ENERGY LABORATORY

MASSACHUSETTS INSTITUTE OF TECHNOLOGY

DOE/ET/37218-2

Development of a Model to Predict Flow Oscillations in Low-Flow Sodium Boiling

by

Alan E. Levin
Peter Griffith

Energy Laboratory Report No. MIT-EL-80-006

April 1980

MASTER

Development of a Model to Predict Flow Oscillations in Low-Flow Sodium Boiling

by

Alan E. Levin
Peter Griffith

Energy Laboratory Report No. MIT-EL-80-006

April 1980

MGW

REPORTS IN REACTOR THERMAL HYDARULICS RELATED TO THE MIT ENERGY LABORATORY ELECTRIC POWER PROGRAM

A. Topical Reports (For availability check Energy Laboratory Headquarters, Room E19-439, MIT, Cambridge, Massachusetts, 02139)

A.1 M. Massoud, "A Condensed Review of Nuclear Reactor Thermal-Hydraulic Computer Codes for Two-Phase Flow Analysis," MIT Energy Laboratory Report MIT-EL-79-018, February 1979.

J.E. Kelly and M.S. Kazimi, "Development and Testing of the Three Dimensional, Two-Fluid Code THERMIT for LWR Core and Subchannel Applications," MIT Energy Laboratory Report MIT-EL-79-046, December 1979.

A.2 P. Moreno, C. Chiu, R. Bowring, E. Khan, J. Liu, N. Todreas, "Methods for Steady-State Thermal/Hydraulic Analysis of PWR Cores," MIT Energy Laboratory Report MIT-EL-76-006, Rev. 1, July 1977 (Orig. 3/77).

J.E. Kelly, J. Loomis, L. Wolf, "LWR Core Thermal-Hydraulic Analysis--Assessment and Comparison of the Range of Applicability of the Codes COBRA-IIIC/MIT and COBRA IV-1," MIT Energy Laboratory Report MIT-EL-78-026, September 1978.

J. Liu, N. Todreas, "Transient Thermal Analysis of PWR's by a Single Pass Procedure Using a Simplified Model Layout," MIT Energy Laboratory Report MIT-EL-77-008, Final, February 1979, (Draft, June 1977).

J. Liu, N. Todreas, "The Comparison of Available Data on PWR Assembly Thermal Behavior with Analytic Predictions," MIT Energy Laboratory Report MIT-EL-77-009, Final, February 1979, (Draft, June 1977).

A.3 L. Guillebaud, A. Levin, W. Boyd, A. Faya, L. Wolf, "WOSUB-A Subchannel Code for Steady-State and Transient Thermal-Hydraulic Analysis of Boiling Water Reactor Fuel Bundles," Vol. II, Users Manual, MIT-EL-78-024. July 1977.

L. Wolf, A Faya, A. Levin, W. Boyd, L. Guillebaud, "WOSUB-A Subchannel Code for Steady-State and Transient Thermal-Hydraulic Analysis of Boiling Water Reactor Fuel Pin Bundles," Vol. III, Assessment and Comparison, MIT-EL-78-025, October 1977.

L. Wolf, A. Faya, A. Levin, L. Guillebaud, "WOSUB-A Subchannel Code for Steady-State Reactor Fuel Pin Bundles," Vol. I, Model Description, MIT-EL-78-023, September 1978.

A. Faya, L. Wolf and N. Todreas, "Development of a Method for BWR Subchannel Analysis," MIT-EL-79-027, November 1979.

A. Faya, L. Wolf and N. Todreas, "CANAL User's Manual," MIT-EL-79-028, November 1979.

A.4 W.D. Hinkle, "Water Tests for Determining Post-Voiding Behavior in the LMFBR," MIT Energy Laboratory Report MIT-EL-76-005, June 1976.

W.D. Hinkle, Ed., "LMFBR Safety and Sodium Boiling - A State of the Art Reprot," Draft DOE Report, June 1978.

M.R. Granziera, P. Griffith, W.D. Hinkle, M.S. Kazimi, A. Levin, M. Manahan, A. Schor, N. Todreas, G. Wilson, "Development of Computer Code for Multi-dimensional Analysis of Sodium Voiding in the LMFBR," Preliminary Draft Report, July 1979.

M. Granziera, P. Griffith, W. Hinkle (ed.), M. Kazimi, A. Levin, M. Manahan, A. Schor, N. Todreas, R. Vilim, G. Wilson, "Development of Computer Code Models for Analysis of Subassembly Voiding in the LMFBR," Interim Report of the MIT Sodium Boiling Project Covering Work Through September 30, 1979, MIT-EL-80-005.

A. Levin and P. Griffith, "Development of a Model to Predict Flow Oscillations in Low-Flow Sodium Boiling," MIT-EL-80-006, April 1980.

M.R. Granziera and M. Kazimi, "A Two Dimensional, Two Fluid Model for Sodium Boiling in LMFBR Assemblies," MIT-EL-80-011, May 1980.

G. Wilson and M. Kazimi, "Development of Models for the Sodium Version of the Two-Phase Three Dimensional Thermal Hydraulics Code THERMIT," MIT-EL-80-010, May 1980.

B. Papers

B.1 J.E. Kelly and M.S. Kazimi, "Development of the Two-Fluid Multi-Dimensional Code THERMIT for LWR Analysis," accepted for presentation 19th National Heat Transfer Conference, Orlando, Florida, August 1980.

J.E. Kelly and M.S. Kazimi, "THERMIT, A Three-Dimensional, Two-Fluid Code for LWR Transient Analysis," accepted for presentation at Summer Annual American Nuclear Society Meeting, Las Vegas, Nevada, June 1980.

B.2 P. Moreno, J. Kiu, E. Khan, N. Todreas, "Steady State Thermal Analysis of PWR's by a Single Pass Procedure Using a Simplified Method," American Nuclear Society Transactions, Vol. 26

P. Moreno, J. Liu, E. Khan, N. Todreas, "Steady-State Thermal Analysis of PWR's by a Single Pass Procedure Using a Simplified Nodal Layout," Nuclear Engineering and Design, Vol. 47, 1978, pp. 35-48.

C. Chiu, P. Moreno, R. Bowring, N. Todreas, "Enthalpy Transfer Between PWR Fuel Assemblies in Analysis by the Lumped Subchannel Model," Nuclear Engineering and Design, Vol. 53, 1979, 165-186.

B.3 L. Wolf and A. Faya, "A BWR Subchannel Code with Drift Flux and Vapor Diffusion Transport," American Nuclear Society Transactions, Vol. 28, 1978, p. 553.

B.4 W.D. Hinkle, (MIT), P.M Tschamper (GE), M.H. Fontana, (ORNL), R.E. Henry (ANL), and A. Padilla, (HEDL), for U.S. Department of Energy, "LMFBR Safety & Sodium Boiling," paper presented at the ENS/ANS International Topical Meeting on Nuclear Reactor Safety, October 16-19, 1978, Brussels, Belgium.

M.I. Autruffe, G.J. Wilson, B. Stewart and M. Kazimi, "A Proposed Momentum Exchange Coefficient for Two-Phase Modeling of Sodium Boiling," Proc. Int. Meeting Fast Reactor Safety Technology, Vol. 4, 2512-2521, Seattle, Washington, August 1979.

M.R. Granziera and M.S. Kazimi, "NATOF-2D: A Two Dimensional Two-Fluid Model for Sodium Flow Transient Analysis," Trans. ANS, 33, 515, November 1979.

NOTICE

DEVELOPMENT OF A MODEL TO PREDICT
FLOW OSCILLATIONS IN LOW-FLOW SODIUM BOILING

by

Alan E. Levin
Peter Griffith

Energy Laboratory,
Department of Nuclear Engineering and
Department of Mechanical Engineering

Massachusetts Institute of Technology
Cambridge, Massachusetts 02139

Topical Report of the
MIT Sodium Boiling Project

sponsored by

U. S. Department of Energy,
General Electric Co. and
Hanford Engineering Development Laboratory

Energy Laboratory Report No. MIT-EL-80-006

April 1980

ABSTRACT

An experimental and analytical program has been carried out in order to better understand the cause and effect of flow oscillations in boiling sodium systems. These oscillations have been noted in previous experiments with liquid sodium, and play an important part in providing cooling during Loss-of-Piping Integrity (LOPI) accidents that have been postulated for the Liquid Metal-Cooled Fast Breeder Reactor.

The experimental program involved tests performed in a small scale water loop. These experiments showed that voiding oscillations, similar to those observed in sodium, were present in water, as well. An analytical model, appropriate for either sodium or water, was developed and used to describe the water flow behavior.

The results of the experimental program indicate that water can be successfully employed as a sodium simulant, and further, that the condensation heat transfer coefficient varies significantly during the growth and collapse of vapor slugs during oscillations. It is this variation, combined with the temperature profile of the unheated zone above the heat source, which determines the oscillatory behavior of the system.

The analytical program has produced a model which qualitatively does a good job in predicting the flow behavior in the wake experiment. Quantitatively, there are some discrepancies between the predicted and observed amplitudes of the oscillations. These discrepancies are attributable both to uncertainties in the experimental measurements and inadequacies in modelling the behavior of the condensation heat transfer coefficient. Currently,

several parameters, including the heat transfer coefficient, unheated zone temperature profile, and amount of mixing between hot and cold fluids during oscillations, are set by the user, and have a deterministic effect on the behavior of the model.

Additionally, criteria for the comparison of water and sodium experiments have been developed. These criteria have not been fully tested.

Several recommendations for future study are proposed, in order to advance the capability of modelling the phenomena observed.

ACKNOWLEDGEMENT

Funding for this project was provided by the United States Department of Energy, the General Electric Co., and the Hanford Engineering Development Laboratory. This support was deeply appreciated.

The authors also thank Dr. William Hinkle and Prof. Neil Todreas for their helpful suggestions, Messrs. Joseph Caloggero and Fred Johnson for their help in acquiring materials for and constructing the Water Test Loop, and Messrs. Chris Mulcahy and Lee Shermelhorn for their help with the data acquisition system.

The work described in this report was performed primarily by the principal author, Alan E. Levin, who has submitted the same report in partial fulfillment for the ScD degree in Nuclear Engineering at MIT.

TABLE OF CONTENTS

TABLE OF CONTENTS (Cont.)

TABLE OF CONTENTS (Cont.)

TABLE OF CONTENTS (Cont.)

TABLE OF CONTENTS (Cont.)

LIST OF FIGURES

LIST OF FIGURES (Cont.)

LIST OF FIGURES (Cont.)

LIST OF TABLES

NOMENCLATURE

Symbol	Explanation	Units
A	Area	in^2
C_o	Turbulent drift flux parameter	
C	Specific heat	BTU/lbm°F
D	Diameter	in
F	Body force	lb_f
f	Volumetric body force (Eq. 2.1)	lb_f/ft^3
f	Friction factor	
g	Acceleration of gravity	ft/sec^2
H	Enthalpy	BTU
h	Specific enthalpy	BTU/lbm
h	Heat transfer coefficient	$BTU/hr\text{-}ft^2 °F$
I	Inertance	$lb_f\text{-}sec^2/ft^5$
Ja	Jakob number	
k	Thermal conductivity	BTU/hr-ft°F
L	Length	in
m	Mass	lbm
P	Pressure	lb_f/in^2
P	Power (App. D)	kw,BTU/hr
Q	Volumetric flow rate	ft^3/sec
q	Heat	BTU
R	Resistance	$lb_f\text{-}sec/ft^5$

NOMENCLATURE (Cont.)

Symbol	Explanation	Units
R'	Resistance	lb_f-sec^2/ft^5
Re	Reynolds number	
St	Stanton number	
T	Temperature	°F
t	Time	sec
U	Internal Energy	BTU
V	Volume	ft^3
v	Velocity	ft/sec
W	Work	BTU
x	Length scale	in
α	Void fraction	
ε	Error	
μ	Viscosity	lbm/hr-ft
ρ	Density	lbm/ft^3
σ	Surface tension	lb_f/ft
τ	Shear stress	lb_f/in^2

NOMENCLATURE (Cont.)

Subscripts

acc	Acceleration
b	Bubble
com	Compressible volume
con	Condensation
evap	Evaporation
fg	Difference between saturated vapor and liquid
fric	Frictional
g	Vapor
grav	Gravitational (hydrostatic)
H	Hydrodynamic
i	Index
l	Liquid
net	Net
S	Source
sat	Saturation
sys	System
T	Thermal
tot	Total
o	Reference
1	Bypass leg

NOMENCLATURE (Cont.)

Subscripts (Cont.)

2	Unheated zone
3	Compressible volume

Superscripts

*	Indicates dimensionless quantity
n	Time step

CHAPTER I

INTRODUCTION

1.1 Background

The liquid metal-cooled fast breeder reactor (LMFBR) is currently under consideration as the prototype for the next generation of nuclear power plants to be built in the United States, Europe, and Japan. A thoroughly different concept than present day water cooled reactors (LWR's), the LMFBR employs liquid sodium as a coolant. This permits operation of the reactor at high temperature and low pressure, thus increasing power cycle efficiency. It also allows the use of a compact core with a high power density, which is then surrounded with a blanket of depleted uranium. This configuration permits breeding - the production of more fuel than is consumed - to occur.

Along with the above advantages inherent in the LMFBR, there are several disadvantages. The fact that sodium is opaque means that the reactor cannot be easily inspected by direct visual means. The coolant may also become highly radioactive. Perhaps the most significant drawback is the possible effects of sodium boiling. When a light water reactor sustains an accident which causes the coolant to boil, the reactor tends to shut itself off due to the decrease in the density of the moderator. In the LMFBR, however, the boiling of the coolant would shift the neutron spectrum in the reactor so as to increase the power, thus creating a possible "autocatalytic" reaction that would cause the reactor power to increase rapidly.

There are also circumstances wherein the boiling of the coolant, while not causing large power excursions, could still have serious detrimental effects on the reactor core. In particular, the loss-of-piping-integrity (LOPI) accident must be considered. In such an accident, a coolant inlet pipe breaks, similar to the loss-of-coolant accident in the LWR. In the case of the LMFBR, this pipe rupture causes a rapid decrease in flow rate. It is assumed in the analysis of this accident that the reactor has been shut down by control rods (scrammed). However, the residual heat remaining in the fuel due to decay of fission products and stored energy, may be sufficient to cause coolant boiling. There is significant uncertainty about the behavior of sodium during boiling. One school of thought asserts that, under conditions such as might occur during a LOPI, voiding process would propagate rapidly due to the high thermal conductivity of sodium, causing a rapid dryout of parts of the core, followed possibly by wide scale core melting and subsequent loss of coolable core geometry.

It is also possible, though, that mitigating factors might come into play to prevent such a rapid dryout. Under this scenario, the stored heat would be rapidly removed without deleterious effects, and subsequent natural circulation and/or forced flow would be sufficient to remove the continuing decay power.

Figures 1.1 and 1.2 are taken from the Department of Energy's report on sodium boiling (1), and illustrate the complex sequences of events which have been developed for sodium boiling accidents. The heavy lines indicate the most likely sequences.

1.2 Scope of the Work

This project was conceived as an attempt both to model and simulate sodium boiling behavior, as part of the total D.O.E. effort in this area. Results from the Thermal-Hydraulic Out-of-Reactor Safety Facility (THORS) tests at Oak Ridge National Laboratory have indicated that stable sodium boiling may be expected under low-power, low flow conditions, such as might occur during a LOPI (2); current models do not accurately predict this type of behavior. In addition, significant flow oscillations occurred during some of these experiments. Upon analysis of the THORS results, it appeared that these oscillations might aid in postponing

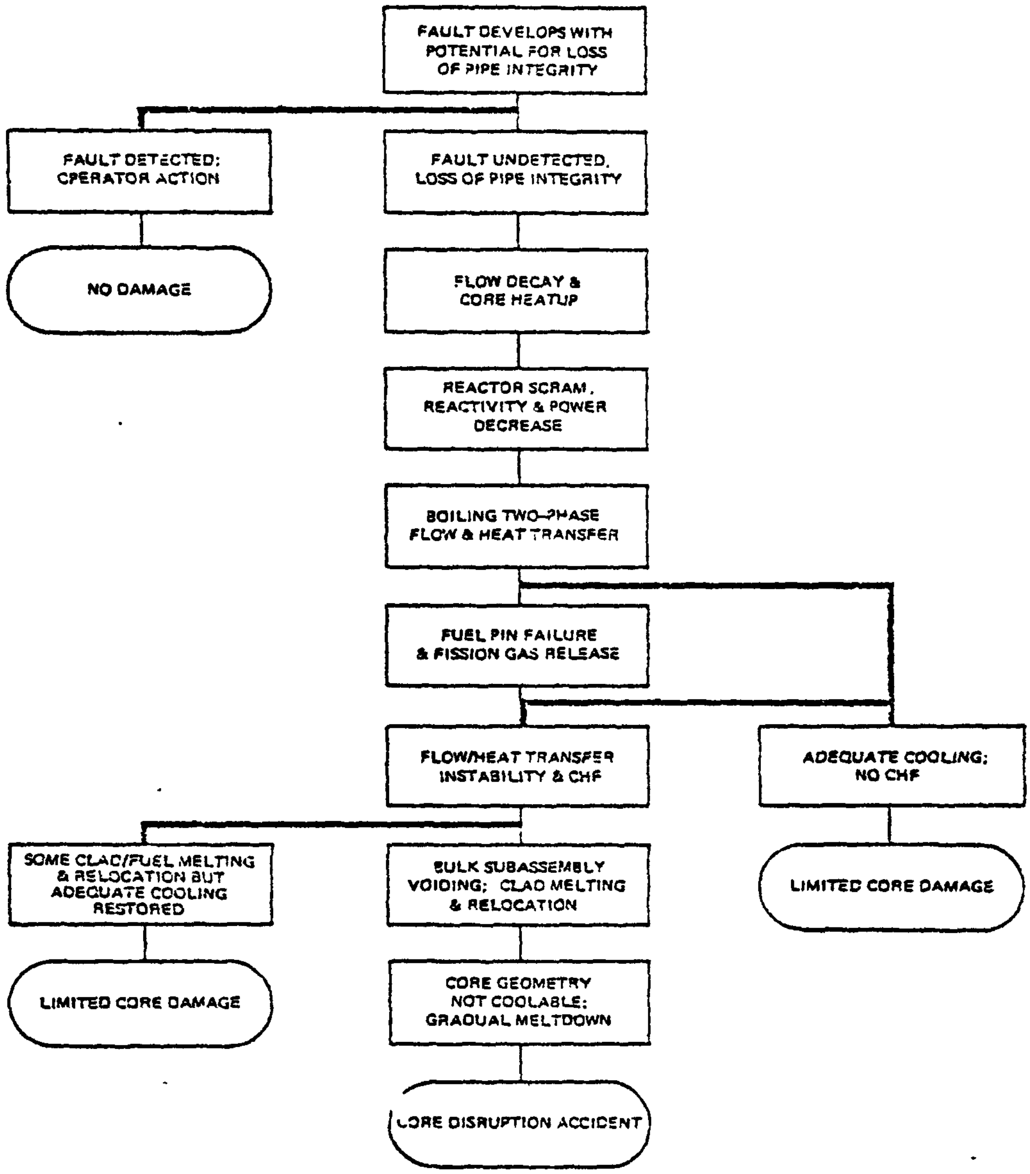

FIGURE 1.1 POTENTIAL SEQUENCE OF EVENTS FOR A LOSS-OF-PIPING-INTEGRITY ACCIDENT

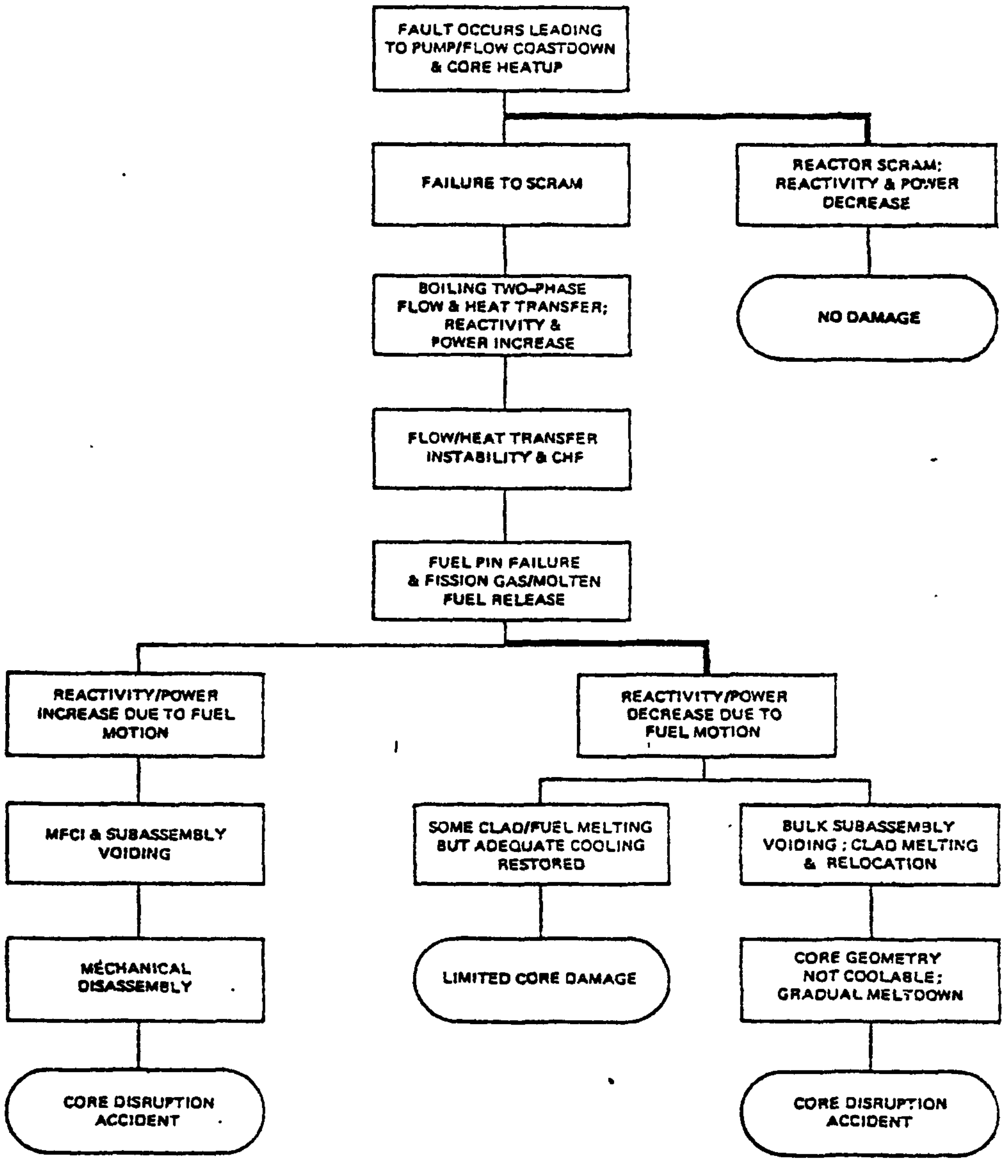

FIGURE 1.2 POTENTIAL SEQUENCE OF EVENTS FOR A LOSS-OF-FLOW ACCIDENT

the dryout of the core.

Since sodium experimentation is both costly and rather hazardous, due to sodium's tendency to ignite spontaneously in oxygen, a simpler approach was developed, using water as a simulant. The objectives of this project were:

1. Development of a simple, one-dimensional model for flow oscillations under low-power, low-flow conditions. This model should be easily understood and incorporate the necessary physical basis for the flow behavior to be modelled.
2. Performance of a series of experiments - with water- to ascertain whether the model would predict observed behavior, as well as to demonstrate the suitability of water as a simulant for liquid sodium.
3. Establishment of a set of criteria through which water and sodium experiments might be compared.
4. Comparison of data from the experiment to sodium data using the criteria developed under 3.

The fourth objective was to be met through comparison of the results obtained from the water experiments to those from the Sodium Boiling Test Facility (SBTF) at ORNL.

The following chapters will cover development of the model, choice of the simulant, criteria for the comparison of water and sodium experimental results, the design of the M.I.T. Water Test Loop, and the results and analysis of experiments performed on the WTL. A brief description of the SBTF will also be included. Finally, the conclusions from this work are presented, along with recommendations for future work in this area.

CHAPTER 2

THE ANALYTICAL MODEL

2.1 Overall Concept

The modelling of two-phase flow is an extremely complex task, due to the interactions of the phases with each other, as well as with their surroundings. Because of this fact, the model developed for this work was derived so as to keep the vapor phase essentially separated from the liquid. In addition, the flow oscillations to be modelled involve the expansion and contraction of a vapor space surrounded by two nearly incompressible liquid columns. The growth and collapse of such a bubble can be the result of either of two effects: a hydrodynamic effect, whereby the vapor space grows or collapses due to the differential pressure between the bubble and the liquid, or a thermal effect, through which the amount of vapor increases or decreases through the evaporation or condensation of the vapor. This second mechanism requires the transfer of heat, either latent or sensible, whereas the first does not. The two effects do not occur independently, however; the collapse of a steam bubble due to hydrodynamic effects would tend to increase the bubble pressure. This would then raise the saturation temperature of the bubble and cause condensation to occur, possibly causing further collapse and starting the cycle again.

Due to the two possible methods of bubble growth and collapse, the model has been developed so as to incorporate both of these factors. This approach was proposed by Ford (3) in his Freon experiments and modelling. While Ford's original reasoning was followed, the details of the models differ, as well as the methods of solution.

In developing this model, the objective was to produce what would eventually be a module in a large system-scale code. There was no attempt made, therefore, to model the single phase flow configuration prior to the inception of boiling and flow oscillations, nor were there any means provided to carry the calculation past the point at which the limitations of model occur. The model limitations are discussed in Section 2.5, and recommendations for further calculational tools are presented in Chapter 6.

2.2 The Hydrodynamic Model

The system under consideration for the development of this model is illustrated in Fig. 2.1. The vapor space is assumed to be at constant pressure throughout, and the top of the upper plenum is assumed to be at atmospheric pressure. The liquid is considered to be incompressible, and acts essentially as a piston. The vapor space is not

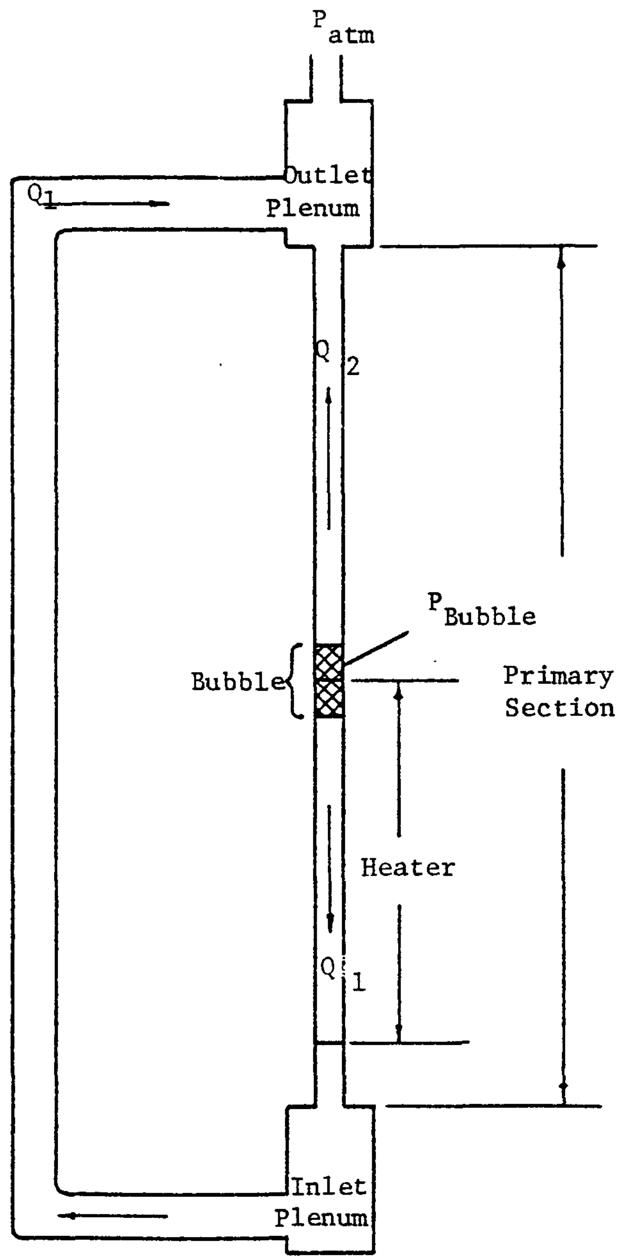

FIGURE 2.1 LOOP MODEL FOR CALCULATION

assumed to be incompressible; in fact, its compressibility is one of the driving forces in the oscillations.

The system is assumed to be in a fixed configuration, with the vapor slug totally separated from the liquid. This "fixed-regime" type of model allows a simple mathematical description of the system.

The momentum equation for one-dimensional, incompressible, single phase flow in a pipe is

$$\frac{dv}{dt} = \frac{1}{\rho_\ell} \frac{dp}{dx} - \frac{1}{\rho} \frac{d\tau}{dy} - f_x \tag{2.1}$$

Integrating over the volume:

$$\rho_\ell \, AL \frac{dv}{dt} = A\Delta P - \frac{A_{shear}}{\bar{A}}\tau - F_x \tag{2.2}$$

This equation can be rearranged to show the contribution of each term:

$$\Delta P_{tot} = \Delta P_{acc} + \Delta P_{fric} + \Delta P_{grav} \tag{2.3}$$

The first term represents the acceleration of the fluid; the second is the pressure drop due to friction, and the third term represents the pressure drop due to body forces, in this case, gravity.

If the area is assumed constant, the term $\rho AL\frac{dv}{dt}$ can be expressed as $\rho L\frac{dQ}{dt}$, where Q is the volumetric flow rate, vA.

Dividing Eq. (2.3) by the area, and combing the gravitational and total pressure drops

$$\Delta P' = \frac{\rho_\ell L}{A} \frac{dQ}{dt} + \tau \frac{A_{shear}}{A} \tag{2.4}$$

where $\Delta P' = \Delta P_{tot} - \Delta P_{grav}$.

The frictional term is now expressed, as is customarily done, using a friction factor, f:

$$\Delta P_{fric} = 4f \frac{L}{D} \frac{\rho_\ell v^2}{2} = \tau \frac{A_{shear}}{A} \tag{2.5}$$

Casting the equation in terms of the volumetric flow rate, Q,

$$\Delta P_{fric} = 2f \frac{L}{D} \frac{\rho_\ell Q^2}{A^2} \tag{2.6}$$

Equation (2.4) now becomes

$$\Delta P' = \left(\frac{\rho_\ell L}{A}\right) \frac{dQ}{dt} + \left(2f \frac{L}{D} \frac{\rho_\ell Q}{A^2}\right) Q \tag{2.7}$$

The term $\frac{\rho L}{A}$ is the inertance of the fluid column indicated by I. The term $2fL\rho Q/DA^2$ is the effective resistance due to friction on the fluid, and is indicated by R. Thus

$$\Delta P' = I \frac{dQ}{dt} + RQ \tag{2.8}$$

This form of the equation is commonly used in system dynamics, and allows the creation of an electrical analog, with pressure drop paralleling voltage and volumetric flow rate analogous to current. The coefficients I and R would correspond to circuit inductances and resistances, respectively.

In Eq. (2.8), the pressure drop $\Delta P'$ represents the non-gravitational pressure difference between the vapor space and the constant upper plenum pressure, and is common to the two liquid legs.

The equation for the vapor space is also derived from system dynamics. For a compressible volume, the conservation of mass equation states

$$\frac{dm}{dt} = \frac{d}{dt}(\rho_g V_g) = \rho_g Q_g \tag{2.9}$$

thus

$$Q_g = \frac{V_g}{\rho_g}\frac{d\rho_g}{dt} + \frac{d\,V_g}{dt} \tag{2.10}$$

If the motion of the boundaries of the compressible volume is examined, it is seen that the motion of the liquid legs, hereafter referred to as Q_1 and Q_2, sum to the volume change, $\frac{dV_g}{dt}$. Therefore,

$$Q_{com} = \frac{V_g}{\rho_g}\frac{d\rho_g}{dt} = Q_3 \tag{2.11}$$

Using Eq. 2.8, the equations for the two liquid legs shown in Fig. 2.1 can be expressed as

$$\Delta P' = I_1 \frac{dQ_1}{dt} + R_1 Q_1 \quad (2.12)$$

$$\Delta P' = I_2 \frac{dQ_2}{dt} + R_2 Q_2 \quad (2.13)$$

since

$$Q_1 + Q_2 = \frac{dV_g}{dt} \quad (2.14)$$

As stated above, Eqs. (2.14) and (2.11) can be combined to define a source volumetric flow rate, Q_s, such that

$$Q_1 + Q_2 + Q_3 = Q_s \quad (2.15)$$

The four equations, 2.8 (one for each liquid leg), 2.11, and 2.12 comprise the hydrodynamic model.

2.3 The Thermal Model

The thermal model for bubble growth is derived directly from the first law of thermodynamics for a closed system. That law states:

$$\delta q - \delta W = \delta U \quad (2.16)$$

The definition of enthalpy

$$H = U + PV \quad (2.17)$$

is substituted into Eq. (2.16). Realizing that the term δW represents pressure-volume work done by the system, so that

$$\delta W = P\delta V \tag{2.18}$$

and making this substitution, as well, Eq. (2.16) becomes

$$\delta q - P\delta V = \delta H - P\delta V - V\delta P \tag{2.19}$$

or

$$\delta q + V\delta P = \delta H \tag{2.20}$$

Equation (2.20) is now divided by δt, and the limit is taken as δt approaches zero. This gives the differential form of the equation

$$\frac{dq}{dt} + V\frac{dP}{dt} = \frac{dH}{dt} \tag{2.21}$$

The enthalpy term for a two-phase system can be separated into its components. Thus

$$H = m_\ell h_\ell + m_g h_g \tag{2.22}$$

and

$$\frac{dH}{dt} = m_\ell \frac{dh_\ell}{dt} + m_g \frac{dh_g}{dt} + h_\ell \frac{dm_\ell}{dt} + h_g \frac{dm_g}{dt} \tag{2.23}$$

The system of bubble and surrounding liquid is chosen to be large enough so that the mass fluxes across the system boundaries are zero. This choice of a closed system sets a model limitation. This assumption is valid only when the vapor through-flow in the bubble is very small, a condition which exists for small bubble lengths only, as in the early stages of a transient. From the definition of a closed system, therefore

$$\frac{dm_{sys}}{dt} = 0 \tag{2.24}$$

and

$$\frac{dm_{\ell}}{dt} = -\frac{dm_g}{dt} \tag{2.25}$$

Substituting into Eq. (2.20):

$$\frac{dH}{dt} = (h_g - h_{\ell})\frac{dm_g}{dt} + m_{\ell}\frac{dh_{\ell}}{dt} + m_g\frac{dh_g}{dt} \tag{2.26}$$

The last two terms represent the change in sensible heat of the system. For small changes in temperature and pressure, these contributions are negligible when compared to the latent heat of vaporization, $(h_g - h_{\ell})$ or h_{fg}. Thus,

$$\frac{dH}{dt} \simeq h_{fg}\frac{dm_g}{dt} \tag{2.27}$$

Substituting back into Eq. (2.18) yields

$$\frac{dq}{dt} + V_g \frac{dP}{dt} = h_{fg} \frac{dm_g}{dt} \qquad (2.28)$$

Since $m_g = \rho_g V_g$

$$\frac{dm_g}{dt} = V_g \frac{d\rho_g}{dt} + \rho_g \frac{dV_g}{dt} \qquad (2.29)$$

and

$$\frac{dV_g}{dt} + \frac{V_g}{\rho_g} \frac{d\rho_g}{dt} = \left(\frac{dq}{dt} + V_g \frac{dP}{dt}\right) / \rho_g h_{fg} \qquad (2.30)$$

It should be noted that the left hand side of Eq. (2.30) corresponds exactly to the source flow Q_s [Eq. (2.15)] derived in Section 2.2. Equation (2.30) comprises the thermal model for the system.

2.4 Solution of the Equations

The thermal and hydrodynamic equations for the system are solved simultaneously and iteratively to find the net source flow and the bubble behavior. The solution is accomplished by means of a digital computer, using a program developed as part of this project.

To review, the equations that must be solved are

$$\Delta P' = I_1 \frac{dQ_1}{dt} + R'_1 Q_1^{\,2} \qquad (2.31)$$

$$\Delta P' = I_2 \frac{dQ_2}{dt} + R'_2 Q_2^{\,2} \qquad (2.32)$$

$$Q_3 = \frac{V_g}{\rho_g} \frac{d\rho_g}{dt} \qquad (2.11)$$

$$Q_s = (\dot{q}_{net} + V \frac{dp}{dt}) / \rho_g h_{fg} = Q_1 + Q_2 + Q_3 \qquad (2.30)$$

In rewriting these equations, the subscripts 1 and 2 refer to the two legs noted on Fig. 2.1; subscript 3 refers to the bubble itself. The total net heat flow to the bubble is symbolized by $\dot{q}_{net}$. Since the resistance term, R, depends on Q [Eq. (2.7], a new coefficient, R', has been introduced in Eqs. (2.31) and (2.32), such that

$$R' = 2f \frac{L}{D} \frac{\rho_\ell}{A^2} \qquad (2.33)$$

There is still a dependence of R' on Q, since the friction factor, f, is a function of the Reynolds number and

$$Re = \frac{\rho Q D}{A\mu} \qquad (2.34)$$

However, since this dependence is normally to a small fraction power in turbulent flow, the form in Eq. (2.33) has been retained.

The number of bypass legs that are part of Leg 1 in Fig. 2.1 is immaterial since, by the analogy of parallel resistances and inductances, these can be combined into an effective single bypass leg. Additional resistances, such as elbows, tees, and other flow obstructions can be accomodated using an equivalent resistance concept, as well.

The solution scheme employed in the computer program sets the equations up in finite-difference form and solves them iteratively. Equations (2.31) and (2.32) are approximated by first order, explicit finite difference equations, while Eqs. (2.11) and (2.30) are solved by implicit first order difference equations. Details of the solution scheme may be found in Appendix A. The iterative technique itself consists of the following steps:

1. The pressure in the bubble is guessed, as well as the bubble lengths and vapor volumes, above and within the heater. The split must be made due to the fact that in the heated zone, evaporation occurs, while in the unheated section above the heater, evaporation occurs. Thus, in order to derive the net heat input to the vapor space, which is the difference between evaporation and condensation, the bubble must be split into two parts. The common vapor space pressure ties the two parts together.

2. The pressure guess allows the determination of the properties in the bubble, since the assumption is made that all vapor (as well as the liquid film on the walls of the heater) is at saturation. The liquid density is assumed to be constant, and

equal to that at saturation. This allows direct solution of Eqs. (2.11) and (2.27), since net heat input is a function of temperature and power to the heater. Other iterative loops determine the amount of power that goes into heating up or cooling the heater wall as pressure changes and the temperature profile of the liquid in the unheated section, as heat is introduced into this liquid by condensation.

3. Equations (2.31) and (2.32) are solved as described above.

4. The source flow $(Q_1+Q_2+Q_3)$ calculated from the thermal model is compared to that calculated from the hydrodynamic model. If these two flows are different by more than a specified convergence error limit, a new pressure is guessed and the calculation starts again from step 1.

5. If the two source flows are within the specified error, new bubble lengths and vapor volumes are calculated and compared to those that were guessed in step 1. If these are within a specified tolerance, time is incremented and the transient calculation proceeds. If they are not within the error limit, a new guess is made of bubble lengths and volumes, and the calculation returns to step 1 for another iteration.

A flow chart is shown in Fig. 2.2 illustrating this technique.

As noted in step 2 above, a temperature-time history of the upper unheated zone is calculated. This is done in order to allow calculation of the condensation of vapor which occurs in that part of the test section. The model used for this calculation is a nodal-averaged temperature scheme, whereby the upper section is split into a number of nodes, each with a single temperature, and new temper-

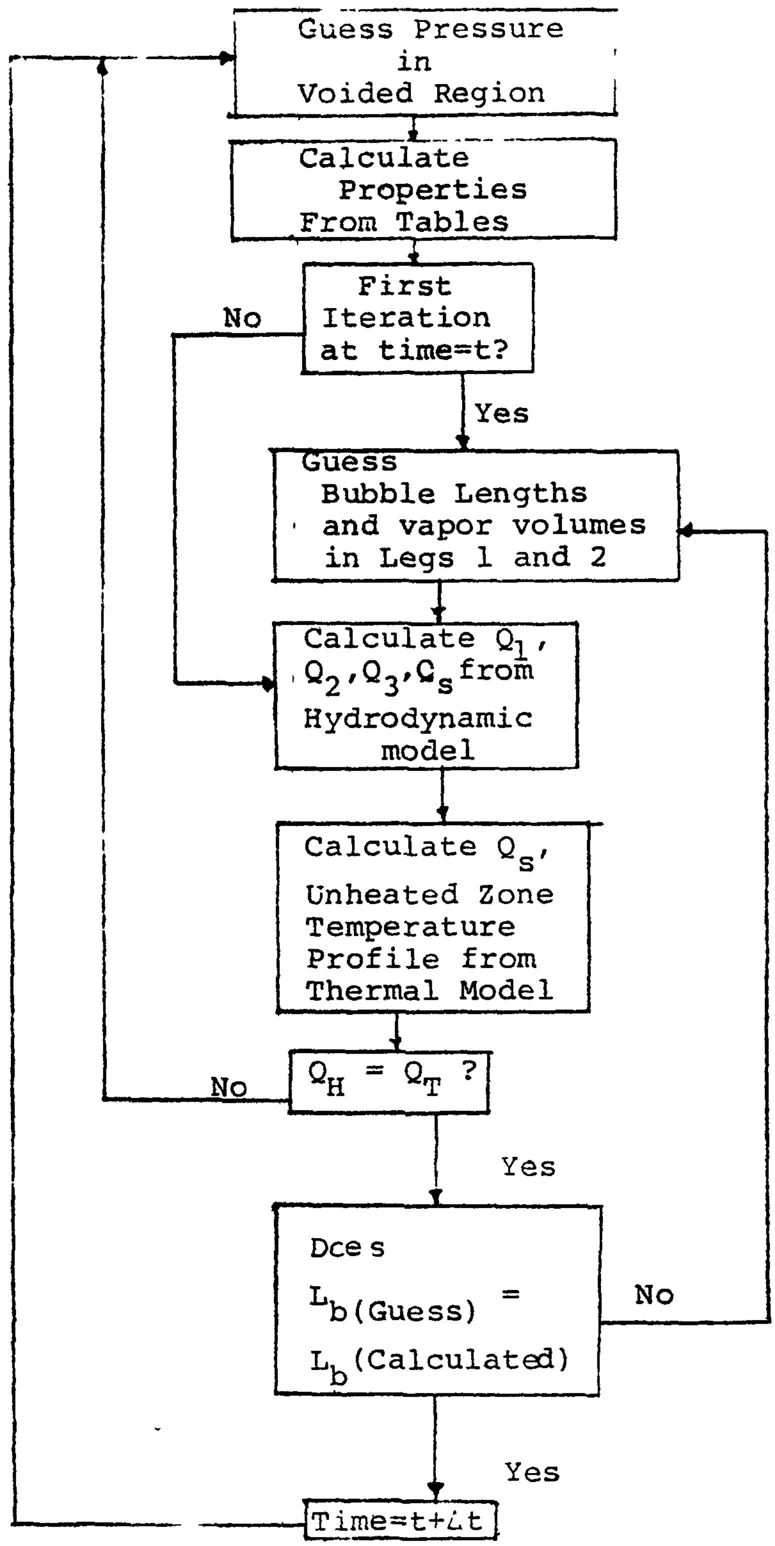

FIGURE 2.2 FLOW CHART OF FLOSS CODE SOLUTION SCHEME

atures are calculated based on the flow of liquid into and out of each node, as well as any condensation which might occur. The changing temperature in the unheated section determines the thermal contribution to bubble growth and collapse, and changes in the amplitude and period of oscillations may be related to this factor. Further discussion of this fact is found in Chapter 5. Details of the temperature calculational scheme can be found in Appendix A.

The method of solution outlined in this section has proven to yield satisfactory and physically realistic results. These results, along with comparison to experimental results can also be found in Chapter 5.

2.5 Limitations of the Model

A "fixed-regime" model is valid only insofar as the regime that is fixed actually exists physically. Once conditions proceed to a point where the assumptions incorporated into the model are no longer justifiable, the model is no longer useful in describing the system.

In the case of the model presented here, the model is valid for small bubble lengths and vapor volumes. Due to the assumptions made in both the hydrodynamic and thermal portions of the model, any deviation from a slug-flow regime would cause the model to fail. In addition, liquid and vapor through-flows are neglected in the formulation of the thermal model. When the bubble becomes large enough to encourage substantial natural circulation flow, this assumption becomes invalid. For these reasons, once net evaporation exceeds net condensation, causing the bubble to grow without collapse, the transient calculation is stopped, and the assumption is made that another calculational tool can be used to determine subsequent occurrences.

CHAPTER 3

CRITERIA FOR THE COMPARISON OF BOILING LIQUID SODIUM TO WATER

3.1 Background

The application of data from water experimentation to the question of what occurs during the boiling of liquid sodium requires that a group of criteria be developed with which to compare water data to sodium data. Several such criteria will be proposed in this chapter.

Clearly, the physical characteristics and properties of the two fluids are quite different, especially those properties dealing with heat transport. Therefore, heat conduction is not included in the comparison criteria. It is assumed that different temperature profiles may exist under the same flow conditions in water and sodium, and differences arising from this fact must be considered. However, from inspection of the equations of the model presented in Chapter 2, it can be seen that the properties that affect the equations are largely hydrodynamic in nature, and there is substantially less disparity between water and liquid sodium in this area. Table 3.1 lists both thermal and hydrodynamic properties of each fluid for comparison.

Table 3.1

Comparison of Water and Sodium Properties

Fluid Property	Water at 14.7 psia	Sodium at 25 psia (Reactor Conditions)
T_{sat}	212°F	1670°F
ρ_ℓ	59.8 lbm/ft^3	46.4 lbm/ft^3
ρ_g	0.0373 lbm/ft^3	0.025 lbm/ft^3
ρ_ℓ/ρ_g	1603	1650
h_{fg}	970.3 BTU/lbm	1650 BTU/lbm
Cp_ℓ	1.0 BTU/lbm°F	0.31 BTU/lbm°F
μ_ℓ	0.687 lbm/hr-ft	0.363 lbm/hr-ft
σ_ℓ	0.004 lb_f/ft	$\sim$0.012 lb_f/ft
k_ℓ	0.394 BTU/hr-ft°F	31.5 BTU/hr-ft°F

The criteria developed in this chapter, then, are mainly hydrodynamic in nature, and may be used under these special circumstances to compare boiling water to boiling liquid sodium.

3.2 Momentum Equations

The approach that is taken throughout this chapter involves the non-dimensionalization of the basic equations.

The momentum equation, as presented in Chapter 2 for unidimensional, single phase flow in a pipe is:

$$\frac{dv}{dt} = \frac{1}{\rho} \frac{dp}{dx} - \frac{\mu}{\rho} \frac{d^2v}{dy^2} - f_x \qquad (2.1)$$

The body force—f_x— is, in this case, due to gravity; thus

$$\frac{dv}{dt} = \frac{1}{\rho} \frac{dp}{dx} - \frac{\mu}{\rho} \frac{d^2v}{dy^2} - g \qquad (3.1)$$

Non-dimensionalization is accomplished by choosing new variables that are dimensionless. For the momentum equation, these variables are:

$$v_o = \sqrt{P_o/\rho_\ell}$$

$$v^* = v/v_o \qquad (3.2)$$

$$t^* = tv_o/D$$

$y^* = y/D$

$\rho^* = \rho/\rho_\ell$

$P^* = P/P_o$

$x^* = x/D$

$\mu^* = \mu/\mu_\ell$

The quantity P_o is a reference pressure, and D is the diameter, and serves as a reference length scale.

Substituting these quantities into Eq. (3.1) yields

$$\frac{v_o^2}{D} \frac{dv^*}{dt^*} = \frac{P_o}{\rho_\ell D} \frac{1}{\rho^*} \frac{dP^*}{dx^*} - \frac{\mu_\ell}{\rho_\ell} \frac{v_o}{D^2} \frac{\mu^*}{\rho^*} \frac{d^2v^*}{dy^{*2}} - g \tag{3.3}$$

Simplifying, and applying the definition of v_o [Eq. (3.2)] to the first term on the right hand side:

$$\frac{dv^*}{dt^*} = \frac{1}{\rho^*} \frac{dp^*}{dx^*} - \frac{\mu_\ell}{\rho_\ell v_o D} \frac{\mu^*}{\rho^*} \frac{d^2v^*}{dy^{*2}} - \frac{Dg}{v_o^2} \tag{3.4}$$

The coefficient of the second term on the right hand side of the equation is the inverse of the Reynolds number. This is the first of the comparison criteria. The Froude number also appears, as the last term in Eq. (3.4). Although this sets another criterion, it reduces essentially to a density ratio for systems of similar geometry and pressure. Applying the definition of v_o to the expression

$\frac{Dg}{v_o^2}$ yields the result

$$\frac{Dg}{v_o^2} = \frac{\rho_\ell Dg}{P_o} \tag{3.5}$$

Since the liquid densities of sodium and water are similar, this criterion is satisfied. The choice of another geometry, however, would necessitate consideration of this parameter.

The appearance of the Reynolds number is not altogether unexpected. As stated above, the driving factors in the oscillatory flow behavior tend to be chiefly hydrodynamic in nature; thus, the prime basis for hydrodynamic scaling should appear.

3.3 The Compressibility Equation

The term expressing the compressibility effects is

$$Q_g = \frac{V_g}{\rho_g} \frac{d\rho_g}{dt} \tag{2.11}$$

The volumetric flow rate is defined in Chapter 2 as

$$Q_g = Av$$

Thus

$$Av = \frac{V_g}{\rho_g} \frac{d\rho_g}{dt} \tag{3.6}$$

or

$$A \frac{dx}{dt} = \frac{V_g}{\rho_g} \frac{d\rho_g}{dt} \tag{3.7}$$

Once again, dimensionless variables are chosen:

$$\begin{aligned} x^* &= x/D \\ A^* &= A/D^2 \\ V_g^* &= V_g/D^3 \\ t^* &= t/\tau \\ \rho^* &= \rho_g/\rho_\ell \end{aligned} \tag{3.8}$$

Equation (3.7) now becomes

$$\frac{D^3 A^*}{\tau} \frac{dx^*}{dt^*} = \frac{D^3 V_g^* \rho_\ell}{\rho_g \tau} \frac{d\rho^*}{dt^*} \tag{3.9}$$

Simplifying:

$$A^* \frac{dx^*}{dt^*} = V_g^* \frac{\rho_\ell}{\rho_g} \frac{d\rho^*}{dt^*} \tag{3.10}$$

The second dimensionless group, then is the liquid-to-vapor density ratio, ρ_ℓ/ρ_g. This term behaves as a kind of variable spring constant, since it changes with pressure, and along with the length of the bubble and heat transfer, helps to determine the oscillatory behavior of the system. From the table of properties, it is clear that the density ratios for sodium and water at pressures near atmospheric are similar.

3.4 The Energy Equation

The energy equation, as derived in Chapter 2, is

$$\frac{dV_g}{dt} + \frac{V_g}{\rho_g}\frac{d\rho_g}{dt} = (\dot{q} + \frac{V_g dP}{dt})/\rho_g h_{fg} \qquad (2.27)$$

The left hand side of the equation is equivalent to a volumetric vapor generation rate, Q_s. The term VdP/dt is very small compared with the net heat flow, $\dot{q}$, and is neglected.

Thus

$$Q_s = \dot{q}_{net}/\rho_g h_{fg} \qquad (3.11)$$

The source flow, Q_s, can be expressed, as in the previous section, in terms of an equivalent velocity and area:

$$Av_s = \dot{q}_{net}/\rho_g h_{fg} \tag{3.12}$$

The velocity, v_s, is now non-dimensionalized:

$$v_s^* = v_s/v_o \tag{3.13}$$

Then

$$Av_o v_s^* = \dot{q}_{net}/\rho_g h_{fg} \tag{3.14}$$

and finally

$$v_s^* = \dot{q}_{net}/\rho_g v_o \; A \; h_{fg} \tag{3.15}$$

The net heat input includes both power input to the lower part of the bubble, as well as condensation which occurs when vapor enters the unheated section above the heat source. The vapor generation occurs via evaporation at the liquid-vapor interface, at saturation, and the condensation is due to the interaction of saturated vapor with subcooled liquid. If this heat input is expressed in terms of an equivalent heat transfer coefficient and temperature difference, Eq. (3.15) becomes

$$v_s^* = \frac{h_{eq} \; (T-T_{sat})}{\rho_g v_o \; h_{fg}} \tag{3.16}$$

where

$$\dot{q}_{net} = h_{eq} \; A \; (T-T_{sat}) \tag{3.17}$$

The quantity on the right hand side of Eq. (3.16) is the Jakob number, Ja, multiplied by the Stanton number, St, since

$$Ja = \frac{\rho_\ell C_{p_\ell}(T-T_{sat})}{\rho_g h_{fg}} \qquad (3.18)$$

and

$$St = \frac{h}{\rho_\ell C_{p_\ell} v} \qquad (3.19)$$

More importantly, this combination serves as a kind of power-to-flow ratio, normalized by the latent heat of vaporization. It is this term which should be used as a comparison criterion. The factor of differing saturation temperatures is also taken into account. One factor which appears indirectly in Eq. (3.16) is the condensation in the unheated zone, since it is combined with the heat input term. The condensation potential in the unheated section appears to be the primary driving force in the flow oscillations under study, a fact that will be discussed more fully in Chapter 5. The heat input to the system is effectively a constant over the duration of the experiments, and it is this condensation term which provides the variation in $\dot{q}_{net}$ and the ultimate potential for bubble growth and collapse. The characterization of the condensation heat transfer in order to determine this potential is therefore crucial.

3.5 Comparison of Sodium Data to Water Data

The Sodium Boiling Test Facility (SBTF) at Oak Ridge National Laboratory is almost an exact analog of the original MIT Water Test Loop, as described in Chapter 4. The SBTF also has a pump to provide for forced-flow experimentation; however, it does not include a bypass loop at this time.

The SBTF is a sodium loop, heated indirectly over its three-foot heated length by a quadelliptical radiant furnace. At the inception of this program, it was expected that some data would be available from SBTF in order to provide a direct comparison to water data. While several of the natural circulation tests performed on the original WTL have been reproduced, budgetary and experimental problems have forced a delay in the performance of forced-flow and flow oscillation testing. It is anticipated that these types of experiments will be performed in the near future, providing a direct test of the comparison criteria herein proposed.

CHAPTER 4

EXPERIMENTAL APPARATUS AND PROCEDURES

4.1 Background and Experimental Apparatus

The expense and hazard involved in the use of liquid metals as an experimental medium led to the concept of the first M.I.T. Water Test Loop, constructed by Dr. W. D. Hinkle in 1976. The WTL was intended to be a simple, easy-to-operate alternative to complex sodium boiling facilities such as THORS. The first experiments performed and reported by Hinkle (4), involved natural circulation tests only, to determine critical heat fluxes under low-power conditions. These results, along with comparison criteria developed by Hinkle, were compared to sodium data obtained under similar conditions from the SBTL loop at Oak Ridge (5). Water was chosen as the simulant in the initial series of tests because of the similar liquid-to-vapor density ratios for the two liquids. Other similarity criteria were not considered.

Flow oscillations such as those observed in the THORS tests could not be modelled using Hinkle's approach, and so a more involved and sophisticated test program was developed. The performance of these experiments required that the Water Test Loop be modified somewhat from its original design. Figure 4.1 shows the loop in its current configuration; Table 4.1 lists the dimensions and properties of the loop. The modifications consisted of the addition of a pump and a bypass leg, which would allow operation in either forced or natural circulation. Four ball valves were installed at the bypass to provide the means to change flow configurations. In addition, an orifice flange was added upstream of the inlet plenum to provide the capacity to vary the inlet flow resistance. Whereas the entire "primary" section - that part between the two plena consisting of the heater and unheated inlet and outlet sections- had been steel, the new loop was built with Pyrex glass tubing making up as much of the unheated sections as practical. This allowed visual observation of bubble growth and collapse patterns during a transient.

The instrumentation was also altered considerably for the new tests. Thermocouples had previously been fastened to the outside of the entire metal primary section, and strain-gauge type pressure transducers were installed in the inlet plenum, heater inlet and heater outlet. There was no flow measuring instrument included. Data acquisition was by means of a chart recorder. The modified version of the loop retained the thermocouples on the outside of the heater rod; however, the Pyrex sections were split into

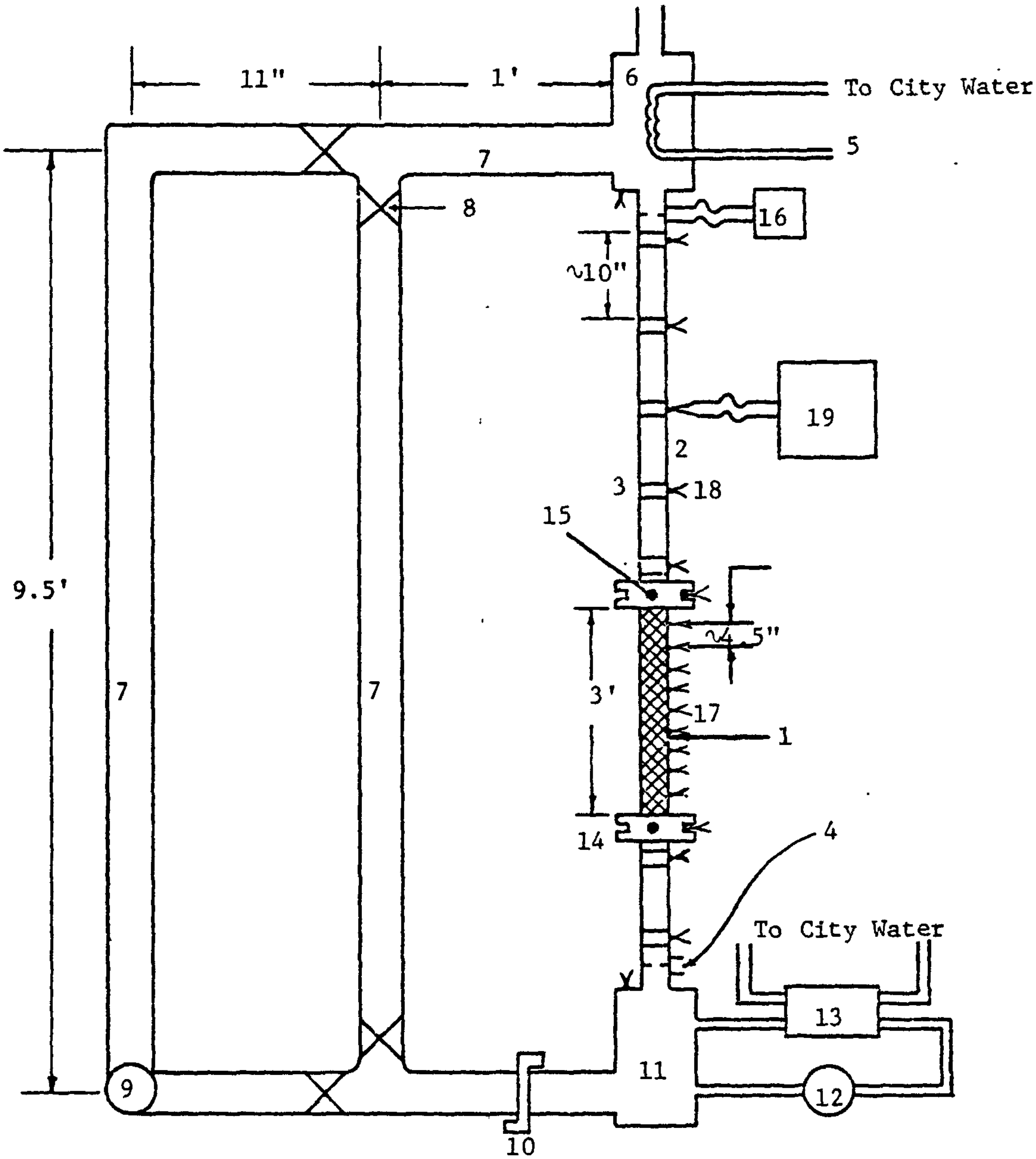

Note: Numbers refer to Table 4.1 on following page

FIGURE 4.1 SCHEMATIC OF THE M.I.T. WATER TEST LOOP

Table 4.1. List of Loop Components

Component Number	Function
1	Heater Tube - 0.25" OD
2	Pyrex Tubing - 6mm OD
3	Swagelok Tee for Thermocouple Insertion
4	Orifice for ΔP Transducer
5	Cooling/Heating Coil for Plenum
6	Upper Plenum - 8"I.D. x 8" ht.
7	Stainless Steel Bypass Pipe - 1" I.D.
8	Ball Valve for Flow Control
9	Pump
10	Orifice Flange
11	Lower Plenum 8" I.D. x 8" ht.
12	Heat Exchange Loop Pump
13	Heat Exchanger
14	Connection to 7kw DC Generator
15	Insulator and Tyco Pressure Transducer
16	Validyne ΔP Cell across Orifice
17	Thermocouple on Outside of Heater Tube
18	Thermocouple Inserted into Swagelok Tee
19	Data Acquisition System

smaller zones, with each end inserted into a Swagelok tee. The third port of the tee was used for insertion of a thermocouple directly into the fluid stream. The thermocouples were sealed into the ports using RTV Silicone Rubber Sealant. All thermocouples were copper-constantan.

Pressure transducers of the same type that Hinkle used were retained for the heater inlet and outlet. The inlet plenum transducer was not used. These gauges were Tyco type AB, with a range of 0-6 psig. When excited by a 6-volt dry cell battery, the response was linear, at a rate of 20 mv/psi.

For the new set of experiments, it was desired to have measurement of inlet and outlet flow rates. To accomplish this, flow orifices were installed just downstream of the inlet plenum and upstream of the outlet plenum. The orifices were about 80% of the test section diameter. They were made this way so as to cause as little interference with the flow as possible, while still generating enough of a pressure drop to measure flow rate. Pressure drop measurements were made using Validyne DP15 differential pressure transducers. These instruments can be adjusted as to the range of their output, from about ± 0-1 to ± 0-10 volts full scale. The transducers themselves are variable reluctance devices with interchangeable diaphragms, permitting operation from ± 0-0.1 psid upward. In order to provide response as accurate as possible and to avoid pinning the data acquisition system at its maximum output, a range of ± 0-1 volt was chosen, with the lower transducer set for ± 0-1.0 psid, and the upper transducer for ± 0-0.5 psid. The Validyne transducers were supplied with their own carrier demodulators, which served as both a power source and voltage output device. Calibration of these transducers was done in place, using both upflow and downflow.

The loop was run in visual observation tests immediately after construction. On the basis of these observations and sodium test results, the decision was made to purchase a fast-scan data acquisition system, in order to collect data at a rapid enough rate to be able to trace the oscillatory motion. The system chosen was a Perkin-Elmer Low-Level Real Time Analog System (RTAS). The RTAS has the capability of scanning individual data points at rates up to 8000 points per second. The low level system permits inputs of ± 0-1.0 volts. To collect and store the data, a Perkin-Elmer Model 1610 minicomputer was acquired. This machine is a 16-bit computer with 64000 bytes of memory, with dual floppy disk drives to provide input-output capability. A Perkin-Elmer 550 CRT terminal was used as the system console, and a Perkin-Elmer 650 Thermal Printer was connected to the rear of the CRT to provide hard copy output, if desired. Operating system software, including FORTRAN support, was supplied by Perkin-Elmer. Using the 1610 computer and driver programs developed by Perkin-Elmer for the RTAS, data acquisition was done at the rate of 600 points per second. The RTAS input supports twenty-four individual instruments, and scans were performed twenty-five times per second. The instrumentation consisted of: The two Validyne differential pressure transducers, the two Tyco gauge pressure transducers, and nineteen thermocouples, one each in the inlet and outlet plena, eight tied onto the outside of the heater at approximately 4.5 inch intervals, and nine in the unheated zones. The twenty-fourth point was connected to an RTD temperature reference on the RTAS termination panel to provide an equivalent ice-point for the thermocouples. The computer, through its line-frequency clock, is able to generate interupts at up to 120 times per second. Each interupt allows the RTAS to scan all 24 points at the maximum scan rate. The interupt interval chosen for these experiments was 40 milliseconds. More detail on the data acquisition system can be found in Appendix B.

Power was supplied to the test section by a 7 kilowatt DC generator. The test section was directly heated (resistance heating) by the generator. Power was measured using a Hewlett Packard Model 3465 B Digital Multimeter. The voltage drop across the test section heater tube was measured, and multiplied by the generator current output. Generator current was ascertained by means of a calibrated shunt providing 50 μv output at 1000 amperes.

The remainder of the test section, aside from the bypass legs, consisted of a heat transfer loop to cool the plena. The lower plenum was cooled by direct fluid exchange, whereby fluid was removed, pumped through a small heat exchanger, and returned to the plenum. The upper plenum, which was open to the atmosphere to provide a constant reference pressure, was cooled by a copper coil loop inside the plenum. Water was run from the city water pipes through this copper coil, and the temperature of this water could be varied, so as to hold the plenum at the desired temperature.

Both the main test section pump and the heat exchanger loop pump were Jabsco "Sturdi-Puppy" self-priming vane pumps, rated at 5 gpm at 8.5 psi. Figure 4.2 represents the pump curve.

The bypass legs were stainless steel piping. The large size of these pipes in relation to the primary tubing was to negate any significant bypass effect on flow dynamics.

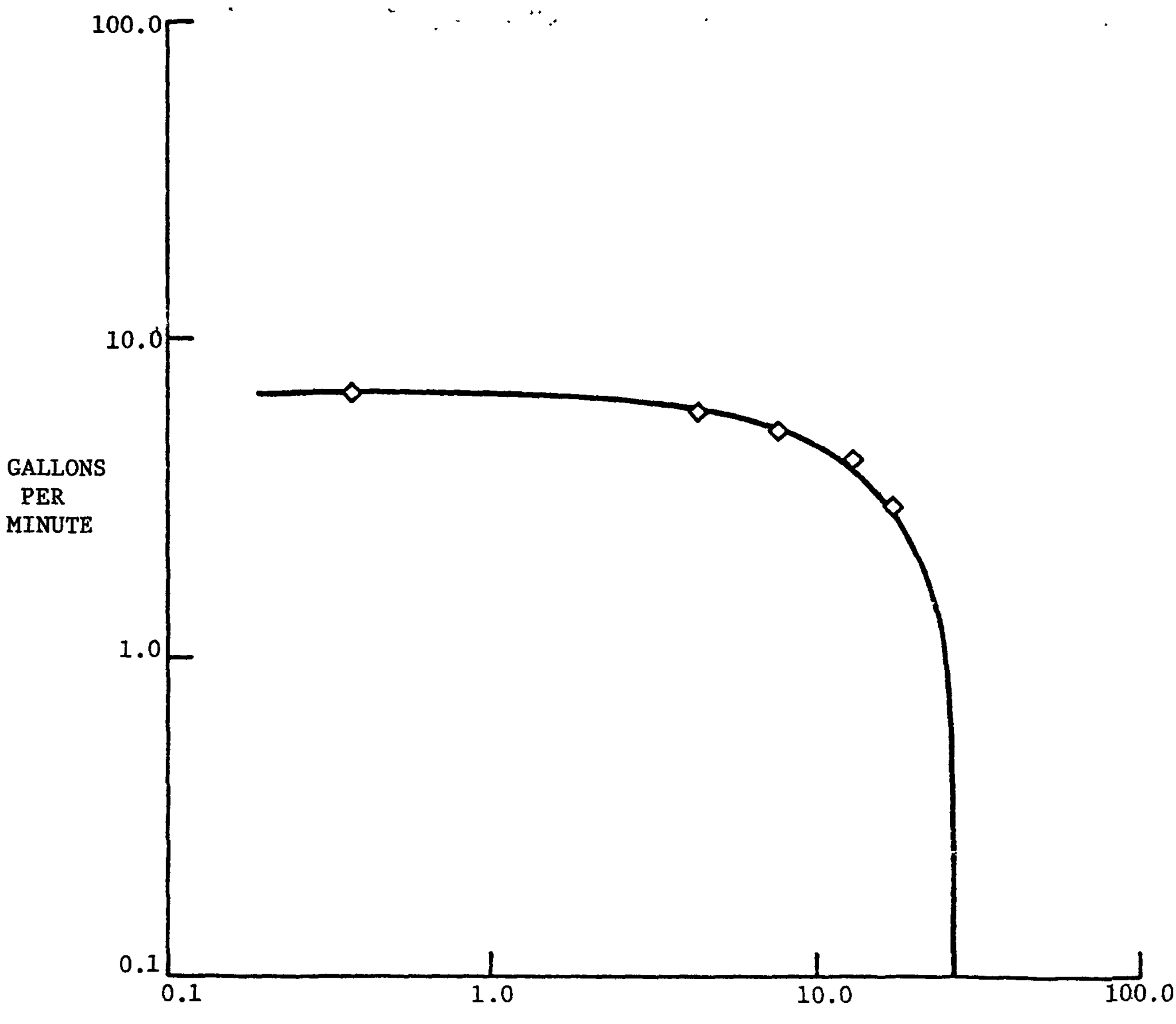

FIGURE 4.2 PUMP PERFORMANCE CHARACTERISTICS

4.2 Experimental Set-up and Procedure

4.2.1 Pretest Set-up and Calibration

Prior to each set of experiments, several steps were followed to insure readings from instruments were as accurate as possible. With the loop filled, the battery for the Tyco pressure transducers was checked to make certain it still was charged at 6 volts. The transducers themselves were then checked for offset from zero. This was accomplished by checking the output from each transducer with a digital multimeter to ascertain the output, and then subtracting from that reading 20 mv for each psi of water head above the transducer.

The second step involved the calibration-in-place of the Validyne differential pressure transducers. Each transducer was calibrated in both upflow and downflow. Calibration in upflow was accomplished via a two step method. The loop was run at the beginning of the experimental program with the bypass line opened and the power at a low level. Using the thermocouples directly upstream and downstream of the heater, a heat balance was performed. Knowing the amount of power input and the temperature size of the water across the heater, it was then possible to determine the flow rate. This single point was used to calibrate the transducers in upflow, with the assumption of linear transducer response. For downflow calibration, the primary side of the loop was isolated to prevent recirculation effect on the transducer. Water was then withdrawn from the lower plenum through the hole where the plenum pressure transducer had been mounted in Hinkle's experiment. Initially, since the water could be withdrawn at variable rates, several different measurements were made. The flow was collected for a timed interval, then measured to find the flow rate. The rate of withdrawal was sufficiently small, so that the driving pressure on the primary side did not change appreciably. This insured constant flow over time. The calibration with several points verified the linearity assumption made in upflow, and in later calibrations, only one point was taken for downflow calibrations. The transducers themselves were first bled, and then zeroed using the carrier demodulator adjusting dial. Output was again read using a digital multimeter.

Before beginning experimentation, the loop was operated for several minutes to remove all trapped air bubbles from the system.

The final step before beginning the experiment was to load the data acquisition system controller programs into memory. Once this was accomplished, the data collection procedure could be started by simply pressing on key the system console.

4.2.2 Experimental Procedure

The experimental procedure for each run was basically the same, with the exception of the final test. The last experiment will therefore be dealt with separately. The conditions for all tests analyzed are presented in Table 4.2.

4.2.2.1 Stagnant Flow Testing

Three preliminary tests were run under stagnant flow conditions to test all of the equipment and to practice data-taking procedures. Six additional experiments were then run in which data was acquired and converted.

Preliminary analytical work using the computer model indicated that the temperature profile in the unheated zone was perhaps the single most important parameter in determining flow oscillatory behavior. It was therfore decided to run the experiment in the same way each time, varying only that temperature profile.

The temperature profile was established by running the loop with bypass flow. This made the velocity in the primary section sufficiently low that any temperature ranging from the lower plenum temperature to saturation could be established in the unheated zone by varying heater power. The temperature would then be uniform from the top of the

Table 4.2. Experimental Conditions

Test Number	Stagnant/ Forced Convection	Unheated Zone Temperature(°F) Prior to Boiling Inception	Heater Power (kw)
4	S	75	0.544
5	S	102	0.544
6	S	80	0.209
7	S	100	0.326
8	S	117	0.417
9	S	140	0.390
10	FC	$\sim$175 decreasing to $\sim$95 at top	1.09

heater to the upper plenum, where the temperature was controlled using the heat transfer loop. Losses to the surroundings were assumed to be negligible. The temperature of the upper unheated zone was measured by connecting an Omega Model 403A digital thermometer connected to the first thermocouple downstream of the heater and in the water.

Once the temperature profile was established, the pump was stopped and the generator was disconnected from the heater. The bypass valve was then closed. The flow path, therefore, consisted of the primary loop with no bypass and a stalled pump in the downcomer. The pump was stalled to permit as little natural circulation as possible to raise the temperature of the unheated zone. Some leakage flow through the stalled pump was present, however. The power was then set at the desired level and applied in a step-change fashion to the test section. Shortly before the inception of boiling, the data acquisition system was started. Boiling and flow oscillations then were observed and data acquired. Upon termination of the data acquisition program in approximately fifteen seconds, the pump was restarted to bring the loop down below saturation at all points. Power was then measured using the procedure outlined in a previous section, and the generator was then shut off. Preparations were then made for the next run.

After the termination of experimentation, data reduction was accomplished using the data acquisition computer. A conversion program was written for the instrumentation present using calibration information to convert the Tyco transducer readings to psig and the Validyne transducer readings to flow rate. The thermocouples were converted by a four step method. Using calibration information supplied with the RTD temperature reference, the temperature of the thermocouple termination panel was determined. This temperature was then converted to millivolts for copper-constantan thermocouples using a standard curve fit with a 32°F reference power. This number was then added to each thermocouple reading. Finally, the adjusted thermocouple output was converted to temperature using a standard curve fit for a 32°F reference temperature. As a last step, bubble lengths in the heated and unheated zones were calculated by a stepwise integration of the flow rates with time. Results of these calculations, and the accuracy of the derived data, will be discussed in Chapter 5.

4.2.2.2 Forced Convection Testing

One experiment was performed using forced, instead of stagnant, flow. This was done both to examine the effect of a nonuniform temperature profile in the unheated zone, and to determine the effect that forced flow would the oscillatory behavior. Procedures for pretest calibration and set-up were the same as described in Section 4.2.1. In this experiment, though, the run was started with the bypass closed and the pump running. This generated a flow rate so large as to make the temperature rise across the heater very small. The bypass was then opened and data acquisition began simultaneously. The opening of the bypass reduced flow drastically to the primary section, allowing boiling to begin. Termination of the experiment and data reduction were then performed as outlined in Section 4.2.2.1.

4.3 Safety Precautions

During all tests, the behavior of the bubble was observed visually in the Pyrex section. This was done to provide verification of the results derived through data reduction, and also to insure that the heater was not about to reach critical heat flux (CHF). Since the heater was clamped at both ends, the rapid heatup of the tube associated with CHF would have caused severe distortion (bowing) of the tube, possibly resulting in permanent heater deformation. The Pyrex was also checked to make certain that it did not crack.

A small amount of leakage was observed, due to the many fittings as well as the manner in which the thermocouples were sealed into the unheated zone. Leaks that were small enough to have no appreciable effect on the experiment were ignored. Large leaks, however, were resealed.

CHAPTER 5

EXPERIMENTAL AND ANALYTICAL RESULTS

5.1 Experimental Results

5.1.1 Stagnant Flow Tests

5.1.1.1 Data Analysis

Data reduction for each experiment was carried out as described in Chapter 4. Upon examination of the data, several facts were immediately evident.

The differential pressure transducer upstream of the upper plenum was nearly useless in trying to determine the bubble length in the unheated section. This was true because of the presence of air in the water. Since the loop was operated open to the atmosphere, it was not degassed, and the water used to fill the loop had a substantial amount of dissolved air in it. At boiling inception, this air was stripped out from the steam, and upon condensation, did not dissolve once again into the water, but instead travelled up the test section to the upper plenum. When these bubbles came near the Validyne transducer, they so distorted the differential pressure reading that any attempt to deduce the flow rate or to integrate the flow rate to find the bubble length yielded unrealistic results, based on what was observed visually during the experiment.

In addition, the Validyne transducer just downstream of the lower plenum registered extremely large pressure drops at times during each run. This pheonomenon was attributed to a "water hammer" effect due to vapor condensation. This conclusion was reached due to the fact that these large pressure drops always occured immediately after the bubble lengths, as calculated from the flow rate, reached zero. After peaking rapidly these shock waves would die away rapidly as well, until the next bubble growth-collapse cycle. The passage of these pressure waves across the orifice taps at the bottom of the test section caused large differential pressures to be recorded by the Validyne transducers, although the flow itself was not significantly affected, due to the high rate of speed of the wave. However, since flow rates are inferred from the readings of the Validynes, the response of the transducers to these pressure waves tended to distort flow rate measurements. No other distortion, such as that mentioned for the upper transducer due to air bubbles, was noted for the lower Validyne.

Several examples of experimental results are shown in Appendix C. The flow rate readings shown in several of the tables illustrates clearly the effect of the "water hammer" shock waves.

The thermocouples performed rather well, although there were cases of bead breakage and subsequent failure to function. In general, though, those couples connected to the outside of the heater tube tended to respond very slowly to changes in temperature inside the tube. This is understandable due to the time lag resulting from the tube wall thickness. The thermocouples in the fluid, though, responded rapidly to temperature changes and were quite valuable in determining bubble movement.

All of the stagnant flow tests exhibited the same basis characteristics. Upon boiling inception, the vapor bubble would begin to grow outward in both directions from the top of the heater. This tended to push warm fluid into the upper unheated zone, causing the temperature of that fluid to rise. In addition, condensation would deposit heat in this fluid. When the bubble grew far enough so that net condensation exceeded net evaporation, it would then begin to collapse. This, in turn, would pull the colder fluid above the bubble down into the heated zone, dropping the temperature at that point below saturation. This cycle was followed by the aforementioned "water hammer" shock effect, and then a short waiting period would occur while the water at the top of the heater was reheated to saturation. This cycle would repeat itself several times. The amplitude and frequency of the bubble growth-collapse cycle tended to change over the course of the transient, due to the changing temperature profile in the unheated zone.

In the subsequent sections, each test will be examined individually in order to discuss its characteristics.

5.1.1.2 Test 4

After the first three preliminary tests, the first run to be analyzed was number 4.

A plot of calculated bubble lengths in the heater versus time is presented in Fig. 5.1. Due to the anomalies in flow rate readings, from which the bubble length is calculated, mentioned in the previous section, these measurements can be treated only as approximate. However, several pieces of valuable information are discernable from these data.

The first thing to notice is, in general, the extremely rapid collapse of the bubbles after they have reached their peak lengths. This is likely due to the variation in condensation heat transfer during the oscillation cycle. This point will be discussed at length in a later section, due to its importance in determining bubble growth and collapse.

Although the growth-collapse pattern appears to be somewhat random at first, after about two seconds, a pattern

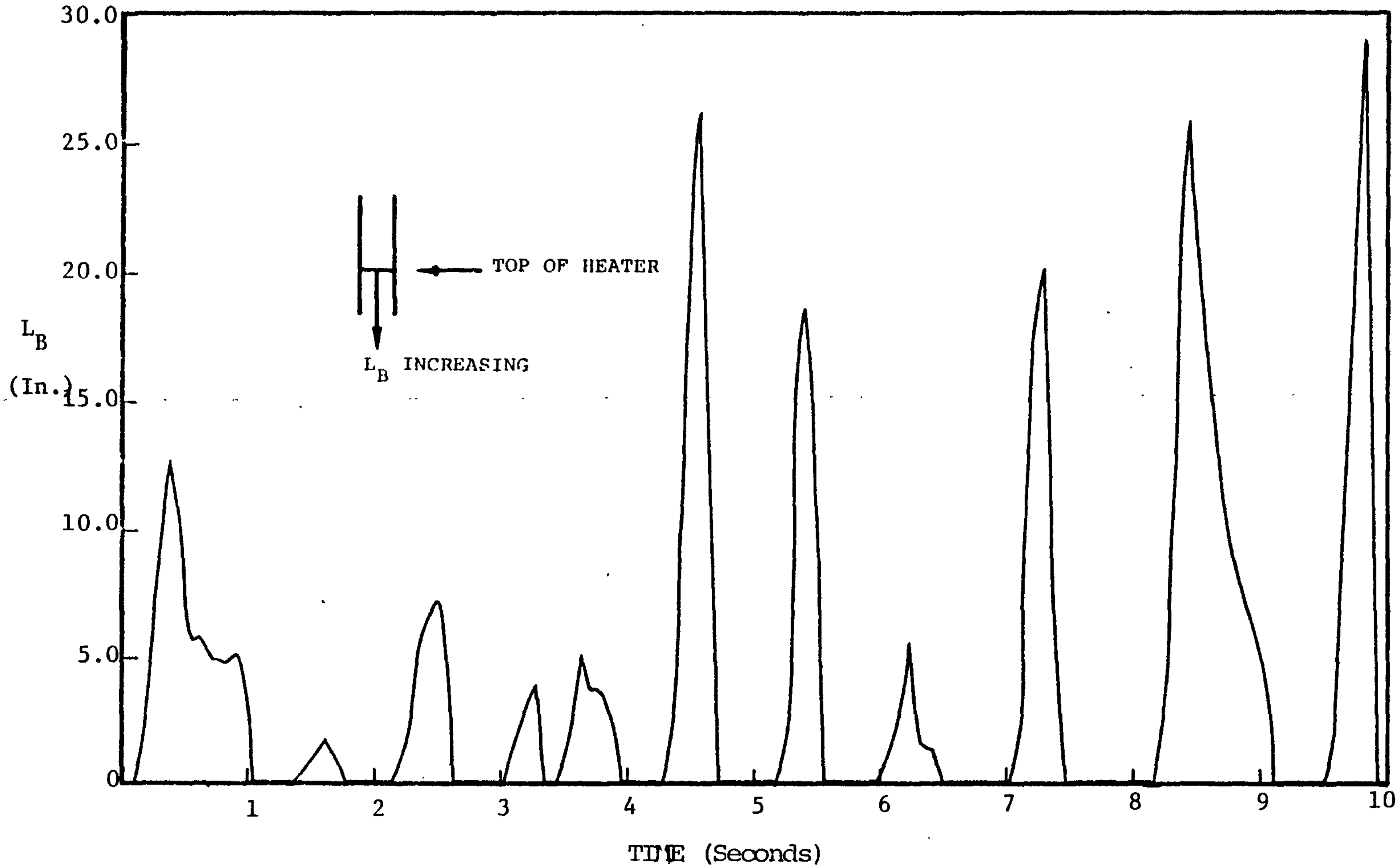

FIGURE 5.1 RESULTS OF TEST 4 - OSCILLATIONS IN BUBBLE LENGTH

of increasing and then decreasing bubble length becomes apparent. This looks very much like a "beat pattern" that is experienced in sound waves. It results from the superposition of two somewhat different frequencies. In this case, it appears that the short frequency is indeed the bubble oscillation frequency. The longer wave pattern is probably due to a sort of "enthalpy wave" flow instability. This instability results, at low flow rates, when a large amount of fluid is heated to saturation. Upon boiling inception, its density decreases, and the fluid accelerates out of the heated zone. It is replaced by colder fluid from below, which increases the density of the fluid once again, and decelerates the column back to its original condition. This beat pattern behavior is consistent with results of liquid metal experiments, another point which will be examined in more detail in a subsequent section.

The temperature at the first thermocouple in the fluid downstream of the heater is shown in Fig. 5.2 as a function of time. This plot clearly illustrates the temperature oscillations which occur as the bubble grows and collapses.

Another point to note is the waiting period evident after each bubble collapse. Part of this time is artifically induced by the pressure waves from the water

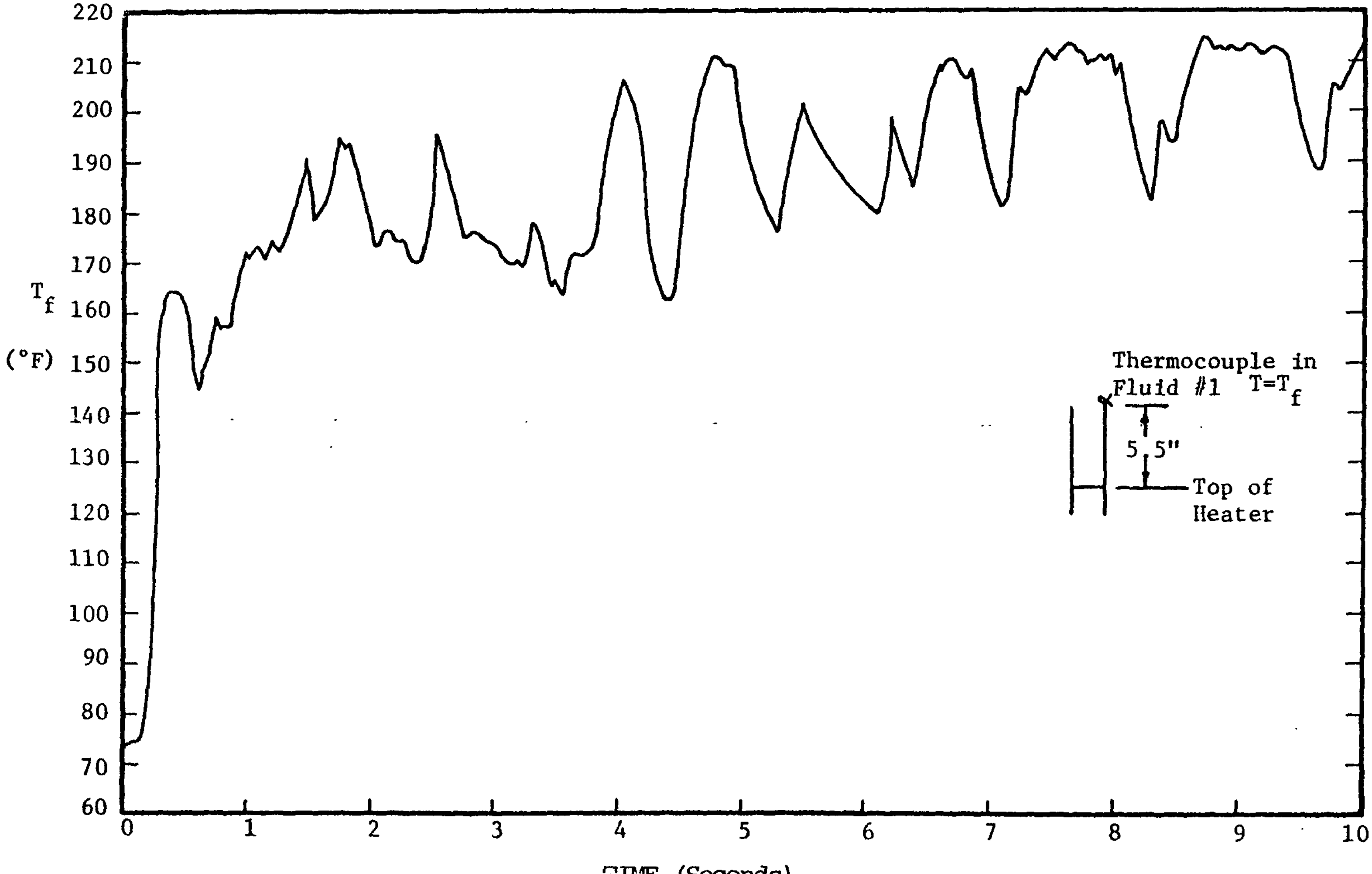

FIGURE 5.2 RESULTS OF TEST 4 - TEMPERATURE OF FIRST UNHEATED NODE

hammer effect. However, some of this period is caused by the necessity to heat the water back to saturation after a bubble collapses.

A final point to note is the amplitude of the oscillation. Since the flow rates are inferred from the pressure transducers, and bubble length is inferred by integrating the flow rate curve, several sources of uncertainty are available to distort the calculation. In addition, since the readings from the upper Validyne were highly unreliable, the bubble length above the heater can be inferred only by applying information gained from the analytical study. This point will be elaborated upon in the section on the comparison of analytical and experimental results, and when the condensation heat transfer coefficient is discussed.

5.1.1.3 Test 5

The power to the heater in Test 5 was the same as that in Test 4; however the temperature in the upper unheated zone was approximately 25°F higher. The purpose of this run, then, was to compare it with the previous run to determine the effect of that temperature on the oscillatory flow behavior. A plot of bubble length within the heater versus time is presented in Fig. 5.3, and temperature of the fluid just downstream of the heater versus time is shown in Fig.

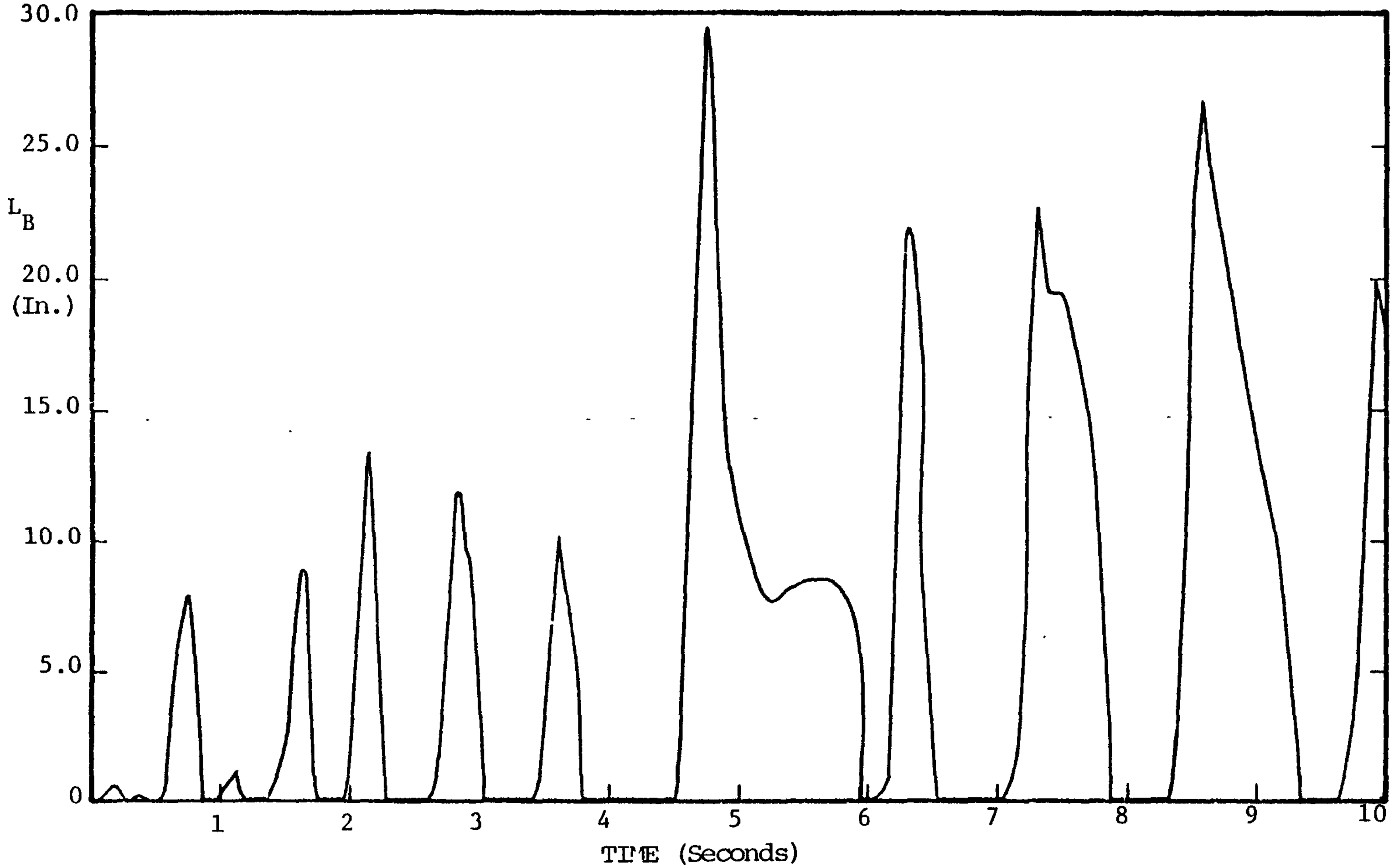

FIGURE 5.3 RESULTS OF TEST 5 - OSCILLATIONS IN BUBBLE LENGTH

5.4. There are some significant differences between Tests 4 and 5 which should be noted, as well as a few similarities.

The similarities basically relate to the character of the flow oscillations in general. The same pattern as that described in the previous section is evident. Some slight evidence of the "beating" that appeared in Test 4 shows again between about 1.5 and 3.5 seconds. However, the difference in amplitude is not as significant in Test 5 as in Test 4, a fact that can be attributed to the difference in unheated zone temperature. A second similarity is the waiting period between oscillations that was noted in Test 4. However, this waiting period tends to be shorter in this test. The higher upper zone temperature means that less time is needed to return the fluid to saturation.

The main differences between the two runs is the difference in oscillation frequency and amplitude over the transient. The average frequency - number of oscillations divided by transient time - is less in this test than in Test 4. This difference is especially clear after t=4 seconds. Related to this fact is the slightly larger amplitude of the oscillations. However, the amplitude of the oscillation is more an inertial effect than a thermal one. Therefore, while the difference in amplitude is not particularly large, for bubbles of similar lengths in the two tests,

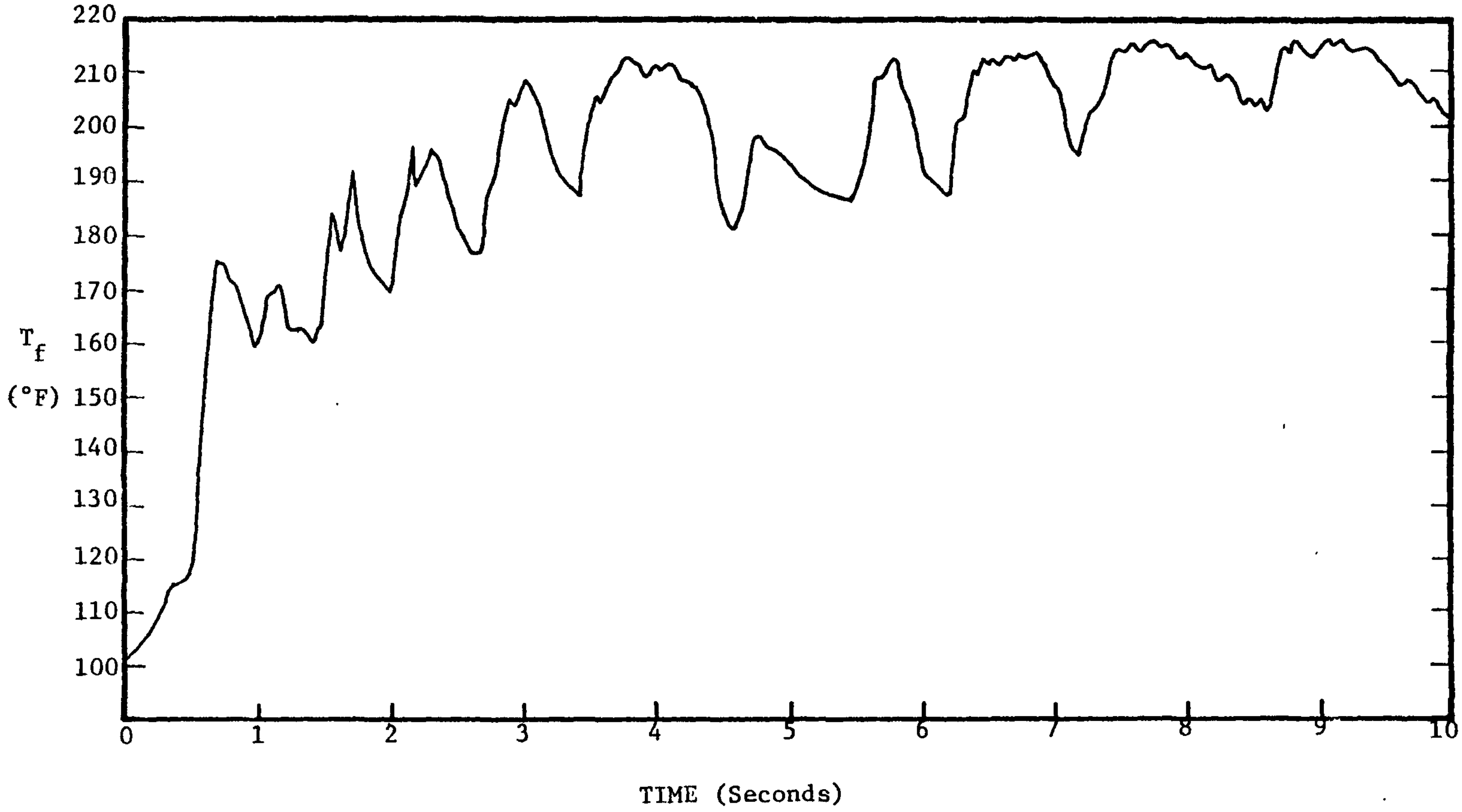

FIGURE 5.4 RESULTS OF TEST 5 - TEMPERATURE OF FIRST UNHEATED NODE

the collapse time in Run #5 is significantly longer, due to the lower temperature difference in condensation. This shows that bubble collapse, in the initial stage at least, is largely thermal in nature.

The remaining four stagnant flow tests were run at lower powers than the first two tests. However, no attempt was made to keep the power exactly the same in the four tests. The temperature of the unheated zone was increased from test to test, though, to further explore the influence of this temperature on flow behavior.

5.1.1.4 Test 6

Conditions during Test 6 featured a very low power as well as a low temperature in the unheated zone. The results of this test are presented in Fig. 5.5 and 5.6. The same general pattern of flow behavior prevails in this test as in the previous two. The beat pattern is especially clear between about 2.5 and 6.5 seconds. However, the amplitudes of the oscillations in this case are smaller than in the previous tests, a fact attributable mainly to the extremely low power level. The average frequency of the oscillations is also much more rapid. This is due partly to the power level and partly to the low upper zone temperature.

An interesting point to note is that there appears

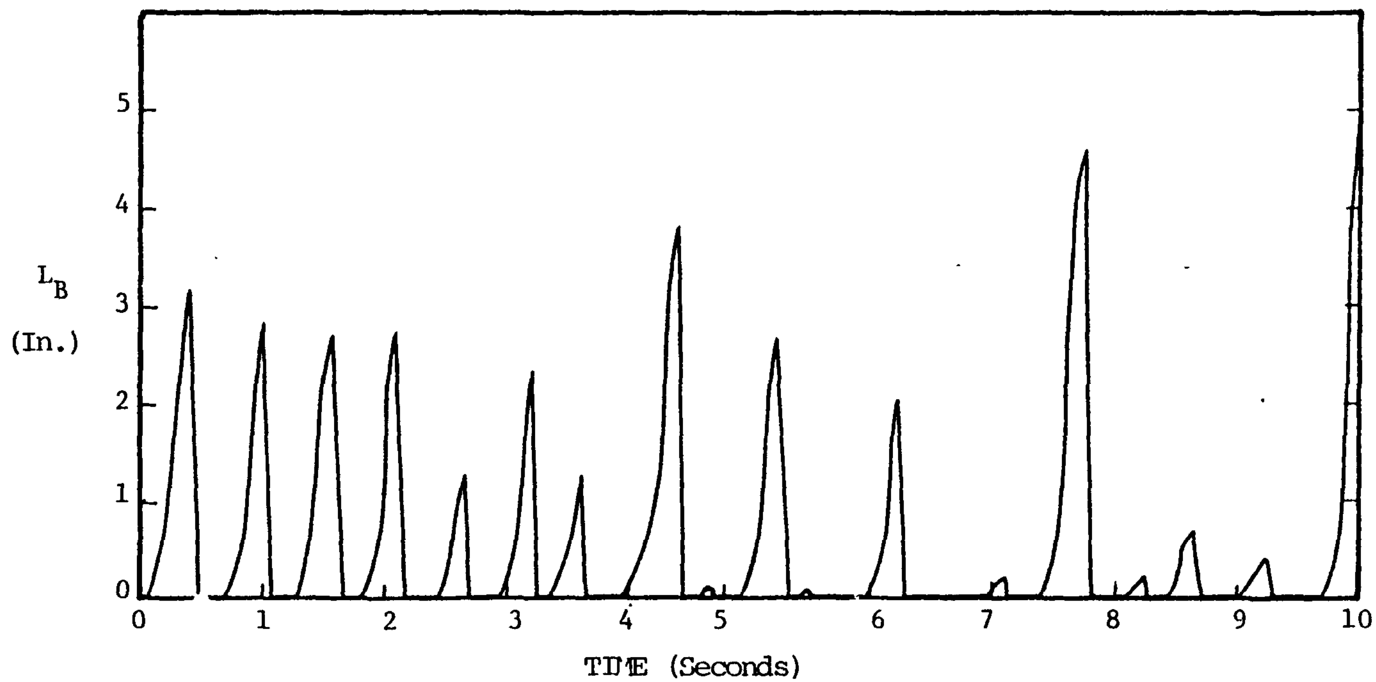

FIGURE 5.5 RESULTS OF TEST 6 - OSCILLATIONS IN BUBBLE LENGTH

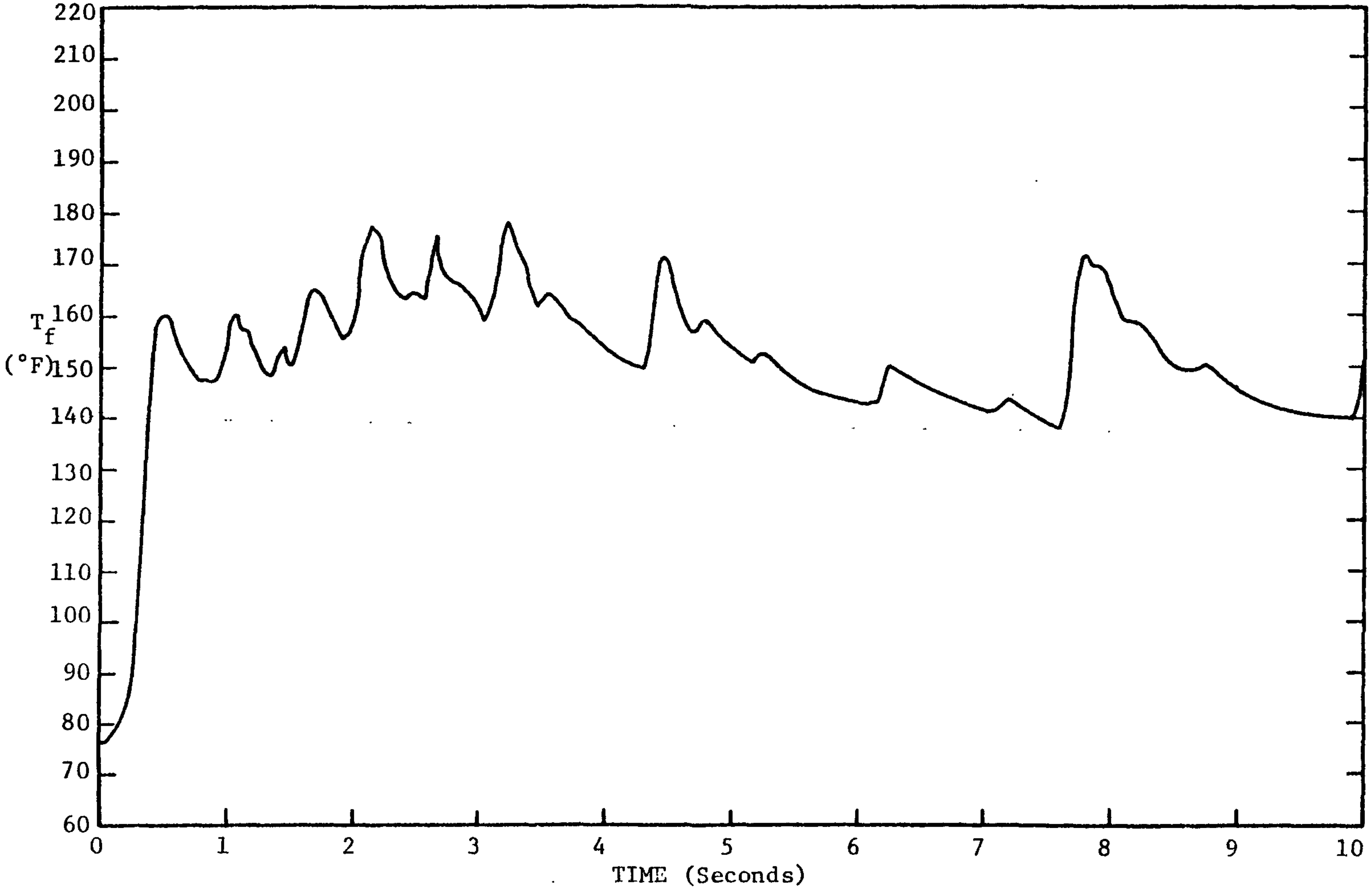

FIGURE 5.6 RESULTS OF TEST 6 - TEMPERATURE OF FIRST UNHEATED NODE

to be less of a waiting period in this test than in previous tests. With a low power and low temperature, this is perhaps the reverse of what would be expected. However, the low amplitudes of the oscillations in this case mean that less cold fluid is pulled down during bubble collapse to mix with the hot fluid at the top of the heater. Even though the power is low, this decreased mixing effect contributes to a short waiting period. The effect of the low upper zone temperature is seen primarily in the extremely fast bubble collapse times. In virtually every cycle, the collapse rate is quite rapid, creating the asymmetrical growth-collapse curve. One additional feature to note is the long temperature coastdown between about 5 and 7 seconds. This temperature decrease was very likely due to two effects. First, there was some loss of heat to the environment, and although those losses were generally quite small, this contributed to the cooling. Second, and more important is the fact that there was a dense, low temperature column of water sitting on top of a warmer, lower density region. During the waiting period, then, colder water diffused into the warmer zone, causing some cooling to occur. The effect of this was to increase the waiting period, as seen between about 6 and 7 seconds in Fig. 5.5.

5.1.1.5 Test 7

The power and unheated zone temperature for this test were both higher than their respective values in Test 6. It is perhaps in this run that the features of the flow behavior that have been discussed previously are most clearly seen. Figures 5.7 and 5.8 illustrate the bubble growth and temperature oscillations. In particular, the superposition of oscillatory patterns to create the "beating" seen in Tests 4, 5, and 6 is quite evident throughout the run. Not only does the beat pattern recur, but the beat frequency and average amplitude of the envelope each increase. This behavior is consistent with the higher power and temperature condition. The average frequency of the oscillation is slightly less than in Test 6, as is the waiting period between bubble growth cycle. In addition, the amplitudes of the oscillations, reflected by the maximum bubble lengths, are clearly larger.

5.1.1.6 Tests 8 and 9

The last two stagnant flow tests are presented in Figs. 5.9 through 5.12. In each case, the features discussed in the previous sections pertaining to bubble growth patterns, beating, and amplitudes and frequencies can be seen. The fact that each test essentially reproduces the same behavior, with changes attributable to slightly differ-

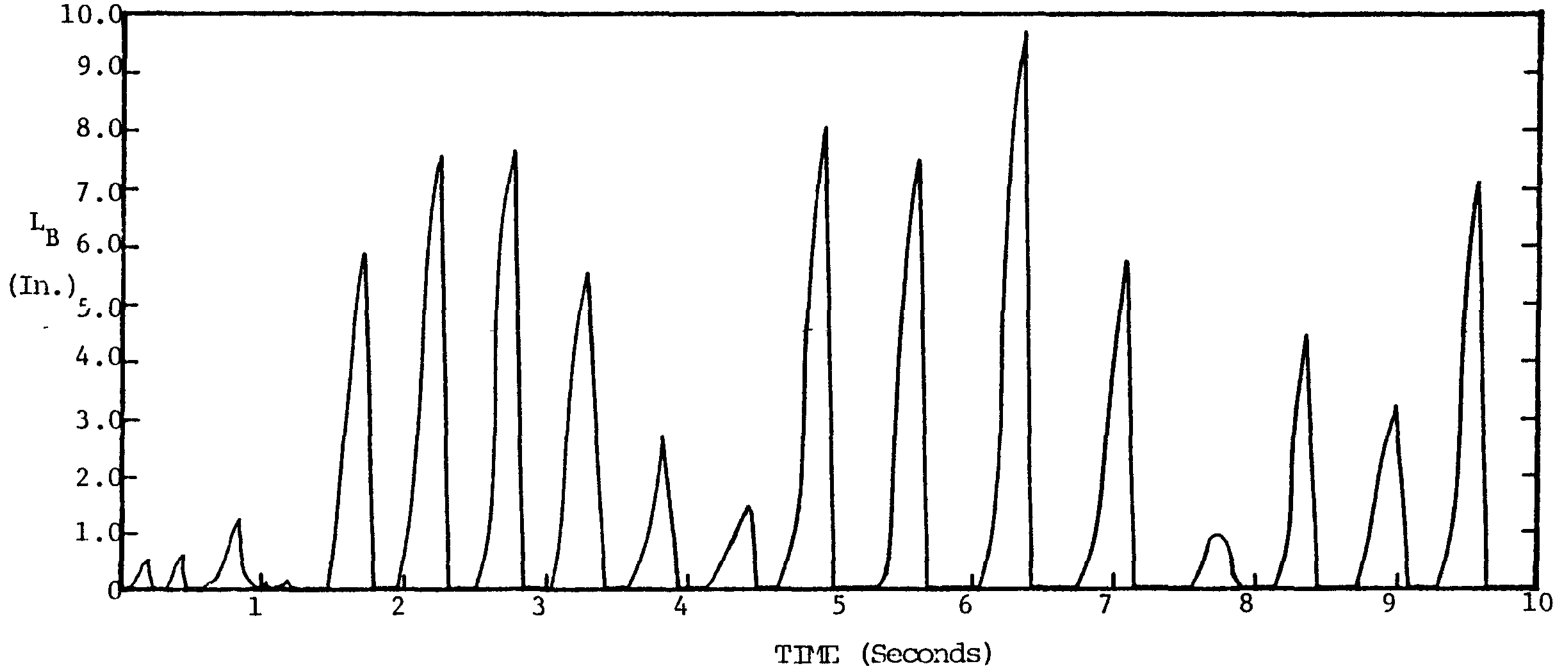

FIGURE 5.7 RESULTS OF TEST 7 - OSCILLATIONS IN BUBBLE LENGTH

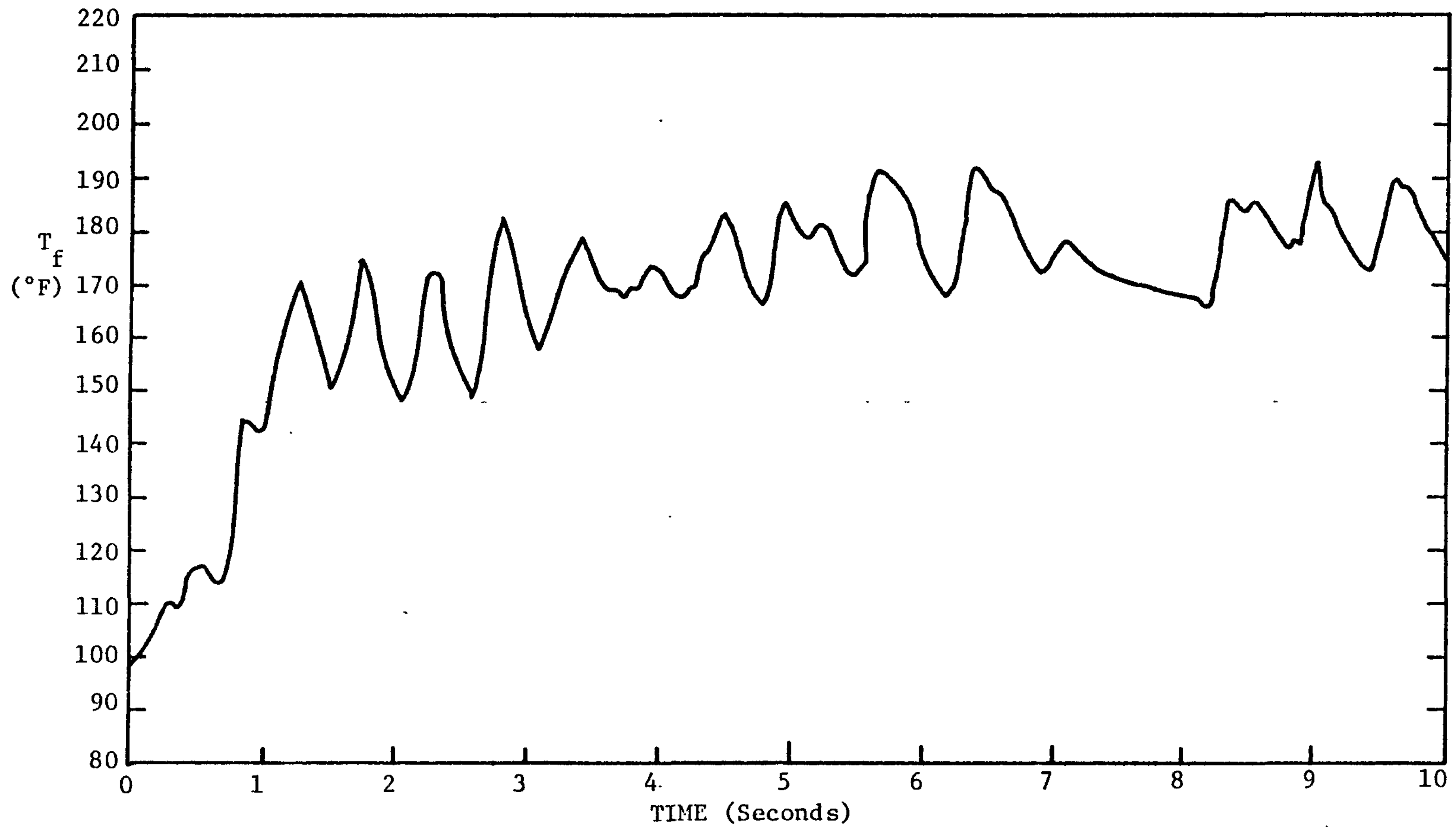

FIGURE 5.8 RESULTS OF TEST 7 - TEMPERATURE OF FIRST UNHEATED NODE

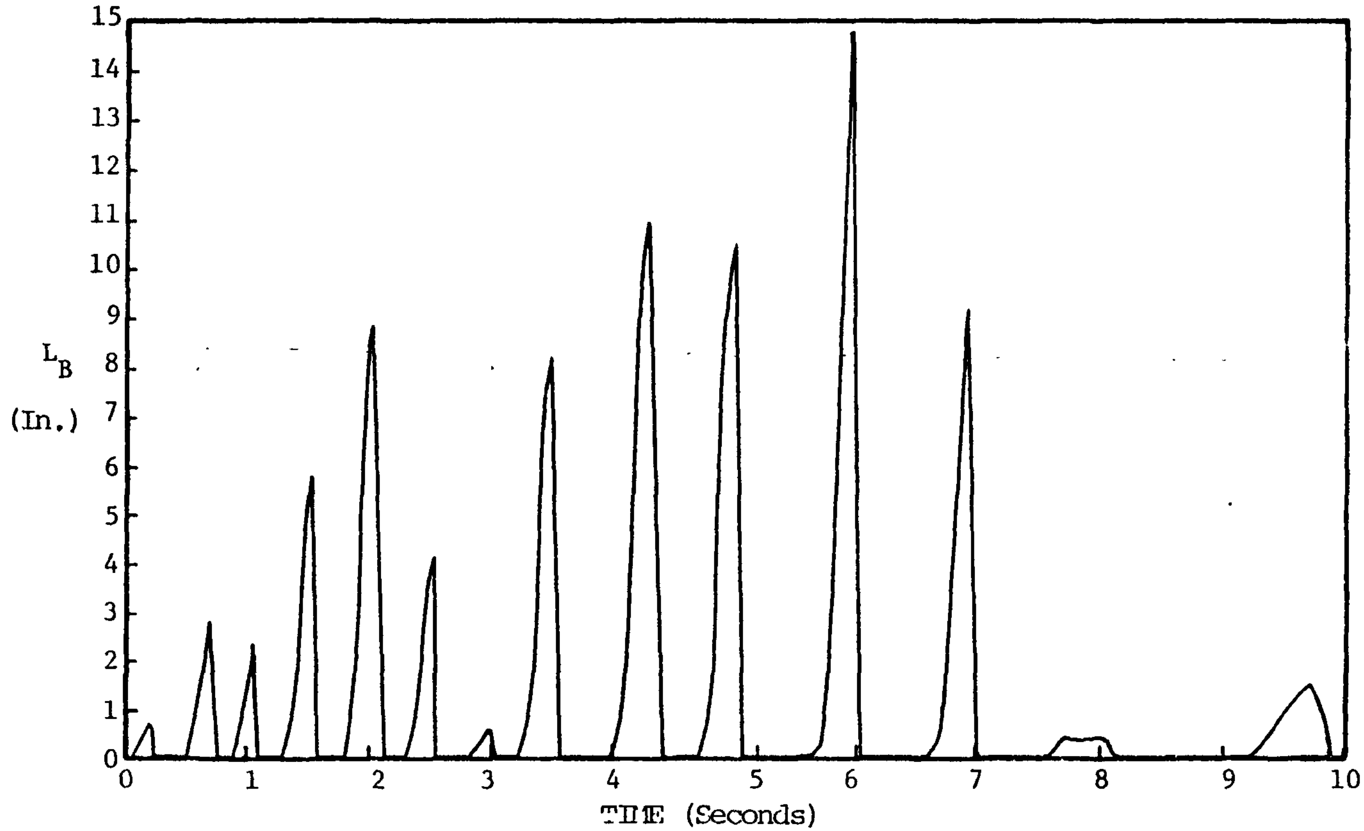

FIGURE 5.9 RESULTS OF TEST 8 - OSCILLATIONS IN BUBBLE LENGTH

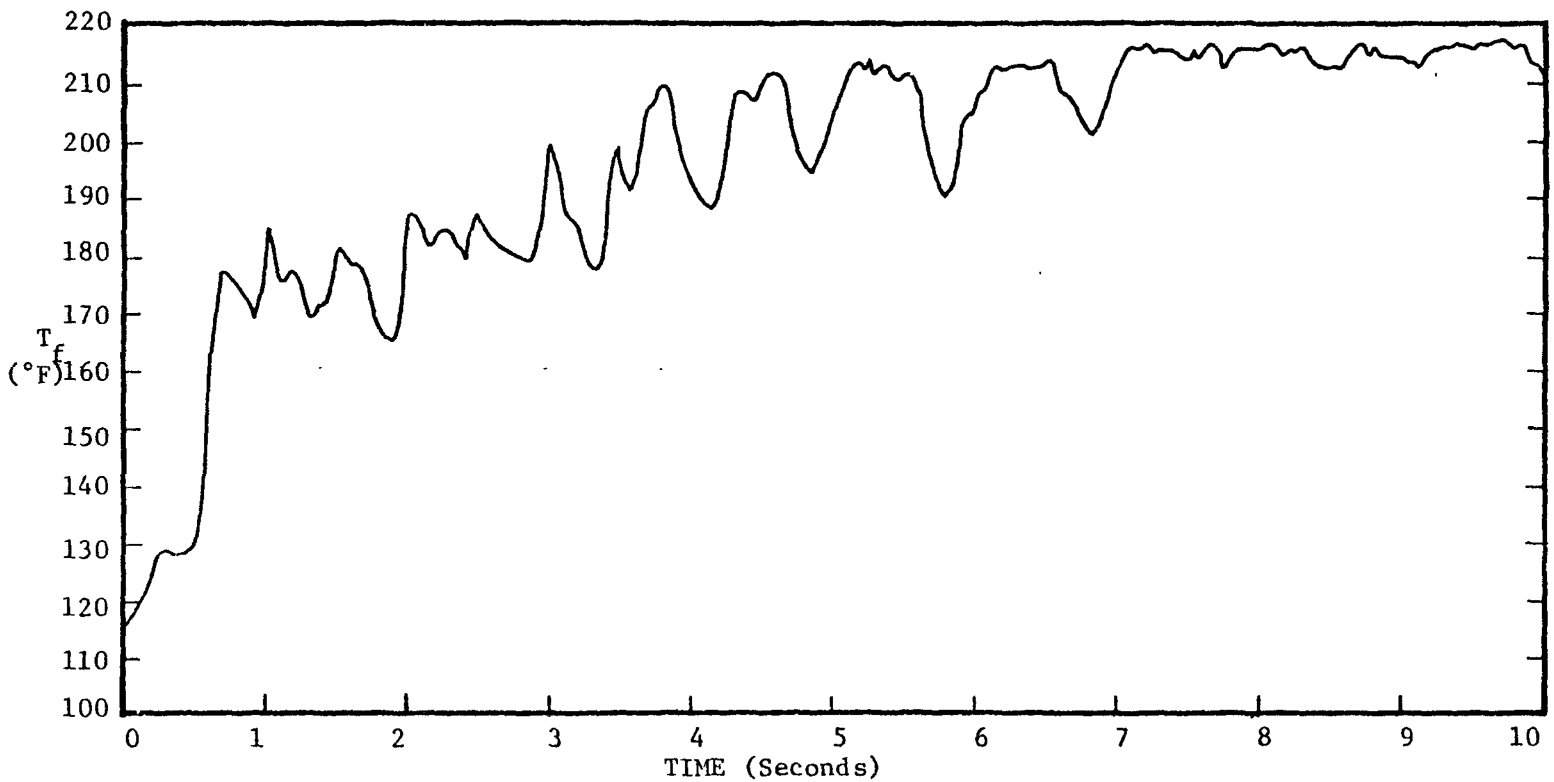

FIGURE 5.10 RESULTS OF TEST 8 - TEMPERATURE OF FIRST UNHEATED NODE

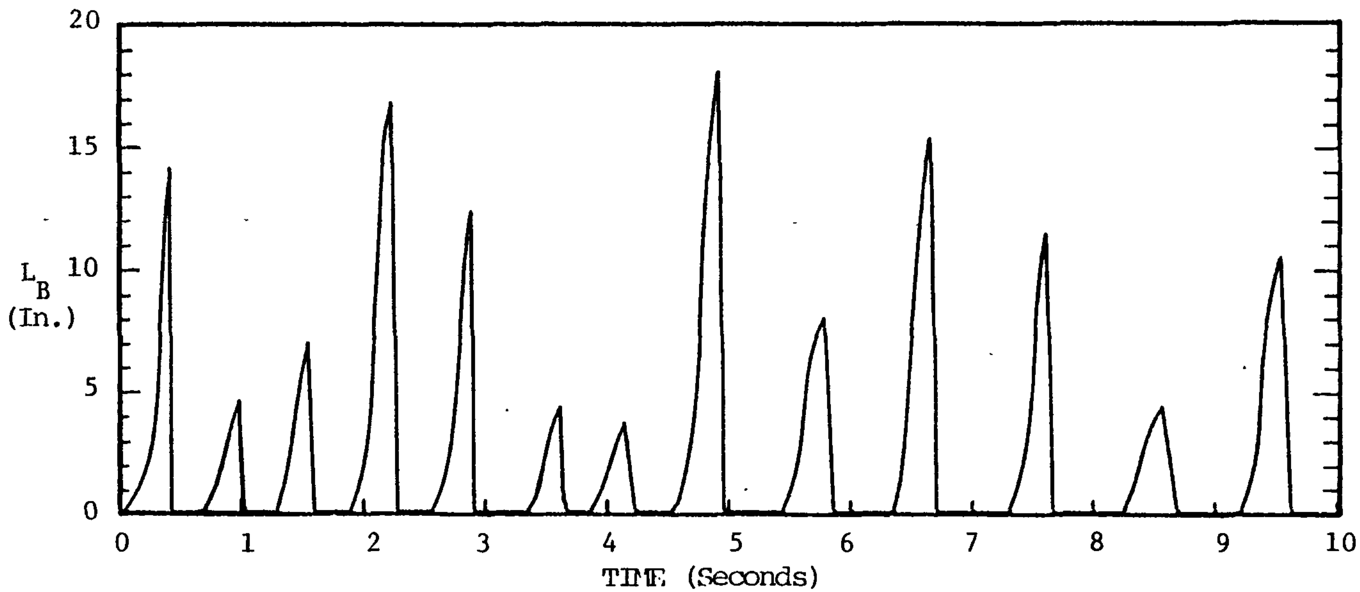

FIGURE 5.11 RESULTS OF TEST 9 - OSCILLATIONS IN BUBBLE LENGTH

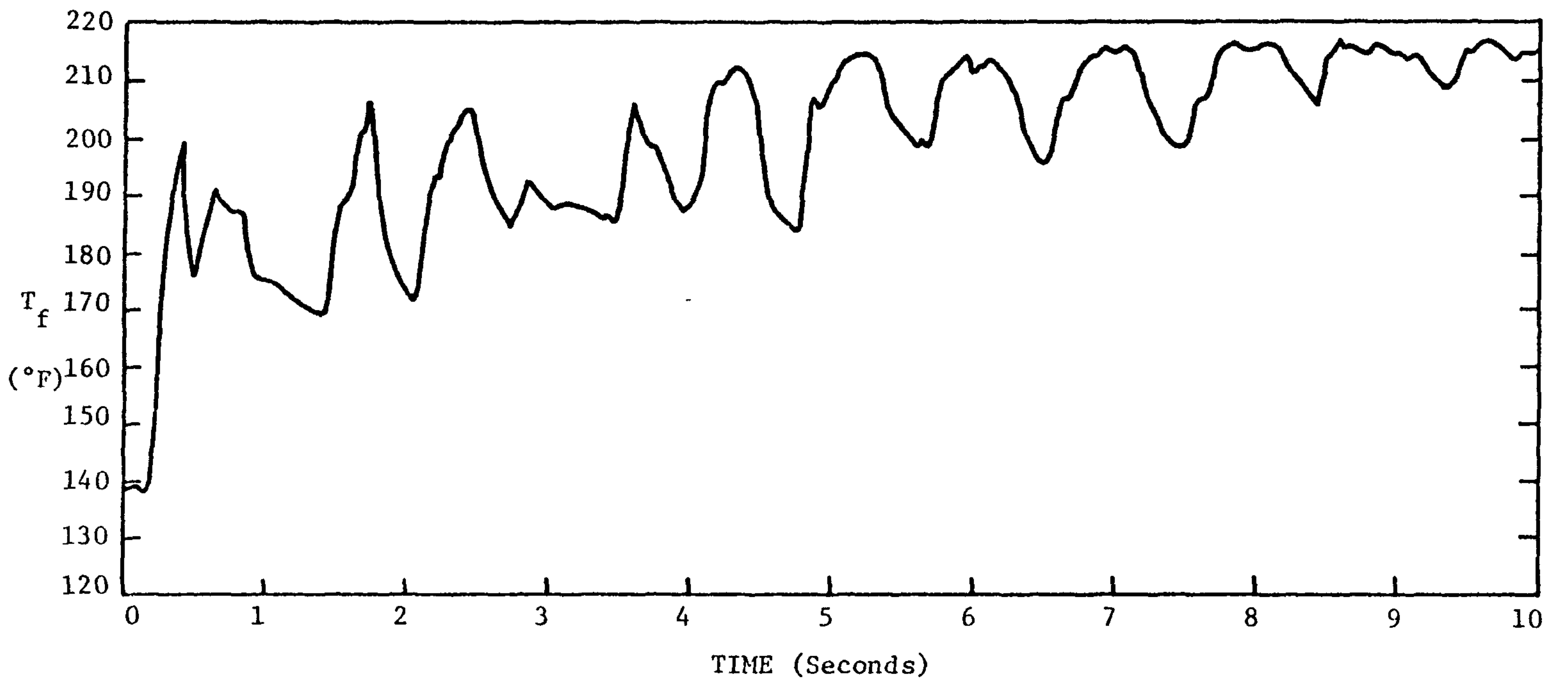

FIGURE 5.12 RESULTS OF TEST 9 - TEMPERATURE OF FIRST UNHEATED NODE

ing test conditions indicate that the same basic mechanisms are at work in creating the oscillatory flow behavior.

5.1.2 Forced Convection Testing

Only one experiment was performed with non-stagnant flow. The results of this experiment are presented in Fig. 5.13. Only the temperature downstream of the heater is shown for this run, due to the highly ambiguous bubble length results for this run. The reason for the ambiguous results will be discussed shortly.

The features discussed in relation to stagnant flow oscillatory behavior are largely absent in this test, and the reason for this is quite evident.

The test was carried out by opening the bypass valve and allowing the flow to coast down from approximately 10-15 feet per second to approximately 0.7 feet per second. However, during this time, the power was constant at a level of about 1.09 kilowatts. Under these conditions, the water in the unheated zone was able to heat up to a substantially higher temperature than was present in the stagnant flow tests. The result of this high temperature at bubble inception was to allow the growth of the vapor volume to such an extent that net condensation never exceeded net evaporation by enough to collapse the bubbles, and steady state forced convection two-phase flow eventually was

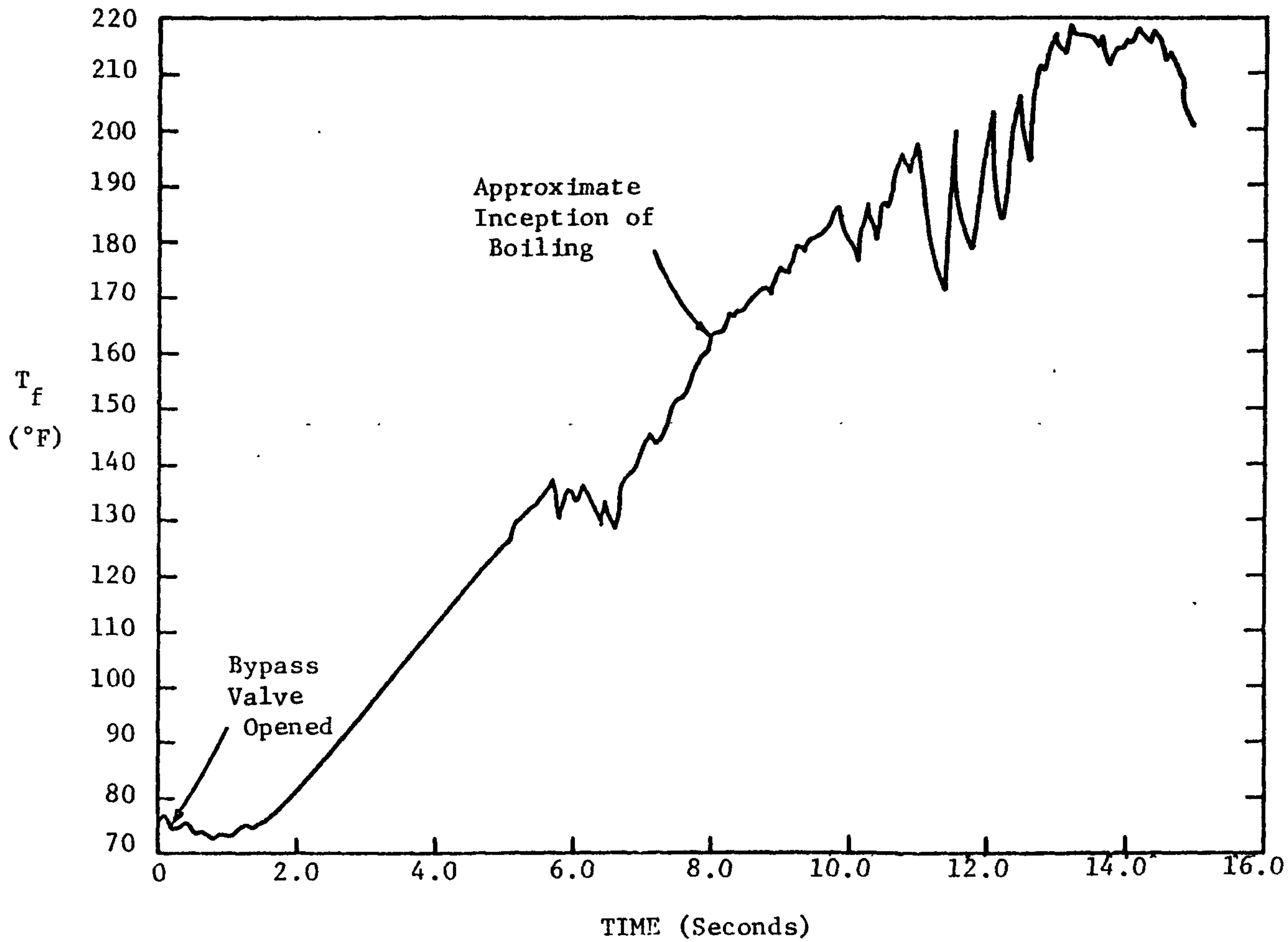

FIGURE 5.13 RESULTS OF FORCED CONVECTION TEST - TEMPERATURE OF FIRST UNHEATED NODE

established. This is the reason for the ambiguous bubble length readings after data reduction. Since no real flow oscillations occurred, except for the normal variations associated with "steady" two-phase flow, integration of the flow rate did not give dependable void readings. In any case, the vapor present was mainly in the form of small bubbles, not a single vapor slug. This fact in itself would indicate a different flow behavior than that present in the stagnant flow tests. It was believed that setting the power high enough to allow boiling inception before the establishment of high unheated zone temperatures might possibly lead to critical heat flux and subsequent damage to the test section. This was not desirable, and further forced convection tests were not conducted. There were also instrumentation problems associated with the forced convection tests, as well as the same sources of uncertainty as in the other tests. These will be discussed in the following section.

5.1.3 Sources of Error and Uncertainties in Experimental Tests

Several factors were present in the experiments that created, or had the potential to create, errors in the measurement of key parameters. These factors were different in the two different types of experiments, and will be examined separately.

5.1.3.1 Stagnant Flow Tests

The sources of uncertainty and error in the stagnant flow tests are connected mainly with two factors: the dissolved air in the water being used, and the water hammer effects mentioned in Section 5.1.1.

The presence of air on the water has been previously discussed. After becoming liberated from the water in boiling, some of the air formed bubbles which travelled upward through the remainder of the test section. As already noted, these bubbles rendered the flow rate readings from the upper differential pressure transducer virtually meaningless. However, not all of the air travelled up out of the test section. Some of it very likely remained mixed with the steam in the bubble. Upon bubble collapse due to condensation, the air would remain to cushion the oscillation. Some of the very low amplitude oscillations seen in the experimental results may indeed be the result of these air bubbles.

The effect of the water hammer pressure waves on the flow rate measurements has also been mentioned previously in Section 5.1.1.2. The extremely high artificial flow rates inferred from differential pressure measurements during these pressure waves certainly distorted the bubble length calculations. This effect also made it more difficult to calculate condensation heat transfer coefficients. It is also probable that the waiting period between bubble growth-collapse cycles is partially due to the decay of these pressure waves, although part of that period is undoubtedly genuine. One further possible effect of these waves involves the measurement of flow rates late in the course of the transients. In this case, though the waves generated by the water hammer do tend to decay rapidly, they also propagate throughout the test section, and would tend to reflect back and forth from the two plena. It is possible that, given enough growth-collapse cycles, as sufficient intensity could still remain to distort flow rate readings throughout the cycle, and not just at the beginning and end of the cycles. This may possible account for the behavior between about 7.5 and 9 seconds in Run 8 (Fig. 5.9), for example.

5.1.3.2 Forced Convection Testing

The uncertainties present in this test are largely due to an effect related to the water hammer pressure waves noted in the previous section. When the bypass valve was opened to permit the flow to coast down, severe pressure waves resulted from this flow disturbance. As a result, the flow rate readings inferred from the pressure transducers are quite unreliable during the first part of the transient.

5.1.3.3 Other Sources of Error

In both types of tests, there are sources of error related to the nature of the instruments themselves. The Validyne transducers proved to be extremely difficult to calibrate and to maintain in a zero-output condition at zero flow. This zero drift was compensated in both the calibration procedure and in the conversion program, but some uncertainties were still possible. The Tyco gauge pressure transducers functioned quite well, in general, and few uncertainties exist in the readings from these instruments. The thermocouples also functioned well, in general. However, thermocouples do have characteristic response times, and cannot record temperature changes instantaneously. The thermocouples in the fluid responded quite rapidly, and the readings were considered reliable. The thermocouples fastened onto the outside of the metal tube tended to respond much more slowly, due to the time constant of the tube itself, the time constant of the thermocouple, and the contact resistance of the thermcouple bead with the metal tube. The resultant response time of these thermocouples was somewhat less rapid, and the readings less reliable. Temperature changes related to the flow oscillations were not recorded by these thermocouples.

One final source of error was the data acquisition system itself. When the RTAS was tested, small offsets were found in the output of each channel. These offsets were subtracted from the instrument readings during data reduction, but there is no way of knowing if these offsets were truly constant during a run. In addition, the data acquisiton system error band as per manufacturer's specifications was on the order of 0.5%, full scale. This inherent error also contributed somewhat to experimental error.

5.1.4 Calculation of Condensation Heat Transfer Coefficient

Examination of the bubble growth-collapse patterns reveals an extremely asymmetrical behavior. Instead of a bubble collapse which parallels the growth curve, what is seen is a relatively long growth period, followed by a rapid collapse. This indicates a non-uniform heat transfer coefficient over the bubble growth-collapse cycle. In order to ascertain the nature of this non-uniformity, several calculations were performed to determine the condensation heat transfer coefficient.

Results of the calculations for various experiments are shown in Table 5.1. Details of the calculational method can be found in Appendix D.

Table 5.1 Example of Condensation Heat Transfer Coefficients

Test Number	Bubble Condition	Heat Transfer Coefficient (BTU/hr-ft^2°F)	hA (BTU/hr°F)
4	Growth	168.5	6.71
	Collapse	3167.1	62.71
5	Growth	325.7	10.91
	Collapse	4456.3	180.03
6	Growth	25.0	0.19
	Collapse	192.0	2.88
7	Growth	102.4	0.36
	Collapse	871.2	25.53
8	Growth	102.2	1.62
	Collapse	3587.2	100.80
9	Growth	109.9	2.86
	Collapse	3457.5	67.08

The most interesting aspect of the results is the extremely large magnitude of the heat transfer coefficient during bubble collapse. The reason for this behavior involves another type of flow instability. When a vapor accelerates into a liquid medium, small waves may form at the liquid-vapor interface. This is due to Taylor instabilities. The waves may then break up into small droplets of liquid, creating a mist-flow regime at the very end of the bubble. This type of behavior was documented by Ford (3) in his Freon experiments. Since the heat transfer coefficient shown is based on an area which does not account for any such mechanisms, the result is a coefficient which is quite large. The important parameter is the product of the heat transfer coefficient and the heat transfer area, and this is also shown in Table 5.1. This product represents the heat removal rate ($q/\Delta T$). The calculational method employed, to determine the heat removal contains some assumptions, as presented in Appendix D, which might tend to distort, the actual numbers; however, the way in which the condensation changes over the period of the bubble growth-collapse cycle is indisputable.

The fact that the heat transfer coefficient effects the oscillatory behavior of the system implies that a circular situation exists; that is, that the system behavior in turn affects the heat transfer coefficient. The more violent the oscillation, the greater the acceleration of vapor into fluid, and the more extensive the fluid misting effect becomes. This is one reason for the behavior noted in Test 6 - the oscillation amplitude was so small and vapor generation reasonably slow, that the heat transfer coefficient did not have a chance to increase to the same magnitude as in the higher-power experiments.

Although it is qualitatively clear what is happening to the heat transfer coefficient in this type of flow, quantifying the behavior mechanistically is more difficult, and was not conceived as part of this work. Further discussion of this point can be found in Chapter 6.

5.1.5 Comparison of Water Data to Sodium Data

Although the Sodium Boiling Test Facility was not able to operate in a mode precisely comparable to the WTL, is is interesting to compare the results of the water experiments to LOPI experiments carried out in the THORS facility at ORNL. It should be noted that the THORS facility is a multipin bundle, in which two-dimensional effects may be important. However, examination of the results of one of the LOPI tests reveals some interesting parallels.

Figure 5.14 shows the results from THORS test 71H-101. Note that the parameter plotted is flow rate

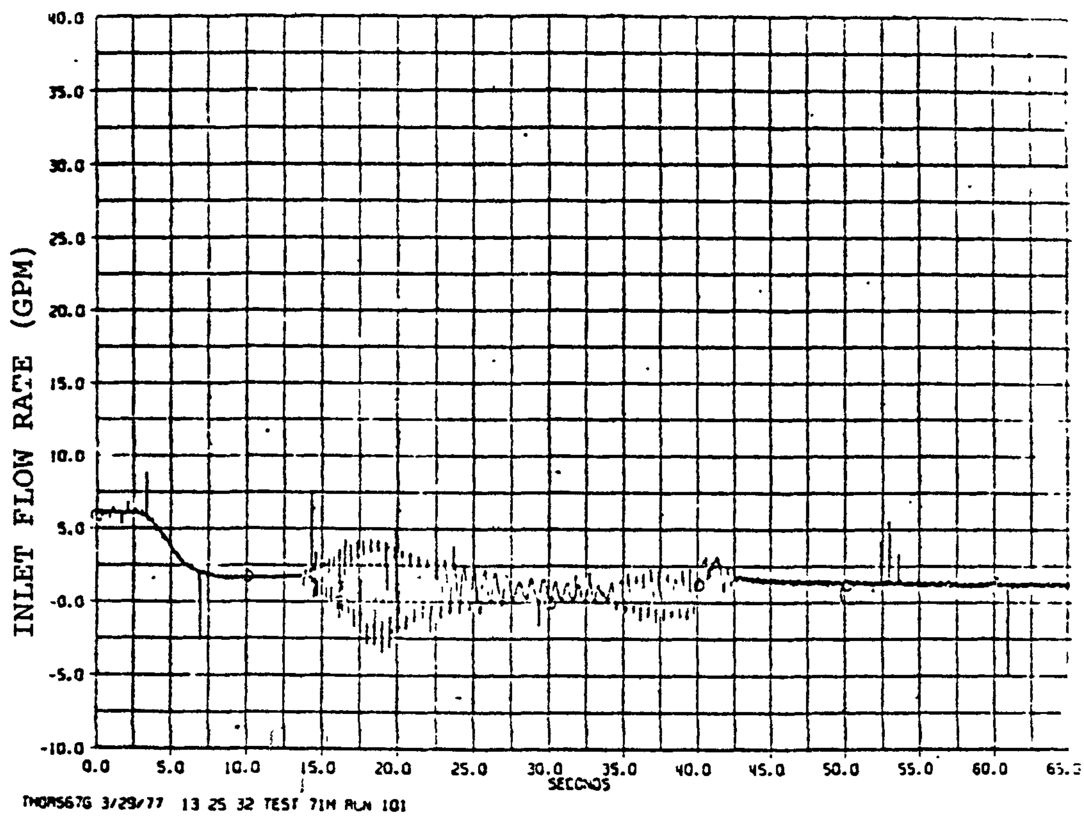

FIGURE 5.14 EXAMPLE OF THORS RESULTS - VOLUMETRIC FLOW OSCILLATIONS

versus time; however, since the flow oscillates about the zero-flow point, it is clear that the integration of the curve to show the bubble length would show the same characteristics. The most outstanding point is the beat pattern that appears during the course of the oscillation cycle. This characteristic is quite similar to the pattern seen in several of the water tests. In addition, there is a change in flow oscillation frequency over the transient, which again parallels the water results.

One other area in which a comparison between water and sodium tests can be drawn is the subject of noncondensable gases. Mention has already been made about some of the effects on dissolved air in the water. It must be noted that in a sodium system, inert gas blankets are used to preclude the potentially dangerous contact of sodium and oxygen. As a result, these gases become dissolved in the sodium, and can behave in much the same manner as air in water. Sodium systems cannot be examined visually during experimentation, of course, to determine the presence of inert gas in the sodium vapor; however, the presence of noncondensables in water experiments should not be considered as a non-prototypic parameter.

5.2 Analytical Results

The results of computer simulations of the stagnant flow tests are presented in Fig. 5.15 through 5.33. The features of the simulations themselves will be discussed in the next section. Comparison of analytical results to those obtained experimentally will be discussed in the Section 5.2.2.

5.2.1 Features of Analytical Simulations

The information obtained from a computer run includes data on flow rates, bubble pressures, areas, and bubble lengths and volumes. An example of the actual output from the computer is presented in Appendix E. There exists, as part of the program, a subroutine which picks specific pieces of information and plots them, using a library plotting routine. Examples of these plots are presented in Figs. 5.15 through 5.18. The conditions for this run correspond to those shown in the output in Appendix E.

Some of the features to be noted in the plots include the rapid oscillation of all variables plotted as the bubble flows and collapses. Note also, the slight delay between oscillatory cycles and the asymmetric pattern of the growth-collapse cycle.

Figures 5.19 through 5.21 present a slightly different perspective. In these plots, the bubble length within the heater is shown. The conditions for these runs correspond to some of the stagnant-flow test conditions.

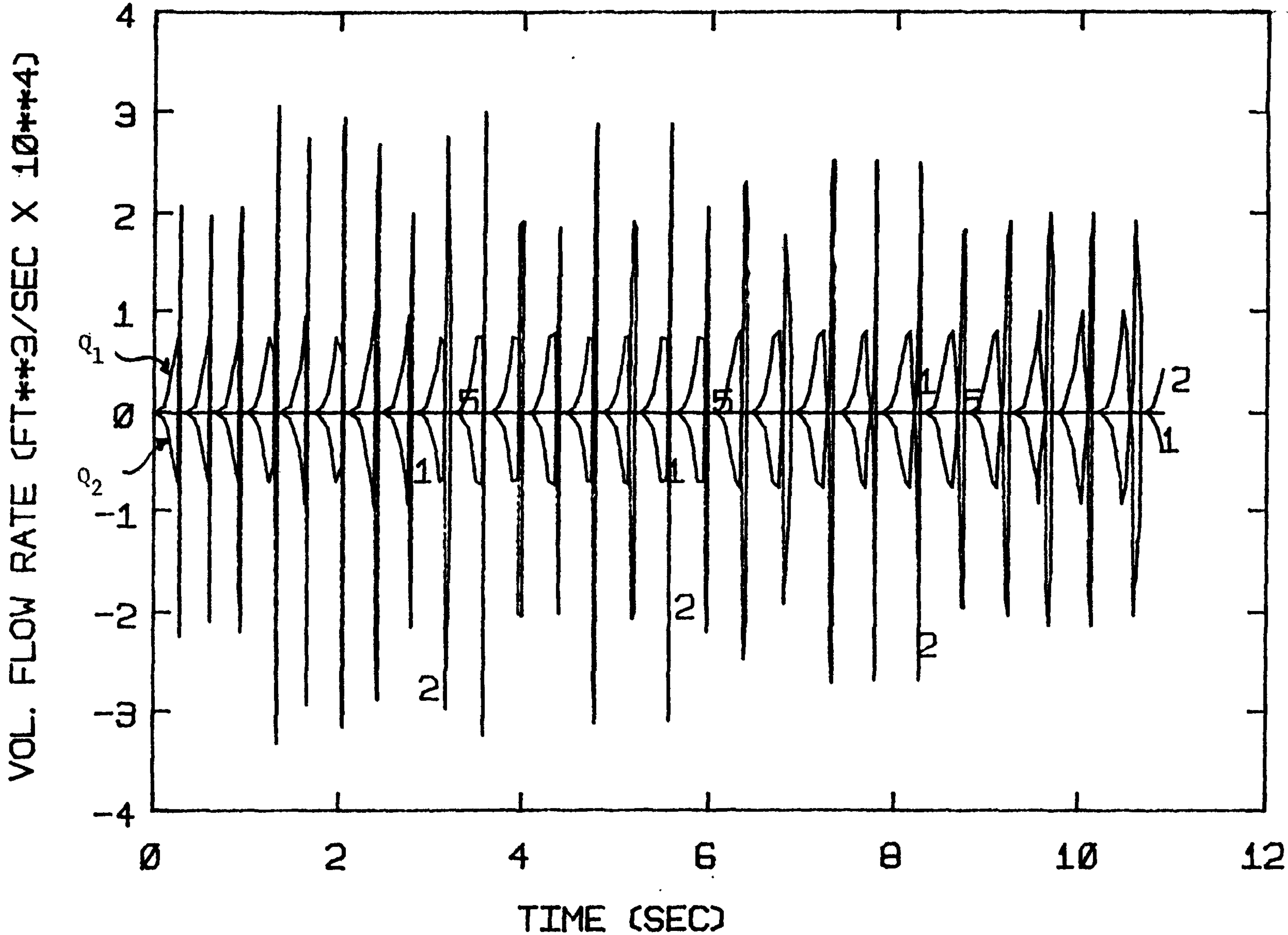

FIGURE 5.15 COMPUTER GENERATED PLOT - SIMULATION OF TEST 9: VOLUMETRIC FLOW RATES IN LEGS 1 AND 2

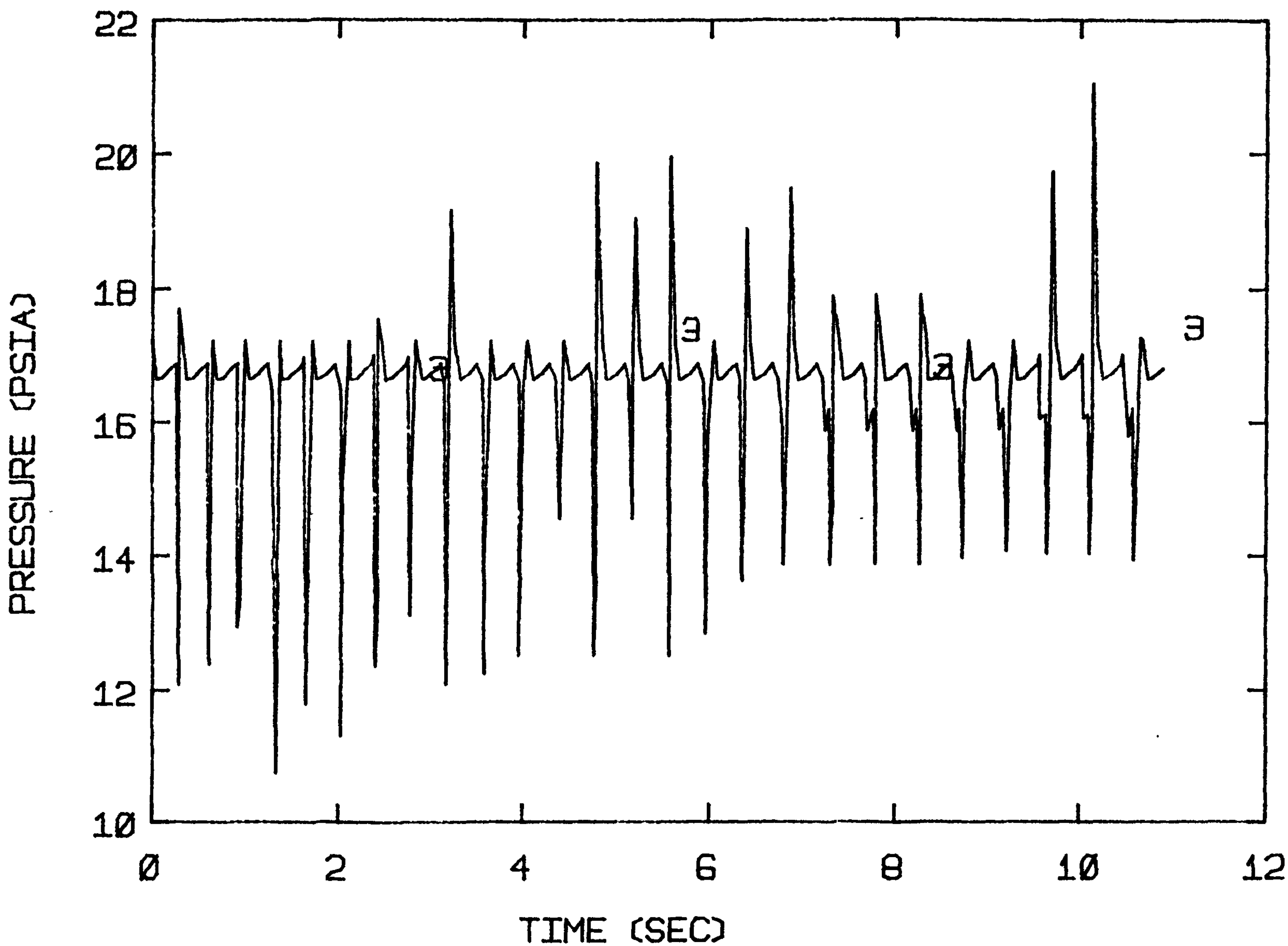

FIGURE 5.16 COMPUTER GENERATED PLOT - SIMULATION OF TEST 9: BUBBLE PRESSURE

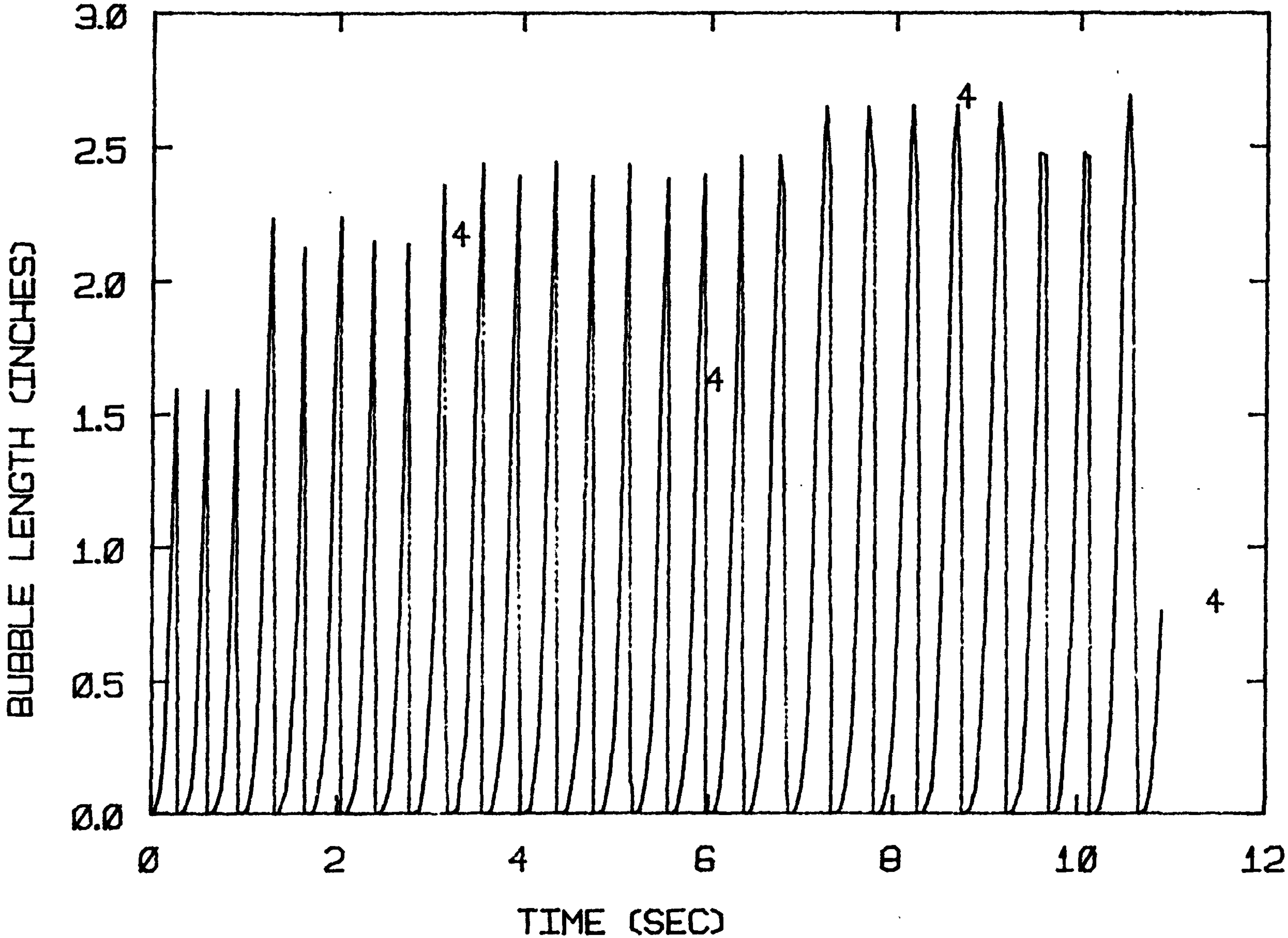

FIGURE 5.17 COMPUTER GENERATED PLOT - SIMULATION OF TEST 9: TOTAL BUBBLE LENGTH

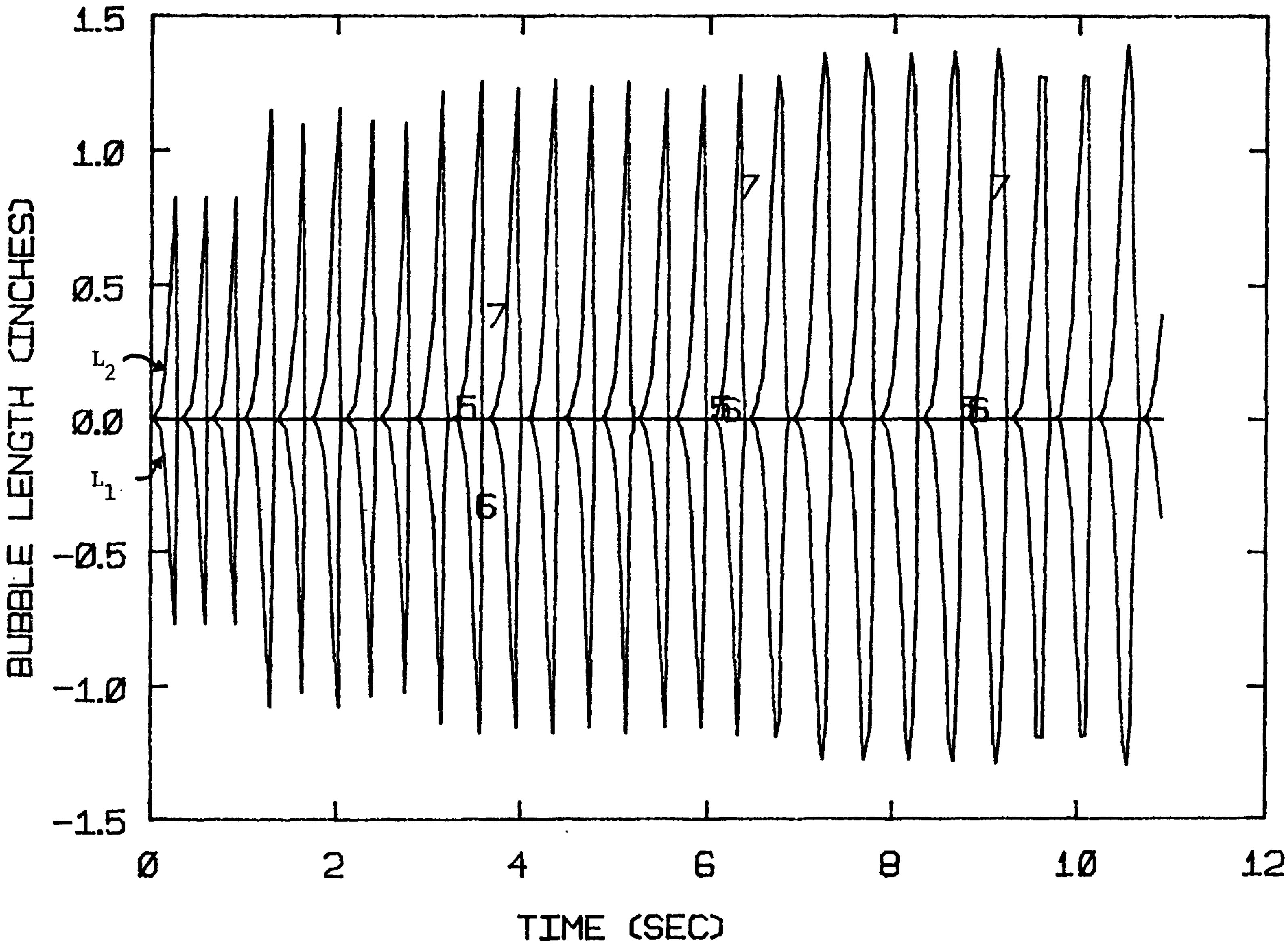

FIGURE 5.18 COMPUTER GENERATED PLOT - SIMULATION OF TEST 9: BUBBLE LENGTHS IN LEGS 1 AND 2.

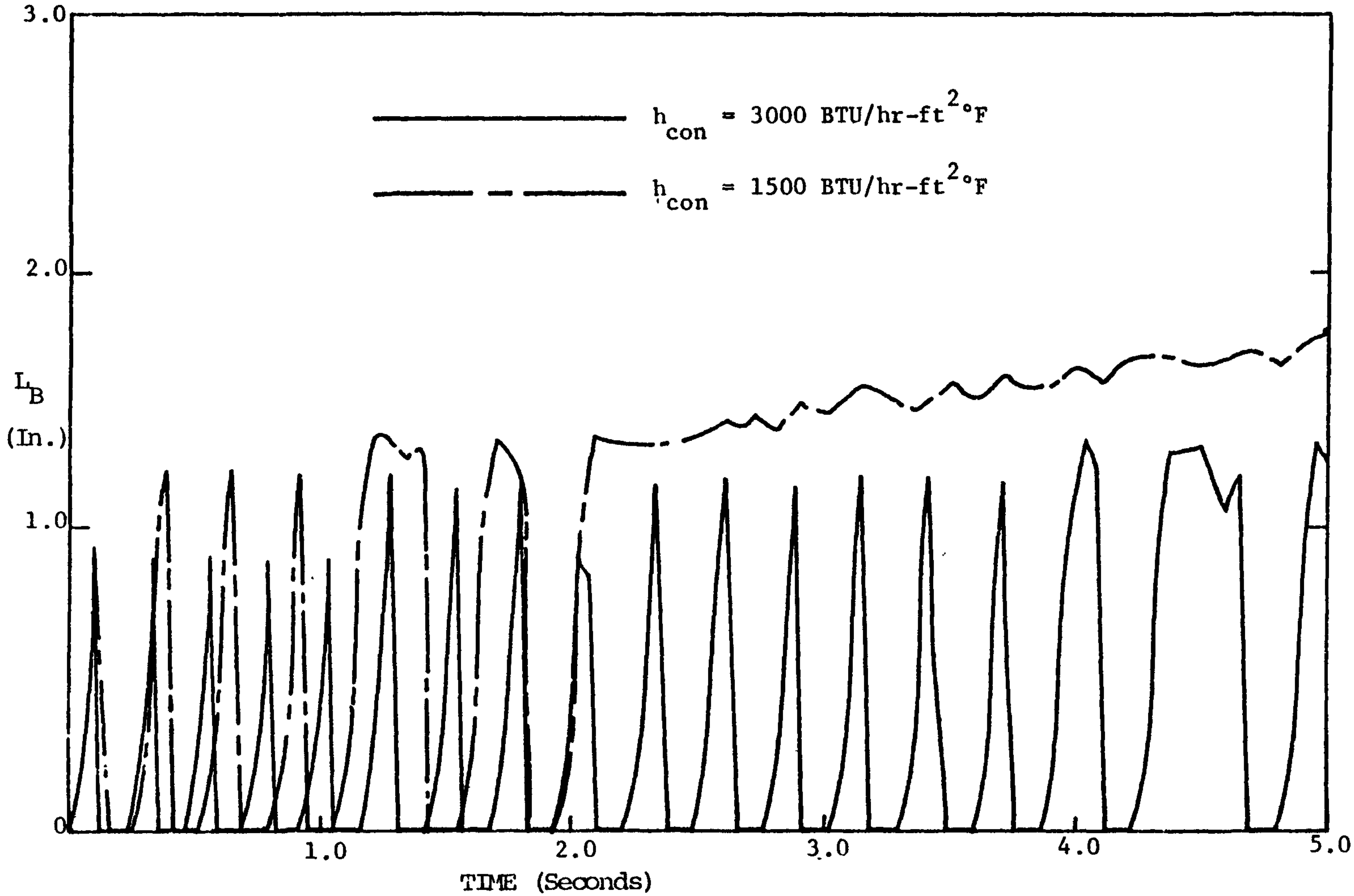

FIGURE 5.19 COMPARISON OF ANALYTICAL RESULTS FOR DIFFERENT HEAT TRANSFER COEFFICIENTS - TEST 4 CONDITIONS

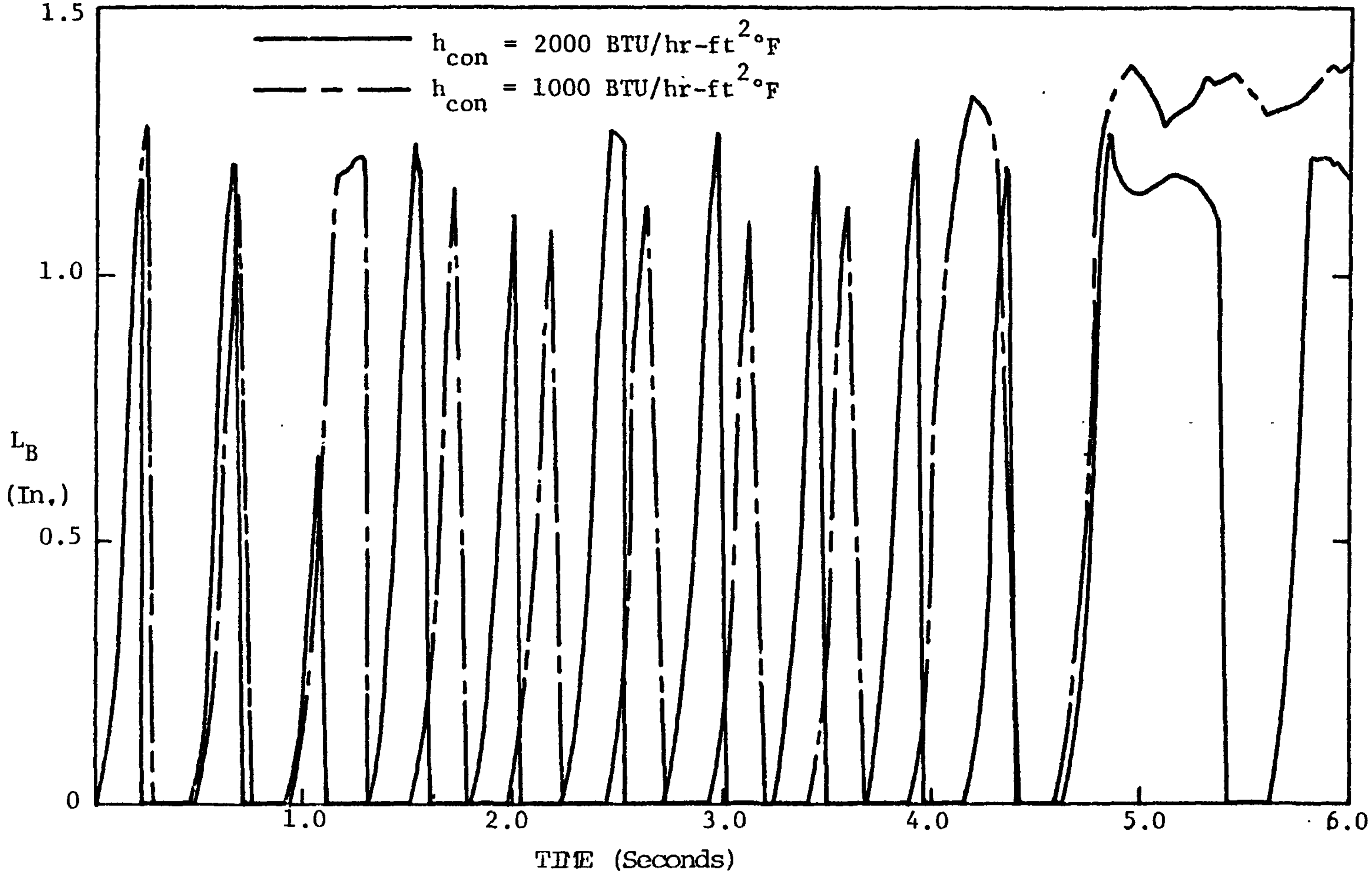

FIGURE 5.20 COMPARISON OF ANALYTICAL RESULTS FOR DIFFERENT HEAT TRANSFER COEFFICIENTS - TEST 6 CONDITIONS

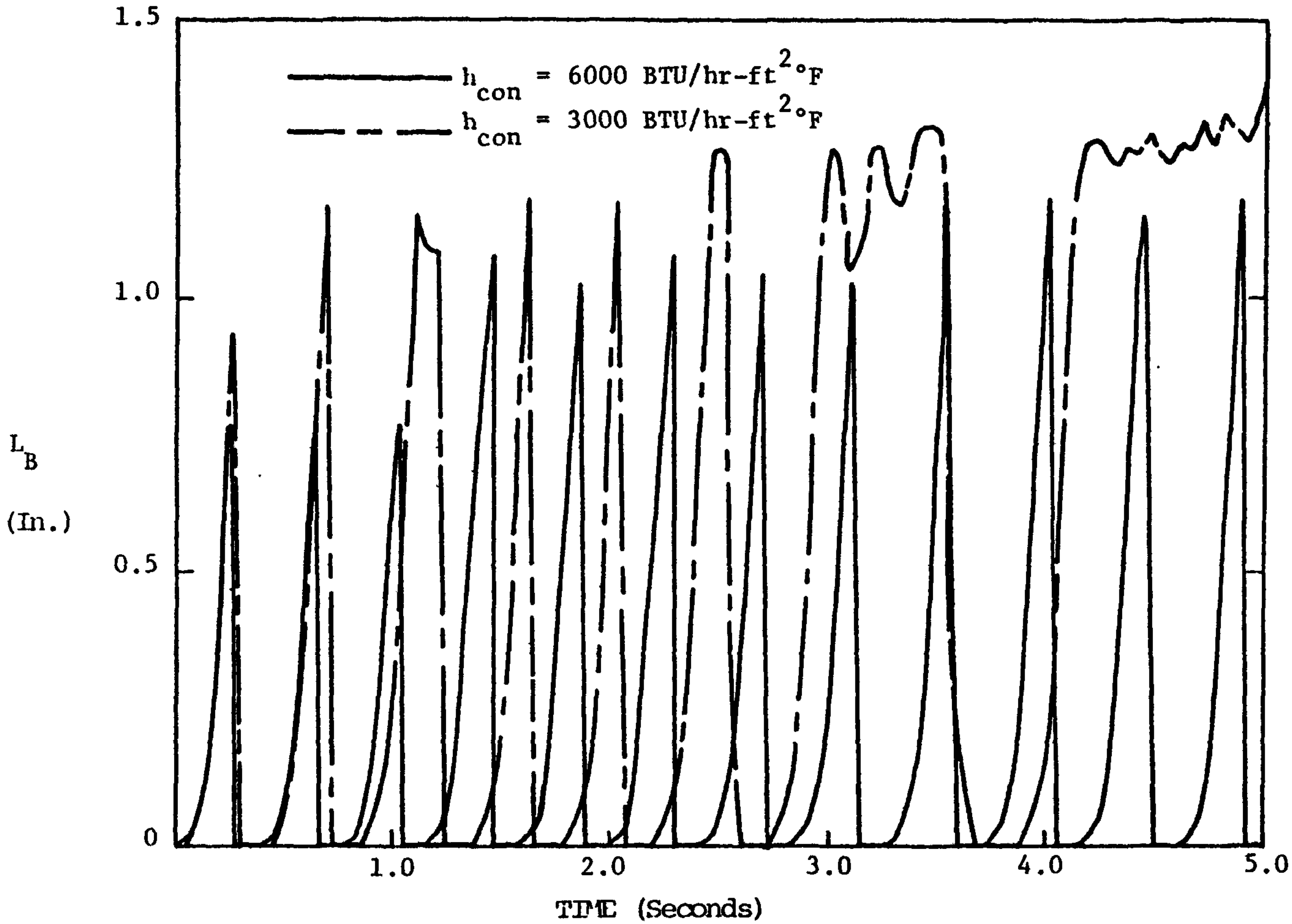

FIGURE 5.21 COMPARISON OF ANALYTICAL RESULTS FOR DIFFERENT HEAT TRANSFER COEFFICIENTS - TEST 9 CONDITIONS

However, the condensation heat transfer coefficient has been varied so as to provide a comparison between the results for different heat removal rates.

It is not surprising that, when a high heat transfer coefficient is used, the cycle period is slightly smaller, and the amplitude of the cycle is considerably smaller. This is due largely to the manner in which the code is currently set up.

When the temperature nodal pattern is input to the code, the first node is normally made quite small - on the order of an inch - and the temperature therein is set at saturation. This permits no condensation to occur in that node. This is done for two reasons. First, from a physical standpoint, some hot fluid must flow into the unheated zone before the inception of boiling, due to natural circulation. The resistance of the stalled pump during the stagnant flow tests, however, made the natural circulation flow rate quite small. Therefore, this relatively small volume of fluid was used as a saturated length. This "zone of no condensation" permits growth of the bubble at the start of the cycle. In addition, the heat transfer coefficient, when input as a constant, as was done in these runs, must be set very high, to correspond to the large heat removal rate attained during bubble collapse. The small initial saturated node provides a de facto variation in condensation heat transfer coefficient. More preferable, of course, would be a mechanistic model of the variation of the heat transfer coefficient during the cycle. However, such a model does not presently exist.

The choice of the length of the saturated node and the condensation heat transfer coefficient together provides a "dial" which the user may adjust. The combination of these two parameters, along with the temperature profile chosen for the unheated zone, legislates, for all intents and purposes, the length of the bubble during the transient. Changes in the temperature profile by virtue of the heat input to or output from the unheated zone during the transient also provide some change in the cycle period and amplitude, and this, too, is demonstrated in all of the figures.

The variation of the heat transfer coefficient during the cycle in the simulations is correct in a broad sense - low at the beginning and high at the peak, and it was felt that trying to vary either the temperature profile or the heat transfer coefficient without some mechanistic base would cause more difficulties than it would solve. The results of this decision are discussed in the next section.

5.2.2 Comparison of Analytical and Experimental Test Results

The parameter which is best suited for comparison between the experimental tests and analytical simulations is the bubble length with the heater. This is true for a combination of reasons. First and foremost, this bubble length is the most reliable nonthermal datum that can be derived from the experimental results. The experimentally determined flow rates were subject to effects that do not show up analytically (non-condensables, "water hammer", etc.). Second, this parameter illustrates quite clearly the frequency, amplitude, and asymmetrical behavior of the oscillations.

The bubble length within the heater is plotted, therefore, in Figs. 5.22 through 5.27, for each stagnant flow test and its corresponding computer simulation. The simulations plotted here correspond to the high heat transfer coefficient runs, examples of which were shown and explained in Section 5.2.1. One small change has been made, however: the waiting period between oscillations has been adjusted in the analytical results to agree with that determined experimentally. Therefore, what is shown is actually a cycle-by-cycle comparison of the results.

The reason for the adjustment involves the method

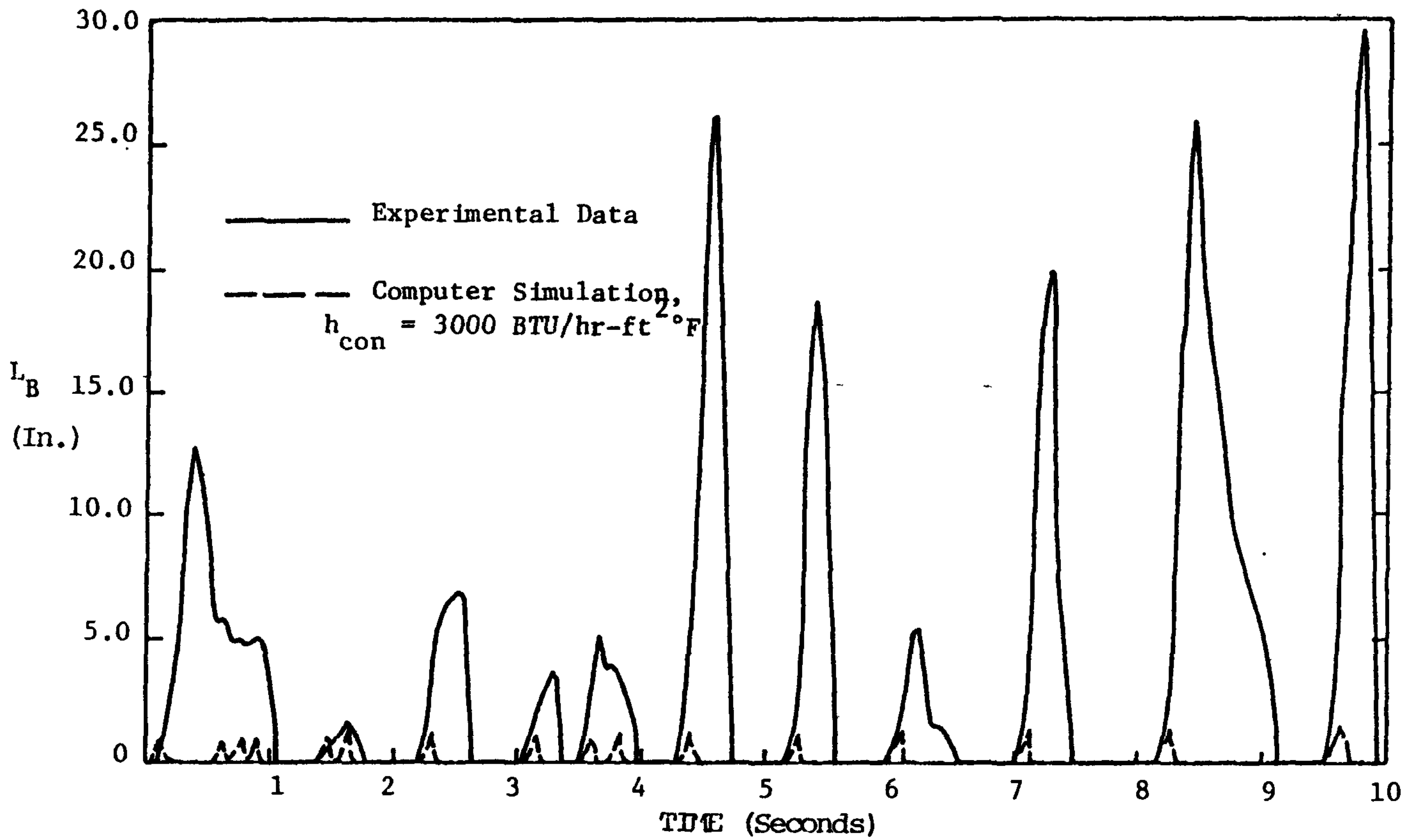

FIGURE 5.22 ANALYTICAL VS. EXPERIMENTAL RESULTS - TEST 4: BUBBLE LENGTH

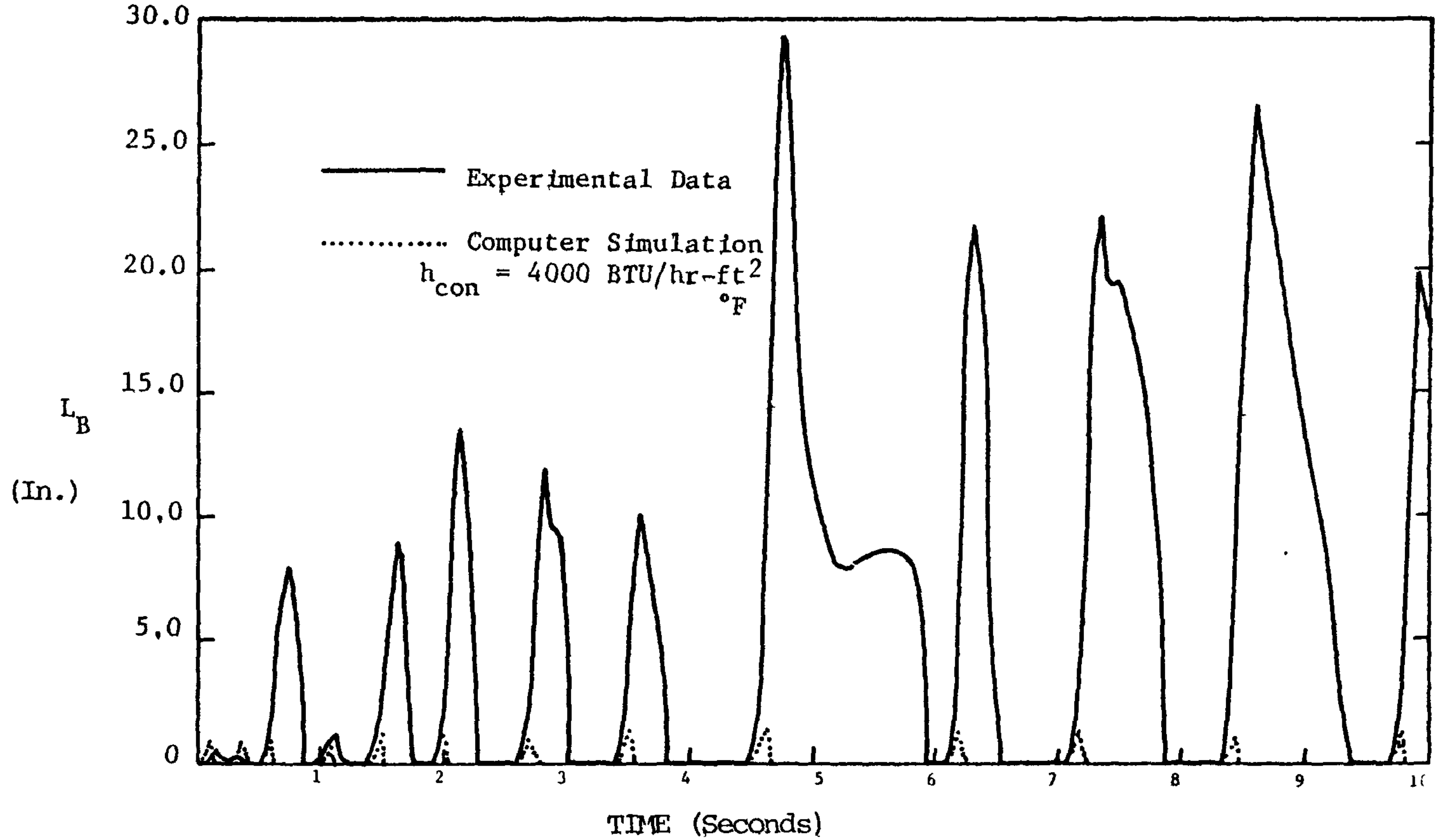

FIGURE 5.23 ANALYTICAL VS. EXPERIMENTAL RESULTS - TEST 5; BUBBLE LENGTH

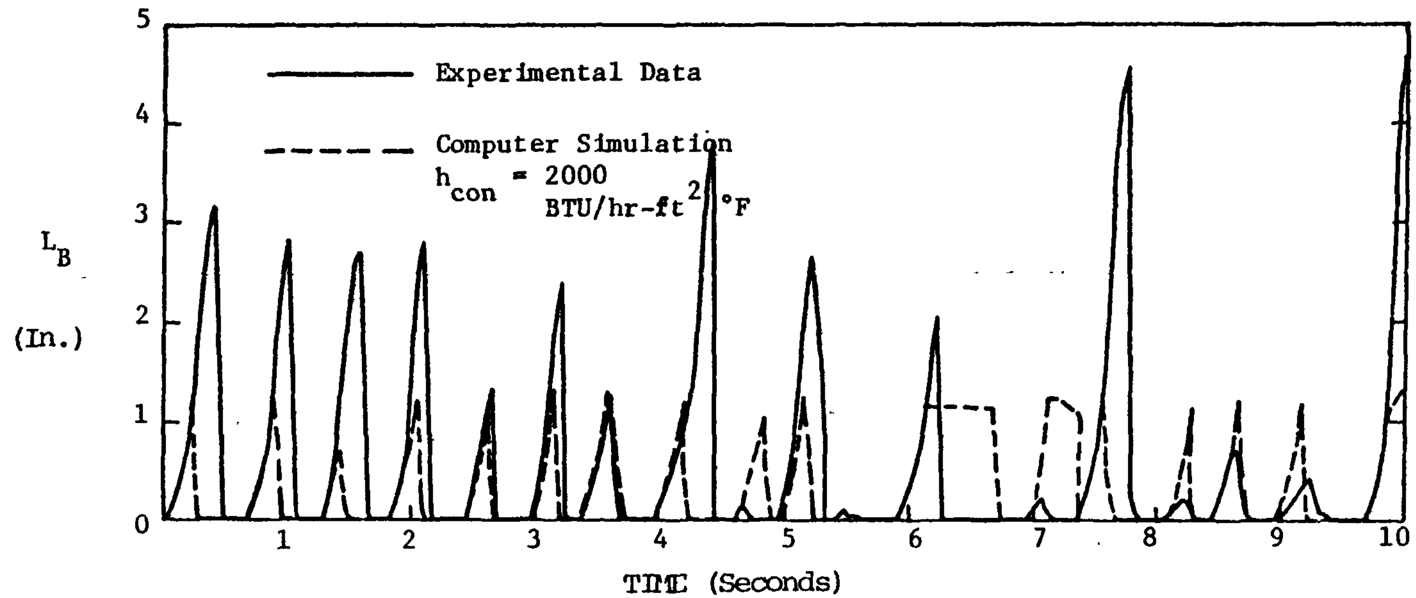

FIGURE 5.24 ANALYTICAL VS. EXPERIMENTAL RESULTS - TEST 6: BUBBLE LENGTH

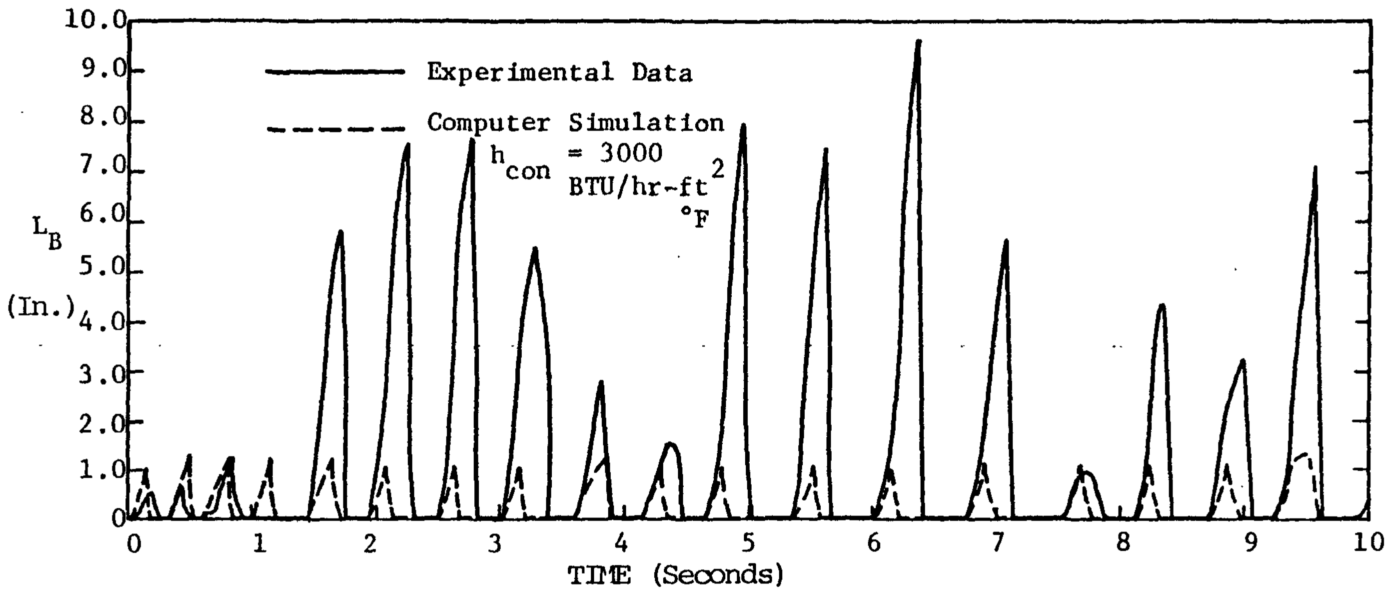

FIGURE 5.25 ANALYTICAL VS. EXPERIMENTAL RESULTS - TEST 7: BUBBLE LENGTH

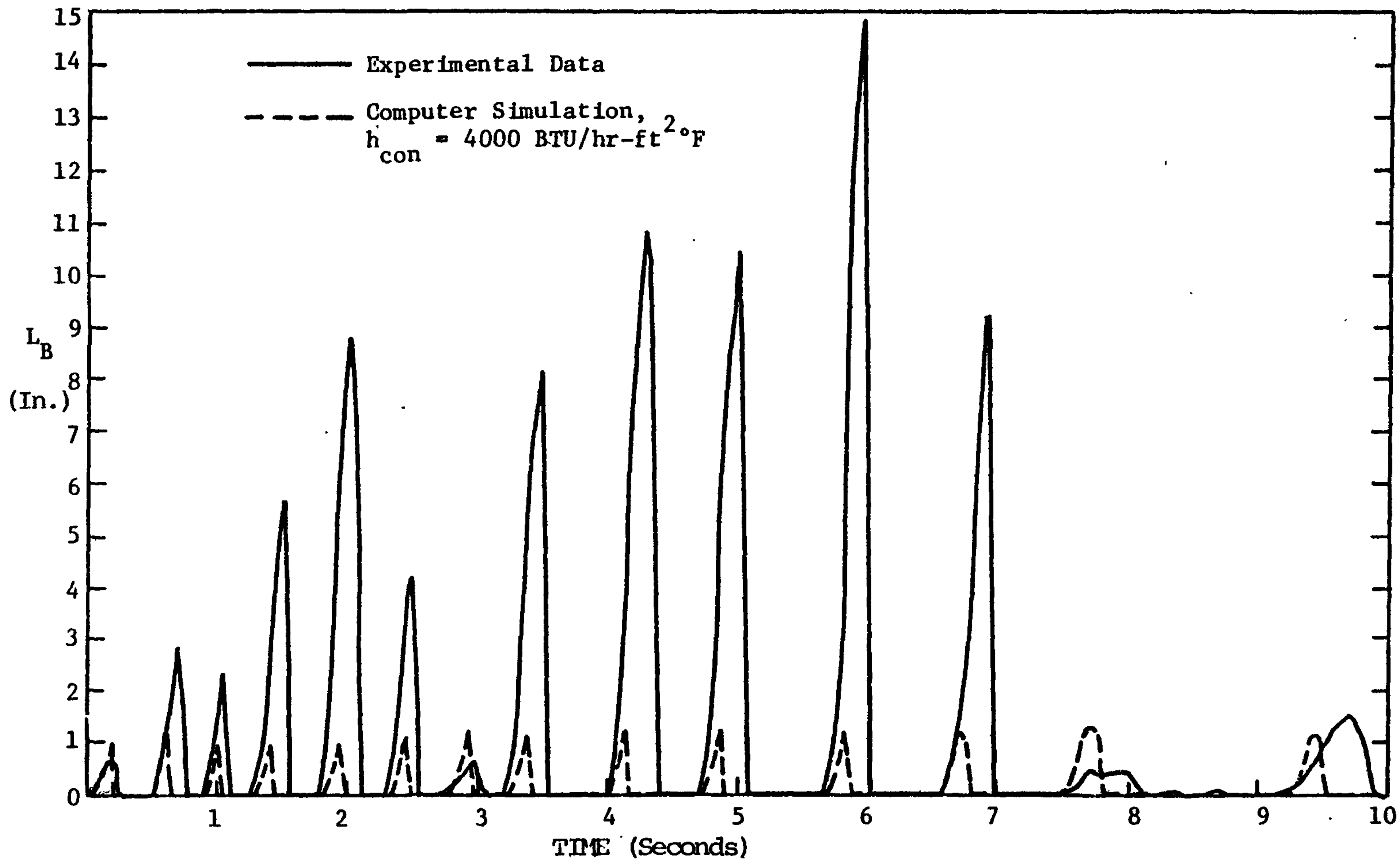

FIGURE 5.26 ANALYTICAL VS. EXPERIMENTAL RESULTS - TEST 8: BUBBLE LENGTH

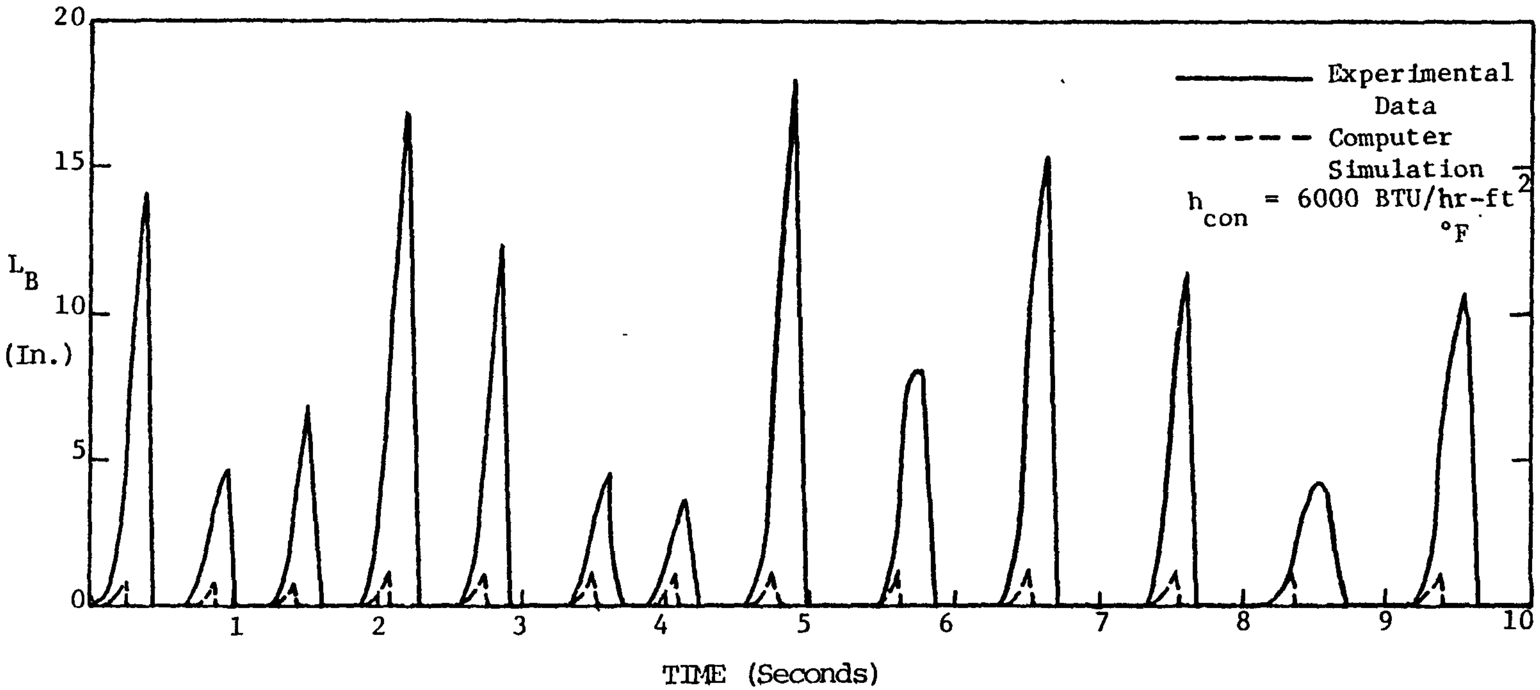

FIGURE 5.27 ANALYTICAL VS. EXPERIMENTAL RESULTS - TEST 9: BUBBLE LENGTH

by which the waiting period is determined in the code. The program uses the First Law of thermodynamics to increment the temperature of the initial node back to saturation. However, the temperature after bubble collapse is determined by mixing an arbitrary amount of fluid at saturation with the colder fluid from above the heater. While this arbitrary amount of fluid is chosen from the standpoint of how much physical mixing can occur, it is essentially another user-adjustable "dial". In addition, the large positive flow rate readings produced by the "water hammer" effect probably had a tendency to bias the calculations of bubble length to some extent. This would have shown up most in the waiting period between cycles, due to the decay of these pressure waves. In light of these facts, it was felt that to try to adjust the code to correspond to the actual experimental output would not be a productive exercise.

To demonstrate how the actual computer output corresponds to the experimental results, Fig. 5.28 has been included on the following page. This is a combination of Fig. 5.11 and Fig. 5.18, and plots length versus time, calculated without adjusting the delay time against the experimental data.

The difference in calculated versus experimental period can also be deduced by examining the temperature versus time plots in Fig. 5.29 through 5.34.

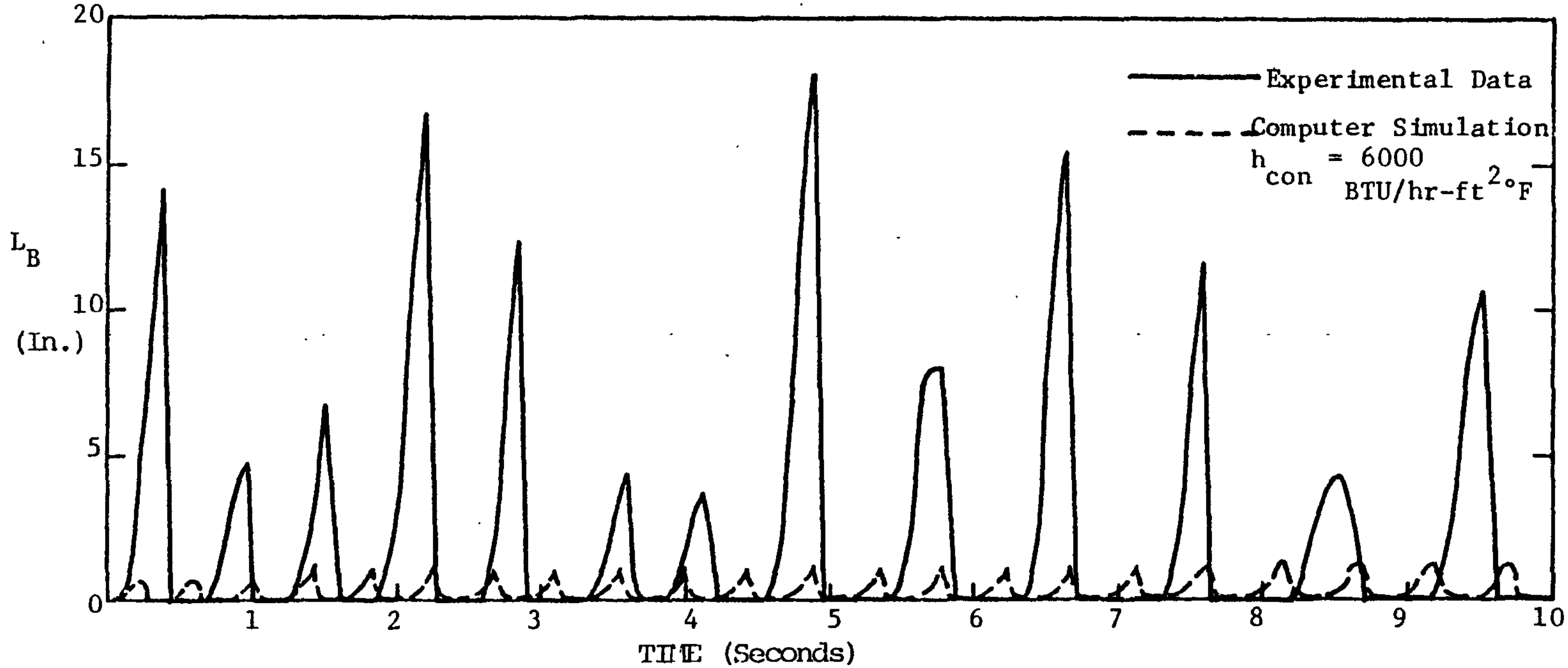

FIGURE 5.28 ANALYTICAL VS. EXPERIMENTAL RESULTS - TEST 9: BUBBLE LENGTHS, NO DELAY TIME ADJUSTMENT

In every case, the first and most obvious fact that is apparent is that the experimental results give much larger bubble lengths than the analytical results. The reasons for this are twofold. First, the previously mentioned bias in the experimental flow rate readings, due to pressure waves, tends to distort the bubble lengths determined from those readings. Second, the way in which the condensation heat transfer coefficient varies, both experimentally and analytically, has been discussed in previous sections. Although the variations in heat transfer coefficient throughout the entire cycle have not been accounted for analytically, it is interesting to note that, in almost every case, the initial rise of the bubble growth pattern is very close analytically to what is seen experimentally. This confirms the lack of condensation during this period of the cycle. In a few cases, in Test 6 especially, the entire cycle is very closely simulated, as well. This would tend to confirm the large jump in condensation heat transfer when the bubble begins to collapse. Other tests are more correct qualitatively, though. The fact that there is a mismatch in the experimental and analytical heat transfer coefficients during various times of the cycle explains much of the quantitative disagreement between the two types of results.

Figures 5.29 through 5.34 show the temperature of the first fluid thermocouple in the experiment compared to that of the first non-saturated analytical node, for each stagnant flow test. Note that while the values of the temperatures are not correct quantitatively, in every case, and that the flow oscillatory patterns are somewhat variant, the trends between experimental temperature results and computer simulations agree quite well.

From a qualitative standpoint, then, the analytical results and the experimental results agree quite well. In general, the period of the oscillatory cycles, as well as the asymmetric shape of the cycle curve are in close agreement. In addition, the variation of the amplitude and period during the transient agree fairly well. Due to the large uncertainties in the experimental results, this qualitative agreement in the areas mentioned are much more important than the quantitative disagreement in the actual magnitude of the parameters measured.

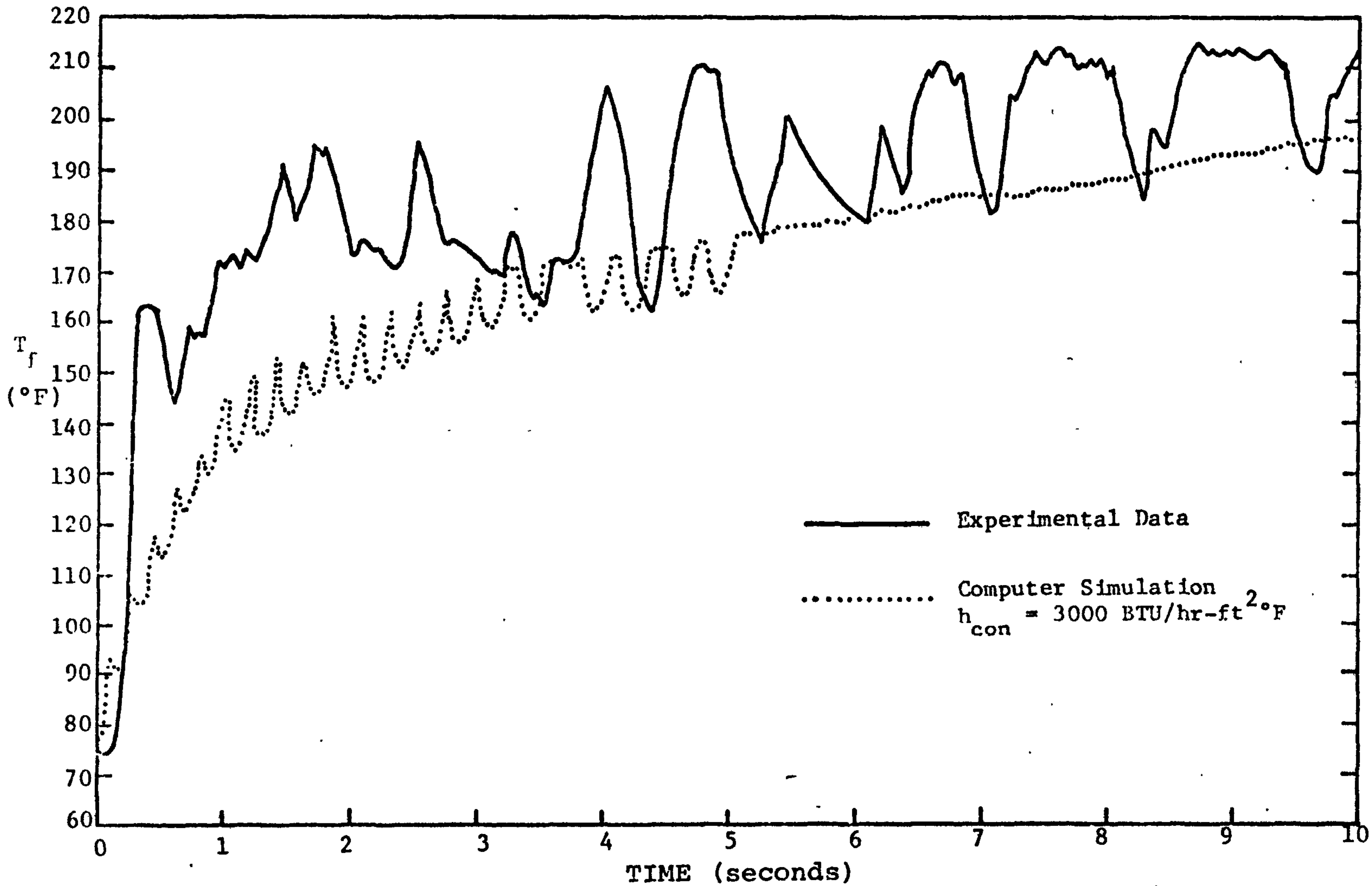

FIGURE 5.29 ANALYTICAL VS. EXPERIMENTAL RESULTS - TEST 4: UNHEATED ZONE TEMPERATURE

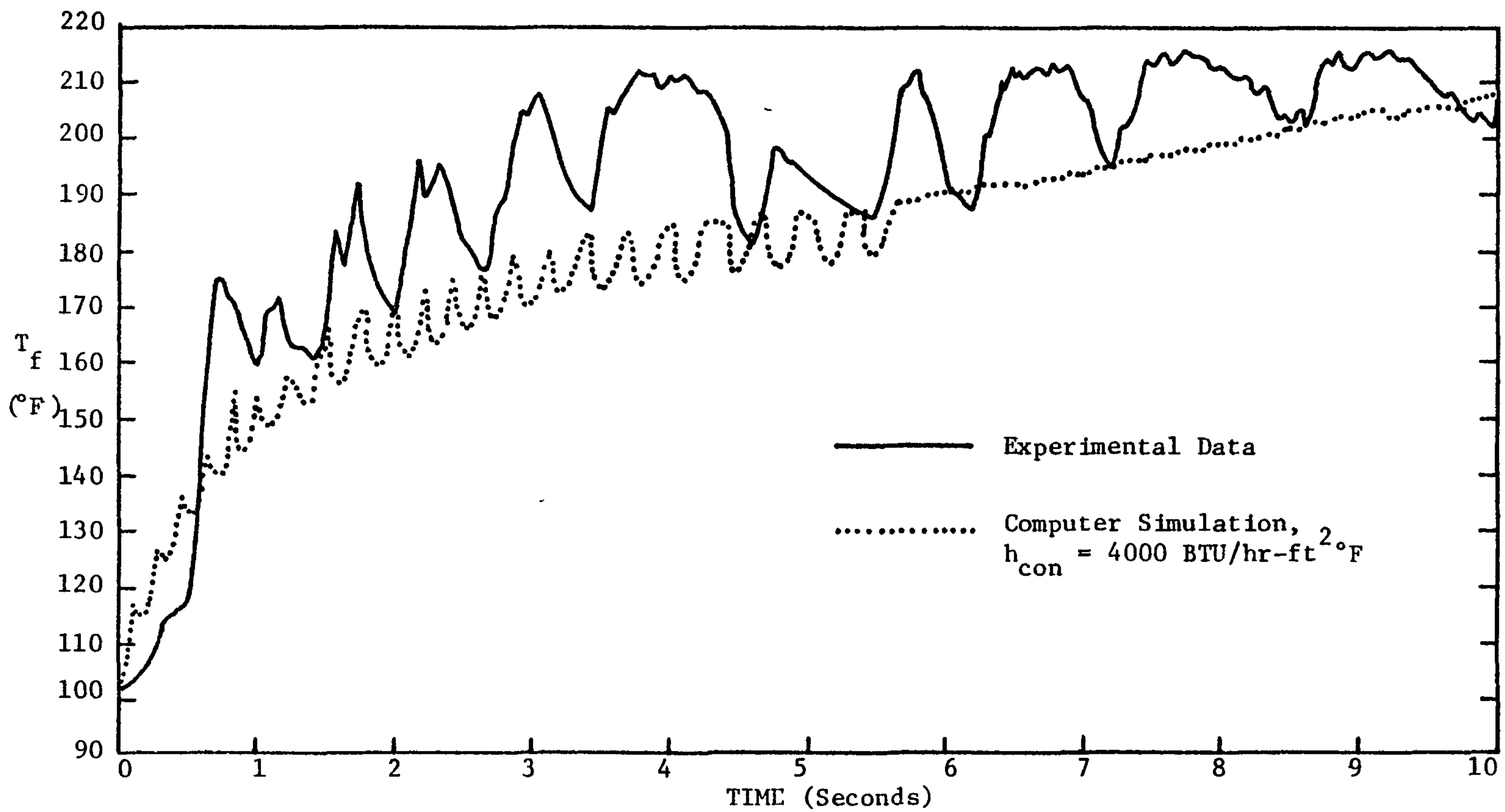

FIGURE 5.30 ANALYTICAL VS. EXPERIMENTAL RESULTS - TEST 5: UNHEATED ZONE TEMPERATURE

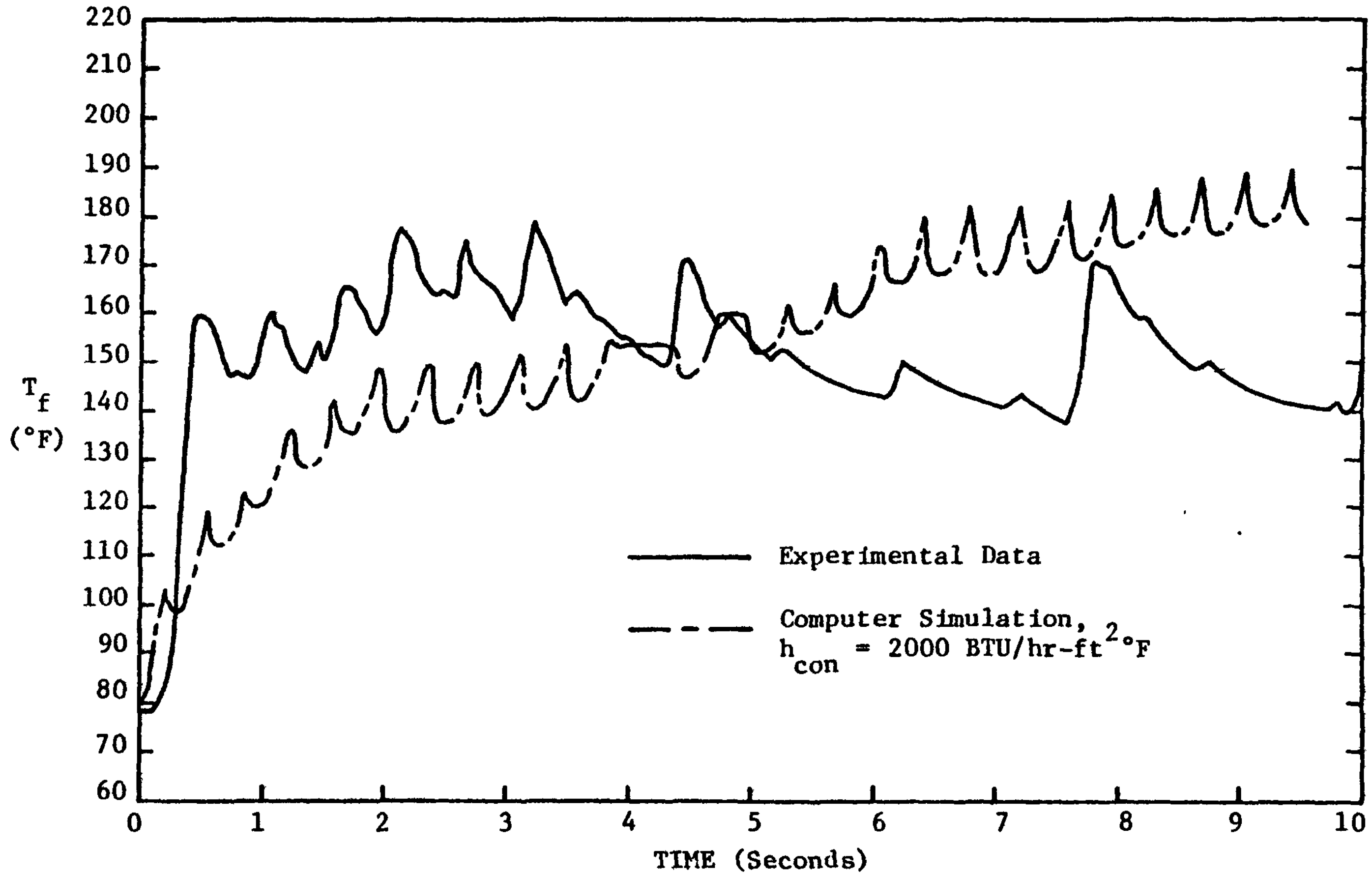

FIGURE 5.31 ANALYTICAL VS. EXPERIMENTAL RESULTS - TEST 6: UNHEATED ZONE TEMPERATURE

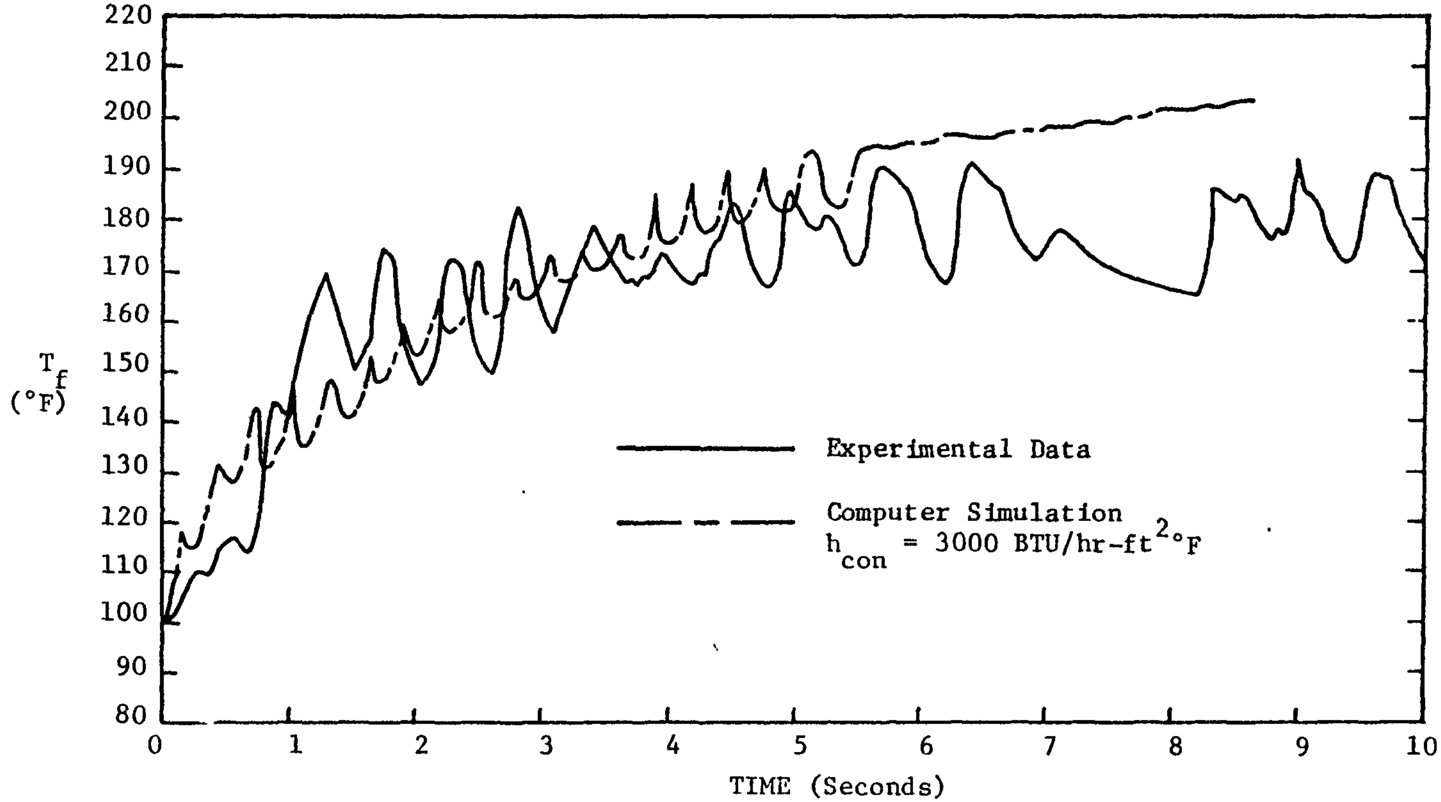

FIGURE 5.32 ANALYTICAL VS. EXPERIMENTAL RESULTS - TEST 7: UNHEATED ZONE TEMPERATURE

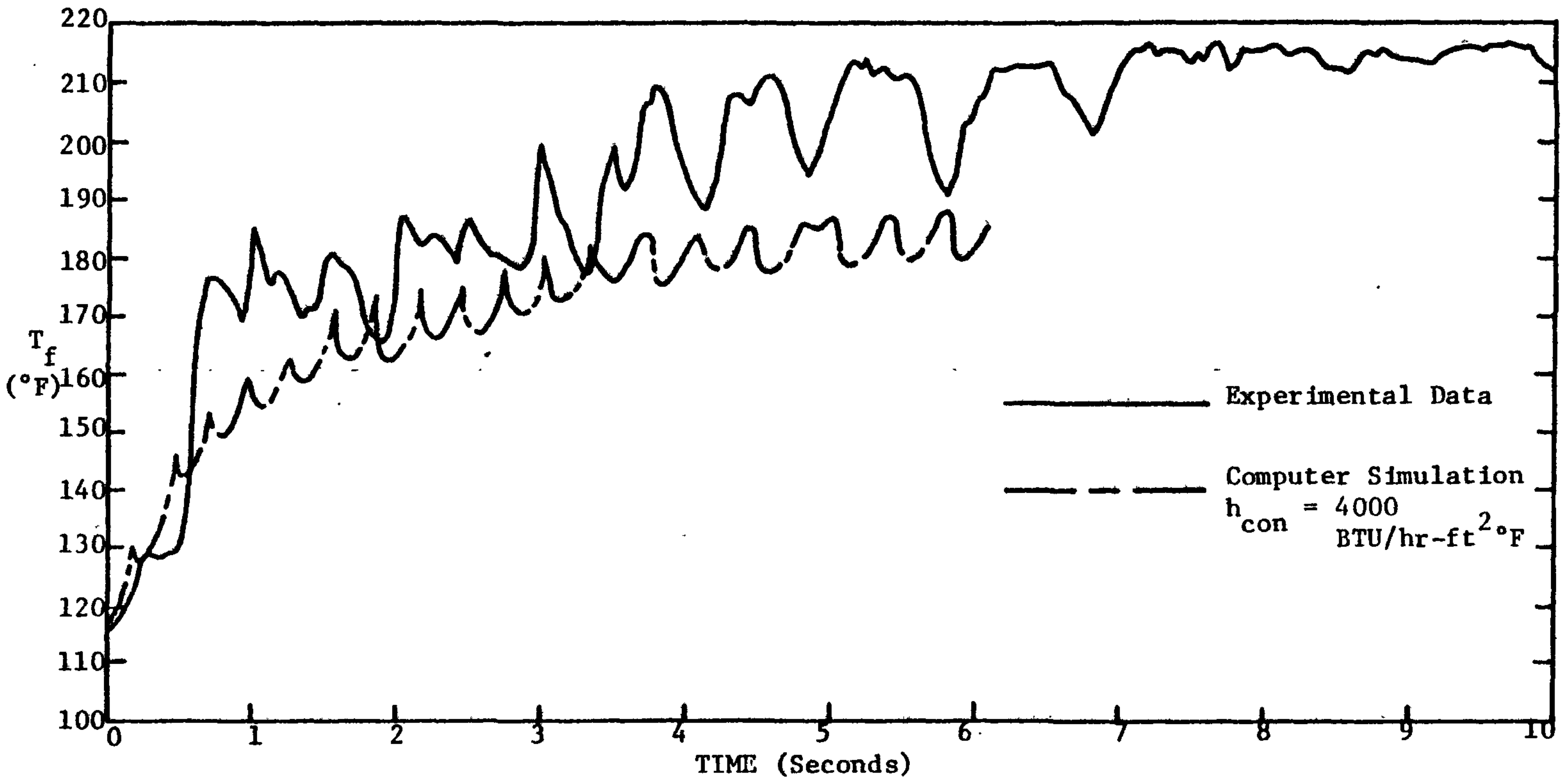

FIGURE 5.33 ANALYTICAL VS. EXPERIMENTAL RESULTS - TEST 8: UNHEATED ZONE TEMPERATURE

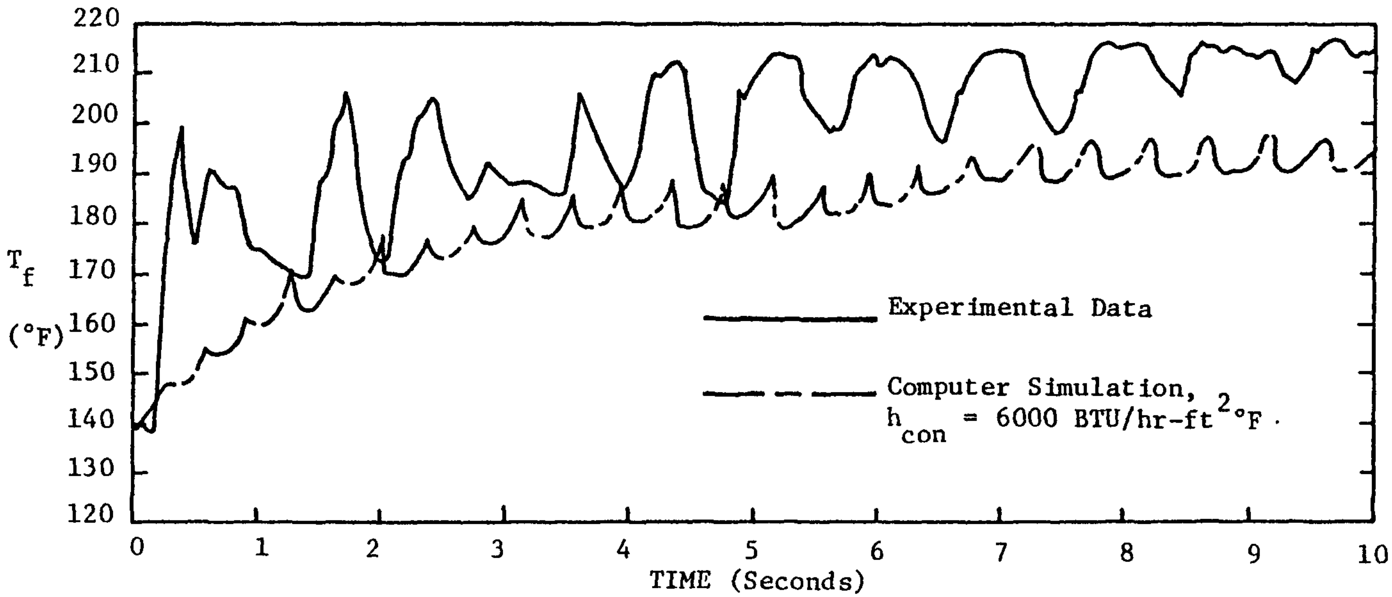

FIGURE 5.34 ANALYTICAL VS. EXPERIMENTAL RESULTS - TEST 9: UNHEATED ZONE TEMPERATURE

CHAPTER 6

CONCLUSIONS AND RECOMMENDATIONS

FUTURE STUDY

6.1 Conclusions

The results of the experimental and analytical work performed for this project have led to the following conclusions.

1. A model has been developed which will qualitatively describe the processes occurring during flow oscillations of the type studied.

2. Experiments with water indicate that sodium behavior can be successfully simulated using water, despite the large disparity in the physical makeup and properties of the two liquids.

3. A set of criteria has been proposed whereby water and sodium data can be compared. Only a very limited amount of mostly qualitative testing of these criteria has been done as part of this work, however.

4. The temperature profile in the unheated region downstream of the source of heat for the fluid (i.e. core, heater pin, heater tube) has a significant effect in determining the behavior of the system during oscillations.

5. The heat transfer coefficient for condensation also has a significant effect on the flow oscillations. In addition, the coefficient changes over perhaps two orders of magnitude during the oscillations, due to the microscale processes at the liquid-vapor interface, and this change may be one of the driving forces during oscillatory behavior.

6. The existence of flow oscillations helps to draw cool fluid down from the unheated zone into the top of the heated zone. This behavior may well

delay dryout of the heater walls and any subsequent temperature excursions, which might otherwise prove detrimental to providing adequate core cooling during transients.

7. More study is needed in many of the areas delineated in points 1-6.

6.2 Recommendations for Future Work

The scope of this project was such that it did not allow detailed study of the condensation heat transfer coefficient. The type of behavior seen was not completely anticipated, and the experiment was not constructed in a way which would easily lead to the development of a mechanistic model of the condensation process during flow oscillations. Clearly, further work is needed in this area.

The criteria proposed for the comparison of sodium and water data have been tested only superficially. It would be useful if the SBTF experiment at ORNL were to be operated in such a way that low-power, low-flow oscillations could be generated for comparison to WTL results. Data from THORS and the multipin experiments is useful from a qualitative standpoint, but the existence of two-dimensional effects due to the radically different experimental geometry may distort efforts to quantitatively compare the data.

The model which has been developed for this project makes a good start toward describing, from a physical basis, the parameters which affect flow oscillatory behavior.

However, it is far from complete, especially with respect to the heat transfer calculational scheme. Further work is required on the model in this area, as well as in the area of expanding the model to a multidimensional tool. A considerable amount of work is underway presently to determine whether multidimensional effects exist in large LMFBR fuel pin bundles. The existence of a multidimensional model to aid in this work would be helpful, and consistent with the original objective of this work to provide a model which might become a module in a large systems code.

Experimentally, there appears to be a wide range of options regarding the simulation of sodium behavior using water. It is clear that certain types of flow behavior can be modelled using water instead of liquid sodium, namely, those types which depend mainly on hydrodynamic processes, rather than thermal ones. Consideration must be given to using small scale water experiments for preliminary investigations of sodium behavior, so that otherwise unexpected effects which might have an adverse effect on sodium experiments may be avoided.

Further work on the effect of loop dynamics on flow behavior should be performed. The means to do this on the Water Test Loop currently exists to some extent, using variable flow orifices in the orifice flange upstream of the inlet plenum. A parametric study using the FLOSS model might also be valuable.

Finally, more work is needed in quantifying the effect of unheated zone temperature profiles on flow oscillations. Judging from the experimental results obtained in this work, there may, for a certain power, be an optimum temperature profile which would provide the best means of accident abatement. The design of LMFBR cores so that such effects could be used to maximum advantage would be the ultimate result of such future work.

REFERENCES

1. W.D. Hinkle, et.al., "LMFBR Safety and Sodium Boiling, A State of the Art Report", Department of Energy (June, 1978).

2. R.J. Ribando, et al., "Sodium Boiling in a Full Length 19-Pin Simulated Fuel Assembly (THORS Bundle 6A)", ORNL/TM-6553, Oak Ridge National Laboratory (January, 1979).

3. W.D. Ford, "Bubble Growth and Collapse in Narrow Tubes with Nonuniform Temperature Profiles", ANL-7746, Argonne National Laboratory (December, 1970).

4. W.D. Hinkle, "Water Tests for Determining Post Voiding Behavior in the LMFBR", M.I.T. Report MIT-EL-76-005, M.I.T. Energy Laboratory (June, 1976).

5. P.W. Garrison, R.H. Morris and B.H. Montgomery, "Dry-out Measurements for Sodium Natural Convection in a Vertical Channel", ORNL/TM-7018, Oak Ridge National Laboratory (December, 1979).

6. R.W. Bowring, "HAMBO: A Computer Programme for the Sub-channel Analysis of the Hydraulic and Burnout Characteristics of Rod Clusters", AEEW-R 582, UKAEA (1968).

7. A.E. Levin, "Simulation of Flow Behavior in BWR Coolant Channels During Transients", S.B. Thesis, M.I.T. (June, 1975).

8. G.H. Golden and J.V. Tokar, "Thermophysical Properties of Sodium", ANL-7323, Argonne National Laboratory (August, 1967).

9. Perkin-Elmer Computer Systems Division, "OS/16 Operator's Handbook", Perkin-Elmer Corporation (1975).

10. Perkin-Elmer Computer Systems Division, "OS/16 User's Handbook", Perkin-Elmer Corporation (1976).

11. Perkin-Elmer Computer Systems Division, "FORTRAN IV Reference Manual and User Guide", Perkin-Elmer Corporation (1976).

12. Perkin-Elmer Computer Systems Division, "FORTRAN IV Run Time Support", Perkin-Elmer Corporation (1977).

13. J. Aberle, et al., "Sodium Boiling Experiments in a 7-Pin Bundle under Flow Rundown Conditions", KFK 2378, GFK, Karlsruhe, FRG.

14. A.E. Bergles, "Review of Instabilities in Two-Phase Systems", Proc. NATO Advanced Study Institute in Two Phase Flows and Heat Transfer, V.1, Hemisphere Publishing Corp., Washington, D.C. (1977).

15. J. Costa and P. Charlety, "Forced Convection Boiling of Sodium in a Narrow Channel", in Liquid Metal Heat Transfer and Fluid Dynamics, A.S.M.E. (1970).

16. A.W. Cronenberg, "A Thermohydrodynamic Model for Molten UO_2-Na Interaction, Pertaining to Fast-Reactor Fuel-Failure Accidents", ANL-7947, Argonne National Laboratory (June, 1972).

17. M.H. Fontana, "THORS Bundle 6A Boiling Stability Test Results", Report presented at D.O.E. Conference, Boston (August, 1977).

18. P.W. Garrison, SBTF Test Results, Personal Communication (January, 1979).

19. R.E. Henry, et al., "OPERA Single-Pin Coastdown Expulsion and Reentry Test", ANL-75-17, Argonne National Laboratory (February, 1975).

20. W. Kowalchuk and A.A. Sonin, "A Model for Condensation Oscillations in a Vertical Pipe Discharging Steam into a Subcooled Water Pool", NUREG/CR-022, M.I.T. (June, 1978).

21. W. Peppler and E. G. Schlechtendahl, "Experimental and Analytical Investigations of Sodium Boiling Events in Narrow Channels", Proc. Winter Annual Meeting, ASME, in Liquid Metal Heat Transfer and Fluid Dynamics, A.S.M.E. (November, 1970).

22. M. Pezzilli, et al., "The NEMI Code for Sodium Boiling, and its Experimental Basis", in Liquid Metal Heat Transfer and Fluid Dynamics, A.S.M.E. (1970).

23. T.A. Shih, "The SOBOIL Program - A Transient, Multichannel, Two-Phase Flow Model for Analysis of Sodium Boiling in LMFBR Fuel Assemblies, G.E. ST-TN-79008, General Electric Corp., A.R.S.D.

24. M.G. Stevenson, et al., "Current Status and Experimental Basis of the SAS LMFBR Accident Analysis Code System", CONF-740401-P3, Proc. Fast Reactor Safety Mtg., Beverly Hills, CA (April, 1974).

25. D.H. Thompson, et al., "SLSF In-Reactor Experiment P3A-Interim Post-Test Report", ANL/RAS 77-, Argonne National Laboratory (November, 1977).

26. J.G. Collier, Convective Boiling and Condensation, McGraw-Hill Book Company, LTD, London (1972).

27. R.H. Sabersky, A.J. Acosta, and E.G. Hauptmann, Fluid Flow, 2nd Ed., The MacMillan Co., New York (1971).

28. W.M. Rohsenow and H.Y. Choi, Heat, Mass and Momentum Transfer, Prentice-Hall, Inc., New Jersey (1961).

29. M. Clark, J. and K.F. Hansen, Numerical Methods of Reactor Analysis, Academic Press, New York (1964).

30. R.H. Perry and C.H. Chilton, Eds., Chemical Engineers' Handbook, 5th Ed., McGraw Hill Book Company, New York (1973).

31. R.L. Powell, et al., "Thermocouple Reference Tables Based on the IPTS-68", NBS Monograph 125, U.S. National Bureau of Standards (March, 1974).

32. F.E. Dunn, et. al., "The SAS2A LMFBR Accident Analysis Computer Code," ANL/RAS 73-39, Argonne National Laboratory (December, 1973).

33. R.E. Barry and R.E. Balshizer, "Condensation of Sodium at High Heat Fluxes," Proc. 3rd Int. Heat Transfer Conf., V.II (1966).

APPENDIX A

THE COMPUTER CODE FLOSS

A.1. General Description of the Code

The computer code FLOSS is a relatively small and simple program designed to solve the equations for the hydrodynamic and thermal models. It was developed as part of this project, and is envisioned as a module of a large system-scale code at some future time. Because of this ultimate aim, many complicating features, such as sophisticated heat transfer models, were omitted. In addition, since the model deals only with a fixed regime, single phase flow before the transient and two-phase flow after the transient have not been modelled. Instead, the primary aim was to develop a code which could be easily understood and would take small amounts of computer time to run, yet would include as much of the essential physics of the problem as possible. This aim has been, for the most part, achieved.

A.2. Solution of the Hydrodynamic and Thermal Models

The solution scheme for the equations presented in Chapter 2 is an amalgam of different techniques for finite difference solutions of differential equations. The entire code is semi-implicit, with an iterative scheme described in Chapter 2.

A.2.1 The Hydrodynamic Model

The equations for the hydrodynamic model are:

$$\Delta P' = I_1 \frac{dQ_1}{dt} + R_1' Q_1^{\,2} \qquad (2.28)$$

$$\Delta P' = I_2 \frac{dQ_2}{dt} + R_2' Q_2^{\,2} \qquad (2.29)$$

$$Q_3 = \frac{V_g}{\rho_g} \frac{d\rho_g}{dt} \qquad (2.11)$$

The first two equations are solved using a first-order, explicit finite difference scheme. The equations can be rearranged into the form

$$\frac{dQ_2}{dt} = \frac{\Delta P'}{I_i} - \frac{R_i'}{I_i} Q_2^{\,2} \qquad (A.1)$$

where i can be either 1 or 2.

This is then transformed into a finite difference equation:

$$\frac{Q_i^{\,n} - Q_i^{\,n-1}}{\Delta t} = \frac{\Delta P'^{\,n}}{I_i^n} - \frac{R'^{\,n-1}}{I_i^n} (Q_i^{\,n-1})^2 \qquad (A.2)$$

where n is a time index.

The final form of the equation, upon rearrangement of terms, is

$$Q_i^n = Q_i^{n-1} + \frac{\Delta t}{I_i^n} [\Delta P'^n - R_i'^{n-1}(Q_i^{n-1})^2] \quad (A.3)$$

Equation (2.11) is solved by an implicit, first order finite difference approximation

$$Q_3^n = \frac{V_g^n}{\rho_g^n} \left(\frac{\rho_g^n - \rho_g^{n-1}}{\Delta t}\right) \quad (A.4)$$

Because of the explicit nature of the equations solved by Eq. (A.3), special attention must be paid to the time step. The time step size is limited by the Courant condition

$$\frac{\Delta x}{\Delta t} \geq v \quad (A.5)$$

That is, the time step must be small enough that the velocity does not allow the calculation to cross more than one node. This becomes important during the temperature profile calculation in the unheated zone. During condensation, the rapidity of the bubble collapse creates extremely large velocities, relative to the bubble growth period. For this reaon, a variable time step is employed in the solution of Eq. (A.3). If the solution fails to converge at a large time step, the step is reduced by a factor of two, and the solution procedure is repeated. If convergence is not achieved after several successive reductions, it is assumed the bubble has collapsed entirely or undergone an expulsion. The method for dealing with this problem is discussed in Section A.3.1.

A.2.2 The Thermal Model

The equation for the thermal model is

$$Q_s = (\dot{q}_{net} + \frac{V_g dP}{dt})/\rho_g h_{fg} \qquad (2.27)$$

This equation is also solved by an implicit, first-order finite difference approximation

$$Q_s^n = [\dot{q}_{net}^n + V_g^n (\frac{P^n - P^{n-1}}{\Delta t})]/(\rho_g^n h_{fg}^n) \qquad (A.5)$$

A.3 The Structure of the Code

To provide ease of handling and understanding, the code is split into a main section and several subroutines. Each routine is briefly explained in this section.

A.3.1 FLOSS-MAIN Program

The MAIN portion of the code provides the basic framework for the simulation of transients. In addition, schemes for variable time step size and non-convergence restarting are included. Initially, data are input and converted to an internally consistent set of units, a proper call sequence for the actual calculational subroutines is established, initial conditions are established, and output is arranged to be easily readable.

One of the limitations that has been determined by use of the code is the necessity to generate a sufficient amount of vapor during the initial time step of the transient. By trial and error, the amount of power required for this to occur is such that

$$(\text{Input Power}) \cdot (\text{time step}) \cong 0.025 \text{ kw-sec} \quad (A.6)$$

This is the only initial constraint. However, for very low powers, large initial time steps must be used. The code, through the variable time step calculation, will adjust the size of the time step as necessary to allow convergence.

If convergence does not occur, as described in Chapter 2, that is, if the thermal and hydrodynamic models cannot be made to generate the same bubble size, a check is made of the temperature in the initial node downstream of the heater. If this temperature is below the saturation temperature at initial pressure, as is usually the case, it is an indication that the bubble has collapsed entirely, and the calculation is restarted. This is accomplished by assuming that a small amount of fluid at the top of the heater, originally at saturation, is mixed with the lower temperature fluid in the first unheated node. The mean temperatures of this fluid is then determined, and a heat balance is performed on this fluid, using the heater power as a heat source. The temperature of the fluid in this node is thereby increased, while temperatures in the upper nodes of the unheated zone are held constant. When the temperature in the first node reaches saturation, the calculation of the transient proceeds anew. In this way, the "waiting period" seen experimentally is reproduced.

If the temperature of the initial unheated node is greater than or equal to saturation at nonconvergence, it is assumed that an expulsion of fluid has occurred, and the transient is ended at that point.

A.3.2 Subroutine HYDRO

This subprogram solves the hydrodynamic model, as previously outlined in A.2.1. The differencing scheme is established, as well as the iterative scheme for calculation of the bubble lengths and volumes. Error convergence limits, read in as data, are applied in this routine.

A.3.3. Subroutine HEAT

This routine solves the thermal model, as previously described. The bubble is split into two volumes, one in the heated zone and one in the unheated zone. The heat inputs and outflows are calculated separately for each "half-bubble", and the total size is then determined. Convergence criteria are set up such that not only must the total bubble size be consistent, but the two separate zones must also converge. There also exists the means to account for wall heat capacity effects.

In addition, the unheated zone temperature profile is calculated. The method for this calculation is quite involved, and the code listing should be referred to in order to understand the details of the scheme. To summarize the scheme, a search is performed to locate the vapor-liquid interface at each time step. That having been accomplished, the temperature of each node is then calculated on a volume-averaged basis:

$$T_i^n = \left(T_i^{n-1} V_i^n + T_i^{n-1} dV_{ij} + \frac{q_i^{n-1} \Delta t}{\rho^{n-1} C_p^{n-1}}\right) / V_i \tag{A.7}$$

In Eq. (A.7), i and j represent the volume being calculated and the adjacent volume respectively. This volume is either above or below volume i, depending on whether the bubble is expanding or contracting. The term $T_i^{n-1} V_i^n$ represents the temperature of the node at the previous time step multiplied by the volume of that fluid remaining in the node at the current time step. The second term represents the temperature of the adjacent node, multiplied by the amount of fluid pushed from node j into node i by bubble movement, and the final term represents any heat input to the node due to condensation at liquid vapor intervaces multiplied by the volume over which the heat transfer occurs. This sum is then divided by the nodal liquid volume, the result being the volume-averaged temperature of the node. This procedure is performed for each node at each time step, during each iteration.

A.3.4 Subroutine AREA

This short subprogram calculates the cross-sectional area of the bubble, based on a weighted average of the film thickness. A constant void fraction is assumed at initial bubble formation, equal to the inverse of the turbulent velocity drift flux constant, i.e. $1/C_o$. Subsequent evaporation in the heated zone is accountable for areal changes. The void fraction in the unheated zone remains $1/C_o$ at all times.

A.3.5 Subroutine HTCOEF

This portion of the code calculates the condensation heat transfer coefficient for the upper unheated zone. Three options exist for the determination of this parameter: a constant heat transfer coefficient which has been input as data (KHT=1); the Dittus-Boelter correlation, based on vapor velocity and properties (KHT=2); or an option that allows the user to input his own correlation or model (KHT=3). If the first option is chosen, the heat transfer coefficient does not change at all over the period of the transient; however heat transfer rates may be changed by changing the unheated zone temperature profile.

A.3.6 Subroutine PGUESS

This subroutine contains the logic for guessing the pressure during the iterative process described in Chapter 2. For each pressure guess, an error is calculated based on the difference between the hydrodynamic and thermal flow rate:

$$\varepsilon = (Q_H - Q_T)/[(|Q_H| + |Q_T|)/2] \tag{A.8}$$

This error may be positive or negative. If positive, the pressure is reduced until a negative error is generated. If the error is negative, the pressure is subsequently increased. When two errors exist of opposite sign, a method of successive linear approximations is employed to continue guessing the pressure until the convergence limits are reached. This method is shown in Fig. A.1 . The equation represented by this linear method is

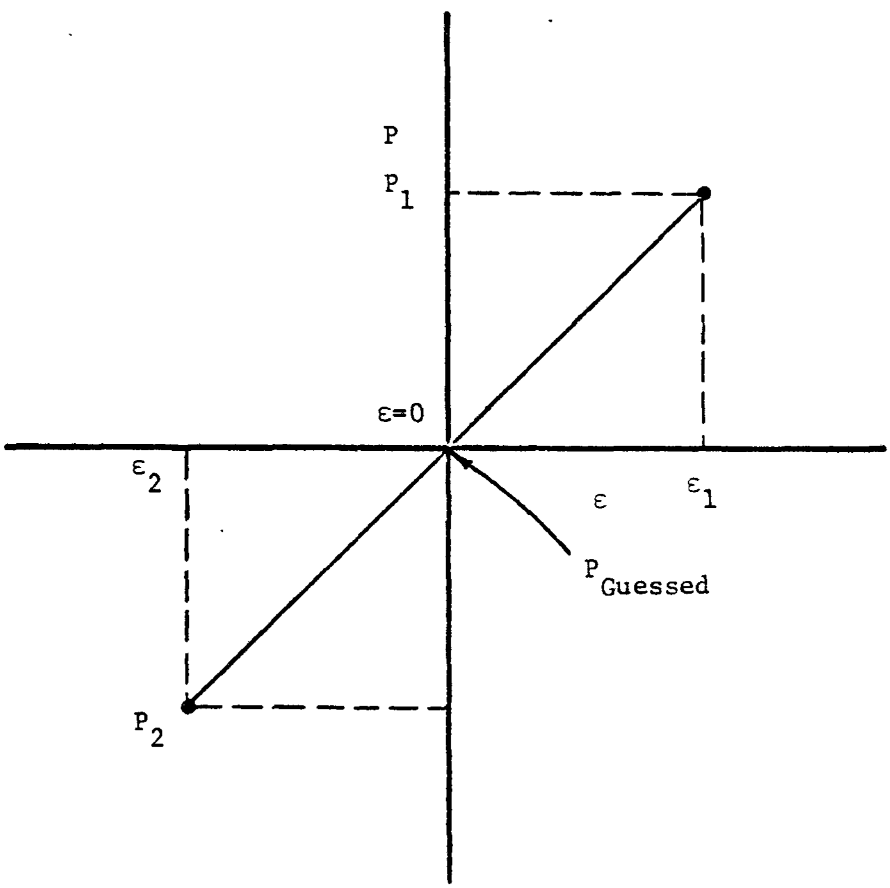

FIGURE A.1 METHOD FOR GUESSING PRESSURES IN FLOSS

$$P = \frac{\Delta P}{\Delta \varepsilon}\varepsilon + B \qquad (A.9)$$

where B is the y-intercept. The method has proven to be reliable, and, for the most part, rapidly convergent.

A.3.7 Subroutine RESIN

This routine calculates resistances and inertances for solution of the hydrodynamic equations. It also contains the logic for deriving equivalent values for parallel bypass loops, using an analog to electrical systems. The numbering scheme for this calculation is shown in Fig. A.2 . The scheme must be followed exactly as shown for the code to calculate the bypass equivalent vales properly.

A.3.8 Subroutine FFACTR

This subprogram calculates the friction factors for the previous subroutine RESIN, for determination of resistance terms. The calculation is based on the Reynolds number of the liquid flow in each part of the system. If the Reynolds number is less than 2000, the laminar value

$$f = \frac{16}{Re} \qquad (A.10)$$

is used.

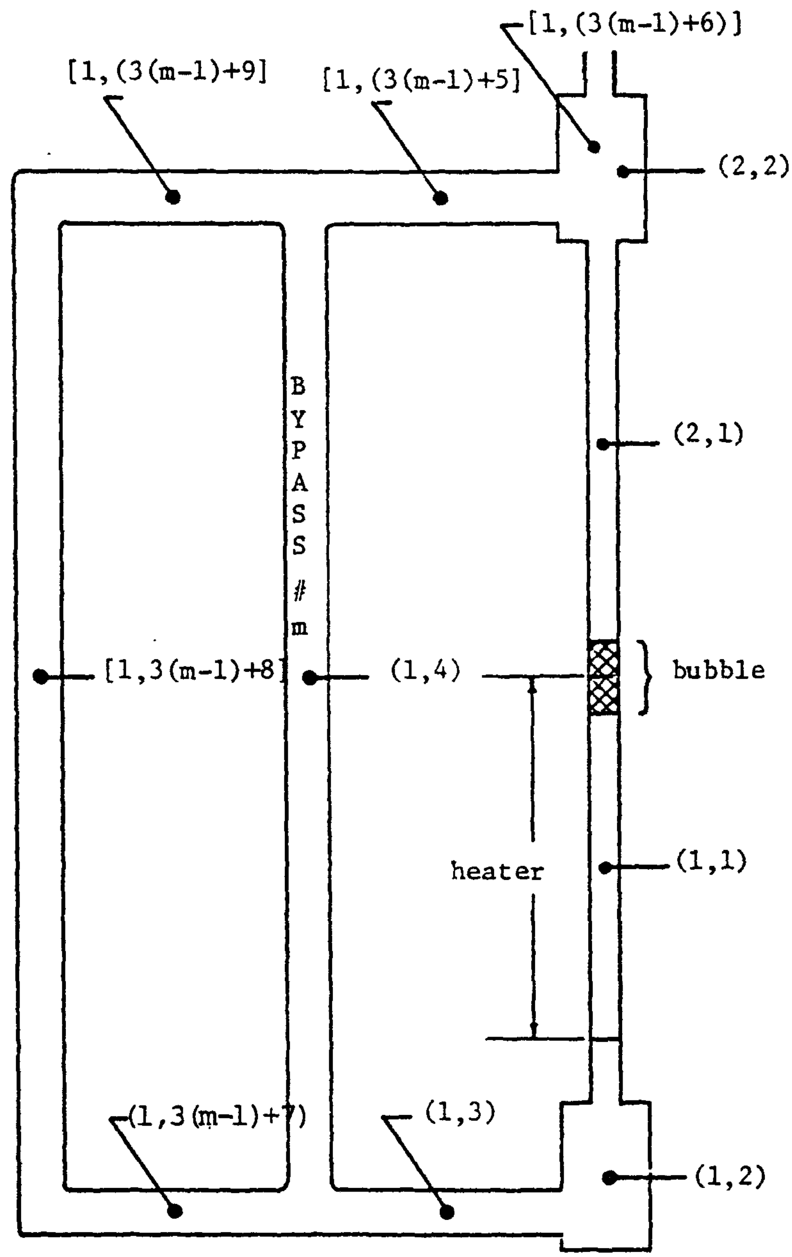

FIGURE A.2 NUMBERING SYSTEM FOR COMPONENTS IN FLOSS

For 2000 <Re <50000

$$f = 0.0791\ Re^{-0.025} \qquad (A.11)$$

If Re > 50000

$$f = 0.046\ Re^{-0.020} \qquad (A.12)$$

A.3.9 Subrountine PROP

This routine calculates properties of either water or liquid sodium, depending on the option chosen. The water properties are based on polynomial expressions derived by Bowring (6), and are taken from Levin (7). The sodium properties were derived by Golden and Tokar (8).

A.3.10 Subroutine PLOTTER

The Joint Computer Facility at M.I.T. maintains a FORTRAN library subroutine called PICTR which enables computer developed plots to be made using a VARIAN electrostatic plotter. This subroutine contains the logic which sets up the output from a simulated transient in a form to be used by the PICTR routines. Information on these routines is available from the JCF.

A.4 Restrictions on Code Use

Several restrictions on the use of the code have been noted already in this Appendix. These will be reviewed, and some other restrictions explained.

1. The energy input to the model during the start of the transient must be about 0.025 kw-sec.

2. The Courant condition $\frac{\Delta x}{\Delta t} > v$ applies during rapid bubble movement. This restriction is automatically considered in the inclusion of a variable time step calculation.

3. The nodalization scheme for the unheated zone is very flexible, as it allows an input not only of the nodal temperatures, but of nodal lengths as well. The initial node should be very short - on the order of two inches or less - and the temperature should be at or near saturation, to allow bubble growth. It is believed that these are the conditions that physically prevail at bubble initiation. The remainder of the nodal lengths should be chosen judiciously. Too long a length will cause the nodal averaged temperature to be far too low, compared to reality, while too short a length would cause temperatures to be too high, and unnecessarily restrict time step size. A sample problem is shown in Appendix D. For most transients, nodel lengths on the order of 0.4 - 1.0 foot have been found to be satisfactory. The scheme for calculation of nodal temperature also breaks down if the bubble interface crosses two nodal interfaces in the same time step. This presents an additional restriction for which the Courant condition must account. Choice of nodal lengths must therefore be chosen such that time step sizes do not become so small as to significantly increase code execution time.

4. The error criterion for convergence of the thermal-to-hydrodynamic comparison has been kept relatively high for most simulations, to cut down on computer time requirements. Reduction of the convergence limit appears to have little effect on the values generated by the code. The convergence criteria for bubble lengths and volumes are related to the error convergence limit, and must be set to approximately the same value. The sample input in Appendix D illustrates this fact.

APPENDIX B

DESCRIPTION AND USE OF THE COMPUTER DATA ACQUISITION SYSTEM

B.1 Background

The general structure of the CCDAS apparatus has been previously described in Chapter 4. The purpose of this appendix is to describe the hardware, software, and operating procedures associated with the system in more detail.

The system is now operating as a data acquisition and data conversion unit in the M.I.T. Heat Transfer Laboratory.

B.2 Hardware

The CCDAS is built from several different components in order to provide a wide range of usage, both as a computer and as a data acquisition system.

The heart of the system is a Perkin-Elmer Model 1610 Minicomputer. This is a 16-bit machine, with a currently installed capacity of 64 kilobytes of semiconductor memory. The memory may be expanded to as much as 128 kilobytes in 32 kb increments. The computer is equipped with a line frequency clock, which can provide processor interrupts at up to twice the line frequency (120 hz). Processor options on the HTL computer include a precision integral clock, a battery backup system, and a hardware multiplication/ division unit. The PIC will provide interrupts at a rate faster than the line frequency clock, if necessary. The battery backup system provides a power system backup to preserve information in memory in the event of a power failure. The hardware multiply/divide option allows the computer to perform these operations directly, instead of through software programming. This allows the operations to be done much more quickly.

These are several peripherals which are connected to the minicomputer. The system command console is a Perkin -Elmer Model 550 CRT. This is an essential piece of equipment, since the minicomputer itself has no built-in command-issuing unit. The CRT is a standard type of visual display unit, with a keyboard and viewing screen, providing interactive use of the computer. In addition, the CRT has a printer port built into the back of the unit, which allows connection to a CRT page printer. The page printer used in this system is the Perkin -Elmer Model 650 "Pussycat" Thermal Printer. The printer will print 24 lines, a full screen display, automatically upon receipt of 24-line feed signals from the CRT. The printer is a single buffer machine, which does not allow data to be received and stored while printing is taking place. Therefore the display must be advanced twenty-four lines and then halted, printing permitted, and then display scrolling advanced in order to allow printing of all information.

Data and program storage are provided by a dual floppy disk system. Each disk contains space for up to 256 kilobytes of information, either in ASCII (source) or binary (object or image) form.

The last peripheral is the data acquisition unit, itself. The RTAS (see Chapter 4) currently allows up to 24 instruments to be connected for input to the computer, and capacity may be expanded to 32 channels in 4-channel increments, in the present configuration. The termination panel is supplied with a calibrated Resistance Temperature Device (RTD) to serve as an equivalent ice-point for thermocouples. If the RTD is used, it must be connected to one of the RTAS channels. Maximum scanning speed is 8000 points per second. Data is stored in the computer by means of software programming. Each data point is stored as a number ranging from -2048 to +2047. To convert these data to meaningful information, the value must be multiplied by a gain factor, which is set by the user. Each channel has a variable gain, which is set through input to the controlling software, which ranges from ±20 to ±1000 millivolts, full scale; the gain factor is then the full scale output divided by 2048. This configuration provides a very flexible system which is not difficult to operate. The system is shown schematically in Fig. B.1.

B.3 Software

The sofware supplied by Perkin-Elmer includes support for all peripherals, and is currently configured for the FORTRAN computer language. Support for other languages is available from the vendor.

The computer is controlled by an operating system, created by means of a system generation (SYSGEN). The SYSGEN procedure, which can be performed by the vendor or the user, sets the operating environment for the system, and tells the computer which peripherals are available and which processing options are necessary for the user's requirements. The SYSGEN is performed by using several assembly language programs supplied by Perkin-Elmer. These include a Configuration Utility Program (CUP), which sets the system environment, and three packages which tell the computer how to perform functions in the given environment. These are the Command Processor, The File Manager, and the System Executive. Once a SYSGEN is performed using these programs, the resultant operating system must be loaded into the computer before any operations can be performed.

The present system provides support for the RTAS,

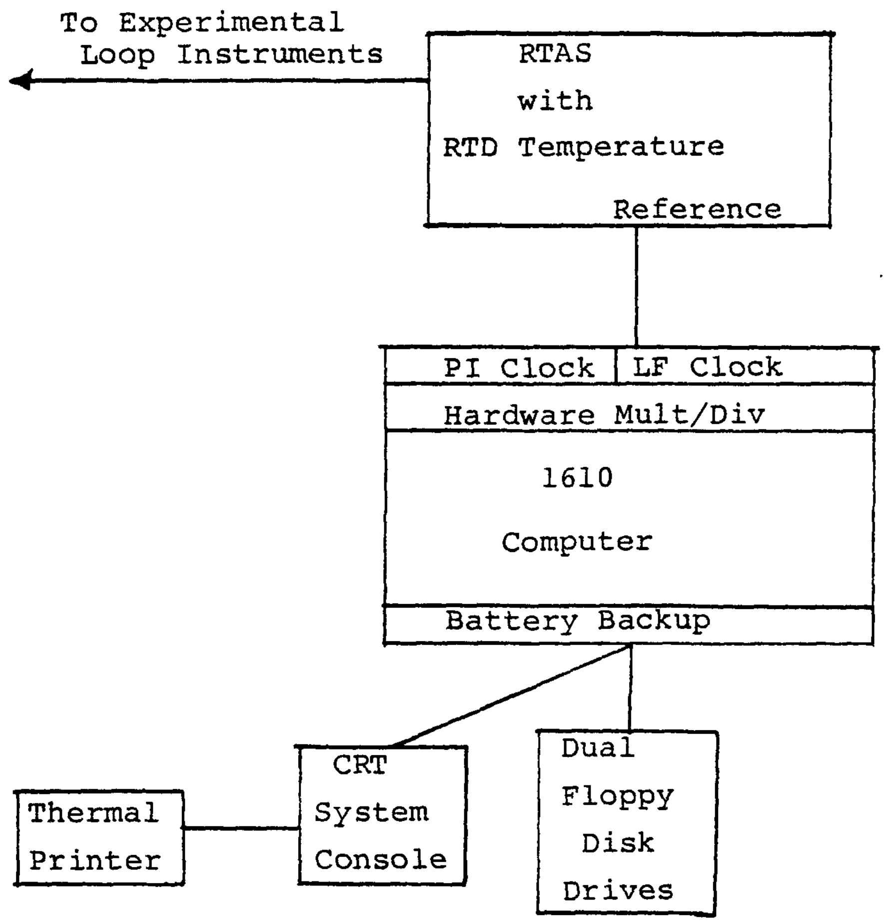

FIGURE B.1 SCHEMATIC OF COMPUTER SYSTEM

CRT, and floppy disk drives. It also includes a partition system for the memory, which allows several programs to be held in memory simultaneously, although only one program may be active at a time. Currently, the system is configured for five foreground partitions and one background partition; the size of each partition may be set by the user. There is also a system partition, which must be allowed to exist for the computer to process information.

The software for FORTRAN programming includes a FORTRAN compiler and a run-time library. The former program allows the FORTRAN source programming to be converted to binary code, and the latter provides support for library mathematical and real-time routines. Linkage between user programs and FORTRAN library functions is provided through use of the vendor-supplied Task Establishment Utility Program. This program also converts the output from the FORTRAN compiler (object code) to executable code (image code).

The remaining software that has been supplied by Perkin-Elmer includes several driver programs to allow the RTAS to be operated. This software includes both assembly language and FORTRAN programming. The function of the programming is to provide for generation of interrupts, data sampling, data storage, disk allocation, and transfer of acquired data from computer memory to disk. Once the data have been put onto the floppy disk, further data processing may be accomplished through user-written data conversion programming.

B.4 Operation of the CCDAS

The operation of the CCDAS involves several steps and will be explained briefly in this section. A detailed instruction manual is under preparation at this time, and Perkin-Elmer's own handbooks are also valuable references.

Initially, the system is started up using the operating system described in Section B.3. The foreground partitions are then set to accomodate two programs: a test supervisory program (TSTSUP) and a data acquisition system driver program (DATACQ). Logical input and output units are then assigned by the user. The input to DATACQ is provided by the RTAS. The input to TSTSUP is provided by the user and includes:

1) The name of the file in which acquired data is to be stored.
2) The time interval at which interrupts are to be generated.
3) The number of channels to be sampled.
4) The list of channels and their respective gains, in the order in which sampling is to be done.
5) The number of scans to be made.

The number of scans to be performed (item 5) is determined by dividing the total transient time, which is not an input, by the sampling interval (item 2).

The TSTSUP program is activated upon the user's START command on the console. This command is issued about 5 seconds before the sampling period is to begin, to allow the programs to start properly. The initial program reads the input data, opens a file on one of the floppy disks for RTAS output, then initiates the DATACQ program and pauses. The DATACQ program generates interrupts at the desired intervals. Each interrupt allows the scanning to proceed. This is done at the maximum rate, and the data is stored in complete memory. After several scans, DATACQ sends a signal to TSTSUP, and TSTSUP activates a small data-logging subroutine, which transfers data from computer memory to the file opened initially by TSTSUP. This procedure continues until the number of samples input as item 3 have been acquired. The program then ceases execution. The user may then load a conversion program into the computer which reads the data from the floppy disk, and converts it, using the gain factors described in the previous section, plus any conversion tables (e.g., calibration curves, thermocouple tables), to engineering units or millivolts, depending on the user's desire.

A flowchart of the data acquisition procedure is shown in Fig. B.2.

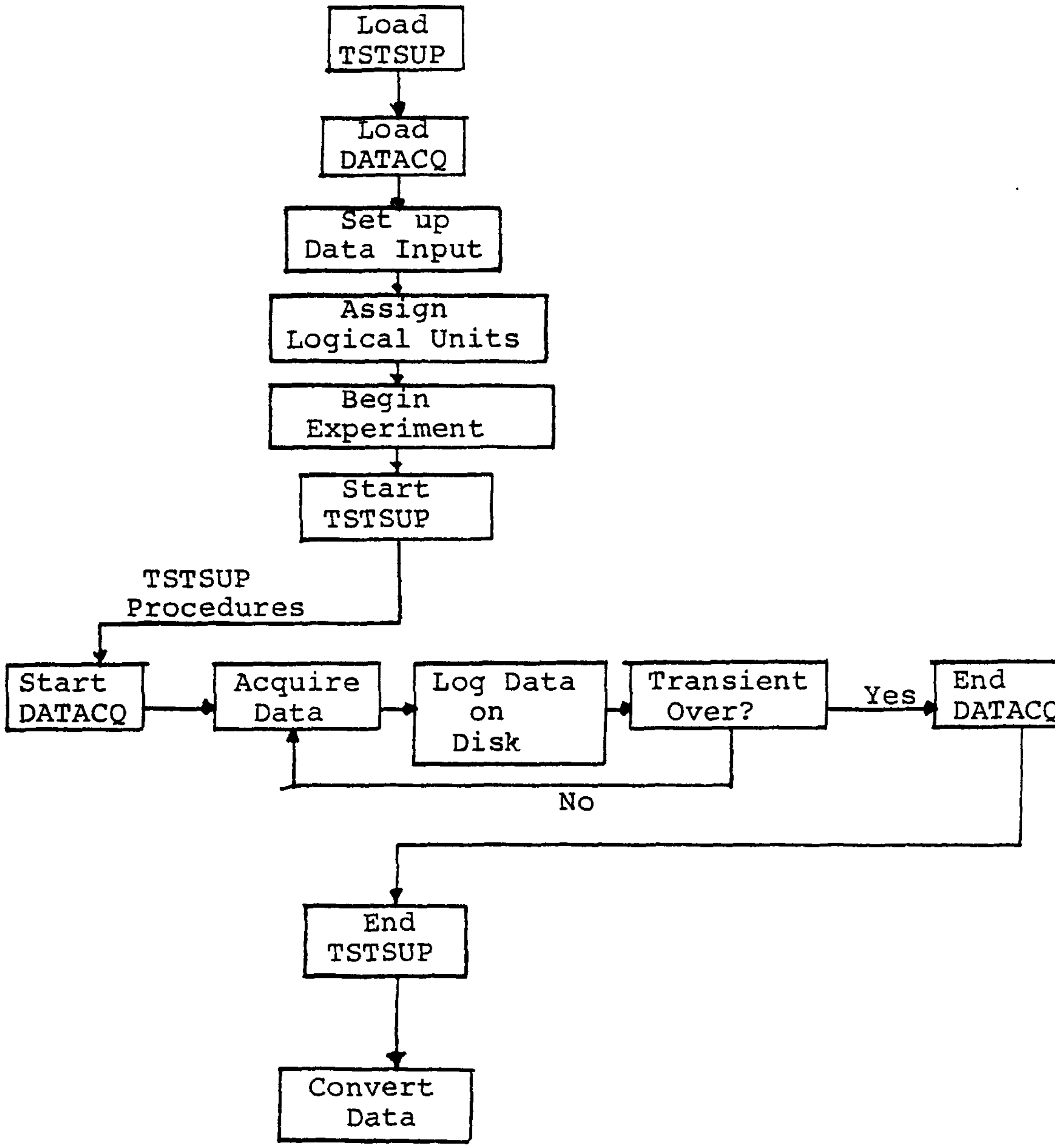

FIGURE B.2 DATA ACQUISITION FLOW CHART

APPENDIX C

EXAMPLE OF EXPERIMENTAL RESULTS

C.1. Data Conversion and Presentation

After the acquisition of data as described in Appendix B, this information was converted to temperatures, pressures, and flow rates by use of calibration information and thermocouple tables, as described in Chapter 4. In addition, a stepwise integration of the flow rates was performed to estimate the length of the vapor bubbles above and below the top of the heater. As explained in Chapter 5, the readings of flow rate from the upper ΔP transducers proved to be quite unreliable. Also, since 375 points were required for each instrument for each transient, it would be impractical to present every piece of data acquired. Therefore, an example of the output from each stagnant flow experiment will be shown in the first six tables. The data shown include:

1. The flow rate, as determined by the lower ΔP cell.
2. The temperature of the first thermocouple in the fluid downstream of the top of the heater.
3. The length of the bubble below the top of the heater.

There are two important points to be made with respect to items 1 and 3. First, a negative flow rate indicates bubble growth downward. A positive flow rate indicates bubble collapse. The second point, then, involves the large positive flow rates generated after bubble collapse. These readings were attributed in Chapter 5 to "water hammer" effects due to bubble collapse. This effect is clearly shown, for example, in Table C.4, at 1.8 and 2.4 seconds. Since a positive flow rate corresponds to bubble collapse, it is clear that continuing to integrate these flow rates after the bubble length has reached zero would provide non-physical results. Thus, upon bubble collapse to zero length, no further integration is performed until a negative flow rate is generated. This explains the form in which the results appear. The data are presented at 0.2-second intervals, which represents five data-taking cycles. Apparent mismatches in flow rate, bubble length, and temperature are attributable in every case to the fact that the duration of bubble growth-collapse cycle is not exactly a multiple of 0.2 seconds; therefore, in Table C.1, for instance, at 0.4 seconds, a positive flow rate (bubble collapsing) is shown, whereas the bubble length is greater than at 0.2 seconds. This indicates that the bubble grew considerably after 0.2 seconds, and had just begun to collapse at 0.4 seconds.

Results from the forced convection test are difficult to decipher because of the effects on the fluid of the valve movement when the flow rate was reduced. Qualitatively, the results indicate that, after boiling inception, the flow oscillates slightly due to normal fluctuations that occur during "steady" two-phase flow. However, there are no real oscillations similar to those in the stagnant flow tests. The temperature downstream of the heater is shown, however, to indicate the high temperature at boiling inception, which caused the transition immediately to bubbly, steady two-phase flow.

Table C.1 - Example of Results from Test 4

Time After Boiling Inception	Flow Rate ($10^{-4} ft^3/sec$)	Calculated Bubble Length (In)	Temperature At First TC Downstream of Heater (°F)
0.0	-0.02	0.00	74.64
0.2	-3.34	2.89	94.63
0.4	1.14	12.19	163.32
0.6	-0.26	5.86	144.52
0.8	0.17	4.86	157.78
1.0	5.41	1.88	171.12
1.2	1.60	0.00	173.54
1.4	-0.28	0.24	184.05
1.6	-0.81	1.69	182.11
1.8	14.49	0.00	193.30
2.0	4.05	0.00	173.93
2.2	-0.22	0.10	174.72
2.4	-1.61	6.60	172.29
2.6	9.20	2.57	188.30
2.8	5.00	0.00	176.59
3.0	0.05	0.00	173.54
3.2	-1.57	2.81	169.62
3.4	10.51	0.00	167.27
3.6	-4.23	4.33	171.98
3.8	0.68	3.60	174.72
4.0	6.63	0.00	206.66
4.2	28.66	0.00	181.72
4.4	-10.35	7.60	162.93
4.6	8.32	22.39	197.82
4.8	4.97	0.00	210.82
5.0	1.72	0.00	194.45

Table C.2 - Example of Results from Test 5

Time After Boiling Inception	Flow Rate ($10^{-4} ft^3/sec$)	Calculated Bubble Length (In)	Temperature At First TC Downstream of Heater (°F)
0.0	-0.01	0.00	102.21
0.2	0.41	0.36	106.40
0.4	0.22	0.11	115.46
0.6	-4.01	2.38	148.93
0.8	4.61	4.70	172.21
1.0	-0.46	0.22	159.68
1.2	5.51	0.00	166.40
1.4	-0.47	0.22	161.27
1.6	-3.50	8.83	182.03
1.8	24.92	0.00	178.92
2.0	-3.11	2.03	169.94
2.2	2.94	12.00	189.38
2.4	13.30	0.00	190.92
2.6	-0.31	0.14	178.92
2.8	-6.69	11.83	189.76
3.0	26.09	0.00	206.96
3.2	2.74	0.00	195.83
3.4	-0.34	0.16	188.22
3.6	-2.49	10.02	204.68
3.8	6.33	0.14	212.25
4.0	11.72	0.00	211.12
4.2	15.07	0.00	208.47
4.4	8.47	0.00	200.49
4.6	-13.62	11.54	181.26
4.8	6.24	26.40	198.20
5.0	1.92	10.81	193.99

Table C.3 - Example of Results from Test 6

Time After Boiling Inception	Flow Rate ($10^{-4} ft^3/sec$)	Calculated Bubble Length (In)	Temperature At First TC Down-stream of Heater (°F)
0.0	-0.03	0.00	78.12
0.2	-0.84	0.92	81.55
0.4	-0.27	3.14	152.63
0.6	21.99	0.00	156.22
0.8	-0.52	0.49	148.24
1.0	0.02	2.80	155.42
1.2	10.99	0.00	154.23
1.4	-1.18	1.09	152.63
1.6	1.99	1.78	163.04
1.8	4.51	0.00	162.56
2.0	-1.81	1.93	160.58
2.2	11.92	0.00	175.13
2.4	1.33	0.00	163.75
2.6	-0.84	1.16	170.83
2.8	10.56	0.00	166.90
3.0	-0.26	0.14	160.98
3.2	-0.30	2.38	178.95
3.4	-0.30	0.14	166.11
3.6	-0.18	1.26	163.35
3.8	5.73	0.00	158.60
4.0	0.18	0.12	155.03
4.2	-0.46	1.03	151.04
4.4	-0.45	3.84	168.47
4.6	2.21	0.00	161.38
4.8	1.97	0.00	159.40
5.0	-0.26	0.17	154.63

Table C.4 - Example of Results from Test 7

Time After Boiling Inception	Flow Rate ($10^{-4} ft^3/sec$)	Calculated Bubble Length (In)	Temperature At First TC Downstream of Heater (°F)
0.0	0.02	0.00	99.56
0.2	-0.03	0.53	105.85
0.4	-0.52	0.42	110.43
0.6	-0.10	0.05	115.91
0.8	-1.02	1.13	131.02
1.0	-0.15	0.07	141.56
1.2	-0.14	0.18	164.30
1.4	16.88	0.00	160.35
1.6	-3.69	3.52	155.59
1.8	31.88	0.00	173.73
2.0	-0.86	0.62	149.68
2.2	-2.90	7.32	161.14
2.4	27.07	0.00	163.91
2.6	-2.07	1.55	149.20
2.8	8.53	3.71	182.30
3.0	1.47	0.00	163.51
3.2	-2.82	4.48	165.09
3.4	8.60	0.00	179.27
3.6	-0.15	0.07	170.20
3.8	-1.46	2.74	169.42
4.0	8.53	0.00	172.95
4.2	-0.33	0.31	167.85
4.4	-0.14	1.57	177.24
4.6	25.50	0.00	176.07
4.8	-2.88	2.41	166.67
5.0	11.78	2.51	183.85

Table C.5 - Example of Results from Test 8

Time After Boiling Inception	Flow Rate ($10^{-4} ft^3/sec$)	Calculated Bubble Length (In)	Temperature At First TC Downstream of Heater (°F)
0.0	-0.03	0.00	116.64
0.2	-0.03	0.66	124.14
0.4	1.36	0.00	128.56
0.6	-1.73	1.38	158.75
0.6	13.36	0.00	174.50
1.0	-1.40	1.55	185.07
1.2	15.64	0.00	176.91
1.4	-2.65	2.12	171.05
1.6	24.70	0.00	178.86
1.8	-0.40	0.18	167.83
2.0	-2.10	8.81	187.77
2.2	15.96	0.00	183.52
2.4	-2.18	1.73	179.56
2.6	12.92	0.00	182.28
2.8	-0.12	0.13	178.78
3.0	-0.11	0.64	199.21
3.2	3.84	0.00	182.28
3.4	-4.77	6.14	186.54
3.6	19.92	0.00	193.47
3.8	4.23	0.00	209.09
4.0	-0.24	0.11	193.09
4.2	-6.59	8.83	197.00
4.4	19.34	0.00	207.66
4.6	7.04	0.00	211.44
4.8	-2.88	1.86	195.77
5.0	-0.26	10.50	205.76

Table C.6 - Example of Results from Test 9

Time After Boiling Inception	Flow Rate ($10^{-4} ft^3/sec$)	Calculated Bubble Length (In)	Temperature At First TC Downstream of Heater (°F)
1.0	-0.03	0.00	139.20
0.2	-3.62	2.82	146.53
0.4	-1.39	14.18	199.29
0.6	28.40	0.00	188.62
0.8	-1.46	1.34	187.38
1.0	8.00	1.04	174.96
1.2	7.31	0.00	171.91
1.4	-3.34	2.74	169.16
1.6	10.00	0.11	192.39
1.8	25.07	0.00	195.08
2.0	-5.90	4.19	172.61
2.2	-0.42	16.84	193.16
2.4	24.54	0.00	205.38
2.6	-0.37	0.22	190.85
2.8	-6.63	11.26	188.93
3.0	11.66	0.00	188.54
3.2	2.23	0.00	188.16
3.4	-0.66	0.55	186.30
3.6	-0.75	4.42	206.14
3.8	7.18	0.00	194.77
4.0	-1.81	1.68	188.54
4.2	4.35	1.24	210.00
4.4	13.43	0.00	211.43
4.6	-0.89	0.44	186.61
4.8	-7.25	13.33	185.45
5.0	46.76	0.00	209.17

Table C.7 - Example of Results from Test 10 (Forced Convection)

Time After Boiling Inception	Temperature at First TC Downstream of Heater (°F)
0.0	165.39
0.2	167.35
0.4	169.71
0.6	171.67
0.8	175.58
1.0	179.09
1.2	179.79
1.4	181.42
1.6	186.46
1.8	180.65
2.0	185.68
2.2	180.65
2.4	187.54
2.6	194.16
2.8	194.92
3.0	178.62
3.2	174.02
3.4	185.68
3.6	180.18
3.8	199.06
4.0	184.14
4.2	204.08
4.4	194.92
4.6	210.90
4.8	212.79
5.0	218.06

APPENDIX D

CALCULATION OF CONDENSATION HEAT TRANSFER COEFFICIENTS

D.1 Calculational Method

Results from the reduction of the experimental data were used to estimate the magnitude of the condensation heat transfer coefficient during different stages of the bubble growth-collapse cycle. These calculated heat transfer coefficients were then used as a guide to the selection of input parameters to the model.

The only assumption that was made for these calculations was that the upper and lower halves of the bubble were approximately equal in length. An assumption of this sort was necessary due to the unreliable flow rate readings from the upper ΔP cell. The assumption of equal lengths was chosen because of the approximately equal inertances of the two halves of the loop (see Chapter 2). Although the lower loop contains all of the bypass and downcomer piping, the fact that most of this piping was approximately six times the diameter of the primary side (and therefore 36 times the area) means that the relative contribution of this piping to the loop inertance was quite small.

Using this assumption, calculations were performed for each of the stagnant flow experiments during bubble growth and collapse. Examples of these calculations are shown in the remainder of this Appendix. The reasons for the large change in magnitude of the heat transfer coefficient have been fully explored in Chapter 5.

For Test 4

Data Taking Conditions

$\Delta t = 0.04$

Test Conditions $P = 0.544$ kw $= 1857.2$ BTU/hr

At $t = 12.32$ sec, Bubble is growing

$p = 18.63$ psia $\rightarrow T_{sat} \cong 223°F$, $\rho_g \cong 0.045$ lbm/ft^3,

$h_{fg} \cong 963$ BTU/lbm

$T_{liq} = 192°F \rightarrow \Delta t = 31°F$

$L_1 = 13.08"$, $Q_1 = 15.23 \times 10^{-4}$ ft^3/sec

Assume

$L_1 = L_2$		$L = 26.16"$
$Q_1 = Q_2$	Thus	$V = 2.29 \times 10^{-4}$ ft^3
$A_1 = A_2$		$A = 3.98 \times 10^{-2}$ ft^2
$\alpha = 1/C_o$		

Since $\frac{V}{\rho}\frac{d\rho}{dt} = \frac{V}{\rho}\frac{dp}{dt}\frac{d\rho}{dp}$; $\Delta p = -0.21$ psi, $\frac{d\rho}{dp}$ 0.002 lbm/ft^3/psi

$$Q_s = Q_1 + Q_2 + A_{com} = 2(15.23\times10^{-4}) + \frac{2.29}{0.045} \cdot \left(\frac{-0.21)(0.002)}{0.04}\right) =$$

$$2.99 \times 10^{-3} \text{ft}^3/\text{sec}$$

$$\dot{q}_s = \rho_g\, h_{fg}\, Q_s = (2.99\times10^{-3})(0.045)(963)(3600) = 466.9 \frac{BTU}{hr}$$

$$\dot{q}_{evap} = (L_{1/L_{HTR}})\ P = \left(\frac{13.08}{36}\right) 1857.2 = 674.8 \frac{BTU}{hr}$$

$$\dot{q}_{con} = \dot{q}_{evap} - \dot{q}_s = 207.9 \ \frac{BTU}{hr}$$

$$h_{con} = \dot{q}_{con}/_{A\Delta T} = \frac{207.9}{(3.98x10^{-2})(31)} = 168.5 \ \frac{BTU}{hrft^2 °F}$$

At t = 14.76 sec, Bubble is collapsing

$$p = 16.52 \text{ psia} \rightarrow T_{sat} \cong 220°F, \ \rho_g \cong 0.041 \ lbm/ft^3,$$

$$h_{fg} \cong 965 \ \frac{BTU}{lbm}$$

$$T_{liq} = 214.5 \ °F \rightarrow \Delta T \simeq 5.5 \ °F$$

$$L_1 = 6.48'' \ , \ Q_1 = -0.34 \ ft^3/sec, \ \Delta p = -0.04 \ psi,$$

$$\frac{d\rho}{dp} = 0.0023 \ \frac{lbm/ft^3}{psi}$$

Same assumptions are made,

Thus $V = 1.1 \times 10^{-4} \ ft^3$

$A = 1.98 \times 10^{-2} \ ft^3$

$$Q_s = -0.68x10^{-4} + \left(\frac{1.1x10^{-4}}{0.041}\right)\left(\frac{0.0023}{-0.04}\right) = -7.42x10^{-5} \ \frac{ft^3}{sec}$$

$$\dot{q}_s = (-7.42x10^{-5})(0.041)(965)(3600) = 10.6 \ \frac{BTU}{hr}$$

$$\dot{q}_{evap} = \left(\frac{6.48}{36}\right) 1857.2 = 334.3 \ \frac{BTU}{hr}$$

$$\dot{q}_{con} = \dot{q}_{evap} - \dot{q}_s = 344.9 \ BTU/hr \rightarrow h_{con} = 344.9/[1.98x10^{-2})(5.5)]$$

$$= 3167.1 \ \frac{BTU}{hrft^2 °F}$$

APPENDIX E

COMPUTER INPUT AND OUTPUT

E.1 Contents of the Appendix

This appendix contains a copy of the FLOSS computer code, a sample input to the code, and a sample of output from the code, as printed out by the computer.

E.2 The FLOSS Code

```
C  ************PROGRAM FLOSS**********************
C ******WRITTEN BY [illegible]******************
C ********M.I.T. NUCLEAR ENGINEERING DEPARTMENT************
C*********ANNOTATED NOVEMBER, 1979**********************
C*********ANNOTATIONS UPDATED, JANUARY, 1980****************
C
C
C        THIS PROGRAM CALCULATES THE GROWTH AND OSCILLATION OF A
C        VAPOR AREA IN A TEST SECTION WHICH SIMULATES A
C        ROD BUNDLE IN AN LMFBR.  THE THERMAL AND INERTIAL
C        EFFECTS ON THE SURFACES ARE BALANCED TO FIND THE POSITION OF
C        THE INTERFACES AT EACH TIME STEP.
C        THE CODE CONTAINS THE OPTION OF USING EITHER SODIUM
C        OR WATER PROPERTIES.  IT ALSO CALCULATES THE TEMPERATURE
C        PROFILE AS A FUNCTION OF TIME IN THE UPPER
C        HEATED ZONE OF THE TEST SECTION.
C        THE CURRENT SET-UP HAS BEEN USED TO SIMULATE TESTS IN
C        THE MIT WATER TEST LOOP.
C  ***********************************************************************
C
       IMPLICIT DOUBLE PRECISION (A-H, O-Z)
       COMMON P(400),VVAP(400),RHOV(400),RHOL(400),VVAP1(400),
      1DT2(400),VVAP2(400),RI1(400),RI2(400),RI(400),R(2,400),
      2Q(2,400),XTEMP(2,400),XX1(2),XX2(2),XX3(2),XX4(2),Q2(400)
       COMMON QTOT(400),[illegible]1(400),XXCP1(400),CPG(400),CPI(400),
      1[illegible](400),[illegible]T1(400),TSAT(400),[illegible]2(400),[illegible]2(400),[illegible](400),
      2[illegible](400),[illegible](400),HTC[illegible](400),[illegible](400),[illegible],[illegible]
       COMMON VISCV(400),VISCL(400),PATM,ML,CZERO,[illegible],GC,
      1[illegible],[illegible](2,10), [illegible](2,10),[illegible](2,10),[illegible](2),[illegible](2,10),[illegible],
      2[illegible],[illegible](400),[illegible],K
       COMMON [illegible],TWALL(400),[illegible](400),CPS,DENS,[illegible],[illegible],
      1[illegible],VVAPI,[illegible],[illegible]
       COMMON [illegible],CLL,[illegible]
       COMMON/[illegible]/[illegible],XI[illegible](20),TI[illegible](20,400),[illegible],[illegible]
       COMMON/[illegible]/[illegible],TIME,[illegible]
       COMMON/CONV/IT,ITI[illegible],ILIM
       COMMON/SODIUM/[illegible]
       COMMON/RESTART/RESTRT
       COMMON/PRINT/[illegible](400),[illegible],[illegible],[illegible]
       CHARACTER*80 TITLE
C
C  ***********************************************************
C        INPUT TO THE CODE--READ FROM DATA FILE FOR005.DAT
C  *******************************************************************
C
C        INPUT THE TITLE OF THE RUN, UP TO 80 CHARACTERS
       READ(5,6200) TITLE
       WRITE(6,6200) TITLE
 6200 FORMAT(A80)
C
C
C        INPUT TIME STEP (SEC), TIME OF TRANSIENT (SEC), GRAVITATIONAL
C        CONSTANT, ATMOSPHERIC PRESSURE (PSIA), PRESSURE AT POINT OF
C        [illegible] FORMATION (PSIA), ORIFICE FLOW CONSTANT FOR TURBULENT
C        FLOW, TUBE RADIUS (INCHES), NUMBER OF [illegible] IN [illegible] 1
C        FOR PARALLEL RESISTANCE/IMPEDANCE CALCULATION,NO.OF ITERATIONS.
C        THE TRANSIENT TIME (INPUT #2) IS APPROXIMATE ONLY AND IS NOT
C        USED BY THE CODE.  THE FINAL INPUT CONTROLS THE NUMBER OF
C        ACTUAL ITERATIONS.  DUE TO THE VARIABLE TIME STEP FEATURE,
C        THE TOTAL TRANSIENT TIME CANNOT BE SPECIFIED A PRIORI.
       READ(5,100) DT1,TIME,GC,PATM,[illegible],CZERO,RTUBE,ML
```

```
     1,NTLIM
 100 FORMAT(7F10.5,2I5)
C
C
C     INPUT WATER TEMPERATURE (NOT USED), CONDENSATION
C     HEAT TRANSFER COEFFICIENT, TUBE POWER (KW), TUBE THICKNESS (IN),
C     DENSITY OF TUBE WALL MATERIAL(LB/CU FT), SPECIFIC HEAT OF WALL
C     MATERIAL (BTU/LB-F), WALL HEAT TRANSFER COEFFICIENT, HEAT
C     TRANSFER OPTION FLAG.  ALL HEAT TRANSFER COEFFICIENTS ARE IN
C     BTU/HR/SQ FT-F.  SEE SUBROUTINE HTCOEF FOR EXPLANATION OF OPTIONS.
C     LAST PARAMETER IS NO. OF ITERATIONS FOR TIME STEP SIZE.
      READ(5,100) TWAT,HTCO,POWER,DELP,DENS,CPS,HWTCO,KHT
     1,NTLIMT
  20  FORMAT(3F10.5,2I5)
C
C
C     INPUT NUMBER OF COMPONENTS IN EACH LEG.  LEG 1 IS THE LOWER
C     LEG AND INCLUDES THE HEATER AND ALL SECONDARY LOOPS.  LEG 2 IS THE UPPER AND
C     INCLUDES THE  UPPER UNHEATED ZONE AND UPPER PLENUM ONLY.  HTRL IS THE
C     HEATED LENGTH IN FEET.
      READ(5,300) (NCOMP(I),I=1,2),HTRL
 300 FORMAT(2I4,F10.4)
      DO 10 I=1,2
      K=NCOMP(I)
      DO 10 J=1,K
C      INPUT THE PIPE DIAMETER, EQUIVALENT RESISTANCE OF ELBOWS (L/D)
C      PIPE LENGTH, AND ANY ADDITIONAL RESISTANCES IN L/D'S
C      FOR EACH COMPONENT IN EACH LOOP.  DIAMETERS AND LENGTHS ARE IN
C      FEET.
      READ(5,400) ETOI(I,J),EL(I,J),PIL(I,J),ADDR(I,J)
 400 FORMAT(4F10.5)
  10 CONTINUE
C
C
C      INPUT  INITIAL BUBBLE LENGTH AND VAPOR VOLUME (TCNII)
C      AND TWO MULTIPLIERS FOR THE FRICTION IN EACH LEG.
C      VVAPIG=BLIG*(BUBBLE CROSS SECTIONAL AREA),
C      AND THAT IS THE ONLY CONSTRAINT.  ADJUST
C      THE TWO MULTIPLIERS TO SIMULATE THE INITIAL STEADY S.
      READ(5,500) BLIG,VVAPIG,FVM1,FVM2
 500 FORMAT(4F10.7)
C
C
C     INPUT THE CONVERGENCE LIMITS FOR THE FLOWRATE
C     ITERATIONS AND THE BUBBLE LENGTH AND VAPOR VOLUME ITERATIONS.
C     INPUT THE ITERATION NUMBER LIMITS FOR NONCONVERGENCE TESTING.
      READ(5,600) FCL,CLI,CLH,ITLIM,IPLIM
 600 FORMAT(3F10.5,2I5)
C
C
C      INPUT NUMBER OF NODES FOR TEMPERATURE PROFILE CALCULATIONS
      READ(5,9000) NT
9000 FORMAT(I5)
      DO 9100 I=1,NT
C      INPUT LENGTH (FT) AND TEMPERATURE (DEG F) OF EACH NODE
      READ(5,9200) XIT(I),TIIQ(I,1)
9200 FORMAT(2F10.5)
9100 CONTINUE
C      INPUT UPPER AND LOWER PLENUM TEMPERATURES (CONSTANT THROUGH TRANSIENT)
      READ(5,9200) TPLENU,TPLENL
C
```

```
C
C     INPUT NUMBER OF PLOTS DESIRED.  KPIT = 1
C     GIVES FLOW RATE VS TIME; =2 GIVES 1 AND PRESSURE VS TIME;
C     = 3 GIVES 2 AND TOTAL BUBBLE LENGTH VS TIME; = 4 GIVES 3 AND
C     INDIVIDUAL BUBBLE LENGTHS VS TIME.
      READ(5,700) KPIT
C
C
C     INPUT SODIUM FLAG:  NA=0 FOR WATER PROPERTIES, NA=1
C     FOR SODIUM PROPERTIES.
      READ(5,700) NA
  700 FORMAT(I5)
C
C
C     SET UP OUTPUT HEADINGS. OUTPUT IS WRITTEN ONTO FILE FOR006.DAT
      WRITE(6,6000) DTI,KPT,CUTCO,POWER,PSTART
 6000 FORMAT(5X,'DTI=',F5.3,3X,'KPT=',I1,3X,'CUTCO='
     1,F .1,3X,'POWER=',F5.2,1X,'KW',3X,'PSTART=',F5.2)
      WRITE(6,6100) [illegible],CIL,CIH
 6100 FORMAT(5X,'ECI=',F5.3,5X,'CLL=',F5.3,5X,'CIH=',F5.3)
      WRITE(6,10000) (TITO(I,1),I=1,NT)
10000 FORMAT(/5X,'INITIAL TEMPERATURE PROFILE',7(3X,F9.3)/
     1,7(3X,F9.3)/,7(3X,F9.3))
      WRITE(6,15000) (/LT(I),I=1,NT)
15000 FORMAT(/5X,'X DEL  ARRANGEMENT, FT/NODE',7(3X,F7.3)/
     1,7(3X,F7.3)/,7(3X,F7.3))
      WRITE(6,5000)
 5000 FORMAT(//3X,'TIME',12X,'Q1',15X,'Q2',10X,'Q12',15X,'Q3',13X,
     1'QTOT',13X,'P',11X,'A1')
      WRITE(6,5100)
 5100 FORMAT( 8X,'BL1',10X,'BL2',15X,'BL',12X,'VVAP1',12X,'VVAP2',
     113X,'VVAP',11X,'A2')
C
C
C     SET INITIAL CONDITIONS FOR TRANSIENT AND CONVERT UNITS
      [illegible]=[illegible]*144.
      [illegible]=DTUBE/12.
      DELR=DTLR/12.
      CUTCO=CUTCO/3600.
      PATM=PATM*144.
      POWER=POWER*0.9484
      NSTEP=0
      ITFLG=0
      KTFLG=0
      TTIME=0.
C     ****************************************************
C
C     START TRANSIENT CALCULATION
      DO 1000 N=1,NTIM
      IF(NRSTRT.EQ.1) GO TO 11115
      IF(N.GT.1) GO TO 5
11115 P(N)=PSTART
      DT(N)=DTI
      IF(N.EQ.1) DT(N)=0.
      CALL PROP
      CALL PSSIN
      CALL HYDRO
      CALL HEAT
      CALL AREA
      GO TO 50000
    5 IF(NRSTRT.EQ.2) GO TO 55000
```

```
      IF(N.GT.2) GO TO 15
55000 P(N)=PSTART
      DT(N)=DTI
      VVALI=VVALIS
      RLI=RLIS
      CALL PROP
      GO TO 25
   15 NTMFLG=0
      DT(N)=DTI
   16 IF(NRSTRT.EQ.3) NRSTRT=0
      P(N)=P(N-1)
      CALL PROP
   25 I =0
      CALL HYDRO
      IF(IP.EQ.IPLIM.OR.IT.EQ.ITLIM) GO TO 4000
50000 TTIME=TTIME+DT(N)
50002 PP=P(N)/100.
C
C     AT THIS POINT, THE PRESSURE IN PSIA AND PSFA ARE WRITTEN ONTO
C     THE CRT SCREEN SO THAT THE USER MAY CHECK ON THE PROGRESS OF
C     THE SIMULATION.
      TYPE *, PP,P(N)
C
C     WRITE THE DATA FOR THE TIME STEP ONTO THE OUTPUT FILE.
      WRITE(6,2000) TTIME,(Q(I,N),I=1,2),Q12(N),Q3(N),QTOT(N),PP,
     1[illegible]1(N)
      WRITE(6,2100) FL1(N),FL2(N),RL(N),VVAP1(N),VVAP2(N),VVAP(N),
     1A[illegible]2(N)
 2000 FORMAT(//1X,F6.3,5(7X,E10.3),7X,F6.3,5X,E10.3)
 2100 FORMAT(5X,E10.3,5(7X,E10.3),4X,E10.3)
      IF(KTFLG.EQ.1) GO TO 12005
      IF([illegible].EQ.1.AND.IPFLG.EQ.1) GO TO 12001
      IF(NRSTRT.EQ.2) NRSTRT=3
      IF(NRSTRT.EQ.1) NRSTRT=2
12005 IF(KTFLG.EQ.1)KTFLG=0
 1000 [illegible]
      [illegible]=NTLIM
      GO TO 31000
C
C
C      VARIABLE TIME STEP ROUTINE--DIVIDES BY SUCCESSIVE FACTORS OF 2.0
 4000 NTMFLG=NTMFLG+1
      XT=FLOAT(NTMFLG)
      DT(N)=DT(N)/(2.**XT)
      IF(NTMFLG.GE.NTIMIT) GO TO 4100
      GO TO 16
 4100 NTMFLG=0
      KT[illegible]=1
      WRITE(6,8000) TTIME
 8000 FORMAT(//10X,'NO CONVERGENCE AT THIS TIME STEP',5X,'T=',F6.3)
      IF(TLIQ(1,N).GT.TSAT(N)) GO TO 11111
C
C     RESTART OPTION--IF CALCULATION FAILS TO CONVERGE AND THE FIRST
C     [illegible] TEMPERATURE IS LESS THAN SATURATION.
      WRITE(6,11112)
11112 FORMAT(/10X,'RESTART')
      NRSTRT=1
12001 IF(IP.LE.[illegible].1) ITFIT=0
      TLIQ(1,N)=(TLIQ(1,N-1)*XLT(1)+TSAT(N-1)*HTRL/(2.*FLOAT(NT)))
     1/(XLT(1)+HTRL/(2.*FLOAT(NT)))+((POWER*DT(N)/FLOAT(NT))/(RHOL(N-1)
     2*CPL(N-1)*3.14159*RTUBE*RTUBE*HTRL/FLOAT(NT)))
```

```
      IF(TLIQ(1,N).LT.TSAT(1)) ITFLG=1
      IF(TLIQ(1,N).GT.TSAT(1)) TLIQ(1,N)=TSAT(1)
      DO 12003 KT=2,NT
      TLIQ(KT,N)=TLIQ(KT,N-1)
12003 CONTINUE
      IF(ITFLG.NE.1) GO TO 12004
      IF(KTFLG.EQ.1) GO TO 50000
      GO TO 1 00
12004 KTFLG=1
      GO TO 11115
11111 WRITE(6,11113)
11113 FORMAT(/10X,'EXPULSION OCCURS')
31000 WRITE(6,30000)
30000 FORMAT(/5X,'TRANSIENT TEMPERATURE PROFILES')
      TTIME=0.
      DO 20000 N=1,NPLTN
      TTIME=TTIME+DT(N)
      WRITE(6,25000) TTIME,(TLIQ(I,N),I=1,NT)
25000 FORMAT(//5X,7(3X,F9.3)/,7(3X,F9.3)/,7(3X,F9.3))
20000 CONTINUE
C  ************************************************
C
C      PLOTTING LOGIC
      KPCNT=0
 7000 KPCNT=KPCNT+1
      IF(KPCNT.GT.KPLT) GO TO 3000
      CALL PLOTTER
      IF(KPLT.GT.1) GO TO 7000
 3000 STOP
      END
C
C
C
      SUBROUTINE HYDRO
      IMPLICIT DOUBLE PRECISION (A-H, O-Z)
C     BUBBLE HYDRODYNAMIC MODEL
      COMMON P(400),VVAI(400),Q10T(400),QHOT(400),VVAP1(400),
     1VAP2(400),VVAP2(400),RL1(400),RL2(400),RI(400),R(2,400),
     2Q(2,400),XINTR(2,400),XK1(2),XK2(2),XK3(2),XK4(2),Q3(400)
      COMMON QTOT(400),AREA1(400),XMCP1(400),CPG(400),CPI(400),
     1DCP1(400),HFAC1(400),TSAT(400),AREA2(400),DCP2(400),QSC(400),
     2TSAT2(400),HFG(400),RTOT(400),TCOND(400),RTUBE,EPACT
      COMMON VISCG(400),VISCL(400),PATM,NI,CZERO,CHTCP,CC,
     1IJ,PIDI(2,10),RI(2,10),RII(2,10),NCOMP(2),ANIB(2,10),KNT,
     2[illegible],IP,XMCP2(400),CPJOB,N
      COMMON DEIP,TWALL(400),CPWALL(400),CPS,DENS,VHTCO,HTPL,
     1RLI,VVAPI,QV1,QV2
      COMMON ECI,CII,CIH
      COMMON/CONV/IT,ITLIM,IPLIM
      COMMON/RESTART/NRSTRT
      COMMON/TRANS/DT(400),TTIME,DTI,NTLIM
      IF(NRSTRT.EQ.1) GO TO 11200
      IF(N.GT.1) GO TO 3100
C   INITIALIZATION OF VOLUMETRIC FLOW RATES AND VAPOR VOLUMES AND LENGTHS
11200 DO 200 L=1,2
      Q(L,N)=0.
  200 CONTINUE
      VVAP1(N)=0.
      VVAP2(N)=0.
      VVAP(N)=0.
      RL1(N)=0.
```

```
      BI2(N)=0.
      Q12(N)=0.
      Q3(N)=0.
      QTOT(N)=0.
      GO TO 40
 3000 IC=0
      IT=
 4000 P(N)=P(N-1)
      IT=IT+1
      IF(IT.EQ.ITLIM) GO TO 55
      CALL PROP
      IP=0
 1000 DELP=P(N)-PATM-((PTL(2,1)+PTL(2,2)-BL2(N))*RHOL(N))
      IC=IC+1
      IF(IP.GT.0) GO TO 25
      VVAP(N)=VVAPI
      BL(N)=BLI
      IF(IC.GT.1) GO TO 20
      IF(NSSIMT.EQ.2) GO TO 50000
      IF(N.GT.2) GO TO 20
50000 VVAP1(N)=VVAPI*PVM1
      VVAP2(N)=VVAPI*PVM2
      BL1(N)=BLI*PVM1
      BL2(N)=BLI*PVM2
      VVAP1I=VVAP1(N)
      VVAP2I=VVAP2(N)
      BL1I=BL1(N)
      BL2I=BL2(N)
      AREA1(N)=3.14159*RTUBE*RTUBE/CZERO
      AREA2(N)=AREA1(N)
      IF(PVM2.EQ.0.) AREA2(N)=0.
      GO TO 25
   20 VVAP1(N)=VVAP1I
      VVAP2(N)=VVAP2I
      BL1(N)=BL1I
      BL2(N)=BL2I
      IF(BL1(N).EQ.0.) GO TO 25
      AREA1(N)=VVAP1(N)/BL1(N)
   25 IF(AREA2(N).EQ.0.) AREA2(N)=3.14159*RTUBE*RTUBE/CZERO
C
C
C     EXPLICIT FIRST ORDER FINITE DIFFERENCE SCHEME FOR CALCULATION OF
C     VOLUMETRIC FLOW RATES IN THE HYDRODYNAMIC MODEL.
      DO 100 L=1,2
      Q(L,N)=Q(L,N-1)+DT(N)*(DELP/XINER(L,N-1)-R(L,N-1)*Q(L,N-1)**2./
     1XI  Q(L,N-1))
  100 CONTINUE
      Q3(N)=VVAP(N)/RHOG(N)*(RHOG(N)-RHOG(N-1))/DT(N)
      Q12(N)=0.
C     Q12 IS THE CHANGE IN VAPOR VOLUME PER UNIT TIME
      DO 110 I=1,2
      Q12(N)=Q12(N)+Q(I,N)
  110 CONTINUE
      CALL RESIN
C
C     QTOT IS THE TOTAL HYDRODYNAMIC MODEL FLOW RATE
      QTOT(N)=Q12(N)+Q3(N)
C     CALCULATE THE THERMAL MODEL VOLUMETRIC FLOW RATE FOR COMPARISON
      CALL HEAT
C     CALCULATE THE ERROR BETWEEN THE TWO MODEL CALCULATIONS
      ETST=ABS(QTOT(N))+ABS(QTS(N))
```

```
      IF(ETST.LE.1.0E-30) ETST=1.0E-30
      ERROR=2.0*(QTOT(N)-QGE(N))/ETST
      IF(ABS(ERROR).LE.ECL) GO TO 10
C
C     IF THE ERROR IS LESS THAN THE ERROR CONVERGENCE LIMIT, CONTINUE
C     WITH THE CALCULATION BASED ON THE PRESSURE GUESSED.  IF THE
C     ERROR IS TOO LARGE, GUESS A NEW PRESSURE BASED ON THE ERROR
C     OF THE OLD ONE.
C
C
      CALL PGUESS
      P(N)=PG
      IF(IP.EQ.IPLIM) P(N)=P(N-1)
      IF(IP.EQ.IPLIM) GO TO 55
      CALL PROP
      GO TO 1000
C     CALCULATE NEW VALUES OF THE VAPOR VOLUME AND BUBBLE LENGTH
   10 VVAP(N)=VVAP(N-1)+(Q12(N)*DT(N))
      IF(VVAP(N).LT.0.) VVAP(N)=0.
      VVAP1(N)=VVAP1(N-1)+(Q(1,N)*DT(N))
      VVAP2(N)=VVAP2(N-1)+(Q(2,N)*DT(N))
      CALL AREA
      IF(AREA1(N).EQ.0.) GO TO 60
      BL1(N)=VVAP1(N)/AREA1(N)
      GO TO 80
   60 BL1(N)=0.
   80 IF(AREA2(N).EQ.0.) GO TO 70
      BL2(N)=VVAP2(N)/AREA2(N)
      GO TO 40
   70 BL2(N)=0.
   40 BL(N)=BL1(N)+BL2(N)
      IF(BL(N).LE.0.) BL(N)=0.
      IF(VVAP1(N).GT.0.0.AND.VVAP2(N).GT.0.0) GO TO 50
      IF(VVAP1(N).LE.0.) GO TO 150
      IF(VVAP2(N).LT.0.) GO TO 160
  150 VVAP1(N)=0.
      BL1(N)=0.
      BL2(N)=BL(N)
      VVAP2(N)=VVAP(N)
      IF(N.EQ.1.OR.NRSTRT.EQ.1) GO TO 55
      GO TO 50
  160 VVAP2(N)=0.
      BL2(N)=0.
      BL1(N)=BL(N)
      VVAP1(N)=VVAP(N)
   50 IF(N.EQ.1.OR.NRSTRT.EQ.1) GO TO 55
      IF(BL1I.EQ.0.) GO TO 101
C
C     COMPARE THE GENERATED VALUES OF BUBBLE LENGTH AND VAPOR
C     VOLUME TO THOSE GUESSED.  IF THEY FALL WITHIN THE BAND BETWEEN
C     THE HIGH AND LOW CONVERGENCE LIMITS, INCREMENT THE TIME AND
C     PROCEED WITH THE CALCULATION.  IF THEY ARE OUTSIDE OF THE BAND,
C     GUESS NEW VALUES AND CONTINUE TO ITERATE.
C
      IF((BL1(N)/BL1I).GE.CLL.AND.(BL1(N)/BL1I).LE.CLH) GO TO 102
      GO TO 111
  101 IF(BL1(N).EQ.BL1I) GO TO 102
      GO TO 111
  102 IF(BL2I.EQ.0.) GO TO 103
      IF((BL2(N)/BL2I).GE.CLL.AND.(BL2(N)/BL2I).LE.CLH) GO TO 104
      GO TO 111
```

```
      103 IF(PL2(N).EQ.PL2I) GO TO 104
          GO TO 111
      104 IF(BLI.EQ.0.) GO TO 105
          IF((BL(N)/BLI).GE.CIL.AND.(BL(N)/BLI).LE.CIH) GO TO 106
          GO TO 111
      105 IF(BL(N).EQ.BLI) GO TO 106
          GO TO 111
      106 IF(VVAP1I.EQ.0.) GO TO 107
          IF((VVAP1(N)/VVAP1I).GE.CIL.AND.(VVAP1(N)/VVAP1I).LE.CIH)
         1GO TO 108
          GO TO 111
      107 IF(VVAP1(N).EQ.VVAP1I) GO TO 108
          GO TO 111
      108 IF(VVAP2I.EQ.0.) GO TO 109
          IF((VVAP2(N)/VVAP2I).GE.CLL.AND.(VVAP2(N)/VVAP2I).LE.CIH)
         1GO TO 112
          GO TO 111
      109 IF(VVAP2(N).EQ.VVAP2I) GO TO 112
          GO TO 111
      112 IF(VVAPI.EQ.0.) GO TO 113
          IF((VVAP(N)/VVAPI).GE.CLL.AND.(VVAP(N)/VVAPI).LE.CLH)
         1GO TO 55
          GO TO 111
      113 IF(VVAP(N).EQ.VVAPI) GO TO 55
      111 PLI=(PL(N)+PLI)/2.
          PL1I=(PL1(N)+PL1I)/2.
          PL2I=(PL2(N)+PL2I)/2.
          VVAPI=(VVAP(N)+VVAPI)/2.
          VVAP1I=(VVAP1(N)+VVAP1I)/2.
          VVAP2I=(VVAP2(N)+VVAP2I)/2.
          GO TO 4000
       55 RETURN
          END
C
C
C
          SUBROUTINE [illegible]
          IMPLICIT DOUBLE PRECISION (A-H, O-Z)
          [illegible](4  ),VVAP(400),[illegible](400),[illegible](400),VVAP1(400),
         1VAP2(400),VVAP2(400),BL1(400),PL2(400),PL(400),[illegible](2,400),
         2[illegible](2,400),[illegible](2,400),XK1(2),XK2(2),XK3(2),[illegible](2),[illegible](400)
         [illegible](400),[illegible](400),[illegible](400),CPS(400),CPI(400),
         1[illegible](  ),[illegible](4  ),[illegible](400),[illegible](400),[illegible](400),[illegible](400),
         2[illegible](400),[illegible](400),[illegible](400),[illegible](400),[illegible],[illegible]
          [illegible] VISCP(400),VISC[illegible](400),[illegible],[illegible]L,[illegible],[illegible],[illegible],
         1[illegible],[illegible](2,10),[illegible](2,10),PII(2,10),[illegible](2),[illegible](2,10),K[illegible]T,
         2[illegible],IP,[illegible](400),[illegible],N
          COMMON DELT,TWALL(400),TPWALL(400),TPS,DENS,WHTCO,HTPL,BII,
         1VV[illegible]I,VV1,VV2
          COMMON /[illegible]/IT,XLT(20),TII(20,400),TPLENU,TPLENL
          COMMON /[illegible]START/[illegible]STRT
          COMMON /TRANS/[illegible](400),TTIME,DTI,NTLIM
          DIMENSION XLTT(21),[illegible](400)
C [illegible] THERMAL MODEL
C [illegible]
          [illegible]=0.
          [illegible]=0.
          I[illegible]=0
          IF([illegible].EQ.1) GO TO 11300
          IF(N.GT.1) GO TO 10
    11300 TWALL(N)=TSAT(N)+POWER/(WHTCO*3.14159*2.0*RTUBE*HTPL)
```

```
      GO TO 50
   10 DP=(P(N)-P(N-1))/779.
C     CALCULATE THE AMOUNT OF HEAT THAT GOES INTO THE HEATER WALL
      CPWALL(N)= DL1(N)*2.0*3.14159*RTUBE*DELR*DENS*CPS
                     CPWALL(N-1)=CPWALL(N)
      TPWP=POWER*DL1(N)/HTPL
      IF(DL1(N).GT.HTPL) TPWR=POWER-(HTCO(N-1)*(TSAT(N)-TLIF[illegible])*
     1(3.14159*D[illegible]S*RGAS+(2.0*3.14159*RGAS*(DL1(N)-HTPL))))
      P[illegible]V=TPWP
   20 ITEMP=ITEMP+1
      IF(ITEMP.GE.50) GO TO 20000
      IF(DL1(N).EQ.0.) GO TO 80000
      TWALL(N)=TSAT(N)+TPWP/(HTCO*3.14159*2.0*RTUBE*DL1(N))
      GO TO 80001
80000 TWALL(N)=TWALL(N-1)
80001 DCPT=((CPWALL(N)*TWALL(N))-(CPWALL(N-1)*TWALL(N-1)))/DT(N)
      TOTP=TPWR+DCPT
      RAT=TOTP/PSAV
      IF(RAT.LT.0.99000) GO TO 45
      IF(RAT.GT.1.01) GO TO 55
      GO TO 30
   45 RAT1=RAT
      TPWRU=TPWR
      GO TO 35
   55 RATO=RAT
      TPWRO=TPWR
      GO TO 35
   35 IF(RATO.NE.0. .AND.RATU.NE.0.0) GO TO 65
      IF(RAT.EQ.0.) RAT=1.
      IF(RAT.GT.0.0.AND.RAT.LT.0.99) GO TO 40
      TPWR=TPWR/RAT
      IF(ABS(TOTP).GT.TPWR) TPWR=PSAV /ABS(RAT)-DCPT
      GO TO 20
   40 TPWR=TPWR+PSAV /1.0
      GO TO 20
   65 TPWR=(TPWRO+TPWRU)/2.
      GO TO 20
20000 TPWR=(TOTP+PSAV)/2.
   30 HTIN=TPWR
      RGAS=SQRT(AREA1(N)/3.14159)
      IF(RGAS.GT.RTUBE) RGAS=RTUBE
      HEAT1(N)=HTIN
C     CALCULATE THE VOLUMETRIC FLOW RATE IN THE NUMBER ONE
      QGS1(N)=(HEAT1(N)+(VVAP1(N)*DP/DT(N)))/(RHOG(N)*HFG(N))
      IF(VVAP1(N).LE.0.) QGS1(N)=HEAT1(N)/(RHOG(N)*HFG(N))
C *BUBBLE 2*
      CALL [illegible]
      IF(N.EQ.2) HTCO(N-1)=HTCO(N)
      TLIQ(NT+1,N)=TFLOWH
      XLTT(1)=0.
      ATUBE=3.14159*RTUBE*RTUBE
      DIFFA1=ATUBE-AREA2(N-1)
      DIFFA=ATUBE-AREA2(N)
      DVOL=ABS(PL2(N)-PL2(N-1))*AREA2(N)
      RGAS=SQRT(AREA2(N)/3.14159)
      IF(VVAP2(N).LE.0.) RGAS=0.
      IF(RGAS.EQ.0.) AREA2(N)=3.14159*RTUBE*RTUBE/CZERO
      NTT=NT+1
C   FIND OUT IN WHICH TEMPERATURE NODE THE BUBBLE INTERFACE IS
      DO 60 J=2,NTT
      XLTT(J)=XLTT(J-1)+XLT(J-1)
```

```
   80 CONTINUE
      DO 90 K=1,NT
      KMARK=K
      IF(BL2(N).GE.XLTT(K).AND.BL2(N).LT.XLTT(K+1)) GO TO 95
   90 CONTINUE
C
C     THE UPPER UNHEATED ZONE TRANSIENT TEMPERATURE PROFILE IS CALCULATED
C     IN THIS  SECTION.  THE TEMPERATURE IS BASED ON A VOLUME AVERAGED
C     NODAL TEMPERATURE, AND IS CALCULATED DIFFERENTLY DEPENDING ON WHETHER
C     THE BUBBLE IS INCREASING OR DECREASING IN SIZE, AND WHETHER IT
C     MOVES ACROSS A NODAL INTERFACE DURING ONE TIME STEP.
C
   95 NTMK(N)=KMARK
      IF(NTMK(N).GT.NTMK(N-1)) GO TO 100
      IF(NTMK(N).EQ.NTMK(N-1).AND.BL2(N).GT.BL2(N-1)) GO TO 110
      IF(NTMK(N).EQ.NTMK(N-1).AND.BL2(N).LE.BL2(N-1)) GO TO 105
      DO 120 L=1,NT
      IF(L.GT.NTMK(N-1)) GO TO 121
      IF(L.EQ.NTMK(N-1)) GO TO 122
      IF(L.EQ.NTMK(N)) GO TO 123
      IF(L.LT.NTMK(N)) GO TO 124
  121 TLIQ(L,N)=((TLIQ(L,N-1)*((XLT(L)*ATUBE)-DVOL))+(TLIQ(L+1,N-1)
     1*DVOL))/(XLT(L)*ATUBE)
      GO TO 125
  122 TLIQ(L,N)=((TLIQ(L,N-1)*(ATUBE*(XLT(L)-(BL2(N-1)-XLTT(L))-
     1(XLTT(L)-BL2(N)))))+((TLIQ(L,N-1)+((HTCO(N-1)*(TSAT(N-1)-TLIQ(L,N-
     21))*DT(N)*(3.14159*PGAS*PGAS+2.0*3.14159*PGAS*(BL2(N-1)-XLTT(L))))
     3/(DIFFA1*(BL2(N-1)-XLTT(L))*RHOL(N)*CPL(N)))))*DIFFA1*(BL2(N-1)
     4-XLTT(L)))+(TLIQ(L+1,N-1)*(3.14159*PGAS*PGAS*(BL2(N-1)-BL2(N)
     5))))/(XLT(L)*ATUBE)
      GO TO 125
  123 TLIQ(L,N)=((TLIQ(L,N-1)+(HTCO(N-1)*(TSAT(N-1)-TLIQ(L,N-1))*DT(N)*2.0
     1*3.14159*PGAS*XLT(L)/(DIFFA1*XLT(L)*RHOL(N)*CPL(N))))
     2*DIFFA1*(XLT(L)-(XLTT(L+1)-BL2(N)))+(TLIQ(L+1,N-1)*ATUBE*
     3(XLTT(L+1)-BL2(N))))/(ATUBE*(XLTT(L+1)-BL2(N))  +(DIFFA*(XLT(L)-
     4(XLTT(L+1)-BL2(N)))))
      GO TO 125
  124 TLIQ(L,N)=TLIQ(L,N-1)+(HTCO(N-1)*(TSAT(N-1)-TLIQ(L,N-1))*DT(N)*2.0
     1*3.14159*PGAS*XLT(L))/(DIFFA1*XLT(L)*RHOL(N)*CPL(N))

  125 IF(TLIQ(L,N).GT.TSAT(N)) TLIQ(L,N)=TSAT(N)
  120 CONTINUE
      GO TO 500
  105 DO 135 L=1,NT
      IF(L.GT.NTMK(N-1)) GO TO 131
      IF(L.EQ.NTMK(N-1)) GO TO 132
      IF(L.LT.NTMK(N-1)) GO TO 133
  131 TLIQ(L,N)=(TLIQ(L,N-1)*(XLT(L)*ATUBE-DVOL)+(TLIQ(L+1,N-1)*
     1DVOL))/(XLT(L)*ATUBE)
      GO TO 134
  132 TLIQ(L,N)=((TLIQ(L,N-1)*(XLTT(L+1)-BL2(N-1))*ATUBE)+(TLIQ(L+1,N-1)
     1*DVOL)+(TLIQ(L,N-1)+ HTCO(N-1)*(TSAT(N-1)-TLIQ(L,N-1))*DT(N)*(3.14159
     2*PGAS*PGAS+(2.0*3.14159*PGAS*(BL2(N-1)-XLTT(L))))/(DIFFA1*
     3(BL2(N-1)-XLTT(L))*RHOL(N)*CPL(N)))*(DIFFA1*(BL2(N-1)-XLTT(L))))
     4/(ATUBE*(XLTT(L+1)-BL2(N))+(DIFFA*(BL2(N)-XLTT(L))))
      GO TO 134
  133 TLIQ(L,N)=TLIQ(L,N-1)+(HTCO(N-1)*(TSAT(N-1)-TLIQ(L,N-1))*DT(N)*2.0
     1*3.14159*PGAS*XLT(L))/(DIFFA1*XLT(L))
  134 IF(TLIQ(L,N).GT.TSAT(N)) TLIQ(L,N)=TSAT(N)
  135 CONTINUE
      GO TO 500
```

```
  104 DO 145 I=1,NI
      IF(I.GT.NTMK(N)) GO TO 141
      IF(I.EQ.NTMK(N)) GO TO 142
      IF(L.LE.NTMK(N)) GO TO 143
  141 TLIQ(L,N)=(TLIQ(I,N-1)*(XLT(I)*ATUBE-DVOL)+TLIQ(L-1,N-1)*DVOL)
     1/(XLT(I)*ATUBE)
      GO TO 145
  142 TLIQ(I, )=(TLIQ(I,N-1)*(XLT(L)*ATUBE-DVOL)+TLIQ(I-1,N-1)*
     1(XLTT(I)-BL2( -1))*ATUBE+(TLIQ(I,N-1)+HTCO(N-1)*(TSAT(N-1)-
     2TLIQ(I,N-1))*DT(N)*(3.14159*RCB*RCAS+2.0*3.14159*RCAS*
     3(BL.(N)-XLTT(I)))/(DIFFA*(BL2(N)- LTT(I))*RHOL(N)*CPL(N)))
     4*(DIFFA*(BL2(N)-XLTT(I)))))/(ATUBE*(XLT(I)-(BL2(N)-XLTT(I)))+
     5( IFF)*(BL2(N)-XLTT(L))))
      GO TO 145
  143 TLIQ(I,N)=TLIQ(I,N-1)+HTCO(N-1)*(TSAT(N-1)-TLIQ(I,N-1))*DT(N)*
     12.0*3.14159*RCAS*XLT(I)/(DIFFA1*XLT(L)*RHOL(N)*CPL(N))
  145 IF(TLIQ(L,N).GT.TSAT(N)) TLIQ(I,N)=TSAT(N)
  146 CONTINUE
      GO TO 500
  110 DO 155 I=1,NT
      IF(I.GT.NTMK(N)) GO TO 151
      IF(I.EQ.NTMK(N)) GO TO 152
      IF(I.LT.NTMK( )) GO TO 153
  151 TLIQ(I,N)=(TLIQ(I,N-1)*(XLT(L)*ATUBE-DVOL)+TLIQ(I-1,N-1)*
     1DVOL)/(XLT(I)*ATUBE)
      GO TO 154
  152 TLIQ(I,N)=(TLIQ(I,N-1)*(XLTT(I+1)-BL2(N))*ATUBE +(TLIQ(I,N-1)
     1+ HTCO( -1)*(TSAT( -1)-TLIQ(I,N-1))*DT(N)*(3.14159*RCAS*RCAS+2.0*
     23.14159*RCAS*(BL2(N)-XLTT(I)))/(DIFFA*(BL2(N)-XLTT(I))*RHOL(N)
     3*CPL( )))*(DIFFA*(BL2(N)-XLTT(I)))))/(ATUBE*(XLTT(I+1)-BL2(N))
     4+(DIFFA*( LT(I)-(XLTT(I+1)-BL2(N)))))
      GO TO 154
  153 TLIQ(I,N)=TLIQ(I,N-1)+HTCO(N-1)*(TSAT(N-1)-TLIQ(L,N-1))*DT(N)*2.0
     1*3.14159*RCAS*XLT(I)/(DIFFA1*XLT(I)*RHOL(N)*CPL(N))
  154 IF(TLIQ(I,N).GT.TSAT(N)) TLIQ(I,N)=TSAT(N)
  155 CONTINUE
  500 HTIN=0.
      NTI=NTMK(N)
C     THE CONDENSATION HEAT OUTPUT FROM THE BUBBLE IS NOW CALCULATED
      DO 200 I=1, NI
      IF(I.EQ.NTI) GO TO 199
      HTIN=HTIN+HTCO(N)*(TLIQ(L,N)-TSAT(N))*2.0*3.14159*RCAS*XLT(I)
      GO TO 200
  199 HTIN=HTIN+HTCO(N)*(TLIQ(I,N)-TSAT(N))*(3.14159*RCAS*RCAS+
     12.0*3.14159*RCAS*(BL2(N)-XLTT(I)))
  200 CONTINUE
      HEAT2(N)=HTIN
C     CALCULATE THE VOLUMETRIC FLOW RATE IN TUBE NUMBER TWO
      QGS2(N)=(HEAT2(N)+(VAL2(N)*DP/DT(N)))/(RHOG(N)*HFG(N))
      IF(VVAR2( ).LE.0.) QGS2(N)=HEAT2(N)/(RHOG(N)*HFG(N))
   50 IF(N.EQ.1.OR.NESTIT.EQ.1) GO TO 70
C
C     CALCULATE THE TOTAL THERMAL MODEL FLOW RATE FOR COMPARISON
C     TO THAT CALCULATED BY THE HYDRODYNAMIC MODEL AND
C      RETURN TO SUBROUTINE "HYDRO."
C
      QG (N)=QGS1(N)+QGS2(N)
   70 RETURN
      END
C
C
```

```
C
      SUBROUTINE AR[illegible]
      IMPLICIT DOUBLE PRECISION (A-H, O-Z)
      COMMON Z(400),VVAP(400),RHOC(400),RHOI(400),VVAP1(400),
     1Q12(400),VVAP2(400),HT1(400),HT2(400),TI(400),F(2,400),
     2Q(2,400),XI[illegible](2,400),XK1(2),XK2(2),XK3(2),XK4(2),Q3(400)
      COMMON DT[illegible](400),AREA1(400),XMCP1(400),CPC(400),CPI(400),
     1QSS1(400),HEAT1(400),TSAT(400),AREA2(400),QSS2(400),QSS(400),
     2HEAT2(400),HFC(400),HTCP(400),TCO[illegible](400),RTUBE,EFECT
      COMMON VISCI(400),VISCC(400),PATM,XI,CZERO,[illegible]TCP,GC,
     1PC,PIDI(2,10),[illegible](2,10),PII(2,10),NCOMP(2),ADDB(2,10),KNT,
     2[illegible]OUR,IP,XMCP2(400),ERROR,N
      COMMON DELP,TWIII(400),T[illegible]IL(400),CPS,DENS,WHTCP
      COMMON/RESTART/RESTRT
      COMMON/TRANS/PP(400),TTIME,DTT,NTIIM
C
C
C     THIS ROUTINE CALCULATES THE AREA OF THE VAPOR SPACE
C     AT EACH TIME STEP.  SINCE THIS IS A FIXED REGIME MODEL,
C     AN ANNULAR FLOW REGIME IS ASSUMED.  ANY CHANGE IN
C     THE CROSS SECTIONAL AREA IS ACCOMPLISHED BY EVAPORATION.
C     THUS, THE AREA IS SET CONSTANT IN THE UNHEATED ZONE (NO
C     EVAPORATION), AND IS RECALCULATED IN THE HEATED ZONE
C     AT EACH TIME STEP.  THE CONSTANT VALUE ASSUMED, WHERE ONE
C     IS ASSUMED, IS EQUAL TO THE TUBE AREA DIVIDED BY THE
C     THE TURBULENT FLOW DRIFT FLUX CONSTANT, CZERO.
C
C
      IF([illegible].EQ.1) GO TO 20
      IF(RESTRT.EQ.1) GO TO 20
      IF(N.EQ.2.OR.RESTRT.EQ.2)    GO TO 5
      IF(VVAP1(N).LT.VVAP1(N-1)) GO TO 10
      IF(VVAP(N).EQ.0.) GO TO 20
      AREA1(N)=((VVAP1(N-1)*AREA1(N-1))+(VVAP1(N-1)*QSS(N)*[illegible](N)*RHOC(N)
     1/([illegible]S(N)*EL(N-1)))+((VVAP1(N)-VVAP1(N-1))*3.14159*RTUBE*RTUBE
     2/CZERO))/VVAP1(N)
      ATUB=3.14159*RTUBE*RTUBE
      IF(AREA1(N).GT.ATUBE) AREA1(N)=ATUBE
      GO TO 15
   10 AREA1(N)=AREA1(N-1)
      GO TO 15
    5 AREA1(N)=3.14159*RTUBE*RTUBE/CZERO
   15 AREA2(N)=3.14159*RTUBE*RTUBE/CZERO
      GO TO 50
   20 AREA1(N)=0.
      AREA2(N)=0.
   50 RETURN
      END
C
C
C
      SUBROUTINE [illegible]
      IMPLICIT DOUBLE PRECISION (A-H, O-Z)
      COMMON Z(400),VVAP(400),RHOC(400),RHOI(400),VVAP1(400),
     1Q12(400),VVAP2(400),HT1(400),HT2(400),HT(400),F(2,400),
     2Q(2,400),XI[illegible](2,400),XK1(2),XK2(2),XK3(2),XK4(2),Q3(400)
      COMMON DT T(400),AREA1(400),XMCP1(400),CPC(400),CPI(400),
     1QSS1(400),HEAT1(400),TSAT(400),AREA2(400),QSS2(400),QSS(400),
     2HEAT2(400),HTC(400),HTCP(400),TCO[illegible](400),RTUBE,EFECT
      COMMON VISCI(400),VISCC(400),PATM,XI,CZERO,[illegible]TCP,GC,
     1PC,PIDI(2,10),EI(2,10),PII(2,10),NCOMP(2),ADDB(2,10),KNT,
```

```
      2POWER,IP,YMCF2(400),ERROR,N
       COMMON DELP,TWALL(400),CPWALL(400),CPS,DENS,WHTCO
C
C
C     SUBROUTINE HTCOND CALCULATES THE CONDENSATION HEAT TRANSFER
C     COEFFICIENT USING ONE OF THREE OPTIONS.  THE FIRST OPTION,
C     SIGNIFIED BY THE INPUT VARIABLE KHT=1 (SEE COMMENTS AT BEGINNING
C     OF MAIN PROGRAM FOR INPUT FORMAT), USES THE NUMBER WHICH IS CHTCO IN
C     THE INITIAL DATA INPUT THROUGHOUT THE TRANSIENT.  EXPERIMENTAL EVIDENCE
C     INDICATES THAT THIS NUMBER IS IN THE RANGE OF 500-2000 BTU/HR-SQ FT-F
C     FOR WATER AND 8000-10000 BTU/HR-SQ FT-F FOR LIQUID SODIUM.
C     THE OPTION KHT=2 USES THE DITTUS-BOELTER CORRELATION TO CALCULATE A
C     COEFFICIENT ON THE BASIS OF FORCED CONVECTION TO THE VAPOR
C     IN AN ANNULAR FLOW PATTERN.  THIS OPTION HAS NOT PROVEN PARTICULARLY ACCURATE.
C     THE THIRD OPTION, AS NOTED IN THE BODY OF THE PROGRAM, CORRESPONDS
C     TO KHT=3, AND IS RESERVED FOR ANY OPTION THAT THE USER MIGHT DESIRE.
C     THE MOST DESIROUS MODEL IS PROBABLY A DETAILED CONDUCTION MODEL.
C
C
       IF(KHT.EQ.2) GO TO 5
       HTCO(N)=CHTCO
       GO TO 10
     5 IF(KHT.EQ.3) GO TO 10
       REG=ABS(Q(2,N)/AREA(N)*2.0*RTUBE*RHOG(N)/VISCG(N)*3600.)
       PRG=VISCG(N)*CPG(N)/TCONG(N)
       HTCO(N)=0.023*(REG**0.8)*(PRG**0.4)
       GO TO 10
C KHT=3--USER SUPPLIED OPTION FOR HTCO, E.G. CONDUCTION MODEL
    10 CONTINUE
       HTC (N)=HTCO(N)/3600.
    50 RETURN
       END
C
C
C
       SUBROUTINE GUESS
       IMPLICIT DOUBLE PRECISION (A-H, O-Z)
       COMMON P(400),VVAP(400),RHOG(400),RHOL(400),VVAP1(400),
      1P12(400),VVAP2(400),PI1(400),PI2(400),PI(400),Q(2,400),
      2Q(2,400),VTUBE(2,400),XK1(2),XK2(2),XK3(2),XK4(2),Q3(400)
       COMMON QTOT(400),ALFA1(400),XMCF1(400),CPG(400),CPL(400),
      1DQ1(400),HEAT2(400),TSAT(400),ALFA2(400),DES2(400),DGS(400),
      2HEAT2(400),HF(400),HFG(400),TCONG(400),RTUBE,FRACT
       COMMON VISCF(400),VISCG(400),PATM,EL,CZERO,CHTCO,CC,
      1EG,PIDI(2,10),EI(2,10),PII(2,10),NCOMP(2),APPR(2,10),KHT,
      2POWER,IP,YMCF2(400),ERROR,N
       COMMON DELP,TWALL(400),CPWALL(400),CPS,DENS,WHTCO
       COMMON/TRANS/DT(400),TTIME,DTI,TLIM
C
C
C     THIS ROUTINE GENERATES GUESSES FOR THE PRESSURE USED IN SUBROUTINE
C     HYDRO FOR CALCULATION OF THE FLOW RATE.  THE PROCEDURE USED IS
C     EXPLAINED FULLY IN THE THESIS.  BRIEFLY, A NEWTON'S METHOD
C     OF SUCCESSIVE LINEAR APPROXIMATIONS BASED ON THE ERROR BETWEEN THE
C     HYDRODYNAMIC AND THERMAL MODEL FLOW RATES IS USED
C     TO GENERATE THE GUESSES.
C
C
       IF(IP.GE.1) GO TO 10
       ERRPOS=0.
       ERRNEG=0.
```

```
C
      SUBROUTINE AREA
      IMPLICIT DOUBLE PRECISION (A-H, O-Z)
      COMMON Z(400),VVAP(400),RHOG(400),RHOI(400),VVAP1(400),
     1DT2(400),VVAP2(400),HT1(400),HT2(400),IT(400),F(2,400),
     2P(2,400),ZIN2(2,400),YK1(2),YK2(2),YK3(2),YK4(2),Q3(400)
      COMMON QTOT(400),AREA1(400),YMOD1(400),CPG(400),CPI(400),
     1QS1(400),HEAT1(400),TSAT(400),AREA2(400),QSS2(400),QSS(400),
     2HEAT2(400),HFG(400),HTC2(400),TCONC(400),RTUBE,EFFCT
      COMMON VISCG(400),VISCI(400),PATM,XI,CZERO,CHTCO,GC,
     1PC,PIDT(2,10),E(2,10),PII(2,10),NCOMP(2),ADDR(2,10),KNT,
     2ZOPLR,IT,YMOD2(400),ERROR,N
      COMMON PAIR,TWALL(400),TOWALL(400),CPS,DENS,WHTCO
      COMMON/RESTART/RESTRT
      COMMON/TRANS/DT(400),TTIME,DTT,NTIM
C
C
C     THIS ROUTINE CALCULATES THE AREA OF THE VAPOR SPACE
C     AT EACH TIME STEP.  SINCE THIS IS A FIXED REGIME MODEL,
C     AN ANNULAR FLOW REGIME IS ASSUMED.  ANY CHANGE IN
C     THE CROSS SECTIONAL AREA IS ACCOMPLISHED BY EVAPORATION.
C     THUS, THE AREA IS SET CONSTANT IN THE UNHEATED ZONE (NO
C     EVAPORATION), AND IS RECALCULATED IN THE HEATED ZONE
C     AT EACH TIME STEP.  THE CONSTANT VALUE ASSUMED, WHERE ONE
C     IS ASSUMED, IS EQUAL TO THE TUBE AREA DIVIDED BY THE
C     THE TURBULENT FLOW DRIFT FLUX CONSTANT, CZERO.
C
C
      IF(N.EQ.1) GO TO 20
      IF(RESTRT.EQ.1) GO TO 20
      IF(N.EQ.2.OR.RESTRT.EQ.2)     GO TO 5
      IF(VVAP1(N).LT.VVAP1(N-1)) GO TO 10
      IF(VVAP(N).EQ.0.) GO TO 20
      AREA1(N)=((VVAP1(N-1)*AREA1(N-1))+(VVAP1(N-1)*QSS(N)*DT(N)*RHOG(N)
     1/( [illegible](N)*[illegible](N-1)))+((VVAP1(N)-VVAP1(N-1))*3.14159*RTUBE*RTUBE
     2/( [illegible])))/VVAP1(N)
      ATUB =3.14159*RTUBE*RTUBE
      IF(AREA1(N).GT.ATUBE) AREA1(N)=ATUBE
      GO TO 15
   10 AREA1(N)=AREA1(N-1)
      GO TO 15
    5 AREA1(N)=3.14159*RTUBE*RTUBE/CZERO
   15 AREA2(N)=3.14159*RTUBE*RTUBE/CZERO
      GO TO 50
   20 AREA1(N)=0.
      AREA2(N)=0.
   50 RETURN
      END
C
C
C
      SUBROUTINE HTCOEF
      IMPLICIT DOUBLE PRECISION (A-H, O-Z)
      COMMON Z(400),VVAP(400),RHOG(400),RHOI(400),VVAP1(400),
     1DT2(400),VVAP2(400),HT1(400),HT2(400),HT(400),F(2,400),
     2P(2,400),ZIN2(2,400),YK1(2),YK2(2),YK3(2),YK4(2),Q3(400)
      COMMON QTOT(400),AREA1(400),YMOD1(400),CPG(400),CPI(400),
     1QS1(400),HEAT1(400),TSAT(400),AREA2(400),QSS2(400),QSS(400),
     2HEAT2(400),HFG(400),HTC2(400),TCONC(400),RTUBE,EFFCT
      COMMON VISCG(400),VISCI(400),PATM,XL,CZERO,CHTCO,GC,
     1PC,PIDI(2,10),EI(2,10),PII(2,10),NCOMP(2),ADDR(2,10),KNT,
```

```
C
C
C     THIS ROUTINE CALCULATES RESISTANCES AND INERTANCES FOR INPUT TO SUBROUTINE
C     HYDRO.  THE INPUT IS EXPLAINED IN THE COMMENTS PREFATORY TO THE
C     MAIN PROGRAM.  TO REVIEW, THE LENGTH AND DIAMETER OF EACH COMPONENT
C     IN THE SYSTEM ARE INPUT.  IN ADDITION, ANY ELBOWS CONTAINED
C     IN A COMPONENT ARE REPRESENTED BY THE TERM FI, IN EQUIVALENT
C     L/D'S, AND ANY ADDITIONAL RESISTANCE IN A COMPONENT (FLOW
C     ORIFICES, STALLED PUMP, ETC.)IS REPRESENTED BY THE TERM ADDR,
C     ALSO IN EQUIVALENT L/D'S.  THE COMPONENT NUMBERING SYSTEM
C     MUST BE FOLLOWED AS EXPLAINED IN THE THESIS IN ORDER FOR THE
C     CALCULATION OF EQUIVALENT LOOP RESISTANCES AND INERTANCES TO BE DONE
C     BY THE CODE.  ANY DEVIATION FROM THIS SCHEME WILL CAUSE ERRONEOUS RESULTS.
C
C
      DIMENSION XINT(2,10),XR(2,10),RBASE(2),RPAR(2),BASEI(2),PARI(2)
      DO 1000 I=1,2
      JI= COMP(I)
      DO 1000 K=1,JI
      CALL FFACTR(I,K)
      C  R=32.0*ET*(*F  T(*)/( C*(PIDI(I,K)**4.0)*(3.14159**2.0))
      CONT=4.*WPOL(N)/(3.14159*PIDI(I,K)*PIDI(I,K)*GC)
      IF(K.GT.1) GO TO 5
      IF(*.EQ.1.OR.UESTET.EQ.1) GO TO 5
      IF(I.EQ.2) GO TO 15
      XR(I,K)=((PIL(I,K)-BL1(N))/PIDI(I,K)+FI(I,K)+ADDR(I,K))*COMR
      XINT(I,K)=( IL(I,K)-BL1(N))*CONT
      GO TO 1000
   15 XR(I,K)=((PIL(I,K)-BL2(N))/PIDI(I,K)+FI(I,K)+ADDR(I,K))*COMR
      XINT(I,K)=(PIL(I,K)-BL2(N))*CONT
      GO TO 1000
    5 XR(I,K)=(PIL(I,K)/PIDI(I,K)+FI(I,K)+ADDR(I,K))*COMR
      XI T(I,K)-PIL(I,K)*CONT
 1000 CONTINUE
      DO 200 I=1,NL
      IF(I.GT.1) GO TO 30
      M =3*(NI-1)+5
      N =  +1
      RBASE(1)=XR(1,1)+XR(1,2)+XR(1,3)+XR(1,MM)+XR(1,NN)
      BASEI(1)=XINT(1,1)+XINT(1,2)+XINT(1,3)+XINT(1,MM)+XINT(1,NN)
      RPAR(1)=XR(1,4)
      PART(1)=XINT(1,4)
   30 IF(I.EQ.1) GO TO 2000
      JJ=I-1
      KK-(3*JJ)+2
      LL=KK+2
      XINT(1,JJ)=0.
      XR(1,JJ)=0.
      DO 100 M=KK,LL
      XR(1,JJ)=XR(1,JJ)+XR(1,M)
      XINT(1,JJ)=XINT(1,JJ)+XINT(1,M)
  100 CONTINUE
 2000 CONTINUE
      JA=NL-1
      IF(JA.EQ.0) GO TO 40
      DO 3000 I=1,JA
      RPAR(1)=(RPAR(1)*XR(1,I))/(RPAR(1)+XR(1,I))
      PART(1)=(PART(1)*XINT(1,I))/(PART(1)+XINT(1,I))
 3000 CONTINUE
   40 R(1,N)=RBASE(1)+RPAR(1)
      XINER(1,N)=PART(1)+BASEI(1)
```

```
      R(2,N)=0.
      XINER(2,N)=0.
      KR=NCOMP(2)
      DO 4000 K=1,KR
      R(2,N)=R(2,N)+/R(2,K)
      XINER(2,N)=XINER(2,N)+XINT(2,K)
 4000 CONTINUE
      RETURN
      END
C
C
C
      SUBROUTINE FRACTR(I,K)
      IMPLICIT DOUBLE PRECISION (A-H, O-Z)
          COMMON R(400),VVAR(400),RHOC(400),RHOL(400),VVAP1(400),
     1Q12(400),VVAP2(400),EL1(400),HI2(400),HI(400),P(2,400),
     2Q(2,400),XINER(2,400),XK1(2),XK2(2),XK3(2),XK4(2),Q3(400)
      COMMON QTOT(400),HEAT1(400),XMCP1(400),CPC(400),CPI(400),
     1QCS1(400),HEAT1(400),TCAT(400),HEAT2(400),QCS2(400),QSF(400),
     2HEAT2(400),HFG(400),HTC1(400),TCONG(400),RTUBE,FFACT
      COMMON VISCF(400),VISCG(400),PATM,NI,CZERO,SHTCO,CC,
     1PG,DIDI(2,10),EL(2,10),DTI(2,10),NCOMP(2),ADDH(2,10),KUT,
     2POWER,IP,XMCP(400),ERROR,N
      COMMON DELL,PWALL(400),CPWALL(400),CPS,DENS,KHTCD
      COMMON/RESTART/NRSTRT
C
C
C     THIS ROUTINE CALCULATES THE FRICTION FACTOR FOR USE IN
C     SUBROUTINE BASIN.  THE CALCULATION IS MADE ON THE BASIS
C     OF A REYNOLDS NUMBER AND IS DIVIDED INTO THREE ZONES;
C     LAMINAR (RE<2000), TURBULENT, BLASIUS APPROXIMATION
C     (2000<RE<50000) AND TURBULENT, RE>50000, WHERE THE
C     EQUATION F=0.046RE**-0.25 IS USED.  THE CALCULATION IS
C     MADE FOR EACH COMPONENT IN THE SYSTEM.
C
C
      IF(NRSTRT.EQ.1) GO TO 10000
      IF(N.GT.1) GO TO 15
10000 FFACT=0.
      GO TO 60
   15 V=4.0*Q(I,K)/(3.14159*DIDI(I,K)*DIDI(I,K))*3600.
      RE=ABS(V*RHOL(N)*DIDI(I,K)/VISCF(N))
      IF(RE.GT.2000.) GO TO 5
      IF(RE.EQ.0.) GO TO 40
      FFACT=16.0/RE
      GO TO 50
    5 IF(RE.GT.50000.) GO TO 10
      FFACT=0.0791/(RE**0.25)
      GO TO 50
   10 FFACT=0.046/(RE**0.20)
      GO TO 50
   40 FFACT=0.
      GO TO 50
   50 IF(Q(I,K).LT.0.) FFACT=-FFACT
   60 RETURN
      END
C
C
C
      SUBROUTINE PROP
      IMPLICIT DOUBLE PRECISION (A-H, O-Z)
```

```
      COMMON P(400),VVAP(400),RHOG(400),RHOL(400),VVAP1(400),
     1912(400),VVAP2(400),RT1(400),RT2(400),SI(400),P(2,400),
     2Q(2,400),YT,PP(2,400),YK1(2),YK2(2),YK3(2),YK4(2),Q3(400)
      COMMON QTOT(400),RHOS1(400),XHCP1(400),CPG(400),CPL(400),
     1OG31(400),HEAT1(400),TSAT(400),AREA2(400),QSF2(400),QGF(400),
     2HEAT2(400),HFG(400),HTC1(400),TCONG(400),PTURB,FFACT
      COMMON VISCL(400),VISCG(400),PATM,NL,CZERO,CHTC0,GC,
     1PG,WIDT(2,10),TI(2,10),PIL(2,10),NCOMP(2),ADDR(2,10),KPT,
     2POWER,IF,XHCP2(400),ERROR,N
      COMMON DELP,TWALL(400),CPWALL(400),CPS,DENS,WHTCO
      COMMON/CODTYM/NA
C
C
C     THIS ROUTINE CALCULATES THE PROPERTIES OF WATER (NA=0)
C     OR LIQUID SODIUM (NA=1).  THE CORRELATIONS ARE TAKEN FROM
C     IRVIN (BACHELOR'S THESIS) FOR WATER, AND FROM ANL-7323 FOR
C     LIQUID SODIUM.  THE PROPERTIES INCLUDED ARE
C     WATER:  TSAT, HFG, VISCOSITY (LIQUID), SPECIFIC HEAT (LIQUID)
C     DENSITY (BOTH PHASES),; SODIUM:  TSAT, DENSITY (BOTH PHASES),
C     HFG, LIQUID SPECIFIC HEAT, VISCOSITY (BOTH PHASES).
C
C
      IF(NA.EQ.1) GO TO 100
      CPG(N)=0.5
      VISCG(N)=0.03
      TCONG(N)=0.05
      PP=P(N)/144.
      U=ALOG(PP)
      A=U-7.0
      IF(PP.GT.265.) GO TO 5
      HLIQ=((((((((-0.4771D-04*U+0.9461PD-03)*U-0.53392(D-02)*U
     1+0.12(37370D-01)*U+0.9695)7D-02)*U-0.6628012D-01)*U
     2+0.41 31929D-01)*U+0.2976(511D-0))*U+0.22225*55D01)*U
     3+0.33320472D02)*U+0.69795537D02
      GO TO 10
    5 HLIQ=((((((-0.58728711D04*A+0.11490811D01)*A+0.74153449D01)
     1*A+0.10631109D02)*A+0.13891594D(2)*A+0.37492429D02)*A
     2+0.16178158D03)*A+0.5C715337D03
   10 X=0.001*H
      X3=X**3.
      CP=0.854+1.66*X-7.0*X*X+10.6*X3-7.0*X*X3
      CPL(N)=1.0/CP
      VISCL(N)=0.009+118.0/HLIQ
      IF(HLIQ-90.) 1,2,2
    1 VISCL(N)=0.009+118.0/(HLIQ+0.25*(90.-HLIQ))
    2 IF(PP.GT.450.) GO TO 15
      HVAP=((((((-0.3674D-04*U-0.5862D-03)*U+0.43597510D-02)*U
     1-0.14515940D-01)*U+0.22775919D-01)*U+0.85550917D0)*U
     2+0.14229318D02)*U+0.11059525D04
      GO TO 20
   15 HVAP=((((0.37170416D01*A-0.31119126D01)*A-0.20447P1D02)*A
     1-0.27217176D02)*A-0.44226896D02)*A-0.46351642D02)*A
     2+0.11276082D04
   20 HFG(N)=HVAP-HLIQ
      IF(PP.GT.450.) GO TO 25
      VL=(((((((0.463D-08*U-0.747D-07)*U+0.39596D-06)*U
     1-0.36945D-06)*U-0.270944D-05)*U+0.6746279PD-05)*U
     2+0.331327390-04)*U+0.103945140-03)*U+0.16140835D-01
      GO TO 30
   25 VL=(((((-0.26331D-03*A+0.142578D-02)*A+0.21252D-02)*
     1A+0.113227D-02)*A+0.197421D-02)*A+0.40469CD-02)*A
```

```
     2+0.2196328CD-01
  30 RHOL(N)=1.0/VL
     IF(PP.GT.450.) GO TO 35
     PVG=(((((((-0.196D-05*U-0.12008D-03)*U+0.67223D-03)
    1*U-0.307139D-2)*U-0.631125D-02)*U+0.60016723D-01)
    2*U+0.11339315D01)*U+0.19257401D02)*U+0.33361356D03
     GO TO 40
  35 PVG=(((((0.47458752D01*A-0.65913524D01)*A-0.22430605D02)*A
    1-0.27967054D02)*A-0.53077282D02)*A-0.61514631D02)*F
    2+0.43397464D03
  40 RHOG(N)=PP/PVG
     IF(H.GT.450.) GO TO 45
     TSAT(N)=(((((((-0.198D-05*U+0.1405D-04)*U-3.265D-5)*U
    1+2.3937D-3)*U+0.43451BD-02)*U+0.17363304D00)*U
    2+0.22808149D01)*U+0.33445776D02)*U+0.10152432D03
     GO TO 50
  45 TSAT(N)=((((-0.16074225D-00*A-0.69678576D0)*A
    1+0.61771119D0)*A+0.14657783D02)*A+0.12405875D03)*A
    2+0.55599436D03
 100 CONTINUE
C    SATURATION PROPERTIES OF LIQUID AND GASEOUS SODIUM
     PPA=P(N)/2116.224
     IF(PPA.GT.0.1) GO TO 105
     TSAT(N)=((14.65*DLOG10(PPA)-9515.4464)/(DLOG10(PPA)-4.57791
    1))-459.7
     GO TO 110
 105 TSAT(N)=((83.16*DLOG10(PPA)-99P1.1961)/(DLOG10(PPA)-4.36383
    1))-459.7
 110 RHOL(N)=59.566-(7.9504D-3*TSAT(N))-(0.2872D-6*(TSAT(N)**2.)
    1)+( .06035D-9*(TSAT(N)**3.))
     TABS=TSAT(N)+459.7
     TWO=EXP(-9.95845+(16598.3/TABS))
     FOUR=EXP(-24.59115+(37589.7/TABS))
     U=PPA*TWO
     W=(PPA**3.)*FOUR
     X1= .8
 115 X1P=X1
     X1=X1-(W*(X1**4)+(U*(X1**2.))+X1-1.)/((4.*W*(X1**3.))+
    1(2.*U*X1)+1.)
     IF((ABS(X1-X1P)/X1)-1.D-6) 120,120,115
 120 X2=U*(X1**2.)
     X4=1.-X1-X2
     ABAR=22.91*(X1+(2.*X2)+(4.*X4))
     VSAT=(0.730227*TABS)/(ABAR*PPA)
     RHOG(N)=1./VSAT
     DHF1=25980.7-(2.21312*TABS)+(7.16279D-4*(TABS**2.))-(1.4526
    1D-7*(TABS**3.))
     DHF2=(2.*DHF1)-18304.
     DHF4=(4.*DHF1)-41472.
     HFG(N)=1.8*((X1*DHF1)+(X2*DHF2)+(X4*DHF4))/ABAR
     CPL(N)=0.389352-(1.10599D-4*TABS)+(3.41173D-8*(TABS**2.))
     TCOND(N)=0.038
     CPG(N)=0.59
     VISCG(N)=0.03427+(6.176D-6*TSAT(N))
     VISL=1.0203+(397.17/TABS)-(0.4925*DLOG10(TABS))
     VISCF(N)=10.**VISL
  50 RETURN
     END
C
C
C
```

```
      SUBROUTINE PLOTTER
      IMPLICIT DOUBLE PRECISION (A-H, O-Z)
      COMMON P(400),VVAP(400),RHOG(400),RHOL(400),VVAP1(400),
     1QI2(400),VVAP2(400),RL1(400),RI2(400),RL(400),Q(2,400),
     2Q(2,400),XINTR(2,400),YK1(2),YK2(2),YK3(2),YK4(2),Q3(400)
      COMMON QTOT(400),AREA1(400),XMCP1(400),CPG(400),CPL(400),
     1QGS1(400),HEAT1(400),TSAT(400),AREA2(400),QGS2(400),QSF(400),
     2HEAT2(400),HFG(400),HTCO(400),TCONC(400),FTUBE,FRACT
      COMMON VISCF(400),VISCG(400),PATM,NL,CTERO,CUTCO,GC,
     1PG,IDI(2,10),IL(2,10),PII(2,10),NCOMP(2),ADDR(2,10),KUT,
     2POWER,IP,XMCP2(400),ERROR,H
      COMMON/PLOTT/KPLT,TIME,KPCNT
      COMMON/TRANS/DT(400),TTIME,DTI,ATIM
C
C
C     THIS ROUTINE USES THE LIBRARY SUBROUTINE PICTR ON THE MIT
C     JOINT COMPUTER FACILITY VAX COMPUTER TO GENERATE
C     GRAPHS OF SELECTED CURVES.  THE ROUTINE PICTR IS ACCESSED
C     THROUGH A CALL STATEMENT THAT USES ARRAYS SET UP BY THE USER
C     AND CREATES THE PLOTS.
C
      REAL*4 CURVE(8,400)
      INTEGER*2 ZIAR(96)
      NPTS=NTLIM
      STIME=0.
C     CREATE THE CURVES USING RESULTS FROM TRANSIENT CALCULATION
      DO 100 I=1,8
      DO 100 N=1,400
      IF(I.GE.2) GO TO 10
      CURVE(I,N)=-Q(I,N)*10000.
      GO TO 100
   10 IF(I.GE.3) GO TO 20
      CURVE(I,N)=Q(I,N)*10000.
      GO TO 100
   20 IF(I.GE.4) GO TO 30
      CURVE(I,N)=P(N)/144.
      GO TO 100
   30 IF(I.GE.5) GO TO 40
      CURVE(I,N)=RL(N)*12.
      GO TO 100
   40 IF(I.GE.6) GO TO 50
      CURVE(I,N)=0.
      GO TO 100
   50 IF(I.GE.7) GO TO 60
      CURVE(I,N)=-RL1(N)*12.
      GO TO 100
   60 IF(I.EQ.8) GO TO 70
      CURVE(I,N)=RL2(N)*12.
      GO TO 100
   70 IF(N.GT.1) GO TO 80
      CURVE(I,N)=0.
      GO TO 100
   80 CURVE(I,N)=CURVE(I,N-1)+DT(N)
  100 CONTINUE
      IF(KPCNT.EQ.2) GO TO 1000
      IF(KPCNT.EQ.3) GO TO 2000
      IF(KPCNT.EQ.4) GO TO 3000
C
C
C     INPUT THE TITLES OF THE PLOTS.  THESE ARE THE LAST
C     FOUR DATA LINES.  THE TITLE FOR THE Y-AXIS OF THE PLOT
```

```
C     GOES IN THE FIRST FORTY COLUMNS OF THE LINE AND THE
C     X-AXIS LABEL GOES IN THE SECOND FORTY COLUMNS.  THE LINES
C     SHOULD BE CENTERED IN THE FORTY COLUMNS TO GET THEM ON THE
C     PLOTS PROPERLY.
C
C
      READ(5,200) (YLAB(I),I=1,40)
  200 FORMAT(40A2)
C
C      CALL THE PLOTTING ROUTINE.  DETAILED INFORMATION OF THE
C      ORIGINAL ARGUMENTS IN THE CALL STATEMENTS IS AVAILABLE
C      FROM MIT-ICF.
C
      CALL PICTR(CURVE,8,XLAB,XSCL,-19,NPTS,8,0,4,1,FTIME,1)
      GO TO 500
 1000 READ(5,200) (YLAB(I),I=1,40)
      CALL PICTR(CURVE,8,XLAB,XSCL,-4,NPTS,8,0,4,1,FTIME,1)
      GO TO 500
 2000 READ(5,200) (XLAB(I),I=1,40)
      CALL PICTR(CURVE,8,YLAB,YSCL,-8,NPTS,8,0,4,1,FTIME,1)
      GO TO 500
 3000 READ(5,200) (YLAB(I),I=1,40)
      CALL PICTR(CURVE,8,XLAB,XSCL,-112,NPTS,8,0,4,1,FTIME,1)
  500 RETURN
      END
```

E.3 Sample Input to FLOSS

```
100       SIMULATION OF TEST 9 CONDITIONS; LARGE HT COEF.
200       0.050     11.000     32.200     14.70000  17.20000    1.20000     .07600     1  300
300     175.000006000.00000     .390      0.04900 488.00000    0.110002000.00000     1    4
400       5   2    3.0
500       .013      0.0        4.00       0.0
600       .6667     0.0         .6667     0.0
700       .083      0.0        1.0        0.0
800       .083    180.0       10.0      250.0
900       .083      0.0        1.0        0.
1000      .013      0.0         4.0        0.0
1100      .6667     0.0        .6667       0.0
1200      .395       .00004    .005        .005
1300      .05        .95       1.05       75   75
1400      9
1500      .100      225.0
1600      .48       140.0
1700      .48       140.0
1800      .48       140.0
1900      .48       140.0
2000      .48       140.0
2100      .48       140.0
2200      .48       140.0
2300      .64       140.0
2400    60.0         75.0
2500      4
2600      0
2700              TIME (SEC)                     VOL. FLOW RATE (FT**3/SEC X 10**4)
2800              TIME (SEC)                            PRESSURE (PSIA)
2900              TIME (SEC)                        BUBBLE LENGTH (INCHES)
3000              TIME (SEC)                         BUBBLE LENGTH (INCHES)
```

E.4 FLOSS Output

SIMULATION OF TEST 9 CONDITIONS: LARGE HT COEF.
DT=0.050 KHT=1 CHTCO=6000.0 POWER= 0.39 KW PSTART=17.20
ECL=0.050 CLL=0.950 CLH=1.050

INITIAL TEMPERATURE PROFILE 225.000 140.000 140.000 140.000 140.000 140.000 140.000
140.000 140.000

NODAL ARRANGEMENT, FT/NODE 0.100 0.480 0.480 0.480 0.480 0.480 0.480
0.480 0.640

TIME	Q1	Q2	Q12	Q3	QTOT	P	A1
BL1	BL2	BL	VVAP1	VVAP2	VVAP	A2	
0.000	0.000E+00	0.000E+00	0.000E+00	0.000E+00	0.000E+00	17.200	0.000E+00
0.000E+00	0.300E+00	0.000E+00	0.000E+00	0.000E+00	0.000E+00	0.000E+00	
0.050	0.151E-05	0.163E-05	0.314E-05	-0.103E-06	0.304E-05	16.646	0.105E-03
0.721E-03	0.774E-03	0.150E-02	0.757E-07	0.813E-07	0.157E-06	0.105E-03	
0.100	0.599E-05	0.643E-05	0.124E-04	0.199E-07	0.124E-04	16.669	0.105E-03
0.357E-02	0.384E-02	0.741E-02	0.375E-06	0.403E-06	0.778E-06	0.105E-03	
0.150	0.179E-04	0.192E-04	0.370E-04	0.166E-06	0.372E-04	16.728	0.105E-03
0.121E-01	0.130E-01	0.250E-01	0.127E-05	0.136E-05	0.263E-05	0.105E-03	
0.200	0.384E-04	0.412E-04	0.796E-04	0.469E-06	0.800E-04	16.794	0.105E-03
0.303E-01	0.326E-01	0.629E-01	0.319E-05	0.342E-05	0.661E-05	0.105E-03	
0.250	0.705E-04	0.756E-04	0.146E-03	0.126E-05	0.147E-03	16.879	0.105E-03
0.634E-01	0.586E-01	0.132E+00	0.671E-05	0.720E-05	0.139E-04	0.105E-03	
0.275	-0.208E-03	-0.224E-03	-0.433E-03	-0.465E-04	-0.479E-03	12.094	0.105E-03
0.143E-01	0.151E-01	0.295E-01	0.151E-05	0.159E-05	0.310E-05	0.105E-03	
0.281	-0.189E-03	-0.204E-03	-0.393E-03	0.311E-04	-0.362E-03	17.707	0.105E-03
0.308E-02	0.300E-02	0.608E-02	0.324E-06	0.315E-06	0.639E-06	0.105E-03	

NO CONVERGENCE AT THIS TIME STEP T= 0.281

RESTART

TIME	Q1	Q2	Q12	Q3	QTOT	P	A1
0.281	0.239E-06	-0.239E-06	0.136E-19	0.424E-35	0.136E-19	17.707	0.000E+00
0.183E-34	0.191E-34	0.380E-34	0.000E+00	0.000E+00	0.399E-38	0.105E-03	
0.331	0.000E+00	0.000E+00	0.000E+00	0.000E+00	0.000E+00	17.200	0.000E+00
0.000E+00	0.000E+00	0.000E+00	0.000E+00	0.000E+00	0.000E+00	0.000E+00	
0.381	0.000E+00	0.000E+00	0.000E+00	0.000E+00	0.000E+00	17.200	0.000E+00

```
    0.000E+00       0.000E+00       0.000E+00       0.000E+00       0.000E+00       0.000E+00       0.000E+00

0.431       0.151E-05       0.163E-05       0.314E-05      -0.103E-06       0.304E-05       16.646       0.105E-03
    0.721E-03       0.774E-03       0.150E-02       0.757E-07       0.813E-07       0.157E-06       0.105E-03

0.481       0.599E-05       0.643E-05       0.124E-04       0.199E-07       0.124E-04       16.669       0.105E-03
    0.357E-02       0.384E-02       0.741E-02       0.375E-06       0.403E-06       0.778E-06       0.105E-03

0.531       0.179E-04       0.192E-04       0.370E-04       0.166E-06       0.372E-04       16.728       0.105E-03
    0.121E-01       0.130E-01       0.250E-01       0.127E-05       0.136E-05       0.263E-05       0.105E-03

0.581       0.384E-04       0.412E-04       0.796E-04       0.469E-06       0.801E-04       16.794       0.105E-03
    0.39[illegible]E-01       0.326E-01       0.629E-01       0.319E-05       0.342E-05       0.661E-05       0.105E-03

0.631       0.705E-04       0.756E-04       0.146E-03       0.126E-05       0.147E-03       16.879       0.105E-03
    0.63[illegible]E-01       0.666E-01       0.132E+00       0.671E-05       0.720E-05       0.139E-04       0.105E-03

0.656      -0.189E-03      -0.204E-03      -0.392E-03      -0.568E-04      -0.449E-03       12.407       0.105E-03
    0.190E-01       0.201E-01       0.391E-01       0.199E-05       0.211E-05       0.410E-05       0.105E-03

0.657      -0.196E-03      -0.212E-03      -0.408E-03       0.000E+00      -0.408E-03       12.407       0.105E-03
    0.175E-01       0.165E-01       0.360E-01       0.184E-05       0.195E-05       0.378E-05       0.105E-03

      NO CONVERGENCE AT THIS TIME STEP     T= 0.657

      RESTART

0.657       0.339E-06      -0.339E-06       0.136E-19       0.640E-35       0.136E-19       12.407       0.000E+00
    0.262E-34       0.277E-34       0.539E-34       0.000E+00       0.000E+00       0.566E-38       0.105E-03

0.707       0.000E+00       0.000E+00       0.000E+00       0.000E+00       0.000E+00       17.200       0.000E+00
    0.000E+00       0.000E+00       0.000E+00       0.000E+00       0.000E+00       0.000E+00       0.000E+00

0.757       0.000E+00       0.000E+00       0.000E+00       0.000E+00       0.000E+00       17.200       0.000E+00
    0.000E+00       0.000E+00       0.000E+00       0.000E+00       0.000E+00       0.000E+00       0.000E+00

0.807       0.151E-05       0.163E-05       0.314E-05      -0.103E-06       0.304E-05       16.646       0.105E-03
    0.721E-03       0.774E-03       0.150E-02       0.757E-07       0.813E-07       0.157E-06       0.105E-03

0.857       0.599E-05       0.643E-05       0.124E-04       0.199E-07       0.124E-04       16.669       0.105E-03
    0.357E-02       0.384E-02       0.741E-02       0.375E-06       0.403E-06       0.778E-06       0.105E-03

0.907       0.179E-04       0.192E-04       0.370E-04       0.166E-06       0.372E-04       16.728       0.105E-03
    0.121E-01       0.130E-01       0.250E-01       0.127E-05       0.136E-05       0.263E-05       0.105E-03

0.957       0.384E-04       0.412E-04       0.796E-04       0.470E-06       0.801E-04       16.794       0.105E-03
```

	0.303E-01	0.326E-01	0.629E-01	0.319E-05	0.342E-05	0.661E-05	0.105E-03
1.007	0.705E-04	0.756E-04	0.146E-03	0.127E-05	0.147E-03	16.879	0.105E-03
	0.639E-01	0.686E-01	0.132E+00	0.671E-05	0.720E-05	0.139E-04	0.105E-03
1.032	-0.156E-03	-0.169E-03	-0.325E-03	-0.631E-04	-0.388E-03	12.933	0.105E-03
	0.267E-01	0.284E-01	0.551E-01	0.280E-05	0.298E-05	0.579E-05	0.105E-03
1.038	-0.205E-03	-0.221E-03	-0.427E-03	0.117E-04	-0.415E-03	13.275	0.105E-03
	0.145E-01	0.152E-01	0.297E-01	0.152E-05	0.160E-05	0.312E-05	0.105E-03

NO CONVERGENCE AT THIS TIME STEP   T= 1.038

RESTART

1.038	0.236E-06	-0.236E-06	-0.305E-19	0.526E-35	-0.305E-19	13.275	0.000E+00
	0.216E-34	0.228E-34	0.445E-34	0.000E+00	0.000E+00	0.467E-38	0.105E-03
1.088	0.000E+00	0.000E+00	0.000E+00	0.000E+00	0.000E+00	17.200	0.000E+00
	0.000E+00	0.000E+00	0.000E+00	0.000E+00	0.000E+00	0.000E+00	0.000E+00
1.138	0.000E+00	0.000E+00	0.000E+00	0.000E+00	0.000E+00	17.200	0.000E+00
	0.000E+00	0.000E+00	0.000E+00	0.000E+00	0.000E+00	0.000E+00	0.000E+00
1.188	0.151E-05	0.163E-05	0.314E-05	-0.103E-06	0.304E-05	16.646	0.105E-03
	0.721E-03	0.774E-03	0.150E-02	0.757E-07	0.813E-07	0.157E-06	0.105E-03
1.238	0.599E-05	0.643E-05	0.124E-04	0.199E-07	0.124E-04	16.669	0.105E-03
	0.357E-02	0.384E-02	0.741E-02	0.375E-06	0.403E-06	0.778E-06	0.105E-03
1.288	0.179E-04	0.192E-04	0.370E-04	0.166E-06	0.372E-04	16.728	0.105E-03
	0.121E-01	0.130E-01	0.250E-01	0.127E-05	0.136E-05	0.263E-05	0.105E-03
1.338	0.384E-04	0.412E-04	0.796E-04	0.470E-06	0.801E-04	16.754	0.105E-03
	0.303E-01	0.326E-01	0.629E-01	0.319E-05	0.342E-05	0.661E-05	0.105E-03
1.388	0.705E-04	0.756E-04	0.146E-03	0.127E-05	0.147E-03	16.879	0.105E-03
	0.639E-01	0.686E-01	0.133E+00	0.672E-05	0.720E-05	0.139E-04	0.105E-03
1.438	0.546E-04	0.581E-04	0.113E-03	-0.912E-05	0.104E-03	16.486	0.105E-03
	0.899E-01	0.962E-01	0.186E+00	0.944E-05	0.101E-04	0.196E-04	0.105E-03
1.463	-0.308E-03	-0.332E-03	-0.640E-03	-0.699E-04	-0.710E-03	10.753	0.105E-03
	0.167E-01	0.171E-01	0.338E-01	0.175E-05	0.180E-05	0.35[illegible]E-05	0.105E-03

NO CONVERGENCE AT THIS TIME STEP   T= 1.463

```
RESTART

1.463      0.789E-06     -0.789E-06      0.177E-17      0.652E-35      0.177E-17     10.753      0.000E+00
    0.257E-34     0.265E-34      0.522E-34      0.000E+00      0.000E+00      0.548E-38     0.105E-03

1.513      0.000E+00      0.000E+00      0.000E+00      0.000E+00      0.000E+00     17.200      0.000E+00
    0.000E+00     0.000E+00      0.000E+00      0.000E+00      0.000E+00      0.000E+00     0.000E+00

1.563      0.000E+00      0.000E+00      0.000E+00      0.000E+00      0.000E+00     17.200      0.000E+00
    0.000E+00     0.000E+00      0.000E+00      0.000E+00      0.000E+00      0.000E+00     0.000E+00

1.613      0.151E-05      0.163E-05      0.314E-05     -0.103E-06      0.304E-05     16.646      0.105E-03
    0.721E-03     0.774E-03      0.150E-02      0.757E-07      0.813E-07      0.157E-06     0.105E-03

1.663      0.599E-05      0.643E-05      0.124E-04      0.199E-07      0.124E-04     16.669      0.105E-03
    0.357E-02     0.384E-02      0.741E-02      0.375E-06      0.403E-06      0.778E-06     0.105E-03

1.713      0.179E-04      0.192E-04      0.370E-04      0.166E-06      0.372E-04     16.728      0.105E-03
    0.121E-01     0.130E-01      0.250E-01      0.127E-05      0.136E-05      0.263E-05     0.105E-03

1.763      0.384E-04      0.412E-04      0.796E-04      0.470E-06      0.801E-04     16.794      0.105E-03
    0.304E-01     0.326E-01      0.629E-01      0.319E-05      0.342E-05      0.661E-05     0.105E-03

1.813      0.705E-04      0.757E-04      0.146E-03      0.127E-05      0.147E-03     16.879      0.105E-03
    0.639E-01     0.686E-01      0.133E+00      0.672E-05      0.720E-05      0.139E-04     0.105E-03

1.838      0.906E-04      0.971E-04      0.188E-03      0.281E-05      0.190E-03     16.951      0.105E-03
    0.855E-01     0.917E-01      0.177E+00      0.898E-05      0.963E-05      0.186E-04     0.105E-03

1.863     -0.209E-03     -0.226E-03     -0.435E-03     -0.120E-03     -0.556E-03     11.774      0.105E-03
    0.357E-01     0.379E-01      0.736E-01      0.375E-05      0.398E-05      0.773E-05     0.105E-03

1.870     -0.273E-03     -0.295E-03     -0.568E-03      0.209E-04     -0.547E-03     12.193      0.105E-03
    0.194E-01     0.203E-01      0.397E-01      0.204E-05      0.213E-05      0.418E-05     0.105E-03

   NO CONVERGENCE AT THIS TIME STEP     T= 1.870

   RESTART

1.870      0.447E-06     -0.447E-06      0.285E-18      0.000E+00      0.285E-18     12.193      0.000E+00
    0.145E-34     0.152E-34      0.297E-34      0.000E+00      0.000E+00      0.313E-38     0.105E-03

1.920      0.000E+00      0.000E+00      0.000E+00      0.000E+00      0.000E+00     17.200      0.000E+00
    0.000E+00     0.000E+00      0.000E+00      0.000E+00      0.000E+00      0.000E+00     0.000E+00
```

```
1.970      0.000E+00    0.000E+00    0.000E+00    0.000E+00    0.000E+00    17.200    0.000E+00
    0.000E+00    0.000E+00    0.000E+00    0.000E+00    0.000E+00    0.000E+00    0.000E+00

2.020      0.151E-05    0.163E-05    0.314E-05   -0.103E-06    0.304E-05    16.646    0.105E-03
    0.721E-03    0.774E-03    0.150E-02    0.757E-07    0.813E-07    0.157E-06    0.105E-03

2.070      0.599E-05    0.643E-05    0.124E-04    0.199E-07    0.124E-04    16.669    0.105E-03
    0.357E-02    0.384E-02    0.741E-02    0.375E-06    0.403E-06    0.778E-06    0.105E-03

2.120      0.179E-04    0.192E-04    0.370E-04    0.166E-06    0.372E-04    16.728    0.105E-03
    0.121E-01    0.130E-01    0.250E-01    0.127E-05    0.136E-05    0.263E-05    0.105E-03

2.170      0.384E-04    0.412E-04    0.796E-04    0.471E-06    0.801E-04    16.794    0.105E-03
    0.304E-01    0.326E-01    0.629E-01    0.319E-05    0.342E-05    0.661E-05    0.105E-03

2.220      0.706E-04    0.757E-04    0.146E-03    0.127E-05    0.148E-03    16.879    0.105E-03
    0.639E-01    0.686E-01    0.133E+00    0.672E-05    0.721E-05    0.139E-04    0.105E-03

2.270      0.551E-04    0.586E-04    0.114E-03   -0.910E-05    0.105E-03    16.490    0.105E-03
    0.901E-01    0.965E-01    0.187E+00    0.947E-05    0.101E-04    0.196E-04    0.105E-03

2.295     -0.274E-03   -0.296E-03   -0.570E-03   -0.881E-04   -0.658E-03    11.787    0.105E-03
    0.249E-01    0.260E-01    0.509E-01    0.262E-05    0.273E-05    0.535E-05    0.105E-03

2.301     -0.294E-03   -0.317E-03   -0.611E-03    0.598E-04   -0.551E-03    15.023    0.105E-03
    0.746E-02    0.716E-02    0.146E-01    0.777E-06    0.751E-06    0.153E-05    0.105E-03

     NO CONVERGENCE AT THIS TIME STEP     T= 2.301

     RESTART

2.301      0.490E-06   -0.490E-06   -0.149E-18    0.565E-35   -0.149E-18    15.023    0.000E+00
    0.236E-34    0.231E-34    0.467E-34    0.000E+00    0.000E+00    0.491E-38    0.105E-03

2.351      0.000E+00    0.000E+00    0.000E+00    0.000E+00    0.000E+00    17.200    0.000E+00
    0.000E+00    0.000E+00    0.000E+00    0.000E+00    0.000E+00    0.000E+00    0.000E+00

2.401      0.000E+00    0.000E+00    0.000E+00    0.000E+00    0.000E+00    17.200    0.000E+00
    0.000E+00    0.000E+00    0.000E+00    0.000E+00    0.000E+00    0.000E+00    0.000E+00

2.451      0.151E-05    0.163E-05    0.314E-05   -0.103E-06    0.304E-05    16.646    0.105E-03
    0.721E-03    0.774E-03    0.150E-02    0.757E-07    0.813E-07    0.157E-06    0.105E-03

2.501      0.599E-05    0.643E-05    0.124E-04    0.199E-07    0.124E-04    16.669    0.105E-03
    0.357E-02    0.384E-02    0.741E-02    0.375E-06    0.403E-06    0.778E-06    0.105E-03
```

```
2.551       0.179E-04      0.192E-04      0.370E-04      0.166E-06      0.372E-04      16.728      0.105E-03
   0.121E-01      0.130E-01      0.250E-01      0.127E-05      0.136E-05      0.263E-05      0.105E-03

2.601       0.384E-04      0.412E-04      0.796E-04      0.471E-06      0.801E-04      16.795      0.105E-03
   0.304E-01      0.326E-01      0.630E-01      0.319E-05      0.342E-05      0.661E-05      0.105E-03

2.651       0.706E-04      0.757E-04      0.146E-03      0.127E-05      0.148E-03      16.879      0.105E-03
   0.640E-01      0.686E-01      0.133E+00      0.672E-05      0.721E-05      0.139E-04      0.105E-03

2.676       0.945E-04      0.101E-03      0.196E-03      0.564E-05      0.201E-03      17.010      0.105E-03
   0.864E-01      0.928E-01      0.179E+00      0.908E-05      0.974E-05      0.188E-04      0.105E-03

2.701      -0.151E-03     -0.164E-03     -0.315E-03     -0.134E-03     -0.449E-03      12.657      0.105E-03
   0.504E-01      0.537E-01      0.104E+00      0.530E-05      0.564E-05      0.109E-04      0.105E-03

2.707      -0.214E-03     -0.232E-03     -0.446E-03     -0.287E-04     -0.475E-03      12.358      0.105E-03
   0.376E-01      0.399E-01      0.776E-01      0.396E-05      0.419E-05      0.815E-05      0.105E-03

2.714      -0.268E-03     -0.289E-03     -0.557E-03      0.281E-04     -0.529E-03      12.893      0.105E-03
   0.217E-01      0.227E-01      0.445E-01      0.228E-05      0.239E-05      0.467E-05      0.105E-03

2.720      -0.250E-03     -0.269E-03     -0.518E-03      0.569E-04     -0.462E-03      17.571      0.105E-03
   0.685E-02      0.676E-02      0.136E-01      0.720E-06      0.710E-06      0.143E-05      0.105E-03

      NO CONVERGENCE AT THIS TIME STEP     T= 2.720

      RESTART

2.720       0.120E-06     -0.126E-06      0.678E-20      0.483E-35      0.678E-20      17.571      0.000E+00
   0.208E-34      0.207E-34      0.415E-34      0.000E+00      0.000E+00      0.436E-38      0.105E-03

2.770       0.000E+00      0.000E+00      0.000E+00      0.000E+00      0.000E+00      17.200      0.000E+00
   0.000E+00      0.000E+00      0.000E+00      0.000E+00      0.000E+00      0.000E+00      0.000E+00

2.820       0.000E+00      0.000E+00      0.000E+00      0.000E+00      0.000E+00      17.200      0.000E+00
   0.000E+00      0.000E+00      0.000E+00      0.000E+00      0.000E+00      0.000E+00      0.000E+00

2.870       0.151E-05      0.163E-05      0.314E-05     -0.103E-06      0.304E-05      16.646      0.105E-03
   0.721E-03      0.774E-03      0.150E-02      0.757E-07      0.813E-07      0.157E-06      0.105E-03

2.920       0.599E-05      0.643E-05      0.124E-04      0.199E-07      0.124E-04      16.669      0.105E-03
   0.357E-02      0.384E-02      0.741E-02      0.375E-06      0.403E-06      0.778E-06      0.105E-03

2.970       0.179E-04      0.192E-04      0.370E-04      0.166E-06      0.372E-04      16.728      0.105E-03
   0.121E-01      0.130E-01      0.250E-01      0.127E-05      0.136E-05      0.263E-05      0.105E-03
```

```
3.020       0.384E-04     0.412E-04     0.797E-04     0.472E-06     0.801E-04     16.795     0.105E-03
   0.304E-01     0.326E-01     0.630E-01     0.319E-05     0.342E-05     0.661E-05    0.105E-03

3.070       0.706E-04     0.757E-04     0.146E-03     0.127E-05     0.148E-03     16.880     0.105E-03
   0.641E-01     0.687E-01     0.133E+00     0.672E-05     0.721E-05     0.139E-04    0.105E-03

3.095       0.911E-04     0.976E-04     0.189E-03     0.311E-05     0.192E-03     16.957     0.105E-03
   0.856E-01     0.919E-01     0.178E+00     0.900E-05     0.965E-05     0.186E-04    0.105E-03

3.120      -0.126E-03    -0.136E-03    -0.262E-03    -0.126E-03    -0.387E-03     13.121     0.105E-03
   0.558E-01     0.595E-01     0.115E+00     0.586E-05     0.625E-05     0.121E-04    0.105E-03

3.145      -0.200E-03    -0.216E-03    -0.416E-03     0.964E-05    -0.407E-03     15.327     0.105E-03
   0.809E-02     0.812E-02     0.162E-01     0.850E-06     0.852E-06     0.170E-05    0.105E-03

     NO CONVERGENCE AT THIS TIME STEP     T= 3.145

     RESTART

3.145       0.307E-06    -0.307E-06    -0.102E-19     0.604E-35    -0.102E-19     15.327     0.000E+00
   0.261E-34     0.262E-34     0.523E-34     0.000E+00     0.000E+00     0.549E-38    0.105E-03

3.195       0.000E+00     0.000E+00     0.000E+00     0.000E+00     0.000E+00     17.200     0.000E+00
   0.000E+00     0.000E+00     0.000E+00     0.000E+00     0.000E+00     0.000E+00    0.000E+00

3.245       0.000E+00     0.000E+00     0.000E+00     0.000E+00     0.000E+00     17.200     0.000E+00
   0.000E+00     0.000E+00     0.000E+00     0.000E+00     0.000E+00     0.000E+00    0.000E+00

3.295       0.151E-05     0.163E-05     0.314E-05    -0.103E-06     0.304E-05     16.646     0.105E-03
   0.721E-03     0.774E-03     0.150E-02     0.757E-07     0.813E-07     0.157E-06    0.105E-03

3.345       0.599E-05     0.643E-05     0.124E-04     0.199E-07     0.124E-04     16.669     0.105E-03
   0.357E-02     0.384E-02     0.741E-02     0.375E-06     0.403E-06     0.778E-06    0.105E-03

3.395       0.179E-04     0.192E-04     0.370E-04     0.166E-06     0.372E-04     16.728     0.105E-03
   0.121E-01     0.130E-01     0.250E-01     0.127E-05     0.136E-05     0.263E-05    0.105E-03

3.445       0.384E-04     0.412E-04     0.797E-04     0.472E-06     0.801E-04     16.795     0.105E-03
   0.304E-01     0.326E-01     0.630E-01     0.319E-05     0.342E-05     0.661E-05    0.105E-03

3.455       0.706E-04     0.757E-04     0.146E-03     0.127E-05     0.148E-03     16.880     0.105E-03
   0.640E-01     0.687E-01     0.133E+00     0.672E-05     0.721E-05     0.139E-04    0.105E-03

3.545       0.649E-04     0.692E-04     0.134E-03    -0.721E-05     0.127E-03     16.570     0.105E-03
   0.949E-01     0.102E+00     0.196E+00     0.997E-05     0.107E-04     0.206E-04    0.105E-03
```

```
3.570     -0.216E-03     -0.233E-03     -0.449E-03     -0.125E-03     -0.574E-03     12.079     0.105E-03
   0.436E-01      0.461E-01      0.896E-01      0.458E-05      0.484E-05      0.942E-05     0.105E-03

3.576     -0.277E-03     -0.298E-03     -0.575E-03      0.224E-04     -0.552E-03     12.410     0.105E-03
   0.271E-01      0.283E-01      0.554E-01      0.285E-05      0.298E-05      0.562E-05     0.105E-03

3.601     -0.107E-03     -0.114E-03     -0.222E-03      0.369E-05     -0.218E-03     19.158     0.105E-03
   0.153E-02      0.119E-02      0.273E-02      0.161E-06      0.125E-06      0.286E-06     0.105E-03

      NO CONVERGENCE AT THIS TIME STEP.    T= 3.601

      RESTART

3.601     -0.652E-06      0.652E-06      0.339E-20      0.000E+00      0.339E-20     19.158     0.000E+00
   0.185E-34      0.144E-34      0.324E-34      0.000E+00      0.000E+00      0.341E-38     0.105E-03

3.651      0.000E+00      0.000E+00      0.000E+00      0.000E+00      0.000E+00     17.200     0.000E+00
   0.000E+00      0.000E+00      0.000E+00      0.000E+00      0.000E+00      0.000E+00     0.000E+00

3.701      0.000E+00      0.000E+00      0.000E+00      0.000E+00      0.000E+00     17.200     0.000E+00
   0.000E+00      0.000E+00      0.000E+00      0.000E+00      0.000E+00      0.000E+00     0.000E+00

3.751      0.151E-05      0.163E-05      0.314E-05     -0.103E-06      0.304E-05     16.646     0.105E-03
   0.721E-03      0.774E-03      0.150E-02      0.757E-07      0.813E-07      0.157E-06     0.105E-03

3.801      0.599E-05      0.643E-05      0.124E-04      0.199E-07      0.124E-04     16.669     0.105E-03
   0.357E-02      0.384E-02      0.741E-02      0.375E-06      0.403E-06      0.778E-06     0.105E-03

3.851      0.179E-04      0.192E-04      0.370E-04      0.166E-06      0.372E-04     16.728     0.105E-03
   0.121E-01      0.130E-01      0.250E-01      0.127E-05      0.136E-05      0.263E-05     0.105E-03

3.901      0.384E-04      0.412E-04      0.797E-04      0.472E-06      0.801E-04     16.795     0.105E-03
   0.304E-01      0.326E-01      0.630E-01      0.319E-05      0.342E-05      0.661E-05     0.105E-03

3.951      0.706E-04      0.758E-04      0.146E-03      0.127E-05      0.148E-03     16.880     0.105E-03
   0.643E-01      0.687E-01      0.133E+00      0.672E-05      0.721E-05      0.139E-04     0.105E-03

4.001      0.716E-04      0.764E-04      0.148E-03     -0.590E-05      0.142E-03     16.625     0.105E-03
   0.980E-01      0.105E+00      0.203E+00      0.103E-04      0.110E-04      0.213E-04     0.105E-03

4.026     -0.200E-03     -0.217E-03     -0.417E-03     -0.139E-03     -0.557E-03     12.221     0.105E-03
   0.504E-01      0.534E-01      0.104E+00      0.529E-05      0.561E-05      0.109E-04     0.105E-03

4.032     -0.263E-03     -0.284E-03     -0.547E-03      0.726E-05     -0.540E-03     12.304     0.105E-03
   0.347E-01      0.365E-01      0.713E-01      0.365E-05      0.384E-05      0.749E-05     0.105E-03
```

```
4.039     -0.301E-03    -0.324E-03    -0.626E-03     0.571E-04    -0.569E-03    13.833     0.105E-03
    0.168E-01     0.172E-01     0.340E-01     0.177E-05     0.181E-05     0.357E-05     0.105E-03

      NO CONVERGENCE AT THIS TIME STEP      T= 4.039

      RESTART

4.039      0.363E-06    -0.303E-06     0.386E-18     0.617E-35     0.386E-18    13.833     0.000E+00
    0.249E-34     0.266E-34     0.504E-34     0.000E+00     0.000E+00     0.530E-38     0.105E-03

4.089      0.000E+00     0.000E+00     0.000E+00     0.000E+00     0.000E+00    17.200     0.000E+00
    0.000E+00     0.000E+00     0.000E+00     0.000E+00     0.000E+00     0.000E+00     0.000E+00

4.139      0.000E+00     0.000E+00     0.000E+00     0.000E+00     0.000E+00    17.200     0.000E+00
    0.000E+00     0.000E+00     0.000E+00     0.000E+00     0.000E+00     0.000E+00     0.000E+00

4.189      0.151E-05     0.163E-05     0.314E-05    -0.103E-06     0.304E-05    16.646     0.105E-03
    0.721E-03     0.774E-03     0.150E-02     0.757E-07     0.813E-07     0.157E-06     0.105E-03

4.239      0.599E-05     0.643E-05     0.124E-04     0.199E-07     0.124E-04    16.669     0.105E-03
    0.357E-02     0.384E-02     0.741E-02     0.375E-06     0.403E-06     0.778E-06     0.105E-03

4.289      0.179E-04     0.192E-04     0.370E-04     0.166E-06     0.372E-04    16.728     0.105E-03
    0.121E-01     0.130E-01     0.250E-01     0.127E-05     0.136E-05     0.263E-05     0.105E-03

4.339      0.384E-04     0.412E-04     0.797E-04     0.472E-06     0.801E-04    16.795     0.105E-03
    0.304E-01     0.326E-01     0.630E-01     0.319E-05     0.342E-05     0.661E-05     0.105E-03

4.389      0.706E-04     0.758E-04     0.146E-03     0.128E-05     0.148E-03    16.880     0.105E-03
    0.640E-01     0.687E-01     0.133E+00     0.672E-05     0.721E-05     0.139E-04     0.105E-03

4.439      0.675E-04     0.720E-04     0.140E-03    -0.673E-05     0.133E-03    16.591     0.105E-03
    0.961E-01     0.103E+00     0.199E+00     0.101E-04     0.108E-04     0.209E-04     0.105E-03

4.464     -0.187E-03    -0.202E-03    -0.388E-03    -0.129E-03    -0.518E-03    12.508     0.105E-03
    0.517E-01     0.549E-01     0.107E+00     0.543E-05     0.576E-05     0.112E-04     0.105E-03

4.489     -0.190E-03    -0.204E-03    -0.394E-03     0.121E-04    -0.382E-03    16.432     0.105E-03
    0.650E-02     0.625E-02     0.128E-01     0.683E-06     0.657E-06     0.134E-05     0.105E-03

      NO CONVERGENCE AT THIS TIME STEP      T= 4.489

      RESTART

4.489      0.914E-07    -0.914E-07    -0.678E-20     0.447E-35    -0.678E-20    16.432     0.000E+00
    0.193E-34     0.202E-34     0.395E-34     0.000E+00     0.000E+00     0.415E-38     0.105E-03
```

```
4.539       0.000E+00      0.000E+00      0.000E+00      0.000E+00      0.000E+00      17.200      0.000E+00
    0.000E+00      0.000E+00      0.000F+00      0.000E+00      0.000E+00      0.000E+00      0.000E+00

4.589       0.000E+00      0.000E+00      0.000E+00      0.000E+00      0.000E+00      17.200      0.000E+00
    0.000E+00      0.000E+00      0.000F+00      0.000E+00      0.000E+00      0.000E+00      0.000E+00

4.639       0.151E-05      0.163E-05      0.314E-05     -0.103E-06      0.304E-05      16.646      0.105E-03
    0.721E-03      0.774E-03      0.150E-02      0.757E-07      0.813E-07      0.157E-06      0.105E-03

4.689       0.599E-05      0.643E-05      0.124E-04      0.199E-07      0.124E-04      16.669      0.105E-03
    0.357E-02      0.384E-02      0.741E-02      0.375E-06      0.403E-06      0.778E-06      0.105E-03

4.739       0.179E-04      0.192E-04      0.370E-04      0.166E-06      0.372E-04      16.728      0.105E-03
    0.121E-01      0.130E-01      0.250E-01      0.127E-05      0.136E-05      0.263E-05      0.105E-03

4.789       0.384E-04      0.412E-04      0.797E-04      0.472E-06      0.801E-04      16.795      0.105E-03
    0.304E-01      0.326E-01      0.630E-01      0.319E-05      0.342E-05      0.661E-05      0.105E-03

4.839       0.699E-04      0.749E-04      0.145E-03      0.116E-05      0.146E-03      16.874      0.105E-03
    0.630E-01      0.683E-01      0.132E+00      0.668E-05      0.717E-05      0.139E-04      0.105E-03

4.889       0.731E-04      0.781E-04      0.151E-03     -0.535E-05      0.146E-03      16.643      0.105E-03
    0.984E-01      0.105E+00      0.204E+00      0.103E-04      0.111E-04      0.214E-04      0.105E-03

4.939      -0.186E-03     -0.202E-03     -0.388E-03     -0.528E-05     -0.394E-03      14.549      0.105E-03
    0.973E-02      0.930E-02      0.190E-01      0.102E-05      0.977E-06      0.200E-05      0.105E-03

     NO CONVERGENCE AT THIS TIME STEP     T= 4.939

     RESTART

4.939       0.835E-06     -0.835E-06     -0.339E-20      0.000E+00     -0.339E-20      14.549      0.000E+00
    0.143E-34      0.146E-34      0.289E-34      0.000E+00      0.000E+00      0.303E-38      0.105E-03

4.989       0.000E+00      0.000E+00      0.000E+00      0.000E+00      0.000E+00      17.200      0.000E+00
    0.000E+00      0.000E+00      0.000E+00      0.000E+00      0.000E+00      0.000E+00      0.000E+00

5.039       0.000E+00      0.000E+00      0.000E+00      0.000E+00      0.000E+00      17.200      0.000E+00
    0.000E+00      0.000E+00      0.000E+00      0.000E+00      0.000E+00      0.000E+00      0.000E+00

5.089       0.151E-05      0.163E-05      0.314E-05     -0.103E-06      0.304E-05      16.646      0.105E-03
    0.721E-03      0.774E-03      0.150E-02      0.757E-07      0.813E-07      0.157E-06      0.105E-03

5.139       0.599E-05      0.643E-05      0.124E-04      0.199E-07      0.124E-04      16.669      0.105E-03
    0.357E-02      0.384E-02      0.741E-02      0.375E-06      0.403E-06      0.778E-06      0.105E-03
```

```
5.189      0.179E-04     0.192E-04     0.370E-04     0.166E-06     0.372E-04     16.728     0.105E-03
    0.121E-01     0.130E-01     0.250E-01     0.127E-05     0.136E-05     0.263E-05     0.105E-03

5.239      0.384E-04     0.412E-04     0.797E-04     0.472E-06     0.801E-04     16.795     0.105E-03
    0.304E-01     0.326E-01     0.630E-01     0.319E-05     0.342E-05     0.661E-05     0.105E-03

5.289      0.706E-04     0.758E-04     0.146E-03     0.128E-05     0.148E-03     16.880     0.105E-03
    0.640E-01     0.687E-01     0.133E+00     0.672E-05     0.721E-05     0.139E-04     0.105E-03

5.339      0.682E-04     0.727E-04     0.141E-03    -0.659E-05     0.134E-03     16.597     0.105E-03
    0.964E-01     0.103E+00     0.200E+00     0.101E-04     0.108E-04     0.210E-04     0.105E-03

5.364     -0.187E-03    -0.203E-03    -0.390E-03    -0.131E-03    -0.521E-03     12.487     0.105E-03
    0.519E-01     0.551E-01     0.107E+00     0.545E-05     0.578E-05     0.112E-04     0.105E-03

5.370     -0.248E-03    -0.267E-03    -0.515E-03     0.000E+00    -0.515E-03     12.487     0.105E-03
    0.372E-01     0.392E-01     0.763E-01     0.390E-05     0.411E-05     0.802E-05     0.105E-03

5.376     -0.290E-03    -0.313E-03    -0.603E-03     0.494E-04    -0.554E-03     13.561     0.105E-03
    0.199E-01     0.206E-01     0.405E-01     0.209E-05     0.216E-05     0.425E-05     0.105E-03

5.383     -0.237E-03    -0.255E-03    -0.492E-03     0.563E-04    -0.436E-03     19.855     0.105E-03
    0.579E-02     0.540E-02     0.112E-01     0.608E-06     0.567E-06     0.118E-05     0.105E-03

        NO CONVERGENCE AT THIS TIME STEP     T= 5.383

        RESTART

5.383      0.581E-07    -0.581E-07     0.169E-19     0.390E-35     0.169E-19     19.855     0.000E+00
    0.176E-34     0.168E-34     0.344E-34     0.000E+00     0.000E+00     0.361E-38     0.105E-03

5.433      0.000E+00     0.000E+00     0.000E+00     0.000E+00     0.000E+00     17.200     0.000E+00
    0.000E+00     0.000E+00     0.000E+00     0.000E+00     0.000E+00     0.000E+00     0.000E+00

5.483      0.000E+00     0.000E+00     0.000E+00     0.000E+00     0.000E+00     17.200     0.000E+00
    0.000E+00     0.000E+00     0.000E+00     0.000E+00     0.000E+00     0.000E+00     0.000E+00

5.533      0.151E-05     0.163E-05     0.314E-05    -0.103E-06     0.304E-05     16.646     0.105E-03
    0.721E-03     0.774E-03     0.150E-02     0.757E-07     0.813E-07     0.157E-06     0.105E-03

5.583      0.599E-05     0.643E-05     0.124E-04     0.199E-07     0.124E-04     16.669     0.105E-03
    0.357E-02     0.384E-02     0.741E-02     0.375E-06     0.403E-06     0.778E-06     0.105E-03

5.633      0.179E-04     0.192E-04     0.370E-04     0.166E-06     0.372E-04     16.728     0.105E-03
    0.121E-01     0.130E-01     0.250E-01     0.127E-05     0.136E-05     0.263E-05     0.105E-03
```

```
5.683      0.384E-04      0.412E-04      0.797E-04      0.472E-06      0.801E-04      16.795      0.105E-03
    0.304E-01      0.326E-01      0.630E-01      0.319E-05      0.342E-05      0.661E-05      0.105E-03

5.733      0.699E-04      0.749E-04      0.145E-03      0.116E-05      0.146E-03      16.674      0.105E-03
    0.634E-01      0.683E-01      0.132E+00      0.668E-05      0.717E-05      0.139E-04      0.105E-03

5.783      0.722E-04      0.770E-04      0.149E-03     -0.555E-05      0.144E-03      16.635      0.105E-03
    0.977E-01      0.105E+00      0.203E+00      0.103E-04      0.110E-04      0.213E-04      0.105E-03

5.833     -0.185E-03     -0.201E-03     -0.386E-03     -0.532E-05     -0.392E-03      14.564      0.105E-03
    0.973E-02      0.931E-02      0.190E-01      0.102E-05      0.978E-06      0.200E-05      0.105E-03

5.833     -0.188E-03     -0.204E-03     -0.392E-03      0.480E-04     -0.344E-03      14.926      0.105E-03
    0.833E-02      0.779E-02      0.161E-01      0.875E-06      0.819E-06      0.169E-05      0.105E-03

5.834     -0.190E-03     -0.206E-03     -0.396E-03      0.703E-04     -0.325E-03      15.603      0.105E-03
    0.692E-02      0.626E-02      0.132E-01      0.727E-06      0.658E-06      0.138E-05      0.105E-03

5.835     -0.189E-03     -0.205E-03     -0.394E-03      0.911E-04     -0.303E-03      16.645      0.105E-03
    0.551E-02      0.474E-02      0.102E-01      0.579E-06      0.498E-06      0.108E-05      0.105E-03

5.836     -0.184E-03     -0.200E-03     -0.384E-03      0.104E-03     -0.280E-03      19.058      0.105E-03
    0.414E-02      0.325E-02      0.739E-02      0.435E-06      0.342E-06      0.776E-06      0.105E-03

       NO CONVERGENCE AT THIS TIME STEP     T= 5.836

       RESTART

5.836      0.782E-06     -0.782E-06      0.678E-20      0.477E-35      0.678E-20      19.058      0.000E+00
    0.245E-34      0.191E-34      0.436E-34      0.000E+00      0.000E+00      0.458E-38      0.105E-03

5.886      0.000E+00      0.000E+00      0.000E+00      0.000E+00      0.000E+00      17.200      0.000E+00
    0.000E+00      0.000E+00      0.000E+00      0.000E+00      0.000E+00      0.000E+00      0.000E+00

5.936      0.000E+00      0.000E+00      0.000E+00      0.000E+00      0.000E+00      17.200      0.000E+00
    0.000E+00      0.000E+00      0.000E+00      0.000E+00      0.000E+00      0.000E+00      0.000E+00

5.986      0.151E-05      0.163E-05      0.314E-05     -0.103E-06      0.304E-05      16.646      0.105E-03
    0.721E-03      0.774E-03      0.150E-02      0.757E-07      0.813E-07      0.157E-06      0.105E-03

6.036      0.599E-05      0.643E-05      0.124E-04      0.199E-07      0.124E-04      16.669      0.105E-03
    0.357E-02      0.384E-02      0.741E-02      0.375E-06      0.403E-06      0.778E-06      0.105E-03

6.086      0.179E-04      0.192E-04      0.370E-04      0.166E-06      0.372E-04      16.728      0.105E-03
    0.121E-01      0.130E-01      0.250E-01      0.127E-05      0.136E-05      0.263E-05      0.105E-03
```

6.136	0.384E-04	0.412E-04	0.797E-04	0.472E-06	0.801E-04	16.795	0.105E-03
0.304E-01	0.326E-01	0.630E-01	0.319E-05	0.342E-05	0.661E-05	0.105E-03	
6.186	0.706E-04	0.758E-04	0.146E-03	0.128E-05	0.148E-03	16.880	0.105E-03
0.64[illegible]E-01	0.687E-01	0.133E+00	0.672E-05	0.721E-05	0.139E-04	0.105E-03	
6.236	0.668E-04	0.712E-04	0.138E-03	-0.688E-05	0.131E-03	16.585	0.105E-03
0.958E-01	0.103E+00	0.198E+00	0.101E-04	0.108E-04	0.2[illegible]8E-04	0.105E-03	
6.261	-0.186E-03	-0.202E-03	-0.388E-03	-0.128E-03	-0.516E-03	12.524	0.105E-03
0.514E-01	0.[illegible]46E-01	0.106E+00	0.540E-05	0.573E-05	0.111E-04	0.105E-03	
6.267	-0.246E-03	-0.266E-03	-0.512E-03	0.000E+00	-0.512E-03	12.524	0.105E-03
0.368E-01	0.388E-01	0.756E-01	0.387E-05	0.407E-05	0.794E-05	0.105E-03	
6.273	-0.288E-03	-0.310E-03	-0.598E-03	0.501E-04	-0.548E-03	13.632	0.105E-03
0.197E-01	0.203E-01	0.400E-01	0.207E-05	0.214E-05	0.420E-05	0.105E-03	
6.280	-0.233E-03	-0.251E-03	-0.484E-03	0.573E-04	-0.426E-03	19.959	0.105E-03
0.581E-02	0.542E-02	0.112E-01	0.610E-06	0.570E-06	0.118E-05	0.105E-03	

NO CONVERGENCE AT THIS TIME STEP T= 6.280

RESTART

6.260	0.614E-07	-0.614E-07	0.102E-19	0.395E-35	0.102E-19	19.959	0.000E+00
0.175E-34	0.171E-34	0.350E-34	0.000E+00	0.000E+00	0.368E-38	0.105E-03	
6.330	0.000E+00	0.000E+00	0.000E+00	0.000E+00	0.000E+00	17.200	0.000E+00
0.000E+00	0.000E+00	0.000E+00	0.000E+00	0.000E+00	0.000E+00	0.000E+00	
6.380	0.000E+00	0.000E+00	0.000E+00	0.000E+00	0.000E+00	17.200	0.000E+00
0.000E+00	0.000E+00	0.000E+00	0.000E+00	0.000E+00	0.000E+00	0.000E+00	
6.430	0.151E-05	0.163E-05	0.314E-05	-0.103E-06	0.304E-05	16.646	0.105E-03
0.721E-03	0.774E-03	0.150E-02	0.757E-07	0.813E-07	0.157E-06	0.105E-03	
6.480	0.599E-05	0.643E-05	0.124E-04	0.199E-07	0.124E-04	16.669	0.105E-03
0.357E-02	0.384E-02	0.741E-02	0.375E-06	0.403E-06	0.778E-06	0.105E-03	
6.530	0.179E-04	0.192E-04	0.370E-04	0.166E-06	0.372E-04	16.728	0.105E-03
0.121E-01	0.130E-01	0.250E-01	0.127E-05	0.136E-05	0.263E-05	0.105E-03	
6.580	0.384E-04	0.412E-04	0.797E-04	0.472E-06	0.801E-04	16.795	0.105E-03
0.304E-01	0.326E-01	0.630E-01	0.319E-05	0.342E-05	0.661E-05	0.105E-03	

```
6.630      0.699E-04      0.749E-04      0.145E-03      0.116E-05      0.146E-03     16.874     0.105E-03
    0.636E-01      0.683E-01      0.132E+00      0.668E-05      0.717E-05      0.139E-04     0.105E-03

6.680      0.693E-04      0.739E-04      0.143E-03     -0.613E-05      0.137E-03     16.611     0.105E-03
    0.966E-01      0.123E+00      0.200E+00      0.101E-04      0.109E-04      0.210E-04     0.105E-03

6.705     -0.163E-03     -0.177E-03     -0.341E-03     -0.131E-03     -0.472E-03     12.853     0.105E-03
    0.577E-01      0.613E-01      0.119E+00      0.606E-05      0.644E-05      0.125E-04     0.105E-03

6.730     -0.205E-03     -0.220E-03     -0.425E-03      0.136E-04     -0.412E-03     15.836     0.105E-03
    0.893E-02      0.883E-02      0.178E-01      0.939E-06      0.927E-06      0.187E-05     0.105E-03

       NO CONVERGENCE AT THIS TIME STEP      T= 6.730

       RESTART

6.730      0.216E-06     -0.216E-06     -0.339E-20      0.000E+00     -0.339E-20     15.836     0.000E+00
    0.140E-34      0.141E-34      0.281E-34      0.000E+00      0.000E+00      0.296E-38     0.105E-03

6.780      0.000E+00      0.000E+00      0.000E+00      0.000E+00      0.000E+00     17.200     0.000E+00
    0.000E+00      0.000E+00      0.000E+00      0.000E+00      0.000E+00      0.000E+00     0.000E+00

6.830      0.000E+00      0.000E+00      0.000E+00      0.000E+00      0.000E+00     17.200     0.000E+00
    0.000E+00      0.000E+00      0.000E+00      0.000E+00      0.000E+00      0.000E+00     0.000E+00

6.880      0.151E-05      0.163E-05      0.314E-05     -0.103E-06      0.304E-05     16.646     0.105E-03
    0.721E-03      0.774E-03      0.150E-02      0.757E-07      0.813E-07      0.157E-06     0.105E-03

6.930      0.599E-05      0.643E-05      0.124E-04      0.199E-07      0.124E-04     16.669     0.105E-03
    0.357E-02      0.384E-02      0.741E-02      0.375E-06      0.403E-06      0.778E-06     0.105E-03

6.980      0.179E-04      0.192E-04      0.370E-04      0.166E-06      0.372E-04     16.728     0.105E-03
    0.121E-01      0.130E-01      0.250E-01      0.127E-05      0.136E-05      0.263E-05     0.105E-03

7.030      0.384E-04      0.412E-04      0.797E-04      0.472E-06      0.801E-04     16.795     0.105E-03
    0.304E-01      0.326E-01      0.630E-01      0.319E-05      0.342E-05      0.661E-05     0.105E-03

7.080      0.699E-04      0.749E-04      0.145E-03      0.116E-05      0.146E-03     16.874     0.105E-03
    0.636E-01      0.683E-01      0.132E+00      0.668E-05      0.717E-05      0.139E-04     0.105E-03

7.130      0.748E-04      0.798E-04      0.155E-03     -0.506E-05      0.150E-03     16.656     0.105E-03
    0.992E-01      0.106E+00      0.205E+00      0.104E-04      0.112E-04      0.216E-04     0.105E-03

7.155     -0.111E-03     -0.120E-03     -0.231E-03     -0.125E-03     -0.356E-03     13.619     0.105E-03
    0.729E-01      0.777E-01      0.151E+00      0.766E-05      0.816E-05      0.158E-04     0.105E-03
```

```
7.180      -0.232E-03      -0.250E-03      -0.482E-03      0.970E-05      -0.472E-03      14.584      0.105E-03
    0.177E-01       0.182E-01       0.359E-01       0.186E-05       0.191E-05       0.378E-05     0.105E-03

7.186      -0.194E-03      -0.209E-03      -0.404E-03      0.435E-04      -0.360E-03      18.903      0.105E-03
    0.619E-02       0.574E-02       0.119E-01       0.650E-06       0.603E-06       0.125E-05     0.105E-03

        NO CONVERGENCE AT THIS TIME STEP     T= 7.186

        RESTART

7.186       0.282E-06      -0.282E-06       0.678E-20      0.414E-35       0.678E-20      18.903      0.000E+00
    0.192E-34       0.181E-34       0.374E-34       0.000E+00       0.000E+00       0.352E-38     0.105E-03

7.236       0.000E+00       0.000E+00       0.000E+00      0.000E+00       0.000E+00      17.200      0.000E+00
    0.000E+00       0.000E+00       0.000E+00       0.000E+00       0.000E+00       0.000E+00     0.000E+00

7.266       0.000E+00       0.000E+00       0.000E+00      0.000E+00       0.000E+00      17.200      0.000E+00
    0.000E+00       0.000E+00       0.000E+00       0.000E+00       0.000E+00       0.000E+00     0.000E+00

7.336       0.151E-05       0.163E-05       0.314E-05     -0.103E-06       0.304E-05      16.646      0.105E-03
    0.721E-03       0.774E-03       0.150E-02       0.757E-07       0.813E-07       0.157E-06     0.105E-03

7.386       0.599E-05       0.643E-05       0.124E-04      0.199E-07       0.124E-04      16.669      0.105E-03
    0.357E-02       0.384E-02       0.741E-02       0.375E-06       0.403E-06       0.778E-06     0.105E-03

7.436       0.179E-04       0.192E-04       0.370E-04      0.166E-06       0.372E-04      16.728      0.105E-03
    0.121E-01       0.130E-01       0.250E-01       0.127E-05       0.136E-05       0.263E-05     0.105E-03

7.486       0.384E-04       0.412E-04       0.797E-04      0.472E-06       0.801E-04      16.795      0.105E-03
    0.304E-01       0.326E-01       0.630E-01       0.319E-05       0.342E-05       0.661E-05     0.105E-03

7.536       0.699E-04       0.749E-04       0.145E-03      0.116E-05       0.146E-03      16.874      0.105E-03
    0.636E-01       0.683E-01       0.132E+00       0.668E-05       0.717E-05       0.139E-04     0.105E-03

7.586       0.750E-04       0.801E-04       0.155E-03     -0.504E-05       0.150E-03      16.658      0.105E-03
    0.993E-01       0.106E+00       0.206E+00       0.104E-04       0.112E-04       0.216E-04     0.105E-03

7.636      -0.111E-04      -0.132E-04      -0.243E-04     -0.168E-04      -0.411E-04      15.922      0.105E-03
    0.940E-01       0.100E+00       0.194E+00       0.988E-05       0.105E-04       0.204E-04     0.105E-03

7.661      -0.178E-03      -0.192E-03      -0.370E-03     -0.585E-04      -0.429E-03      13.899      0.105E-03
    0.517E-01       0.543E-01       0.106E+00       0.544E-05       0.571E-05       0.111E-04     0.105E-03

7.711      -0.100E-03      -0.107E-03      -0.207E-03      0.291E-05      -0.204E-03      17.142      0.105E-03
    0.413E-02       0.359E-02       0.773E-02       0.434E-06       0.377E-06       0.812E-06     0.105E-03
```

```
7.717     -0.562E-04    -0.594E-04    -0.116E-03     0.157E-05    -0.114E-03    19.494     0.105E-03
    0.787E-03     0.566E-04     0.844E-03     0.827E-07     0.594E-08     0.887E-07     0.105E-03

      NO CONVERGENCE AT THIS TIME STEP     T= 7.717

      RESTART

7.717     -0.463E-06     0.463E-06     0.847E-21     0.242E-34     0.847E-21    19.494     0.105E-03
    0.302E-33     0.230E-34     0.325E-33     0.317E-37     0.000E+00     0.342E-37     0.105E-03

7.767      0.000E+00     0.000E+00     0.000E+00     0.000E+00     0.000E+00    17.200     0.000E+00
    0.000E+00     0.000E+00     0.000E+00     0.000E+00     0.000E+00     0.000E+00     0.000E+00

7.817      0.000E+00     0.000E+00     0.000E+00     0.000E+00     0.000E+00    17.200     0.000E+00
    0.000E+00     0.000E+00     0.000E+00     0.000E+00     0.000E+00     0.000E+00     0.000E+00

7.867      0.151E-05     0.163E-05     0.314E-05    -0.103E-06     0.304E-05    16.646     0.105E-03
    0.721E-03     0.774E-03     0.150E-02     0.757E-07     0.813E-07     0.157E-06     0.105E-03

7.917      0.599E-05     0.643E-05     0.124E-04     0.199E-07     0.124E-04    16.669     0.105E-03
    0.357E-02     0.384E-02     0.741E-02     0.375E-06     0.403E-06     0.778E-06     0.105E-03

7.967      0.179E-04     0.192E-04     0.370E-04     0.166E-06     0.372E-04    16.728     0.105E-03
    0.121E-01     0.130E-01     0.250E-01     0.127E-05     0.136E-05     0.263E-05     0.105E-03

8.017      0.384E-04     0.412E-04     0.797E-04     0.472E-06     0.802E-04    16.795     0.105E-03
    0.304E-01     0.326E-01     0.630E-01     0.319E-05     0.342E-05     0.661E-05     0.105E-03

8.067      0.699E-04     0.750E-04     0.145E-03     0.117E-05     0.146E-03    16.874     0.105E-03
    0.636E-01     0.683E-01     0.132E+00     0.669E-05     0.717E-05     0.139E-04     0.105E-03

8.117      0.758E-04     0.809E-04     0.157E-03    -0.493E-05     0.152E-03    16.664     0.105E-03
    0.997E-01     0.107E+00     0.206E+00     0.105E-04     0.112E-04     0.217E-04     0.105E-03

8.142      0.293E-04     0.306E-04     0.599E-04    -0.439E-04     0.160E-04    15.860     0.105E-03
    0.107E+00     0.114E+00     0.221E+00     0.112E-04     0.120E-04     0.232E-04     0.105E-03

8.192     -0.237E-04    -0.233E-04    -0.441E-04     0.827E-05    -0.358E-04    16.190     0.105E-03
    0.968E-01     0.103E+00     0.200E+00     0.102E-04     0.108E-04     0.210E-04     0.105E-03

8.217     -0.189E-03    -0.204E-03    -0.393E-03    -0.669E-04    -0.460E-03    13.881     0.105E-03
    0.519E-01     0.544E-01     0.106E+00     0.545E-05     0.571E-05     0.112E-04     0.105E-03

8.224     -0.228E-03    -0.246E-03    -0.474E-03     0.000E+00    -0.474E-03    13.881     0.105E-03
    0.383E-01     0.397E-01     0.780E-01     0.403E-05     0.417E-05     0.820E-05     0.105E-03
```

```
8.230      -0.253E-03    -0.272E-03    -0.525E-03     0.443E-04    -0.481E-03     14.798     0.105E-03
    0.233E-01     0.235E-01     0.468E-01     0.245E-05     0.247E-05     0.492E-05     0.105E-03

8.236      -0.230E-03    -0.247E-03    -0.477E-03     0.503E-04    -0.427E-03     17.905     0.105E-03
    0.964E-02     0.880E-02     0.184E-01     0.101E-05     0.924E-06     0.194E-05     0.105E-03

        NO CONVERGENCE AT THIS TIME STEP     T= 8.236

        RESTART

8.236       0.174E-06    -0.174E-06     0.678E-20     0.649E-35     0.678E-20     17.905     0.105E-03
    0.293E-34     0.272E-34     0.565E-34     0.308E-38     0.000E+00     0.594E-38     0.105E-03

8.286       0.000E+00     0.000E+00     0.000E+00     0.000E+00     0.000E+00     17.200     0.000E+00
    0.000E+00     0.000E+00     0.000E+00     0.000E+00     0.000E+00     0.000E+00     0.000E+00

8.336       0.000E+00     0.000E+00     0.000E+00     0.000E+00     0.000E+00     17.200     0.000E+00
    0.000E+00     0.000E+00     0.000E+00     0.000E+00     0.000E+00     0.000E+00     0.000E+00

8.386       0.151E-05     0.163E-05     0.314E-05    -0.103E-06     0.304E-05     16.646     0.115E-03
    0.721E-03     0.774E-03     0.150E-02     0.757E-07     0.813E-07     0.157E-06     0.105E-03

8.436       0.599E-05     0.643E-05     0.124E-04     0.199E-07     0.124E-04     16.669     0.105E-03
    0.357E-02     0.384E-02     0.741E-02     0.375E-06     0.403E-06     0.778E-06     0.105E-03

8.486       0.179E-04     0.192E-04     0.371E-04     0.166E-06     0.372E-04     16.728     0.105E-03
    0.121E-01     0.130E-01     0.250E-01     0.127E-05     0.136E-05     0.263E-05     0.105E-03

8.536       0.384E-04     0.412E-04     0.797E-04     0.472E-06     0.802E-04     16.795     0.105E-03
    0.304E-01     0.326E-01     0.630E-01     0.319E-05     0.342E-05     0.661E-05     0.105E-03

8.586       0.699E-04     0.750E-04     0.145E-03     0.117E-05     0.146E-03     16.874     0.105E-03
    0.637E-01     0.683E-01     0.132E+00     0.669E-05     0.717E-05     0.139E-04     0.105E-03

8.636       0.758E-04     0.809E-04     0.157E-03    -0.493E-05     0.152E-03     16.664     0.105E-03
    0.997E-01     0.107E+00     0.206E+00     0.105E-04     0.112E-04     0.217E-04     0.105E-03

8.661       0.294E-04     0.307E-04     0.601E-04    -0.439E-04     0.162E-04     15.861     0.105E-03
    0.107E+00     0.114E+00     0.221E+00     0.112E-04     0.120E-04     0.232E-04     0.105E-03

8.711      -0.206E-04    -0.232E-04    -0.437E-04     0.826E-05    -0.355E-04     16.191     0.105E-03
    0.969E-01     0.103E+00     0.200E+00     0.102E-04     0.108E-04     0.210E-04     0.105E-03

8.736      -0.189E-03    -0.204E-03    -0.393E-03    -0.671E-04    -0.460E-03     13.881     0.105E-03
    0.520E-01     0.545E-01     0.107E+00     0.547E-05     0.572E-05     0.112E-04     0.105E-03
```

```
9.255     -0.188E-03     -0.203E-03     -0.391E-03     -0.674E-04     -0.459E-03     13.884     0.105E-03
     0.523E-01      0.548E-01      0.107E+00      0.550E-05      0.576E-05      0.112E-04      0.105E-03

9.261     -0.225E-03     -0.243E-03     -0.469E-03      0.109E-04     -0.458E-03     14.012     0.105E-03
     0.389E-01      0.404E-01      0.793E-01      0.409E-05      0.424E-05      0.833E-05      0.105E-03

9.267     -0.250E-03     -0.269E-03     -0.519E-03      0.399E-04     -0.479E-03     14.811     0.105E-03
     0.241E-01      0.243E-01      0.484E-01      0.253E-05      0.256E-05      0.509E-05      0.105E-03

9.274     -0.227E-03     -0.244E-03     -0.471E-03      0.548E-04     -0.416E-03     17.921     0.105E-03
     0.106E-01      0.982E-02      0.204E-01      0.111E-05      0.103E-05      0.214E-05      0.105E-03

     NO CONVERGENCE AT THIS TIME STEP     T= 9.274

     RESTART

9.274      0.182E-06     -0.182E-06      0.339E-20      0.000E+00      0.339E-20     17.921     0.000E+00
     0.15?E-34      0.148E-34      0.307E-34      0.000E+00      0.000E+00      0.323E-38      0.105E-03

9.324      0.000E+00      0.000E+00      0.000E+00      0.000E+00      0.000E+00     17.200     0.000E+00
     0.000E+00      0.000E+00      0.000E+00      0.000E+00      0.000E+00      0.000E+00      0.000E+00

9.374      0.000E+00      0.000E+00      0.000E+00      0.000E+00      0.000E+00     17.200     0.000E+00
     0.000E+00      0.000E+00      0.000E+00      0.000E+00      0.000E+00      0.000E+00      0.000E+00

9.424      0.151E-05      0.163E-05      0.314E-05     -0.103E-06      0.304E-05     16.646     0.105E-03
     0.721E-03      0.774E-03      0.150E-02      0.757E-07      0.813E-07      0.157E-06      0.105E-03

9.474      0.599E-05      0.643E-05      0.124E-04      0.199E-07      0.124E-04     16.669     0.105E-03
     0.357E-02      0.384E-02      0.741E-02      0.375E-06      0.403E-06      0.778E-06      0.105E-03

9.524      0.179E-04      0.192E-04      0.371E-04      0.166E-06      0.372E-04     16.728     0.105E-03
     0.121E-01      0.130E-01      0.250E-01      0.127E-05      0.136E-05      0.263E-05      0.105E-03

9.574      0.384E-04      0.412E-04      0.797E-04      0.472E-06      0.802E-04     16.795     0.105E-03
     0.304E-01      0.326E-01      0.630E-01      0.319E-05      0.342E-05      0.661E-05      0.105E-03

9.624      0.699E-04      0.750E-04      0.145E-03      0.117E-05      0.146E-03     16.874     0.105E-03
     0.636E-01      0.683E-01      0.132E+00      0.665E-05      0.717E-05      0.139E-04      0.105E-03

9.674      0.761E-04      0.813E-04      0.157E-03     -0.487E-05      0.152E-03     16.666     0.105E-03
     0.996E-01      0.107E+00      0.207E+00      0.105E-04      0.112E-04      0.217E-04      0.105E-03

9.699      0.304E-04      0.318E-04      0.622E-04     -0.436E-04      0.186E-04     15.872     0.105E-03
     0.107E+00      0.115E+00      0.222E+00      0.113E-04      0.120E-04      0.233E-04      0.105E-03
```

```
9.749      -0.193E-04     -0.218E-04     -0.410E-04      0.809E-05     -0.329E-04      16.193       0.105E-03
    0.979E-01      0.104E+00      0.202E+00      0.103E-04      0.109E-04      0.212E-04      0.105E-03

9.774      -0.181E-03     -0.196E-03     -0.377E-03     -0.665E-04     -0.443E-03      13.983       0.105E-03
    0.549E-01      0.576E-01      0.112E+00      0.577E-05      0.604E-05      0.118E-04      0.105E-03

9.799      -0.183E-03     -0.197E-03     -0.380E-03      0.127E-04     -0.367E-03      16.460       0.105E-03
    0.113E-01      0.107E-01      0.220E-01      0.119E-05      0.112E-05      0.231E-05      0.105E-03

      NO CONVERGENCE AT THIS TIME STEP     T= 9.799

      RESTART

9.799       0.166E-06     -0.166E-06      0.678E-20      0.000E+00      0.676E-20      16.460       0.000E+00
    0.169E-34      0.159E-34      0.328E-34      0.000E+00      0.000E+00      0.345E-38      0.105E-03

9.849       0.000E+00      0.000E+00      0.000E+00      0.000E+00      0.000E+00      17.200       0.000E+00
    0.000E+00      0.000E+00      0.000E+00      0.000E+00      0.000E+00      0.000E+00      0.000E+00

9.899       0.000E+00      0.000E+00      0.000E+00      0.000E+00      0.000E+00      17.200       0.000E+00
    0.000E+00      0.000E+00      0.000E+00      0.000E+00      0.000E+00      0.000E+00      0.000E+00

9.949       0.151E-05      0.163E-05      0.314E-05     -0.103E-06      0.304E-05      16.646       0.105E-03
    0.721E-03      0.774E-03      0.150E-02      0.757E-07      0.813E-07      0.157E-06      0.105E-03

9.999       0.599E-05      0.643E-05      0.124E-04      0.199E-07      0.124E-04      16.669       0.105E-03
    0.357E-02      0.384E-02      0.741E-02      0.375E-06      0.403E-06      0.778E-06      0.105E-03

10.049      0.179E-04      0.192E-04      0.371E-04      0.166E-06      0.372E-04      16.728       0.105E-03
    0.121E-01      0.130E-01      0.250E-01      0.127E-05      0.136E-05      0.263E-05      0.105E-03

10.099      0.384E-04      0.412E-04      0.797E-04      0.472E-06      0.802E-04      16.795       0.105E-03
    0.304E-01      0.326E-01      0.630E-01      0.319E-05      0.342E-05      0.661E-05      0.105E-03

10.149      0.699E-04      0.750E-04      0.14?E-03      0.117E-05      0.146E-03      16.874       0.105E-03
    0.635E-01      0.683E-01      0.132E+00      0.669E-05      0.717E-05      0.139E-04      0.105E-03

10.199      0.764E-04      0.815E-04      0.158E-03     -0.483E-05      0.153E-03      16.668       0.105E-03
    0.100E+00      0.107E+00      0.207E+00      0.105E-04      0.112E-04      0.218E-04      0.105E-03

10.224      0.320E-04      0.335E-04      0.655E-04     -0.4 4E-74      0.231E-04      15.894       0.105E-03
    0.108E+00      0.115E+00      0.223E+00      0.113E-04      0.121E-04      0.234E-04      0.105E-03

10.274     -0.178E-04     -0.202E-04     -0.380E-04      0.753E-05     -0.305E-04      16.192       0.105E-03
    0.991E-01      0.105E+00      0.205E+00      0.104E-04      0.111E-04      0.215E-04      0.105E-03
```

```
10.299     -0.174E-03     -0.189E-03     -0.363E-03     -0.670E-04     -0.430E-03     14.065     0.105E-03
     0.576E-01      0.605E-01      0.118E+00      0.606E-05      0.636E-05      0.124E-04      0.105E-03

10.324     -0.191E-03     -0.205E-03     -0.396E-03      0.130E-04     -0.383E-03     16.235     0.105E-03
     0.123E-01      0.117E-01      0.240E-01      0.129E-05      0.123E-05      0.252E-05      0.105E-03

        NO CONVERGENCE AT THIS TIME STEP     T=10.324

        RESTART

10.324      0.201E-06     -0.201E-06      0.339E-20      0.430E-35      0.339E-20     16.235     0.000E+00
     0.193E-34      0.185E-34      0.379E-34      0.000E+00      0.000E+00      0.398E-38      0.105E-03

10.374      0.000E+00      0.000E+00      0.000E+00      0.000E+00      0.000E+00     17.200     0.000E+00
     0.000E+00      0.000E+00      0.000E+00      0.000E+00      0.000E+00      0.000E+00      0.000E+00

10.424      0.000E+00      0.000E+00      0.000E+00      0.000E+00      0.000E+00     17.200     0.000E+00
     0.000E+00      0.000E+00      0.000E+00      0.000E+00      0.000E+00      0.000E+00      0.000E+00

10.474      0.151E-05      0.163E-05      0.314E-05     -0.103E-06      0.304E-05     16.646     0.105E-03
     0.721E-03      0.774E-03      0.150E-02      0.757E-07      0.813E-07      0.157E-06      0.105E-03

10.524      0.599E-05      0.643E-05      0.124E-04      0.199E-07      0.124E-04     16.669     0.105E-03
     0.357E-02      0.384E-02      0.741E-02      0.375E-06      0.403E-06      0.778E-06      0.105E-03

10.574      0.179E-04      0.192E-04      0.371E-04      0.166E-06      0.372E-04     16.728     0.105E-03
     0.121E-01      0.130E-01      0.250E-01      0.127E-05      0.136E-05      0.263E-05      0.105E-03

10.624      0.384E-04      0.412E-04      0.797E-04      0.472E-06      0.802E-04     16.795     0.105E-03
     0.304E-01      0.326E-01      0.630E-01      0.319E-05      0.342E-05      0.661E-05      0.105E-03

10.674      0.699E-04      0.750E-04      0.145E-03      0.117E-05      0.146E-03     16.874     0.105E-03
     0.636E-01      0.683E-01      0.132E+00      0.669E-05      0.717E-05      0.139E-04      0.105E-03

10.699      0.934E-04      0.100E-03      0.193E-03      0.550E-05      0.159E-03     17.002     0.105E-03
     0.858E-01      0.921E-01      0.178E+00      0.902E-05      0.967E-05      0.187E-04      0.105E-03

10.724      0.576E-04      0.611E-04      0.119E-03     -0.501E-04      0.688E-04     16.046     0.105E-03
     0.995E-01      0.107E+00      0.206E+00      0.105E-04      0.112E-04      0.217E-04      0.105E-03

10.774     -0.457E-06     -0.148E-05     -0.194E-05      0.217E-05      0.235E-06     16.129     0.105E-03
     0.993E-01      0.105E+00      0.205E+00      0.104E-04      0.111E-04      0.216E-04      0.105E-03

10.799     -0.159E-03     -0.173E-03     -0.332E-03     -0.714E-04     -0.404E-03     14.028     0.105E-03
     0.614E-01      0.648E-01      0.126E+00      0.645E-05      0.681E-05      0.133E-04      0.105E-03
```

```
10.824      -0.199E-03     -0.214E-03     -0.413E-03      0.130E-04     -0.400E-03      15.877      0.105E-03
     0.141E-01      0.139E-01      0.280E-01      0.140E-05      0.146E-05      0.294E-05     0.105E-03

10.830      -0.149E-03     -0.161E-03     -0.310E-03      0.299E-04     -0.280E-03      19.746      0.105E-03
     0.524E-02      0.433E-02      0.956E-02      0.550E-06      0.455E-06      0.100E-05     0.105E-03

      NO CONVERGENCE AT THIS TIME STEP      T=10.830

      RESTART

10.830       0.142E-06     -0.142E-06      0.339E-20      0.617E-35      0.339E-20      19.746      0.105E-03
     0.321E-34      0.273E-34      0.594E-34      0.337E-38      0.000E+00      0.624E-38     0.105E-03

10.880       0.000E+00      0.000E+00      0.000E+00      0.000E+00      0.000E+00      17.200      0.000E+00
     0.000E+00      0.000E+00      0.000E+00      0.000E+00      0.000E+00      0.000E+00     0.000E+00

10.930       0.000E+00      0.000E+00      0.000E+00      0.000E+00      0.000E+00      17.200      0.000E+00
     0.000E+00      0.000E+00      0.000E+00      0.000E+00      0.000E+00      0.000E+00     0.000E+00

10.980       0.151E-05      0.163E-05      0.314E-05     -0.103E-06      0.304E-05      16.646      0.105E-03
     0.721E-03      0.774E-03      0.150E-02      0.757E-07      0.813E-07      0.157E-06     0.105E-03

11.030       0.599E-05      0.643E-05      0.124E-04      0.199E-07      0.124E-04      16.[illegible]69      0.105E-03
     0.357E-02      0.384E-02      0.741E-02      0.375E-06      0.403E-06      0.7[illegible]E-06     0.105E-03

11.080       0.179E-04      0.192E-04      0.371E-04      0.166E-06      0.372E-04      16.728      0.105E-03
     0.121E-01      0.130E-01      0.250E-01      0.127E-05      0.136E-05      0.263E-05     0.105E-03

11.130       0.384E-04      0.412E-04      0.797E-04      0.472E-06      0.802E-04      16.795      0.105E-03
     0.304E-01      0.326E-01      0.630E-01      0.319E-05      0.342E-05      0.661E-05     0.105E-03

11.180       0.699E-04      0.750E-04      0.145E-03      0.117E-05      0.146E-03      16.874      0.105E-03
     0.63[illegible]E-01      0.683E-01      0.132E+00      0.669E-05      0.717E-05      0.139E-04     0.105E-03

11.205       0.934E-04      0.100E-03      0.193E-03      0.550E-05      0.199E-03      17.003      0.105E-03
     0.858E-01      0.921E-01      0.178E+00      0.902E-05      0.967E-05      0.187E-04     0.105E-03

11.230       0.575E-04      0.611E-04      0.119E-03     -0.502E-04      0.683E-04      16.095      0.105E-03
     0.995E-01      0.107E+00      0.206E+00      0.105E-04      0.112E-04      0.217E-04     0.105E-03

11.280      -0.643E-06     -0.168E-05     -0.232E-05      0.218E-05     -0.144E-06      16.128      0.105E-03
     0.992E-01      0.106E+00      0.205E+00      0.104E-04      0.111E-04      0.215E-04     0.105E-03

11.305      -0.159E-03     -0.173E-03     -0.332E-03     -0.712E-04     -0.403E-03      14.033      0.105E-03
     0.613E-01      0.647E-01      0.126E+00      0.644E-05      0.680E-05      0.132E-04     0.105E-03
```

-221-

11.330	-0.199E-03	-0.214E-03	-0.414E-03	0.130E-04	-0.401E-03	15.867	0.105E-03
	0.139E-01	0.137E-01	0.276E-01	0.146E-05	0.144E-05	0.290E-05	0.105E-03
11.336	-0.148E-03	-0.159E-03	-0.307E-03	0.301E-04	-0.277E-03	19.871	0.105E-03
	0.512E-02	0.421E-02	0.934E-02	0.539E-06	0.443E-06	0.982E-06	0.105E-03
11.337	-0.139E-03	-0.150E-03	-0.289E-03	0.489E-04	-0.240E-03	21.057	0.105E-03
	0.409E-02	0.310E-02	0.719E-02	0.430E-06	0.325E-06	0.755E-06	0.105E-03

NO CONVERGENCE AT THIS TIME STEP T=11.337

RESTART

11.337	0.136E-06	-0.136E-06	0.339E-20	0.425E-35	0.339E-20	21.057	0.000E+00
	0.241E-34	0.184E-34	0.425E-34	0.000E+00	0.000E+00	0.446E-38	0.105E-03
11.387	0.000E+00	0.000E+00	0.000E+00	0.000E+00	0.000E+00	17.200	0.000E+00
	0.000E+00	0.000E+00	0.000E+00	0.000E+00	0.000E+00	0.000E+00	0.000E+00
11.437	0.000E+00	0.000E+00	0.000E+00	0.000E+00	0.000E+00	17.200	0.000E+00
	0.000E+00	0.000E+00	0.000E+00	0.000E+00	0.000E+00	0.000E+00	0.000E+00
11.487	0.151E-05	0.163E-05	0.314E-05	-0.103E-06	0.324E-05	16.646	0.105E-03
	0.721E-03	0.774E-03	0.150E-02	0.757E-07	0.813E-07	0.157E-06	0.105E-03
11.537	0.599E-05	0.643E-05	0.124E-04	0.199E-07	0.124E-04	16.669	0.105E-03
	0.357E-02	0.384E-02	0.741E-02	0.375E-06	0.403E-06	0.778E-06	0.105E-03
11.587	0.179E-04	0.192E-04	0.371E-04	0.166E-06	0.372E-04	16.728	0.105E-03
	0.121E-01	0.130E-01	0.250E-01	0.127E-05	0.136E-05	0.263E-05	0.105E-03
11.637	0.384E-04	0.412E-04	0.797E-04	0.472E-06	0.802E-04	16.795	0.105E-03
	0.304E-01	0.326E-01	0.630E-01	0.319E-05	0.342E-05	0.661E-05	0.105E-03
11.687	0.699E-04	0.750E-04	0.145E-03	0.117E-05	0.146E-03	16.874	0.105E-03
	0.636E-01	0.683E-01	0.132E+00	0.669E-05	0.717E-05	0.139E-04	0.105E-03
11.712	0.934E-04	0.100E-03	0.193E-03	0.553E-05	0.199E-03	17.003	0.105E-03
	0.859E-01	0.921E-01	0.178E+00	0.902E-05	0.967E-05	0.187E-04	0.105E-03
11.737	0.733E-04	0.786E-04	0.151E-03	-0.349E-04	0.116E-03	16.302	0.105E-03
	0.103E+00	0.111E+00	0.214E+00	0.109E-04	0.116E-04	0.225E-04	0.105E-03
11.762	0.222E-04	0.229E-04	0.451E-04	-0.289E-04	0.163E-04	15.784	0.105E-03
	0.109E+00	0.116E+00	0.225E+00	0.114E-04	0.122E-04	0.236E-04	0.105E-03

```
11.812      -0.272E-04     -0.304E-04     -0.576E-04      0.102E-04     -0.474E-04      16.194     0.105E-03
     0.956E-01      0.102E+00      0.197E+00      0.101E-04      0.107E-04      0.207E-04     0.105E-03

11.837      -0.190E-03     -0.205E-03     -0.395E-03     -0.622E-04     -0.457E-03      13.968     0.105E-03
     0.506E-01      0.528E-01      0.103E+00      0.531E-05      0.554E-05      0.108E-04     0.105E-03

11.887      -0.973E-04     -0.103E-03     -0.201E-03      0.288E-05     -0.198E-03      17.249     0.105E-03
     0.422E-02      0.357E-02      0.779E-02      0.443E-06      0.375E-06      0.818E-06     0.105E-03

         NO CONVERGENCE AT THIS TIME STEP     T=11.887

         RESTART

11.887      -0.546E-06      0.546E-06      0.508E-20      0.458E-35      0.508E-20      17.249     0.000E+00
     0.251E-34      0.226E-34      0.471E-34      0.000E+00      0.000E+00      0.495E-38     0.105E-03

11.937       0.000E+00      0.000E+00      0.000E+00      0.000E+00      0.000E+00      17.200     0.000E+00
     0.000E+00      0.000E+00      0.000E+00      0.000E+00      0.000E+00      0.000E+00     0.000E+00

11.987       0.000E+00      0.000E+00      0.000E+00      0.000E+00      0.000E+00      17.200     0.000E+00
     0.000E+00      0.000E+00      0.000E+00      0.000E+00      0.000E+00      0.000E+00     0.000E+00

12.037       0.151E-05      0.163E-05      0.314E-05     -0.103E-06      0.304E-05      16.646     0.105E-03
     0.721E-03      0.774E-03      0.150E-02      0.757E-07      0.813E-07      0.157E-06     0.105E-03

12.087       0.599E-05      0.643E-05      0.124E-04      0.199E-07      0.124E-04      16.669     0.105E-03
     0.357E-02      0.364E-02      0.741E-02      0.375E-06      0.403E-06      0.778E-06     0.105E-03

12.137       0.179E-04      0.192E-04      0.371E-04      0.166E-06      0.372E-04      16.728     0.105E-03
     0.121E-01      0.130E-01      0.250E-01      0.127E-05      0.136E-05      0.263E-05     0.105E-03

12.187       0.384E-04      0.412E-04      0.797E-04      0.472E-06      0.802E-04      16.795     0.105E-03
     0.304E-01      0.326E-01      0.630E-01      0.319E-05      0.342E-05      0.661E-05     0.105E-03
    TRANSIENT TEMPERATURE PROFILES

          0.000     225.000     140.000     140.000     140.000     140.000     140.000
    140.000     140.000     140.000

          0.050     218.468     140.120     140.000     140.000     140.000     140.000
    140.000     140.000     140.000

          0.100     218.464     140.514     140.001     140.000     140.000     140.000
    140.000     140.000     140.000

          0.150     218.473     141.678     140.008     140.000     140.000     140.000
```

140.000		140.000		140.000					
140.000	0.200	140.000	218.513	140.000	144.128	140.062	140.000	140.000	140.000
140.000	0.250	140.000	218.736	140.000	148.491	140.300	140.004	140.000	140.000
140.000	0.275	140.000	183.149	134.477	147.737	140.273	140.004	140.000	140.000
140.000	0.281	139.885	179.659	133.310	147.581	140.267	140.003	140.000	140.000
140.000	0.281	139.885	205.917	133.310	147.581	140.267	140.003	140.000	140.000
140.000	0.331	139.885	220.161	133.310	147.581	140.267	140.003	140.000	140.000
140.000	0.381	139.885	218.468	133.317	147.683	140.277	140.004	140.000	140.000
140.000	0.431	139.885	218.468	133.342	148.039	140.315	140.005	140.000	140.000
140.000	0.481	139.887	218.473	133.415	149.091	140.430	140.010	140.000	140.000
140.000	0.531	139.891	218.513	133.570	151.305	140.706	140.023	140.000	140.000
140.000	0.581	139.897	218.737	133.848	155.253	141.329	140.063	140.002	140.000
139.991	0.606	139.356	188.252	129.261	154.099	141.224	140.058	140.002	140.000
139.989	0.607	139.359	187.570	129.071	154.052	141.220	140.058	140.002	140.000
139.989	0.607	139.359	197.656	129.071	154.052	141.220	140.058	140.002	140.000
139.989	0.657	139.359	220.161	129.071	154.052	141.220	140.058	140.002	140.000

-224-

139.989	0.707	139.370	218.468	129.082	154.145	141.238	140.060	140.002	140.000
139.989	0.757	139.363	218.468	129.120	154.469	141.303	140.066	140.002	140.000
139.990	0.807	139.372	218.473	129.235	155.425	141.500	140.084	140.003	140.000
139.990	0.857	139.392	218.513	129.478	157.437	141.944	140.129	140.006	140.000
139.990	0.907	139.427	218.737	129.915	161.029	142.855	140.236	140.013	140.000
139.950	0.932	138.747	193.132	126.163	159.729	142.668	140.220	140.012	140.000
139.922	0.938	138.450	189.011	124.992	159.326	142.610	140.215	140.012	139.999
139.922	0.938	138.450	200.277	124.992	159.326	142.610	140.215	140.012	139.999
139.922	0.988	138.450	220.161	124.992	159.326	142.610	140.215	140.012	139.999
139.922	1.038	138.452	218.468	125.007	159.412	142.634	140.218	140.012	139.999
139.922	1.088	138.459	218.468	125.057	159.709	142.718	140.231	140.013	139.999
139.923	1.138	138.481	218.473	125.208	160.586	142.972	140.268	140.016	139.999
139.926	1.188	138.527	218.513	125.525	162.435	143.534	140.354	140.024	139.999
139.930	1.238	138.609	218.737	126.100	165.737	144.647	140.541	140.044	140.001
139.934	1.288	138.683	217.973	126.624	171.205	145.825	140.771	140.071	140.003

139.762	1.313	137.028	172.769	119.776	162.785	145.132	140.675	140.062	139.994
139.762	1.313	137.028	187.776	119.766	162.785	145.132	140.675	140.062	139.994
139.762	1.363	137.028	220.161	119.766	162.785	145.132	140.675	140.062	139.994
139.763	1.413	137.032	218.468	119.784	162.866	145.156	140.681	140.063	139.994
139.764	1.463	137.046	218.468	119.849	163.145	145.245	140.704	140.066	139.994
139.767	1.513	137.066	218.473	120.042	163.971	145.513	140.771	140.076	139.995
139.775	1.563	137.172	218.515	120.450	165.712	146.102	140.923	140.098	139.998
139.788	1.613	137.325	218.736	121.189	168.623	147.258	141.228	140.146	140.004
139.795	1.638	137.407	219.000	121.588	170.471	147.979	141.427	140.182	140.008
139.565	1.663	135.885	186.966	117.144	168.307	147.340	141.307	140.165	139.988
139.449	1.670	135.295	183.892	115.796	167.647	147.151	141.271	140.160	139.975
139.449	1.670	135.295	195.742	115.796	167.647	147.151	141.271	140.160	139.975
139.449	1.720	135.295	220.161	115.796	167.647	147.151	141.271	140.160	139.975
139.450	1.770	135.301	218.468	115.817	167.721	147.186	141.280	140.161	139.975
139.453	1.820	135.322	218.468	115.890	167.976	147.283	141.309	140.167	139.976

1.870	218.473	168.730	147.592	141.399	140.184	139.979	139.461	135.384	116.108
1.920	218.513	170.319	148.267	141.596	140.223	139.985	139.477	135.514	116.579
1.970	218.738	173.161	149.568	141.990	140.304	139.999	139.507	135.748	117.407
2.020	217.984	178.270	150.912	142.421	140.400	140.017	139.535	135.962	118.191
2.045	180.382	170.245	149.860	142.171	140.352	139.957	139.093	133.761	112.787
2.051	178.964	169.589	149.613	142.113	140.340	139.929	138.921	133.087	111.515
2.051	200.281	169.589	149.613	142.113	140.340	139.929	138.921	133.087	111.515
2.101	220.161	169.589	149.613	142.113	140.340	139.929	138.921	133.087	111.515
2.151	218.468	169.661	149.641	142.123	140.342	139.930	138.923	133.095	111.537
2.201	218.468	169.906	149.742	142.161	140.351	139.932	138.928	133.125	111.619
2.251	218.473	170.632	150.043	142.274	140.378	139.938	138.943	133.211	111.860
2.301	218.513	172.161	150.701	142.523	140.439	139.952	138.975	133.395	112.372
2.351	218.738	174.897	151.968	143.005	140.562	139.981	139.032	133.724	113.302
2.376	219.144	177.045	153.091	143.445	140.682	140.009	139.079	133.984	114.053
2.401	193.942	175.333	152.402	143.247	140.634	139.943	138.715	132.560	111.156
2.407	190.934	174.744	152.167	143.180	140.616	139.911			

138.556	132.010	110.170				
2.414	188.264	174.043	151.888	143.100	140.594	139.869
138.353	131.332	109.001				
2.420	186.450	173.426	151.643	143.031	140.574	139.827
138.158	130.710	107.979				
2.420	208.216	173.426	151.643	143.031	140.574	139.827
138.158	130.710	107.979				
2.470	220.161	173.426	151.643	143.031	140.574	139.827
138.158	130.710	107.979				
2.520	218.468	173.492	151.674	143.043	140.577	139.828
138.160	130.721	108.093				
2.570	218.468	173.719	151.784	143.086	140.590	139.832
138.169	130.758	108.088				
2.620	218.47[illegible]	174.387	152.111	143.216	140.627	139.843
138.193	130.809	108.342				
2.670	218.513	175.797	152.824	143.500	140.710	139.868
138.246	131.103	108.883				
2.720	218.739	178.319	154.180	144.051	140.874	139.918
138.342	131.525	109.867				
2.745	219.020	179.763	155.043	144.413	140.988	139.952
138.398	131.766	110.447				
2.770	197.384	178.263	154.397	144.205	140.925	139.858
137.996	130.474	108.150				
2.795	189.697	176.150	153.495	143.915	140.831	139.693
137.330	128.498	104.953				
2.795	205.041	176.150	153.495	143.915	140.831	139.693
137.330	128.498	104.953				
2.845	220.161	176.150	153.495	143.915	140.831	139.693
137.330	128.498	104.953				
2.895	218.468	176.212	153.527	143.928	140.835	139.695
137.333	128.510	104.978				

2.945	218.460	176.425	153.641	143.976	140.851	139.700
137.345	128.555	105.067				
2.995	218.473	177.053	153.982	144.121	140.897	139.717
137.390	128.686	105.330				
3.045	218.513	178.377	154.719	144.436	141.000	139.755
137.455	128.964	105.890				
3.095	218.739	180.740	156.117	145.044	141.203	139.829
137.591	129.416	106.913				
3.145	218.234	185.441	157.528	145.678	141.423	139.908
137.719	129.931	107.882				
3.170	169.[illegible]	179.150	156.363	145.256	141.273	139.690
136.947	127.744	104.319				
3.176	187.693	178.406	155.990	145.126	141.221	139.601
136.646	126.979	103.234				
3.201	186.386	177.348	155.478	144.942	141.145	139.461
136.190	125.859	101.704				
3.201	211.620	177.348	155.478	144.942	141.145	139.461
136.190	125.859	101.704				
3.251	220.161	177.348	155.478	144.942	141.145	139.461
136.190	125.859	101.704				
3.301	218.468	177.408	155.509	144.957	141.150	139.464
136.195	125.873	101.730				
3.351	218.468	177.615	155.619	145.010	141.169	139.472
136.211	125.925	101.821				
3.401	218.473	178.225	155.947	145.168	141.227	139.498
136.260	126.079	102.091				
3.451	218.513	179.512	156.660	145.513	141.353	139.553
136.363	126.405	102.666				
3.501	218.739	181.817	158.010	146.172	141.599	139.659
136.552	126.993	103.718				

3.551	218.404	186.408	159.358	146.842	141.857	139.769
136.728	127.534	134.706				
3.576	191.173	180.814	158.188	146.376	141.662	139.485
135.869	125.401	101.573				
3.582	189.332	180.090	157.810	146.225	141.593	139.369
135.533	124.638	100.575				
3.589	187.520	179.319	157.409	146.065	141.516	139.236
135.156	123.605	99.521				
3.589	201.112	179.319	157.409	146.065	141.516	139.236
135.156	123.865	99.521				
3.639	220.161	179.319	157.409	146.065	141.516	139.236
135.156	123.865	99.521				
3.689	218.464	179.376	157.440	146.081	141.522	139.239
135.162	123.821	99.547				
3.739	218.468	179.573	157.550	146.138	141.545	139.251
135.172	123.878	99.638				
3.789	218.473	180.154	157.879	146.308	141.614	139.285
135.243	124.047	99.910				
3.839	218.513	181.379	158.591	146.678	141.764	139.360
135.372	124.405	100.469				
3.889	218.739	183.574	159.936	147.382	142.054	139.502
135.608	125.053	101.549				
3.939	218.303	188.125	161.391	148.107	142.361	139.649
135.833	125.672	102.566				
3.964	192.799	182.722	160.143	147.602	142.123	139.314
134.939	123.633	99.762				
3.989	189.706	180.827	159.090	147.142	141.887	138.947
133.990	121.630	97.259				
3.989	207.266	180.827	159.090	147.142	141.887	138.947
133.990	121.630	97.259				

4.039	220.161	180.827	159.090	147.142	141.887	138.947	133.990	121.620	97.259
4.089	218.468	180.882	159.121	147.159	141.895	138.951	133.937	121.647	97.285
4.139	218.468	181.071	159.230	147.219	141.921	138.966	134.022	121.709	97.376
4.189	218.473	181.630	159.556	147.399	142.000	139.010	134.096	121.893	97.649
4.239	218.513	182.809	160.262	147.787	142.173	139.105	134.253	122.283	98.231
4.289	218.727	184.819	161.532	148.490	142.489	139.278	134.5[illegible]6	122.957	99.246
4.339	218.460	189.318	162.877	149.243	142.836	139.464	134.801	123.626	100.273
4.389	189.817	179.136	160.605	148.176	142.274	138.687	132.939	119.735	95.241
4.389	203.439	179.136	160.605	148.176	142.274	138.687	132.939	119.735	95.241
4.439	220.161	179.136	160.605	148.176	142.274	138.687	132.939	119.735	95.241
4.489	218.468	179.194	160.631	148.193	142.282	138.692	132.947	119.763	95.267
4.539	218.468	179.392	160.725	148.256	142.312	138.710	132.976	119.820	95.359
4.589	218.473	179.975	161.004	148.442	142.401	138.764	133.062	120.010	95.633
4.639	218.513	181.207	161.610	148.844	142.594	138.880	133.244	120.433	96.218
4.689	218.729	183.411	162.769	149.598	142.963	139.099	133.577	121.191	97.291
4.739	218.317	187.963	163.956	150.356	143.345	139.322			

133.895		121.963		98.322					
132.839	4.764	119.827	192.700	95.792	182.823	162.758	149.738	142.991	138.844
132.439	4.770	119.088	190.944	94.966	182.206	162.358	149.531	142.863	138.659
131.997	4.776	118.289	189.662	94.098	181.549	161.933	149.310	142.724	138.453
131.637	4.783	117.655	188.738	93.427	181.035	161.602	149.137	142.612	138.284
131.637	4.783	117.655	213.086	93.427	181.035	161.602	149.137	142.612	138.284
131.637	4.833	117.655	220.161	93.427	181.035	161.602	149.137	142.612	138.284
131.647	4.663	117.674	218.466	93.453	181.090	161.630	149.155	142.621	138.290
131.640	4.933	117.745	218.470	93.544	161.278	161.728	149.218	142.654	138.312
131.779	4.983	117.953	218.475	93.815	181.833	162.020	149.405	142.752	138.377
131.990	5.033	118.355	218.513	94.395	183.005	162.653	149.808	142.965	138.517
132.358	5.083	119.161	218.727	95.408	185.004	163.799	150.531	143.350	138.767
132.729	5.133	119.926	218.435	96.441	189.505	165.029	151.301	143.767	139.033
130.609	5.183	116.037	190.005	91.915	179.663	162.755	150.053	142.983	137.989
130.566	5.183	115.965	189.863	91.844	179.613	162.718	150.032	142.968	137.967
130.523	5.184	115.895	189.726	91.774	179.564	162.681	150.011	142.953	137.945

5.185	189.588	179.514	162.643	149.990	142.938	137.923	130.479	115.823	91.703
5.186	189.459	179.466	162.607	149.970	142.924	137.902	130.438	115.754	91.635
5.186	212.001	179.466	162.607	149.970	142.924	137.902	130.438	115.754	91.635
5.236	220.161	179.466	162.607	149.970	142.924	137.902	130.438	115.754	91.635
5.286	218.468	179.523	162.631	149.988	142.934	137.909	130.449	115.775	91.661
5.336	218.466	179.719	162.716	150.052	142.969	137.934	130.476	115.849	91.752
5.386	218.473	180.298	162.970	150.241	143.075	138.010	130.597	116.067	92.022
5.436	218.513	181.519	163.524	150.648	143.304	138.172	130.834	116.522	92.599
5.486	218.739	183.705	164.587	151.409	143.738	138.475	131.268	117.377	93.660
5.536	218.281	188.257	165.693	152.171	144.182	138.779	131.665	118.183	94.688
5.561	192.888	183.223	164.511	151.473	143.710	138.159	130.535	116.120	92.415
5.567	191.258	182.656	164.116	151.238	143.542	137.927	130.069	115.409	91.678
5.573	189.913	182.046	163.693	150.985	143.357	137.670	129.568	114.630	90.898
5.580	189.093	181.577	163.367	150.789	143.211	137.462	129.264	114.021	90.303
5.580	213.392	181.577	163.367	150.789	143.211	137.462	129.264	114.021	90.303

5.630	220.161	181.577	163.367	150.789	143.211	137.462
129.204	114.021	90.303				
5.680	218.468	181.631	163.393	150.807	143.222	137.470
129.215	114.042	90.329				
5.730	218.468	181.816	163.485	150.870	143.260	137.499
129.257	114.119	90.418				
5.780	218.473	182.364	163.759	151.059	143.374	137.585
129.380	114.345	90.684				
5.830	218.513	183.519	164.354	151.465	143.620	137.770
129.643	114.826	91.251				
5.880	218.727	185.489	165.433	152.191	144.062	138.100
130.190	115.660	92.247				
5.930	218.361	189.996	166.608	152.967	144.538	138.449
130.559	116.576	93.276				
5.955	195.540	185.584	165.563	152.321	144.071	137.845
129.491	114.726	91.363				
5.980	192.052	183.771	164.364	151.574	143.508	137.089
128.155	112.611	89.234				
5.980	206.965	183.771	164.364	151.574	143.508	137.089
128.155	112.611	89.234				
6.030	220.161	183.771	164.364	151.574	143.508	137.089
128.155	112.611	89.234				
6.080	218.468	183.823	164.391	151.592	143.519	137.098
128.167	112.633	89.258				
6.130	218.468	183.997	164.489	151.656	143.560	137.130
128.212	112.711	89.346				
6.180	218.473	184.512	164.780	151.848	143.681	137.226
128.345	112.942	89.608				
6.230	218.513	185.598	165.412	152.262	143.942	137.433
128.629	113.435	90.168				

6.280	218.727	187.453	166.549	153.003	144.411	137.799	129.125	114.291	91.151
6.330	218.501	191.826	167.766	153.792	144.911	138.185	129.631	115.155	92.162
6.355	200.409	188.834	166.983	153.294	144.534	137.705	128.820	113.867	90.811
6.380	194.594	186.607	165.588	152.401	143.838	136.799	127.235	111.516	88.455
6.386	194.251	186.157	165.306	152.218	143.687	136.596	126.958	111.023	87.999
6.386	213.529	186.157	165.306	152.218	143.687	136.596	126.958	111.023	87.999
6.436	220.161	186.157	165.306	152.218	143.687	136.596	126.958	111.023	87.999
6.486	218.468	196.205	165.335	152.236	143.700	136.606	126.971	111.046	88.023
6.536	218.468	186.368	165.440	152.302	143.742	136.642	127.020	111.120	88.110
6.586	218.473	186.847	165.753	152.499	143.870	136.748	127.164	111.303	88.368
6.636	218.513	187.859	166.428	152.923	144.146	136.976	127.470	111.809	88.919
6.686	218.726	189.587	167.636	153.684	144.641	137.380	126.036	112.748	89.890
6.736	218.507	193.873	168.930	154.506	145.174	137.808	128.559	113.648	90.900
6.786	213.112	193.268	168.657	154.330	145.035	137.633	128.277	113.218	90.462
6.811	200.092	191.237	167.475	153.563	144.424	136.861	127.034	111.340	88.577
6.661	198.137	189.150	166.253	152.760	143.760	135.998			

125.656	109.341	86.695				
6.867	197.934	189.010	166.170	152.705	143.712	135.935
125.556	109.202	86.572				
6.867	215.926	189.010	166.170	152.705	143.712	135.935
125.556	109.202	86.572				
6.917	220.161	189.010	166.170	152.705	143.712	135.935
125.556	109.202	86.572				
6.967	218.468	189.054	166.203	152.724	143.725	135.946
125.571	109.215	86.596				
7.017	218.468	189.202	166.318	152.792	143.770	135.985
125.623	109.308	86.681				
7.067	218.473	189.639	166.659	152.994	143.905	136.101
125.778	109.551	86.935				
7.117	218.513	190.561	167.395	153.431	144.196	136.351
126.108	110.070	87.478				
7.167	218.728	192.138	168.702	154.219	144.717	136.793
126.686	110.975	88.434				
7.217	218.525	196.326	170.105	155.086	145.286	137.268
127.291	111.916	89.446				
7.242	215.988	196.466	170.436	155.276	145.409	137.369
127.417	112.110	89.658				
7.292	215.988	196.359	170.234	155.144	145.303	137.237
127.213	111.811	89.362				
7.317	199.594	190.886	168.914	154.283	144.597	136.360
125.866	109.847	87.436				
7.324	198.213	190.264	168.500	154.009	144.364	136.063
125.413	109.214	86.854				
7.330	197.001	189.625	168.075	153.726	144.120	135.750
124.937	108.557	86.262				
7.336	196.288	189.076	167.709	153.481	143.907	135.474
124.519	107.988	85.760				

7.336	212.515	189.076	167.709	153.481	143.907	135.474
124.519	107.988	85.760				
7.386	220.161	185.076	167.709	153.481	143.907	135.474
124.519	107.968	85.760				
7.436	218.468	189.119	167.739	153.501	143.920	135.486
124.535	108.012	85.784				
7.486	218.468	189.267	167.846	153.573	143.968	135.529
124.550	108.095	65.868				
7.536	218.473	189.703	168.166	153.786	144.112	135.655
124.753	108.341	86.117				
7.586	218.513	190.624	168.856	154.246	144.421	135.925
125.102	108.816	86.650				
7.636	218.728	192.197	170.084	155.070	144.976	136.405
125.713	109.782	87.590				
7.686	218.525	196.383	171.498	155.970	145.580	136.918
126.353	110.736	88.587				
7.711	215.992	196.523	171.725	156.165	145.712	137.028
126.487	110.935	88.798				
7.761	215.992	196.432	171.518	156.027	145.597	136.888
126.261	110.640	88.511				
7.786	199.671	191.075	170.164	155.115	144.835	135.961
124.913	108.766	86.642				
7.792	198.310	190.485	169.739	154.824	144.585	135.649
124.455	108.063	86.077				
7.799	197.209	189.078	169.303	154.525	144.323	135.321
123.977	107.439	65.505				
7.865	196.419	189.347	168.921	154.262	144.091	135.028
123.550	106.873	85.011				
7.805	212.572	189.347	168.921	154.262	144.091	135.028
123.550	106.873	85.011				

7.855	220.161	189.347	168.921	154.262	144.091	135.028	123.550	106.873	85.011
7.905	218.468	189.390	168.950	154.282	144.105	135.041	123.566	106.896	85.034
7.955	218.468	189.536	169.053	154.356	144.156	135.087	123.623	106.980	85.117
8.005	218.473	189.969	169.359	154.576	144.309	135.222	123.795	107.229	85.362
8.055	218.513	190.881	170.018	155.049	144.637	135.513	124.180	107.759	85.886
8.105	218.728	192.440	171.195	155.893	145.225	136.028	124.801	108.684	86.812
8.155	218.526	196.616	172.469	156.811	145.865	136.579	125.474	109.651	87.796
8.180	215.988	196.756	172.786	157.016	146.008	136.701	125.620	109.858	88.011
8.230	215.980	196.674	172.577	156.870	145.884	136.554	125.410	109.568	87.731
8.255	199.907	191.408	171.206	155.911	145.070	135.581	124.078	107.662	85.916
8.261	198.557	190.838	170.775	155.606	144.803	135.256	123.566	107.049	85.368
8.267	197.476	190.255	170.334	155.292	144.525	134.916	123.086	106.419	84.815
8.274	196.708	189.746	169.949	155.017	144.280	134.614	122.660	105.867	84.340
8.274	212.702	189.746	169.949	155.017	144.280	134.614	122.660	105.867	84.340
8.324	220.161	189.746	169.949	155.017	144.280	134.614	122.660	105.867	84.340

8.374	218.468	189.789	169.977	155.038	144.295	134.627	122.677	105.891	84.363
8.424	218.468	189.933	170.077	155.113	144.349	134.676	122.737	105.975	84.444
8.474	218.473	190.360	170.374	155.336	144.510	134.820	122.916	106.225	84.685
8.524	218.513	191.259	171.013	155.817	144.856	135.130	123.297	106.759	85.202
8.574	218.728	192.797	172.156	156.675	145.475	135.679	123.964	107.653	86.114
8.624	218.533	196.959	173.396	157.605	146.148	136.268	124.668	108.671	87.087
8.649	216.026	197.099	173.705	157.812	146.298	136.397	124.820	108.860	87.299
8.699	216.026	197.024	173.492	157.658	146.165	136.242	124.617	108.591	87.024
8.724	200.424	191.991	172.140	156.677	145.318	135.249	123.240	106.750	85.295
8.749	197.849	190.362	170.872	155.745	144.492	134.264	121.867	104.990	83.739
8.749	210.377	190.362	170.872	155.745	144.492	134.264	121.847	104.990	83.739
8.799	220.161	190.362	170.872	155.745	144.492	134.264	121.867	104.990	83.739
8.849	218.468	190.404	170.899	155.767	144.508	134.278	121.965	105.014	83.761
8.899	218.468	190.545	170.998	155.843	144.565	134.330	121.967	105.099	83.841
8.949	218.473	190.963	171.290	156.069	144.733	134.483	122.152	105.351	84.079
8.999	218.513	191.843	171.919	156.556	145.096	134.811			

122.546	105.889	84.590				
9.049	218.728	193.348	173.044	157.423	145.743	135.391
123.238	106.829	85.491				
9.099	218.539	197.489	174.268	158.365	146.447	136.015
123.971	107.818	86.456				
9.124	216.099	197.626	174.572	158.573	146.603	136.152
124.129	108.030	86.666				
9.174	216.099	197.560	174.359	158.414	146.464	135.992
123.915	107.746	86.400				
9.199	201.214	192.826	173.045	157.429	145.601	134.997
122.582	105.966	84.766				
9.224	198.512	191.160	171.729	156.433	144.708	133.951
121.184	104.199	83.203				
9.224	210.183	191.160	171.729	156.433	144.708	133.951
121.184	104.199	83.203				
9.274	220.161	191.160	171.729	156.433	144.708	133.951
121.184	104.199	83.203				
9.324	218.468	191.201	171.757	156.454	144.724	133.966
121.202	104.223	83.226				
9.374	218.468	191.338	171.855	156.531	144.783	134.020
121.2 6	104.308	83.305				
9.424	218.473	191.743	172.146	156.760	144.959	134.181
121.457	104.562	83.540				
9.474	218.513	192.598	172.773	157.253	145.336	134.526
121.864	105.132	84.045				
9.524	218.728	194.061	173.892	158.129	146.009	135.136
122.579	106.048	84.936				
9.549	219.109	195.244	174.859	158.885	146.590	135.658
123.181	106.841	65.696				
9.574	216.585	197.063	175.523	159.405	146.991	136.014
123.587	107.373	86.212				

9.624	216.585	197.261	175.680	159.522	147.081	136.093	123.678	107.491	86.328
9.649	201.531	193.134	174.462	158.585	146.253	135.158	122.458	105.897	84.840
9.674	198.608	191.489	173.064	157.498	145.276	134.039	120.949	104.042	83.199
9.680	198.158	191.186	172.808	157.298	145.091	133.825	120.721	103.659	82.913
9.680	216.436	191.186	172.808	157.298	145.091	133.825	120.721	103.659	82.913
9.730	220.161	191.186	172.808	157.298	145.091	133.825	120.721	103.699	82.913
9.780	218.468	191.227	172.834	157.320	145.108	133.841	120.739	103.723	82.935
9.830	218.468	191.364	172.926	157.398	145.170	133.898	120.805	103.809	83.013
9.880	218.473	191.769	173.202	157.630	145.352	134.066	121.091	104.013	83.246
9.930	218.513	192.624	173.796	158.128	145.745	134.427	121.419	104.655	83.746
9.980	218.726	194.085	174.859	159.012	146.444	135.066	122.153	105.554	84.629
10.005	219.109	195.268	175.782	159.773	147.048	135.612	122.773	106.311	85.382
10.030	216.581	197.089	176.417	160.295	147.463	135.985	123.192	106.887	85.895
10.060	216.581	197.268	176.570	160.414	147.557	136.070	123.286	107.007	86.012
10.105	201.556	193.232	175.357	159.449	146.695	135.110	122.064	105.430	84.547

10.130	198.682	191.665	173.962	158.331	145.679	133.967
120.606	103.600	82.933				
10.136	198.243	191.377	173.708	158.125	145.489	133.749
120.329	103.263	82.653				
10.137	198.182	191.339	173.674	158.098	145.464	133.720
120.292	103.219	82.616				
10.137	218.590	191.339	173.674	158.098	145.464	133.720
120.292	103.219	82.616				
10.187	220.161	191.339	173.674	158.098	145.464	133.720
120.292	103.219	82.616				
10.237	218.468	191.380	173.699	158.120	145.481	133.737
120.311	103.243	82.638				
10.287	218.468	191.516	173.788	158.198	145.545	133.796
120.379	103.329	82.716				
10.337	218.473	191.919	174.053	158.431	145.734	133.971
120.579	103.584	82.947				
10.387	218.513	192.768	174.625	158.931	146.140	134.348
121.008	104.128	83.442				
10.437	218.728	194.222	175.649	159.817	146.862	135.013
121.761	105.081	84.318				
10.462	219.111	195.403	176.544	160.580	147.487	135.584
122.399	105.884	85.068				
10.487	217.397	196.693	177.026	160.988	147.821	135.888
122.736	106.306	85.467				
10.512	215.743	197.033	177.194	161.123	147.932	135.989
122.847	106.445	85.599				
10.562	215.743	196.928	176.900	160.882	147.714	135.749
122.548	106.064	85.249				
10.587	199.908	191.846	175.490	159.723	146.661	134.587
121.097	104.232	83.582				

119.657	10.637	102.469	198.431	82.071	190.449	174.144	158.608	145.630	133.435
119.657	10.637	102.469	212.106	82.071	190.449	174.144	158.608	145.630	133.435
119.657	10.687	102.469	220.161	82.071	190.449	174.144	158.608	145.630	133.435
119.676	10.737	102.493	218.468	82.093	190.491	174.167	158.630	145.648	133.452
119.745	10.787	102.579	218.460	82.179	190.632	174.249	158.708	145.713	133.514
119.9[illegible]1	10.537	102.8[illegible]6	218.473	82.399	191.048	174.494	158.940	145.908	133.696
120.3[illegible]1	10.887	103.363	218.513	82.889	191.925	175.023	159.438	146.325	134.087

APPENDIX F

A COMPARISON OF FLOSS TO THE SAS COMPUTER CODE

F.1 THE SAS Code

Argonne National Laboratory developed the first SAS computer code, SAS1A, in 1970. The code has undergone virtually continuous revision and updating since then, and is currently in its fourth generation, with SAS4A. The code is a one dimensional, multichannel code, for the purpose of studying accidents involving sodium voiding in the LMFBR. It contains calculational modules for transient and steady state thermalhydraulics, both in single phase and two phase flow. In addition, it has the means to consider fuel and clad melting and motion, fission gas release, and other factors present during postulated LMFBR accidents. The code is structured so as to be able to follow an entire reactor accident from the initiation phase through until gross fuel motion and reactor disassembly begin. Other codes, such as VENUS, can then use the SAS results to predict the events during the core disruptive phase of the accident.

The current SAS model can handle multiple bubbles in a single channel, and multiple channels across the core. However, each bundle is considered as a unit which behaves one-dimensionally. Therefore, although corewide incoherencies in voiding behavior can be tracked, multi-dimensional bubble behavior across a single bundle cannot be considered. Due to its versatility, the SAS code is one of the most widely used tools in the United States LMFBR accident analysis program.

F.2 Comparing FLOSS to SAS

Since the FLOSS code also uses a one-dimensional thermal-hydrodynamic model to calculate conditions during a transient, it is not surprising to find that the equations used in both codes are quite similar. The technique used to track the solution of the transient was derived from one of the reports used in the development of the original SAS code, as well. Though the intent of this project was not to reproduce SAS, the system of solution for both codes is basically similar.

The major differences between SAS and FLOSS are in scope and in the handling of the heat transfer during condensation. The scope of SAS is far greater than that of FLOSS; in fact, the FLOSS code would comprise no more than two or three modules in the entire SAS code. This is due to the assumption made when the project was begun that FLOSS would eventually become a module in a larger, system-scale code. The second difference is more fundamental. The SAS code contains only a single input for a constant heat transfer coefficient. In the manual consulted (32) this value was set at approximately 11000 $BTU/hr\text{-}ft^2{}^\circ F$, which falls in the range suggested by Barry and Balzhiser (33). However, there is no methodology presented for describing the changes in condensation heat transfer which have been documented here. The FLOSS code accomplishes this change in heat transfer by slightly changing the initial temperature profile, thereby causing a step change in heat transfer coefficient. The high value of the coefficient causes the code to underpredict experimental results. However, the failure of SAS to consider this phenomenon may lead to overprediction of experimental results causing an unrealistically conservative solution. Table F.1, presented on the next page, spotlights some of the areas where further research is needed to improve the predictive abilities of SAS.

The entire question of multidimensional effects in sodium boiling is another area with which neither FLOSS nor SAS are capable of dealing. As mentioned in Chapter 6, this, as well as several other questions, remain to be resolved in further research.

Table F.1 Comparison of FLOSS to SAS

Issue	Water (FLOSS)	SAS	Recommendations for Sodium work
Initial Temperature Profile in Unheated Zone	Experimentally determined, except for small saturated zone at start of unheated zone	As calculated during initial stages of transient	A physically realistic and accurate temperature profile is necessary to adequately characterize the flow behavior. This factor is one of the prime determinants of how the flow will behave. It is essential that any simulation which purports to chart the best estimate of the oscillation take account of the importance of this factor, and calculate an accurate temperature profile history as well.
Initial Temperature Profile in Core (Heated Zone)	Not considered	As calculated	The identical comment as above is applicable here, as well. This profile will also influence flow behavior, especially if it is steep.
Condensation Heat Transfer	Step change from zero to values approximating those present during bubble collapse	Constant	Investigation is needed to determine whether the sodium condensation coefficient behaves like the water coefficient. A mechanistic model for h_{con} versus time over the period of an oscillation, accounting for interfacial breakup and augmentation of heat transfer, is needed.

Table F.1 Comparison of FLOSS TO SAS (Cont.)

Issue	Water(FLOSS)	SAS	Recommendations for Sodium Work
Loop Dynamics	Present implicit in model	Present in later versions of SAS	The characteristics of the external loop can have a significant effect on flow oscillatory behavior.
Comparison of Simulants to Sodium	--	--	Investigation into the relevance of simulant behavior to sodium behavior is clearly needed.
Non-condensable gas	Implicit in choice of heat transfer coefficient	Implicit in choice of heat transfer coefficient	While work has been done regarding condensation in liquid metals, the presence of non-condensibles in sodium systems provides both a mechanism for nucleation and a retarding factor in condensation. Work is needed to provide accurate models for the effect of these noncondensibles on heat transfer. This is especially relevant if fission gases are released into the coolant.